

22nd Canadian Rock Mechanics Symposium
Canadian Strengths & Future Directions



— Symposium Proceedings —

Editors:

Jennifer J. Day & Mark S. Diederichs



Proceedings of RockEng22, the 22nd Canadian Rock Mechanics Symposium

CANADIAN STRENGTHS AND
FUTURE DIRECTIONS

August 8 – 10, 2022
Kingston, Ontario, Canada

Edited by

Jennifer J. Day

*Department of Geological Sciences and Geological Engineering
Queen's University
Kingston, Ontario, Canada*

Mark S. Diederichs

*Department of Geological Sciences and Geological Engineering
Queen's University
Kingston, Ontario, Canada*

Organized by the

Canadian Rock Mechanics Association

*Canada's National Group of the
International Society for Rock Mechanics and Rock Engineering (ISRM)*

Symposium Committee

Jennifer J. Day (Symposium Chair)
Mark S. Diederichs (Technical Chair)
Navid Bahrani
Davide Elmo
Giovanni Grasselli
Kathy Kalenchuk
Doug Milne
Mohsen Nicksiar
Brad Simser

Student Volunteers

Evan Dressell (Lead)
Caitlin Fischer
Émélie Gagnon
Fedilberto Gonzalez
Amanda Hyslop
Liam Kelly
Simone Markus
Mark McDonald
Timothy Packulak
Jack Park
Samuel Woodland

Editors: Jennifer J. Day and Mark S. Diederichs

A Publication of:
The Canadian Rock Mechanics Association
<http://carma-rocks.ca/>

© Copyright 2025 Canadian Rock Mechanics Association

Copyright of the individual extended abstract or abstract contributions rests with the respective authors.

ISBN-13: 978-1-55339-736-6

All rights reserved.

Requests to the Publisher for permission should be addressed to the Canadian Rock Mechanics Association,
email: contactus@carma-rocks.ca

Published in Canada

Preface

The 22nd Canadian Rock Mechanics Symposium, RockEng22, represents a renewal of this Symposia series by the Canadian Rock Mechanics Association (CARMA), which first started in 1962, and was previously held in 2012 in Edmonton, Alberta, Canada. RockEng22 was the 47th anniversary since the last CARMA Symposium was held in beautiful Kingston, Ontario.

RockEng22 brought together 36 invited speakers in a single-track programme from the Canadian rock mechanics and rock engineering community, with representation from both academia and industry. We highlighted speakers from all career levels (veterans, mid-career, and rising stars) and engineering disciplines involving rock mechanics and rock engineering. In addition to the invited speakers, 32 poster presentations were exhibited at the event.

The social program at RockEng22 featured a 1000 Islands Sunset Dinner Boat Cruise and a combined Technical Tour and Banquet Dinner inside the Brockville Tunnel, where nearly 200 participants experienced some of the spectacular natural and human built vistas in the greater Kingston area.

A special concluding workshop for all participants provided an opportunity to discuss and develop, as the Canadian rock mechanics and rock engineering community, our shared vision for the 23rd Canadian Rock Mechanics Symposium and other future CARMA Symposia.

Thank you to members of the symposium committee for their review of abstract submissions, as well as to the student volunteers who helped ensure the smooth operations of this event.

Thank you to the City of Brockville for granting us access to the Brockville Tunnel for our tour and banquet dinner, and to the Isabel Bader Centre for the Performing Arts at Queen's University for offering a stunning venue at the shore of Lake Ontario for the symposium.

Thank you to our sponsors for their generous support of this event, which would otherwise have truly not been possible.

Jennifer J. Day
Symposium Chair
RockEng22, the 22nd Canadian Rock Mechanics Symposium

Contents

Introductory Remarks	10
Recent Award Winners	12
From common to best practices in underground rock engineering <i>Kaiser, P.K.</i>	14
State-of-the-art, Finite-Discrete Element Method (FDEM) modelling in rock mechanics <i>Tatone, B. and Lisjak, A.</i>	16
Utilization of multi-scale modelling for geomechanical hazard management <i>Kalenchuk, K.</i>	21
The Influence of Release Mechanisms in Rock Slope Engineering: A Three-Dimensional Perspective <i>Stead, D.¹ and Donati, D.²</i>	24
Hydraulic fracture complexity in shale rock <i>Grasselli, G.</i>	29
Characterization of rock salt response to blasting using terrestrial laser scanner technology <i>Aubertin, J.D.</i>	32
Heterogeneous rockmass characterization for numerical rock engineering design <i>Day, J.J.¹, Clark, M.D., Rudderham, G.A., and Gagnon, É.</i>	37
Building slope process models considering engineering geology <i>Hutchinson, D.J.</i>	42
The role of rock mechanics in the geological storage of CO ₂ through the lens of the Aquistore CO ₂ Storage Project <i>Chalaturnyk, R.J.</i>	45
Is it really necessary to quantify GSI? <i>Elmo, D.¹ and Yang, B.²</i>	50
Underground construction in complex rock environments: promises and pitfalls of observational design <i>Diederichs, M.S.</i>	55
Rock mass characterization using DFNs, LiDAR and distributed optical sensing <i>Vlachopoulos, N.¹, Vazaios, I.², and Forbes, B.³</i>	56
Rock Mechanics and Rock Testing	61
Damage during stress relaxation in brittle rocks – recent findings from laboratory experiments <i>Walton, G.¹, Shirole, D.², Hedayat, A.¹, Paraskevopoulou, C.³, Perras, M.A.⁴</i>	63
Micro-mechanical modelling of core damage <i>Bahrani, N.</i>	66
The Leeb Hardness Test for use in rock engineering practice <i>Corkum, A.G.</i>	71
The Wild and Wonderful Adventures of Applying Rock Mechanics to Volcanology <i>Villeneuve, M.C.</i>	76

Rockmass Mechanics and Structure Networks	81
Influence of joint stiffness on a shale slope behaviour	83
<i>Martin, C.D.¹, Rafiei Renani, H.², Stevenson, G.², and Watson, A.³</i>	
Managing scale with empirical and simple numerical analysis techniques	88
<i>Milne, D.</i>	
Post-peak deformation behaviours of brittle rocks	93
<i>Cai, M.</i>	
Challenges in rock engineering	98
<i>Bewick, R.P.</i>	
Innovations in Rock Mechanics Modelling	103
The evolution of factor of safety computation in slope stability analyses	105
<i>Corkum, B.</i>	
Challenges in the modelling of ground support	110
<i>Karampinos, E.¹ and Hadjigeorgiou, J.²</i>	
Incorporating probability in modelling – from DFN to numerical modelling	115
<i>Carvalho, J.L.</i>	
Recent advances in discrete element modelling	120
<i>Hazzard, J.F., Potyondy, D.O., Purvance, M.</i>	
Application of strain-softening in analysis of underground mining	125
<i>Ghazvinian, E.¹, Fuenzalida, M.¹, Garza-Cruz, T.¹, Cancino, C.¹, and Pierce, M.²</i>	
Geotechnical domain determination and characterization – what assumptions have you inherited?	128
<i>Palleske, C.K.</i>	
Mining deeper: The need for new numerical tools for brittle rock failure	133
<i>Eberhardt, E., Rahjoo, M., Lavoie, T., Roy, J., and McMillan, R.</i>	
In Situ Monitoring and Rock Engineering	139
Rock engineering innovations in mine design	141
<i>Espley, S.J. and Larsen, S.</i>	
Residential hillside development and rockfall mitigation	146
<i>Tannant, D.D.</i>	
Characterizing complex seismicity in mines	151
<i>Brown, L.¹, Carusone, O.², and Pelletier, D.²</i>	
The design of the tunnels & caverns for the Rozelle Interchange	156
<i>Hunt, C.¹, Trim, M.², Bateman, J.², and Tepavac, D.³</i>	
Making connections towards data driven underground excavation models	161
<i>Perras, M.A., Morgenroth, J., Vasileiou, A., Alcaino-Olivares, R., Golabchi, Y., and Khan, U.T.</i>	
Transforming underground: A case study on the design of the Long Baseline Neutrino Facility Far Site	166
<i>Stewart, H.¹ and Pollak, S.²</i>	
Making sense of geomechanical data in mine design or the good, the bad and the missing	169
<i>Coulson, A.L.</i>	
Seismic hazard metrics	174
<i>Moreau-Verlaan, L.</i>	
A few underground observations in deep mining: hard igneous rock	179
<i>Simser, B.P.</i>	

Evolution of seismic risk management strategies at Vale's Ontario Operations over the last decade <i>Yao, M., Chinnasane, D., Forsythe, A., and Landry, D.</i>	182
Geology, safety, value: +/- 40 years <i>Falmagne, V.</i>	187
Poster Presentation Abstracts	193
Multi-modal limit equilibrium analysis of open pit mines using LIPS-R <i>Li, S.¹, Cami, B.², Javankhoshdel, S.², Corkum, B.², and Yacoub, T.²</i>	194
Numerical and machine learning based approaches to study the influence of environmental conditions on crack growth in the Theban Necropolis, Egypt <i>Vasileiou, A.¹, Alcaino-Olivares, R.¹, Loprieno-Gnirs, A.², Bickel, S.², Ziegler, M.³, Khan, U.T.¹, and Perras, M.A.¹</i>	195
A geomechanics research program in support of deep geological disposal in Canada <i>Kasani, H.</i>	197
2022 database update and UCS-Leeb Hardness correlation <i>Séguin, K.¹, Kinakin, D.¹, and Corkum, A.G.²</i>	198
Numerical study of the effects of yielding rockbolts on controlling self-initiated strainbursts <i>Wang, J., Apel, D.B., Wei, C., and Xu, H.</i>	200
Innovation in underground mapping – digital data collection and streamlined post-processing in industry standard software <i>Morgenroth, J., Yee, S., and Andrew, J.</i>	202
Forecasting of seismic hazard based on numerical modelling of future mining <i>Rebuli, D.B.</i>	204
Assessing the extent of blast-induced damage in an open pit bench blast using Discrete Fracture Network (DFN) and combined finite/discrete element methods (FDEM) <i>Karimi, O.¹, Fillion, M.H.¹, and Dirige, P.²</i>	205
Investigating the effect of bedding plane orientation on the mechanical and elastic behaviour of shale rock <i>Rizehbandi, A., Popoola, A., Seyed Ghafouri, S.M.S., and Grasselli, G.</i>	207
Implementation of Epiroc Cabletec in permafrost condition <i>Hammoum, S.</i>	209
Empirical stability analysis of stopes using MineRoc software® considering the three-dimensional stress condition, Alamos Gold Mine <i>Vallejos, J.¹, Espinoza, G.¹, Cepeda, E.¹, Espinoza, J.¹, Barberán, A.¹, Xu, Y.H.², Boame, M.², and Blake, T.²</i>	211
The pulverization mechanism of host rocks induced in faulting: Insights from grain-scale fracturing by OpenFDEM <i>Li, X.¹, Zhao, Q.², and Grasselli, G.¹</i>	212
Improving confidence in caving-induced subsidence forecasting through surface monitoring validation <i>Lalang, M.¹, Eberhardt, E.¹, Campbell, R.², and Taylor, K.³</i>	214
Study of bulking displacement and depth of stress fracturing for deformation-based ground support design calibration <i>Primadiansyah, A.A.¹, Eberhardt, E.¹, Silaen, H.², and Campbell, R.³</i>	216
High resolution imaging and characterization of laboratory fractures in layered anisotropic rocks – geometry, morphology and permeability <i>Li, M., Magsipoc, E., Sun, L., Peterson, K., and Grasselli, G.</i>	218
Controlled lab-scale evaluation of the secondary permeability represented in a 3D printed discrete fracture network (DFN) model <i>Baidoo, M.¹, Fillion, M.-H.¹, Hutchison, A.², and González, C.³</i>	220

Studying the effect of roughness-based filtering on structural geology analysis and JRC measurements from LiDAR mapping	222
<i>Niloufarsadat, S., Akram, D., and Aubertin, J.D.</i>	
Delineating numerical excavation damage zone depth limits using machine learning	224
<i>Golabchi, Y., Morgenroth, J., and Perras, M.A.</i>	
Verification of numerical models using seismic source mechanisms	226
<i>Meyer, S.G.¹ and Rigby, A.²</i>	
Representative Elementary Volume (REV) of a jointed rock mass for determination of the block size	227
<i>Mahdavi-rad, M., Shahbazi, A., and Saeidi, A.</i>	
Indication of in situ stress orientation by pressuremeter hold test – experiment and field tests	229
<i>Liu, L. and Chalaturnyk, R.</i>	
Impact of layering and fractures in Buckinghamshire shale on strain measurement using digital image correlation (DIC)	231
<i>Magsipoc, E., Haile, B.F., and Grasselli, G.</i>	
Investigating the thermal cracking process of granitic rocks using digital image correlation (DIC)	233
<i>Haile, B.F., Aboyanah, K.R., and Grasselli, G.</i>	
Entropy-based probabilistic characterization of rock shear strengths from triaxial tests and its application in rock slope risk	235
<i>Deng, J.¹, Li, S.J.², Jiang, Q.², and Chen, B.R.²</i>	
Reconstructing roughness of rock discontinuities by geostatistical procedure	237
<i>Belhaj, M.¹, Rivard, P.¹, and Moradian, O.²</i>	
Studying the strength and fracturing properties of rock-concrete interfaces under tensile loading at the microscale	239
<i>Shams, G.¹, Rivard, P.¹, and Moradian, O.^{2,3}</i>	
25 years of monitoring ground movements around underground excavations: 5 takeaways	240
<i>Hyett, A.</i>	
Excavation and pillar analysis with peak and residual properties in implicit and explicit rockmass models	242
<i>Fischer, C., Dressel, E., and Diederichs, M.S.</i>	
Innovations in direct shear testing under various boundary conditions	244
<i>Packulak, T.R.M., MacDonald, N.R., Diederichs, M.S., and Day, J.J.</i>	
Laboratory testing for the characterization of heterogeneous rockmasses	246
<i>Gagnon, É., Woodland, S.K., Packulak, T.R.M., Hegger, S., Clark, M., and Day, J.J.</i>	
Modelling sea stack and shoreline cliff failure modes in RS3	248
<i>Hyslop, A., Hoyle, W. and Day, J.J.</i>	
Challenges in calibration and verification of hydromechanical models for excavations in rock	249
<i>Markus, S.¹, Kennedy, M.¹, Vazaios, I.², and Diederichs, M.S.¹</i>	
Awards	251
Kingston and 1000 Islands Dinner Boat Cruise	253
Brockville Tunnel Tour and Banquet Dinner	255
Symposium Sponsors	257



Introductory Remarks

August 8, 2022

Good morning. I wish I could have been with you in Kingston today, but that's not to be. I would like to present a brief message to welcome you to this conference, which I hope you will find to be both enjoyable and informative.

Professor R.G.K. Morrison, sometimes known as the father of rock mechanics in Canada, published a paper on the rockburst situation in Ontario mines in 1942. Eighty years later, we can look back on how far we have come with the development of the subject of rock mechanics and many of you at this conference will have been or will be participants in this development.

The early years of rock mechanics were dominated by the application of elastic theory to the calculation of stresses induced by excavations in stress drop masses and the consequent propagation of failure induced by these stresses. It was not until the introduction of personal computers in the 1980s that individual engineers and geologists could explore and apply the more complex properties and behaviour of non-elastic and jointed rockmasses.

I'm sure that the four themes of your program over the next three days will provide ample opportunities for the exploration of many of the advances that have been made in both theoretical and hands-on practical applications during the past 30 years.

I wish you all the best in the presentations and discussions, at this meeting and in the times that you will spend together in the social events which have been set up or will be created by you.

Evert Hoek





Special Session

Recent Award Winners



ISRM Müller Lecture

From common to best practices in underground rock engineering

Kaiser, P.K.

Laurentian University, Sudbury, Ontario, Canada

GeoK Inc., Sudbury, Ontario, Canada

EXTENDED ABSTRACT

Common practices are not necessarily best practices when judged from an economic or workplace safety perspective. As in other engineering disciplines, it is necessary to systematically improve engineering design practices. This lecture addresses some deficiencies in common practice that may lead to flawed or ineffective rock engineering solutions. More than ever, as we go deeper in underground construction, are rock engineers challenged by a number of opportunities that exist for improvements.

In the past, common practices that worked well at shallow depth may need to be replaced as the rock mass behavior has changed and poses new hazards at depth. This lecture focuses specifically on opportunities resulting from better means to assess the vulnerability of excavations, to characterize the rock mass, for ground control, and rockburst damage mitigation. Theoretical considerations and field observations are used to justify the proposed changes and highlight practical implications and benefits. In the spirit of Prof. L. Muller, this lecture aims at pointing the way to future improvements in rock engineering, i.e. 'im Felsbau', and offers guidance on how to move from common to best practices.

Common practices are often not best practices when judged from an economic or workplace safety perspective, and common practices that worked well at shallow depth may need to be replaced because the rock mass behavior has changed and poses new hazards at depth. This lecture focused specifically on opportunities resulting from better means to assess the vulnerability of excavations, to characterize the rock mass, for ground control, and rockburst damage mitigation.

It is demonstrated that ample opportunities exist to derive benefits from moving from common to best practices. In summary, opportunities are identified in the following areas:

- Identification of engineering design parameters EDPs that characterize vulnerability and fragility;
- Rock mass characterization following a systematic process of moving from inferred to proven;
- Grouping of rock mass qualities into classes that reflect rock mass and excavation behavior modes;
- Methods to obtain rock mass strength envelopes for peak, post-peak and residual strength;
- Practices that respect the limitations of classification and characterization systems;
- Deformation-based support selection for ground control in highly stressed, brittle failing ground.
- Utilization of the self-stabilizing capacity of well-constrained broken rock;
- Quantification of support capacity consumption as a critical design criteria;
- Proactive maintenance based on support deformation monitoring to restore consumed support capacity;
- Consideration of the impact of pre-burst support deformation and bulking displacements from strainbursts;
- Replacement of energy-based by displacement-based support designs for burst-prone ground.



2 x ISRM Rocha Medal Winners

State-of-the-art, Finite-Discrete Element Method (FDEM) modelling in rock mechanics

Tatone, B. and Lisjak, A.

Geomechanica Inc., Toronto, Ontario, Canada

EXTENDED ABSTRACT

Over the past 15 years, investigations of rock deformation and fracturing processes using the finite-discrete element method (FDEM) have been proposed by several researchers. The method offers the distinctive advantage of being able to simulate fracturing and fragmentation of discontinuous rock masses without any a priori assumption regarding failure mode and path, thus allowing complex, non-linear processes to be numerically captured. In this talk, advances in the development and application of FDEM will be discussed. As outlined in the abstract, the presentation consists of four main parts. In the first and second parts, two cases studies are presented where FDEM is used to investigate (i) the excavation damaged zone (EDZ) formation process in Opalinus Clay (OPA) and (ii) the shear behaviour of rock discontinuities. The case studies are part of the doctoral research of the presenters at the University of Toronto, which were awarded the 2015 and 2017 Rocha Medals of the ISRM, respectively. In the third part, the more recent application of high-performance computing techniques, namely GPU acceleration, to improve the computational performance of FDEM simulation is discussed together with recent development targeting coupled, thermo-hydro-mechanical (THM) problems and 3D simulations. In the final part, some geomechanical applications of the latest generation of the FDEM implementation by several international research groups are explored.

ASSESSMENT OF EXCAVATION DAMAGED ZONE (EDZ) IN AN ANISOTROPIC CLAY SHALE

OPA is a shale formation currently being assessed as possible host rock formations for the deep geological disposal of radioactive waste in Switzerland. One main concern is that the favourable long-term isolation properties of the intact rock mass could be negatively affected by the formation of an EDZ around the underground openings. Confidence in the performance and safety assessment calculations would increase significantly if a sound understanding of the EDZ generation process and behaviour could be obtained. The ultimate goal of this study was to develop and validate a new robust numerical approach that could capture the deformational and fracturing behaviour of shales and that could, therefore, aid the design and safety assessment of deep geological repositories (DGRs). Prior to this study, most numerical models of OPA had been based on continuum mechanics principles using classic shear failure theory for elasto-plastic materials. However, a number of experimental observations demonstrate that shales may fail in a brittle manner under low-confinement conditions (e.g., near field of excavations). The selected modelling platform was therefore the FDEM software named Y-Geo (Mahabadi et al., 2012) as it allows rock fracturing and fragmentation to be explicitly simulated. New modelling procedures and algorithms were developed to account for stiffness and strength anisotropy of the bedded OPA by: (i) smearing the transversely isotropic elastic deformation of the material in the continuum, finite element formulation and (ii) developing a directional cohesive fracture formulation (Lisjak et al., 2014). The numerical model was validated

by reproducing the results of laboratory tests on bedded OPA, including stress-strain curves, strength variation with loading angle, and fracture patterns. It was observed that for tunnels excavated parallel to the bedding strike, failure initiates with shearing along bedding planes and later evolves with extensional fracturing in the direction perpendicular to the bedding. Spalling and buckling failures were also simulated and shown to be promoted by bedding plane delamination. In 2012, the excavation of a test tunnel at the Mont Terri Underground Rock Laboratory (URL) as part of a long-term research project (“FE experiment”) offered the opportunity to analyze for the first time the behaviour of OPA under geometric and structural-geological conditions similar to those of planned repository tunnels. The deformational behaviour measured in the field was used to calibrate FDEM models with the goal of obtaining a quantitative model of the EDZ formation process in OPA (Lisjak et al., 2015). An overall good fit of the experimental data was obtained for the FDEM model, which reproduced well the anisotropic response of the rock mass. The simulated evolution of fracture pattern (Figure 1) and displacement field around the tunnel showed the formation of (i) a square-shaped inner shell oriented along the bedding planes and dominated by rock mass fragmentation and bulking and (ii) an outer shell characterized by sensibly smaller deformation magnitudes with extensional fracturing inhibited by an increase of confining stress.

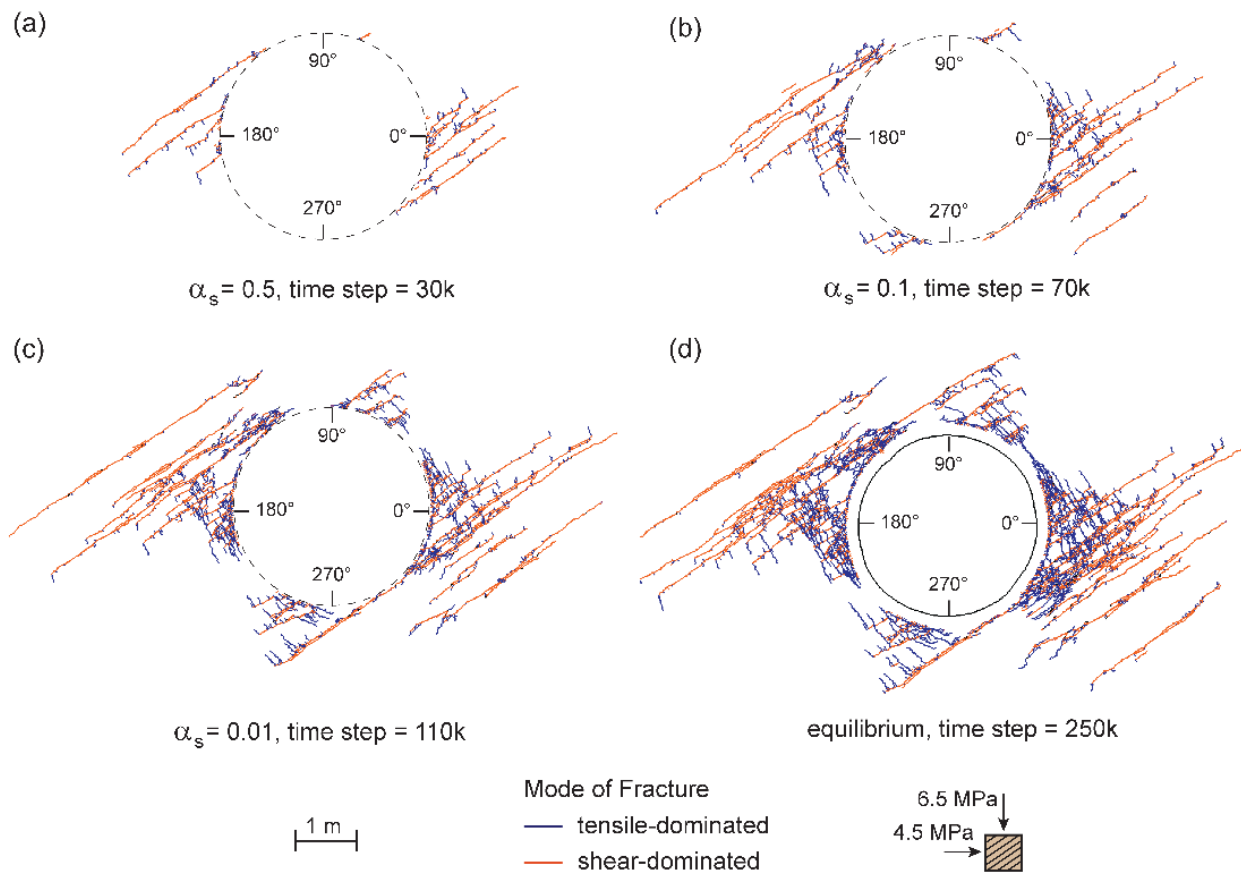


Figure 1: Evolution of fracture growth around the FE tunnel at increasing simulation times.

INVESTIGATION OF THE SHEAR BEHAVIOUR OF ROCK DISCONTINUITIES

Rock mass discontinuities represent planes of relative weakness and enhanced hydraulic conductivity and, thus, have a substantial influence on the hydro-mechanical behaviour of rock masses. While the shearing of rock mass discontinuities has been extensively studied, there remained uncertainty surrounding the mechanisms by which surface asperities deform and degrade during shear and how this degradation influences the aperture distribution. The overall goal of this study was to combine two recent technologies, micro-X-ray Computed Tomography (μ CT) and hybrid continuum/discontinuum modelling techniques, to develop an improved understanding, and confirm empirical assumptions, regarding the evolution of asperity degradation and fracture geometry due

to shearing. Experimentally, a methodology including the design, fabrication, and shear testing of discontinuity replicas, together with μ CT imaging, image processing, and image analysis procedures was developed and used to quantitatively characterize the morphology of specimens (Tatone and Grasselli, 2015a). Numerically, a comprehensive model calibration and direct shear test simulation procedure using FDEM, as implemented in the Y-Geo code, was developed to understand the stress state and failure mechanisms responsible for the damage patterns observed in μ CT images (Tatone and Grasselli, 2015b). A key aspect of the study was the use of the novel experimental and numerical methods in concert to cross-validate the results of each. Experimental direct shear results and μ CT imaging were used to verify the emergent strength and failure patterns obtained in FDEM simulations of direct shear tests. And at the same time, the results of the FDEM simulations provided information regarding the mechanics of the failure processes responsible for the fracture morphology (Figure 2).

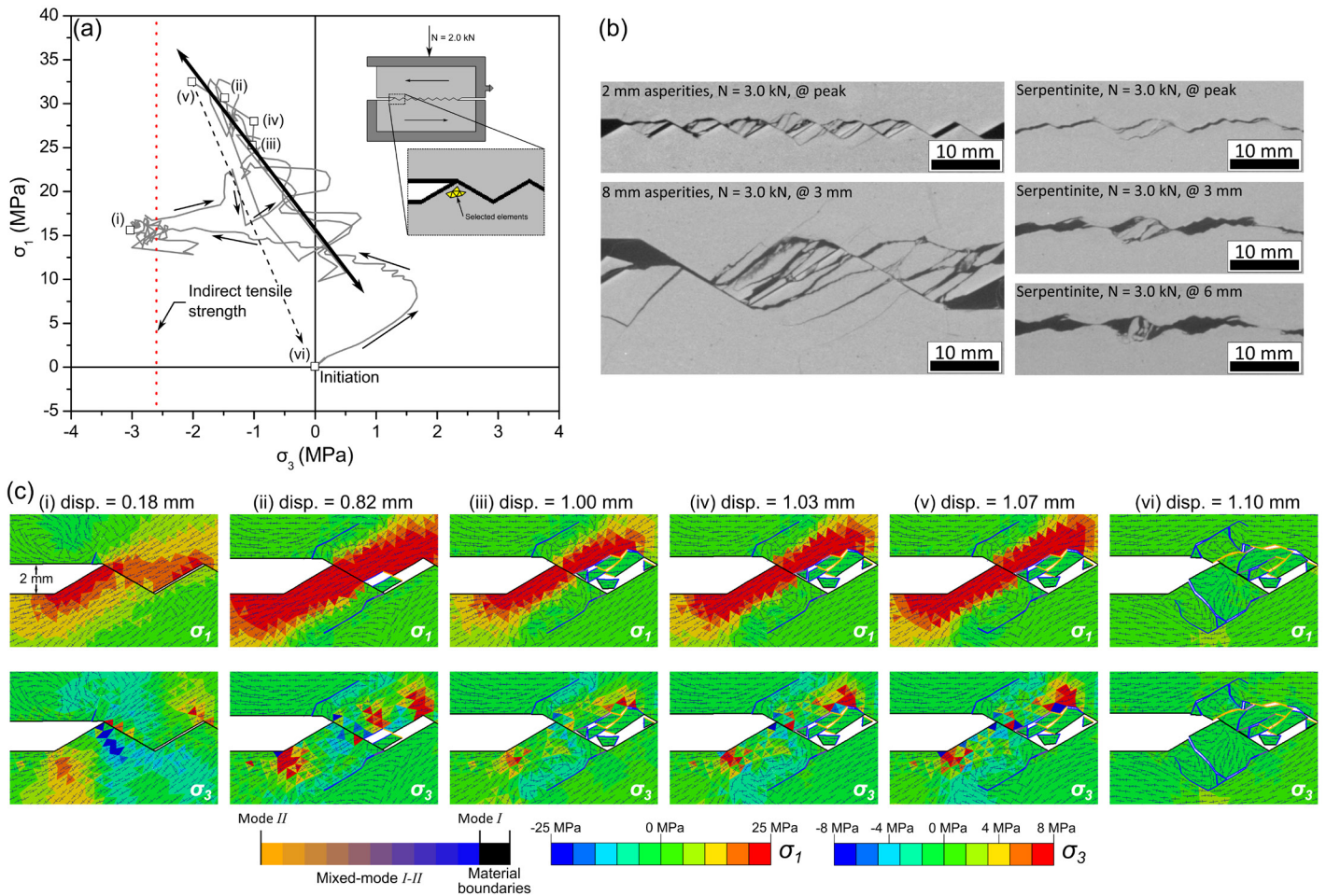


Figure 2: Example of (a) Evolution of asperity stress state; (b) Damage patterns observed via μ CT imaging in 'sawtooth' and natural discontinuity geometries; and (c) simulated stress distribution and damage evolution.

The μ CT imagery obtained in this study provided the first glimpses of asperity damage within the interior of a direct shear specimen without separating the joint walls or destroying the sample via serial sectioning. The modelling approach, which marked the first comprehensive attempt at simulating discontinuity shearing using an FDEM code, was shown to reasonably reproduce the experimentally observed progressive degradation of asperities in direct shear tests in terms of the shear resistance and dilation as a function of shear displacement. Overall, this study improved understanding of the link between the asperity damage and the corresponding stress conditions. In particular, the relationship between the observed asperity fracture pattern and the magnitude and orientation of the principal stresses was established. Tensile failure was identified as the dominant failure mechanism with shear failures playing a secondary role and, based on these findings, a new generalized conceptual model for the

breakdown of asperities was proposed. This model clarifies the mechanisms of progressive asperity degradation which were ambiguous prior to the current study. The improved understanding gained through this study will be of value to several areas of rock engineering and hydrogeology. Namely, those where discontinuity shear can affect stability (e.g., slopes and underground openings) or rock mass permeability (e.g., deep geologic repositories).

APPLICATION OF HIGH-PERFORMANCE COMPUTING TECHNIQUES

A major limitation of the FDEM method is its computational cost, as simulations often involve hundreds of thousands or millions of degrees of freedom (particularly in 3D), thus effectively reducing the spatio-temporal scale of the problems that can be practically simulated. This limitation has motivated R&D efforts at Geomechanica to reduce computational times to run spatially larger, higher-resolution, and multi-physics simulations in less time. To do so, the first ever parallel implementation of a complete FDEM code in 2D and 3D enhanced with coupled fluid flow capabilities was realized (Lisjak et al., 2018). The implementation formed the proprietary FDEM software package Irazu and took advantage of the computing parallelism offered by graphics processing units (GPUs). A heterogeneous co-processing approach was adopted whereby the main control loop of FDEM is executed serially on the host (CPU), while all the compute-intensive tasks are run using a large amount of compute cores on a GPU device. A benchmarking study indicated speedups of up to 400x compared to sequential CPU execution, depending on the total number of degrees of freedom of the simulation. Over the past few years, continuous software development has been focusing on additional modelling logic, including thermo-hydro-mechanical capabilities, proppant transport, rockbolt (structural) elements, and gas dynamics.

OVERVIEW OF GEOMECHANICAL APPLICATIONS OF FDEM

Last part of the talk will showcase the application of FDEM to a variety of geomechanical problems across different fields. These applications include EDZ in hard, brittle rock masses and strain bursting phenomena, shotcrete lining design, stability of deep geothermal boreholes, longwall coal mining, rock pillar behaviour, rock mass pre-conditioning for in situ leaching of copper, landslide runout simulation, caving phenomena, fracture nucleation and growth in heterogeneous rocks, thermally-induced borehole fracturing, hydraulic fracture propagation and interaction with existing discontinuities, and behaviour of skeletal material in biological systems.

ACKNOWLEDGEMENTS

The authors wish to acknowledge the financial support of NSERC, OCE, NAGRA, and the Mont Terri Consortium. A special thanks is also given to Omid Mahabadi, Liqiang He, Giovanni Grasselli, and several other co-collaborators for their important contributions over the last 15 years.

REFERENCES

- Mahabadi, O. K. M., Lisjak, A., Grasselli, G., and Munjiza, A. 2012. Y-Geo: a new combined finite-discrete element numerical code for geomechanical applications. *International Journal of Geomechanics* 12(6), 676–688.
- Lisjak, A., Garitte, B., Grasselli, G., Müller, H. R., and Vietor, T. 2015. The excavation of a circular tunnel in a bedded argillaceous rock (Opalinus Clay): Short-term rock mass response and FDEM numerical analysis. *Tunnelling and Underground Space Technology* 45, 227–248.
- Tatone, B. S. A. and Grasselli, G. 2015a. Characterization of the effect of normal load on the discontinuity morphology in direct shear specimens using X-ray micro-CT. *Acta Geotechnica* 10 (1), 31–54.
- Tatone, B. S. A. and Grasselli, G. 2015b. A calibration procedure for two-dimensional laboratory-scale hybrid finite–discrete element simulation. *International Journal of Rock Mechanics and Mining Sciences* 75, 56–72.
- Lisjak, A., Mahabadi, O. K. M., He, L., Tatone, B. S. A., Kaifosh, P., Haque, S. A., Grasselli, G., and Vietor, T. 2018. Acceleration of a 2D/3D finite-discrete element code for geomechanical simulations using General Purpose GPU computing. *Computers and Geotechnics* 100, 84–96.



CGS Colloquium Winner

Utilization of multi-scale modelling for geomechanical hazard management

Kalenchuk, K.

RockEng Inc., Kingston, Ontario, Canada

EXTENDED ABSTRACT

To develop strategic and tactical strategies to safely and economically manage geomechanical hazards in mines, it is necessary to establish an understanding of likely ground reaction mechanisms, and how ground reaction may vary spatially throughout a mining operation and temporally over the life of mine (LOM). Global mine-scale numerical stress modelling provides a means to forward predict susceptibility to geomechanical hazards and local-scale modelling provides focussed mechanistic analyses. These combined global and local efforts facilitate informed decision making for the development and implementation of risk mitigation measures.

NUMERICAL MODELS FOR GEOMECHANICAL HAZARD MANAGEMENT

The application of numerical models in geomechanical hazard management can be broadly grouped based on the modelling objective; Susceptibility vs. Mechanistic (Kalenchuk, 2021). Susceptibility modelling investigates the likelihood that a geomechanical system will be exposed to a particular ground reaction; global mine-scale stress modelling is often a Susceptibility modelling exercise. Mechanistic modelling aims improve the understanding of fundamental mechanics; this becomes more critical for local-scale engineering analyses. Multi-scale simulations, making use of both susceptibility and mechanistic analyses, are critical for effective geomechanical hazard management. Global mine modelling provides susceptibility forecasting for global and local-scale hazards. Local-scale analyses must be coupled with mine-scale modelling so that local mechanistic evaluations account for broader geological controls on boundary conditions and material competencies. With a holistic understanding of global geological controls on stress and material domains, a picture of mine-scale

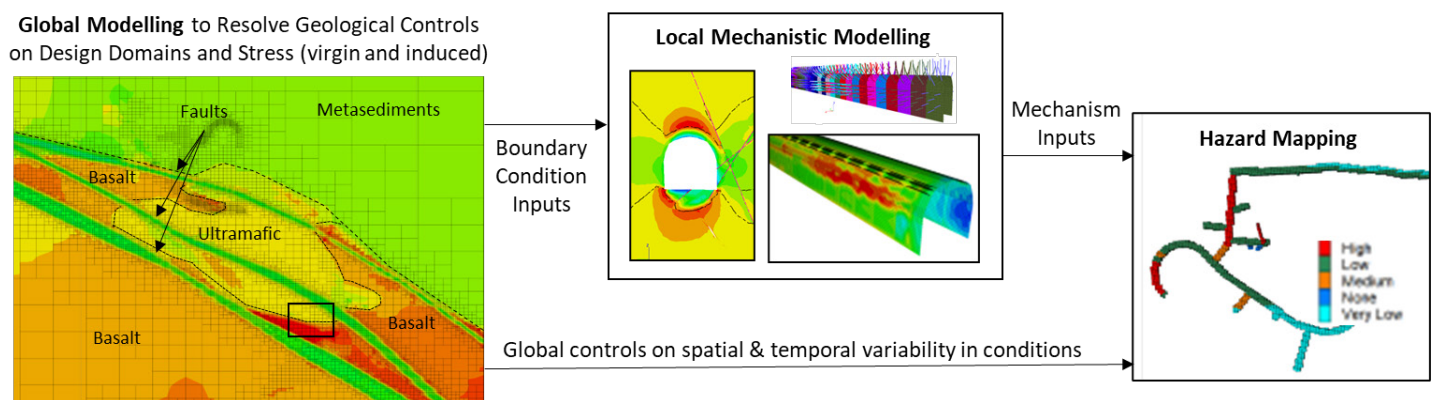


Figure 1: Coupled utilization of global mine-scale Susceptibility modelling and local Mechanistic modelling to identify and map geomechanical hazards (modified after Kalenchuk, 2022).

stress, strain and yield evolution over the LOM, and a local understanding of hazard mechanisms, a global interpretation of the spatial and temporal distribution of hazard intensity can be achieved (Figure 1).

IMPORTANCE OF CALIBRATION – WITH FOCUS BEYOND MATERIAL PROPERTIES

To make forward predictions of hazard susceptibility using global stress models with reasonable confidence, it is necessary to rigorously calibrate numerical stress models to the observed history of ground reaction. Any numerical simulation should have some degree of model calibration, with the exception of green-field studies (which must instead rely on thorough sensitivity testing). Model calibration traditionally focuses on material strength parameterization; however rigorous calibration efforts must also consider the initialization of boundary conditions and constitutive model.

The importance of calibrating stress initialization is often overlooked. Calibration of virgin stress state, which is often complex, is a critical component of global stress modelling. And, local-scale modelling efforts should rely on global models to establish boundary conditions in areas of interest. Strain-based stress initialization is fundamental to global mine-scale stress modelling, particularly in high stress environments where geological controls can impose significant stress gradients and tensor rotations across geotechnical domains and structures. Strain-based stress initialization relies heavily on a reliable geological model to define the approximate boundaries between lithological units, or a solid-model representing three-dimensional geotechnical domains. In the absence of at least one or the other it is nearly impossible to estimate how in situ stresses may vary spatially.

Further to the calibration of in situ stress; calibrating the applied constitutive model is also important. Multiple constitutive models should be trialled during the calibration process to explore numerical output sensitivities prior to selecting best-fit constitutive behaviour for forward looking hazard prediction studies.

SUMMARY

Numerical modelling analyses provide means to quantify geomechanical hazard susceptibility and mechanisms. This requires multi-scale Susceptivity and Mechanistic analyses using rigorously calibrated numerical models. Susceptibility models incorporate mine-scale stress modelling exercises to characterize ground reaction and mine-wide ground behaviour. Detailed Mechanistic modelling at the excavation-scale improves the understanding of hazard triggers and fundamental mechanics of failure processes by identifying failure mechanisms. Mechanistic modelling, combined with mine-scale susceptibility analyses allow for anticipation of hazardous conditions and controlling parameters; which are vital inputs for strategic mine planning and tactical engineering.

ACKNOWLEDGEMENTS

This talk expands on my 2019 CGS Colloquium presented at the 72nd Canadian Geotechnical Conference. Thank you Canadian Geotechnical Society and Canadian Foundation for Geotechnique for providing the opportunity to Present the Colloquium and subsequent Cross Canada Colloquium lecture series.

REFERENCES

- Kalenchuk K. 2021. 2019 Canadian Geotechnical Colloquium: Mitigating a fatal flaw in modern geomechanics: understanding uncertainty, applying model calibration and defying the hubris in numerical modelling. Canadian Geotechnical Journal, 59(3), <https://doi.org/10.1139/cgj-2020-0569>.
- Kalenchuk, K. 2022. Predicting Mine-Wide Seismogenic Risk with Confidence Using Calibrated Numerical Models. In Proceedings Rockbursts and Seismicity in Mines, Tucson, USA.



CGS Cross-Canada Lecture Winner¹

The Influence of Release Mechanisms in Rock Slope Engineering: A Three-Dimensional Perspective

Stead, D.¹ and Donati, D.²

¹*Earth Sciences, Simon Fraser University, Vancouver, British Columbia, Canada*

²*University of Bologna, Bologna, Italy*

EXTENDED ABSTRACT

The combined use of state-of-the-art remote sensing (characterization and monitoring) and numerical modelling has over the last two decades provided strong evidence on the true three-dimensional nature of landslides, rendering previous simplistic assumptions on the nature of release surfaces increasingly problematic. The role of slope kinematics and its evolution over time is a critical factor in understanding rock slope failure mechanisms. The importance of considering rock slope failures in terms of the characteristics of all release surfaces and the number/geometry of the blocks involved in failure is clear.

INTRODUCTION

Early research on rock slopes provided highly practical stereographic and limit equilibrium approaches for planar, toppling and wedge analysis. These methods involved several important assumptions to apply methods of statics and to a certain degree these assumptions have led to less emphasis being placed on release mechanisms than sliding processes. The authors will provide herein an overview of the characteristics and importance of release surfaces in rock slope stability.

LATERAL AND REAR RELEASE SURFACES

A wide variety of lateral and rear release geometries exist dependent on slope scale, tectonics, and landform evolution. Lateral release surfaces are commonly sub-vertical in dip but may strike in a direction oblique to the strike of the slope face, with important implications for both the three-dimensionality of the failure mechanisms and for support design. Simple planiform lateral and rear release surfaces may be more commonly observed in small bench scale and rockfall scale failures. As the scale of the failure increases to large pit slope failures and landslides then release surfaces tend to be more complex and may involve multiple structures with the global release surface branching across different structural and geotechnical domains. Release surfaces may be stepped in plan or encompass zones of localised (often secondary) wedge/toppling instability. Variations in the rock mass quality may see more retrogression in weaker, more weathered rock masses. In such cases it is important to consider different generations of release surfaces with primary release surfaces for the main failure and secondary release surfaces corresponding to post-main failure instability. The existence of multiple rear and lateral release surfaces is evident in long-term failures which progress both into and along a slope (e.g., Downie Slide, Hope Slide, and La Clapiere Slide, Figure 1a-c). The engineer should also consider that in a retrogressing failure the main failure process may involve multiple “internal” lateral and rear release surfaces with sometimes evidence

only of the final release surface at the boundaries of the landslide (e.g., Hope Slide). In practice, lateral kinematic release may be provided by topography e.g., gully incision on both sides of a landslide or on one side. Where two gullies exist or where there is a change in slope strike such as at a promontory then lateral release structures may not be required. Where a gully exists on one side only, a structure is required on the other side. Where no gullies are present then structural surfaces for lateral release, or a combination of structures and intact rock fracture may be required. (Brideau 2010). Progressive damage accumulation due to stress concentration (e.g., basal release surface within a toppling hinge zone, e.g., La Clapiere landslide), seismic damage (e.g., Madison Canyon landslide, Figure 1d), and excavation- or mining-induced damage processes (e.g., Frank Slide, Figure 1e) may also play a role in the development of persistent release surfaces.

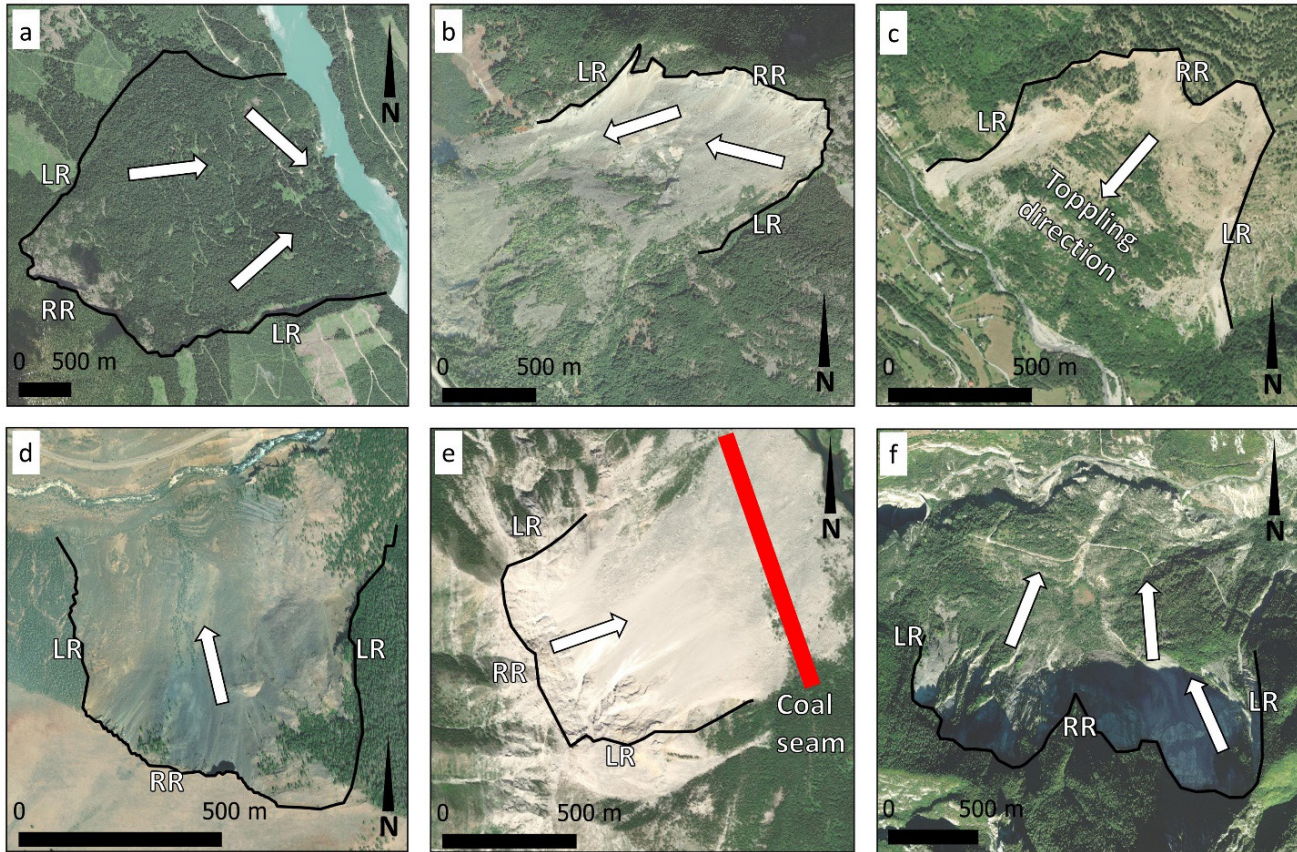


Figure 1: Major landslide lateral and rear release surfaces; a. Downie Slide, BC, b. Hope Slide BC, c. La Clapiere, France, d. Madison Canyon landslide, MT, USA, e. Frank Slide, AB, F. Vajont Slide, Italy. LR: lateral release. RR: rear release. SF: secondary failure. White arrow: inferred displacement direction (toppling direction for C). Black lines: landslide outline.

Traditionally rear and lateral releases surface have been considered two-dimensionally as sub vertical planes parallel or orthogonal to the slope respectively and offering limited shear resistance to failure. Remote sensing has shown that the morphology of release surfaces may be complex with significant release surface roughness necessitating dilation, and even intact rock fracture for a failure block to move. The roughness of the lateral release surface and the failure block geometry may lead to complex translational and rotational block movements. It is thus important to consider not only the dip and dip direction of release surfaces but also the plunge of the intersection between the sliding or basal release surface and the lateral release surfaces. The plunges and trends of all major structure intersections should be systematically compared to three-dimensional monitoring data from remote sensing, (e.g., InSAR, LiDAR) and survey methods (dGNSS/GeoCubeTM).

Understanding the importance of tectonic control on release surfaces is paramount. It is recommended that tectonic structures be treated in a 1st, 2nd, 3rd, 4th order manner as is done in groundwater studies. 1st order faults or shears spanning the entire slope clearly have the potential to form release surface for major failures.

Corresponding minor 4th order lower persistence joint sets are more liable to provide release for rockfall/bench scale instabilities. Where major fault zones exist along a valley the possibility of tectonic damage at the toe and associated fault structures/splays forming release surfaces should be considered. The concept of connectivity in rock slopes has received limited attention to date yet the lower the connectivity in a fracture network the more likely that intact fracture of so-called “rock bridges” will be required for kinematic release of a landslide. The observed progressive failure of post-glacial slopes and deep-seated gravitational displacements may involve ongoing fracture of the rock mass until lateral or rear release is through-going and the slope is brought to a state of failure. The importance of lateral and rear release surface morphology has not been investigated in detail, either through field observations or numerical modelling. It is observed that these surfaces may range from smooth to extremely rough both in section and plan and this may result in landslide dilatational behaviour. Landslide blocks may be released along smooth surfaces with limited dilation, whereas, on very rough, stepped surfaces or non-persistent surfaces, a significant degree of dilation may occur which may lead to a combination of sliding and rotational movements and/or oblique slip on a basal release surface. Brittle stress-dependent fracture occurs along rough non-persistent lateral/rear release surfaces in addition to gradual reduction of the surface shear strength.

THE SLIDING OR BASAL RELEASE SURFACE

Simple translation along a planar or curvilinear structure is normally assumed in most failure mechanisms. Often the true three-dimensional nature of landslide failure displacement mechanisms is dictated by a more complex failure surface morphology. At the bench scale the failure surface may be approximated as a planar surface but at the larger landslide scale, variations in dip and dip direction may occur both along dip and strike due to metamorphic foliations and the influence of faults, shears and folding (e.g., Downie Slide). In such cases a landslide may move as multiple blocks with different magnitudes and in different directions. Landslides in such cases may be divided into domains. On a smaller scale the roughness of the basal release surface may be influenced by sedimentary structures or tectonic features such as interference fold patterns, fault steps and slickensides. Inherited brittle fractures associated with fracture propagation may be mapped using fractography and may influence rockfall and localised failure in steep rock slopes.

THE IMPORTANCE OF SLOPE SCALE, BLOCK NUMBER, BLOCK SIZE AND SHAPE

It is important to consider the changes in release surface with respect to landform evolution, slope damage and the importance of kinematic confinement both in-slope and along slope. Toe release due to undercutting (glaciation/river/coastal erosion) may remove keyblocks mobilising new release surfaces bounding previously unremovable blocks. Failure of a block within a slope may result in a loss of confinement and lateral progression of instability. Multiple potential internal lateral release surfaces may exist within a slope and be mobilised progressively over time. The possibility of the kinematics changing with block removal should always be considered (i.e., one block failing by out of slope translation allowing an adjacent block to fail along slope by toppling/rotation). Similarly, the role of pre-cursor rockfall/local failures may require release surfaces at multiple scales over time. Small scale release surfaces and block failures may provide the kinematic conditions (removal of toe and/or lateral confinement) for larger scale failures that mobilise larger slope-scale release surfaces. Failure zones may grow in area and coalesce both retrogressively into the slope and along slope in what is an inherently three-dimensional process. Failure of a surface layer of a steep rock slope may occur within a stress-relief loosened damage skin that migrates into the slope over time through continuing rockfall at multiple scales. Such a migration of the damage skin may lead to larger scale landslides where the necessary large scale release surfaces are present. In 2D simple failure mechanism are assumed to involve one block (planar/wedge), two-three blocks (active passive blocks with a Prandtl deformation zone, e.g., Vajont Slide, Figure 1e). When a slope is considered in three dimensions it is common to see multiple blocks along slope in addition to in-slope blocks. The blocks interact along internal lateral and rear release surfaces often with varying dip/dip direction of the basal sliding surface. The shape of

the blocks is critical in three-dimensional stability and requires a 3D-distinct element keyblock approach. The more faces and complex the blocks shape the less likely it is to slide without yielding, brittle or block removal. Constraining 3D rock slope modelling using combined remote sensing (characterisation-monitoring) and boreholes is essential.

IMPORTANCE OF GEOMORPHIC PROCESSES

The interaction between slope stability and geomorphic processes such as glacial retreat, river and coastal erosion is often controversial, viz., is it the removal of the support of the ice or the changing kinematics that is important. Notwithstanding, the observed slope toe that follows glacier retreat is both damaged by glacial processes and steeper due to glacier erosion; this can facilitate either daylighting of incipient basal release/failure surfaces, rock mass failure, or both. In foliated metamorphic rocks of low rock mass strength failure may occur concurrent with glacier retreat with the failure developing laterally and in-slope almost instantaneously. In stronger, brittle rocks the undercut toe may fail long after the glacier has disappeared sometimes in a violent, energetic manner. It is important to also consider the effect of the sea eroding weak rock/faulted rock masses to form lateral or rear release to major coastal landslide blocks or rivers/gullies incising into mountain slope to form lateral release. Geomorphic processes include both the removal of toe/lateral keyblocks and the effects of stress-relief, and weathering.

FUTURE CHALLENGES IN UNDERSTANDING RELEASE MECHANISMS

The role of groundwater pressures on release surfaces in three-dimensional rock slope/landslides models has been the subject of limited research. The water pressures along the base of landslide blocks have been considered in 3D distinct element models and similarly the influence of rear release (tension crack) water pressures has received considerable emphasis in rock slope stability. The role of water pressures on lateral release surfaces however requires further investigation. It is known that the same structures that may function as lateral release of landslides also can result in compartmentalisation of groundwater pressures. It is thus highly likely that different blocks within landslides may be influenced to varying degrees by groundwater. Similarly, the role of fracturing has been suggested to result in amplification of earthquake waves and releases surfaces both internal and bounding may interact with seismicity in a complex manner. The time dependency of displacements in slopes and their relationship to lateral release surfaces (block shape) is an area for future research. Remote sensing should be used to characterise lineaments related to release surfaces and the three-dimensional plunge/trend of displacement vectors over time observed both in the field and numerically compared with the plunge/trend of release structures. Emphasis should be given to constraining and differentiating time dependent movements related to release surfaces and to the rock mass. Further research is required to characterise lateral, rear and sliding surfaces in detail using remote sensing, geophysics, borehole methods and numerical modelling. The mechanical properties assumed for numerical modelling of large-scale release surfaces also requires further investigation and constraint through combined remote sensing and numerical modelling of rock slopes and landslides at varying engineering scales.

ACKNOWLEDGEMENTS

The authors wish to acknowledge funding from an NSERC Discovery grant to the first author.

REFERENCES

Brideau, M-A. 2010. Three-dimensional kinematic controls on rock slope stability conditions, Ph.D. Thesis, Simon Fraser University.



CGS Franklin Award Winner

Hydraulic fracture complexity in shale rock

Grasselli, G.

University of Toronto, Toronto, Ontario, Canada

EXTENDED ABSTRACT

The significant surge in hydrocarbon production from unconventional resources in the past decades is largely due to the technological advances in horizontal drilling and hydraulic fracturing (i.e., fracking), which made it possible to extract hydrocarbon from low-permeability (tight) reservoirs formerly inaccessible or uneconomical to exploit, such as the Triassic Montney formation sitting on the Alberta-British Columbia boundary, northwest of Edmonton, which is now considered one of North America's premier natural shale gas resource plays. During the process of hydraulic fracture stimulation, pre-existing fractures and other zones of weakness in the rock may be activated and generate brittle failures, with potentially associated seismicity, through what is generally thought to be a combination of pore-pressure and stress perturbations (e.g., March 4, 2019, Mw = 3.4 induced earthquake in Red Deer, AB, most likely related to Vesta Energy's operations). In the Montney, hydraulic fracturing techniques have proven to significantly enhance production and well performance, and have become a vital enabling component of industry practice to continue the economic exploitation of shale gas. Despite these technological advancements, hydraulic fracturing is difficult to design, and many wells still underperform. At the planning and operational stages one of the primary limitations and source of uncertainty is related to the ability to accurately understand the fracturing processes, including the complex interaction between fluid-pressure-driven fractures and rock mass micro-structures (i.e., pre-existing discontinuities, bedding planes). These processes are ultimately responsible for creating the network of interconnected fractures used to channel and extract the targeted hydrocarbon resource.

Testing and analyzing rock under controlled laboratory condition, mimicking those in situ, is a powerful approach for studying the complex failure processes that are associated with hydraulic fracturing in the field. A Montney shale cube, obtained from a full-diameter shale core, was hydraulically fractured in the lab under stress conditions similar to those experienced by the rock at the reservoir depth (Figure 1) (Abdelaziz et al, 2019).

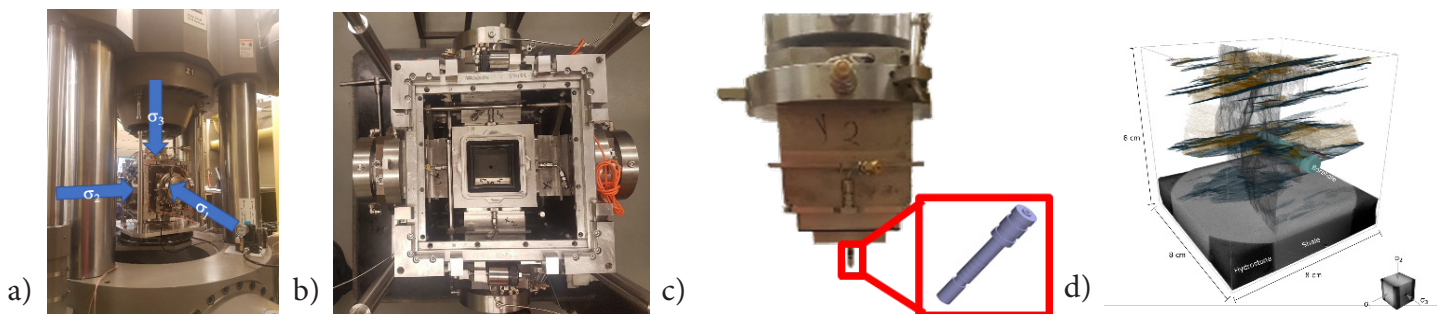


Figure 1: a) polyaxial testing system. b) polyaxial cell; c) minipacker system used to inject hydraulic fracturing fluids into the sample (Abdelaziz et al. 2019); d) fracture network imaged from the tested sample (Li et al, 2021).

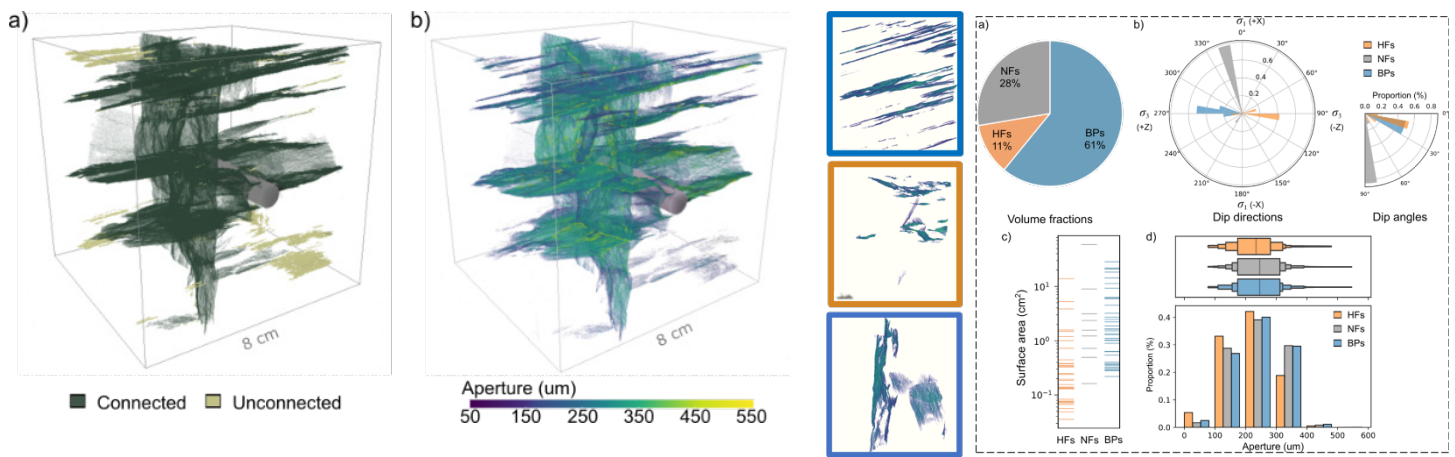


Figure 2: The complex fracture network obtained during the hydraulic fracturing test was quantitatively analyzed. The fracture connectivity (a) and the fracture aperture (b) maps visually highlight the complexity of the fracture geometries. (c) Quantitative analysis of the tested sample shows that almost 90% of activated fractures were associated to pre-existing of discontinuities (Li et al, 2023).

The newly created fracture network, visualized at a high spatial resolution utilizing the serial-section reconstruction method (Li et al, 2021), was complex and strongly influenced by the presence of pre-existing natural fractures and bedding planes. The injected fluid generated a few new hydraulic fractures dipping 40–60° to the horizontal injection hole, but mainly activated the crosscut bedding planes, dipping 17° to horizontal, creating a large volume of interconnected fluid paths, very different with respect to the expected planar fracture. Given the testing conditions, this fracture network pattern can be expected to be a reliable proxy for the fracturing process occurring near the wellbore in similar shale formations.

SUMMARY

This experimental work highlights the fundamental role played by parting of bedding planes during hydraulic fracturing and helps to explain the physical process underneath the creation of complex interconnected fracture network in shale formations.

ACKNOWLEDGEMENTS

The authors wish to acknowledge the scientific contributions made by Mei Li, Earl Magsipoc, Aly Abdelaziz, Johnson Ha, Karl Peterson. This work was supported by the NSERC DG 341275, NSERC CRDPJ 543894-19, and NSERC/Energi Simulation Industrial Research Chair program.

REFERENCES

- Abdelaziz, A., Ha, J., Abul Khair, H., Adams, M., Tan, C. P., Musa, I. H., Grasselli, G. 2019. Unconventional Shale Hydraulic Fracturing Under True Triaxial Laboratory Conditions, the Value of Understanding Your Reservoir (p. 16). Presented at the SPE ATCE 2019.
- Li, M., Magsipoc, E., Abdelaziz, A., Ha, J., Peterson, K., Grasselli, G. 2021. Mapping fracture complexity of fractured shale in laboratory: three-dimensional reconstruction from serial-section images. *Rock Mechanics and Rock Engineering*, 1–12.
- Li, M., Magsipoc, E., Sun, L., Peterson, K., Grasselli, G. 2023. High-resolution Mapping and Characterization of Shale Fractures Hydraulically Induced in the Laboratory. Presented at the RockEng22 Symposium.



CARMA Prof. Doug Stead PhD Thesis Award

Characterization of rock salt response to blasting using terrestrial laser scanner technology

Aubertin, J.D.

École de Technologie Supérieure, Montréal, Québec, Canada

EXTENDED ABSTRACT

Blasting rock salt differs significantly from conventional hard rock methods due to the unique geomechanical properties of rock salt. Unlike hard rock, rock salt has low mechanical strength, low density, minimal porosity, and moderate stiffness, which affect its behavior during blasting. Traditional blast designs, developed for hard rock, are often ineffective in salt mining. To adapt, engineers use low-velocity explosives to reduce energy loss and create large mechanical cuts to enhance free surfaces. These techniques have evolved through decades of field trials, yet the underlying mechanisms remain poorly understood. Site-specific variations further complicate blast design, leaving engineers with limited technical guidance. The article addresses fundamental aspects of blast design in rock salt mines and describe a unified blastability indexing method to assess site-specific blasting needs and rock mass response, aiming to improve design accuracy and operational efficiency in underground salt mining. A new cratering mechanism prevalent in low porosity soft rocks is introduced to rationalize the distinctive nature of blasting in rock salt and potash bearing minerals.

EXPERIMENTAL METHODS

Experimental field work consisted of an adaptation to Single Hole Blast (SHB) testing methodology (Rustan 1995, Wimmer 2007, Wimmer et al. 2008, Ouchterlony and Moser 2012). SHB testing consists in blasting individual holes with two degrees of freedom (i.e. two free surfaces) to investigate blastability conditions and quantify relevant trends from varying the burden dimension. SHB testing was used in the present research to capture and investigate the breakout shape of craters under realistic operational conditions. The detailed procedure is outlined in Aubertin et al. (2021a, 2021b).

Figure 1 presents SHB (Single-Hole Blasting) craters surveyed at three underground rock salt mines, each with distinct geological and geomechanical characteristics shaped by their depositional history. Despite these differences, the craters consistently show an elliptical breakout profile. The crater geometry was analyzed by measuring cross-sections perpendicular to the blasthole axis. Figure 2(a) illustrates the variation of burden (B) and breakout angle (α) along the blasthole, while Figure 2(b) plots breakout profiles and crater areas against burden. Incremental measurements along the blasthole enhance data resolution, allowing for a more detailed understanding of crater formation and blast behavior in rock salt environments.

It can be shown that the relationship for the specific charge to burden can be represented by an expending Taylor series of the form $\sum_1^k m_i B^{n_i}$ where k is the number of components considered in the series (Langefors and Kihlstrom 1963). Following this rationale, a generic formulation of the crater extent Y (m) is proposed by

considering one primary component of the series expansion:

$$Y = \psi(B) \cdot b^{\epsilon^*} \quad (1)$$

where ψ and ϵ^* are model parameters; b is the burden axis, and B is the burden. The special case where $\epsilon^*=1$ defines a triangular crater shape. Values of ϵ^* below 1 are elliptical like craters as illustrated in Figure 1, while $\epsilon^*>1$ presents a convex shape (e.g. Wimmer 2007).

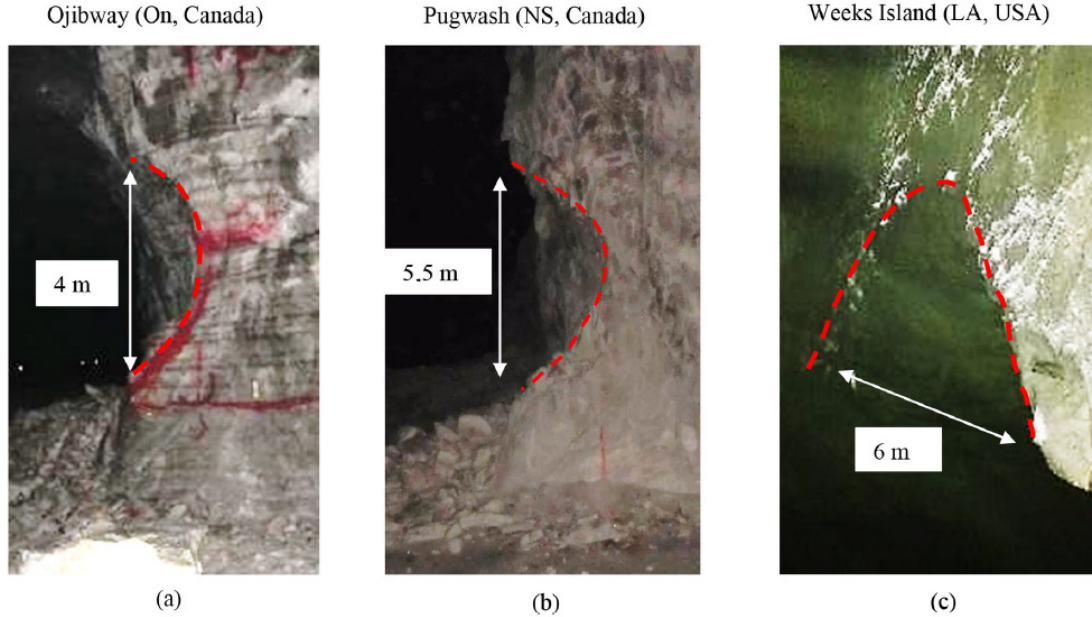


Figure 1: Single hole blast (SHB) craters in three underground rock salt mines with distinct geological and geomechanical characteristics (taken from Aubertin et al. 2021a).

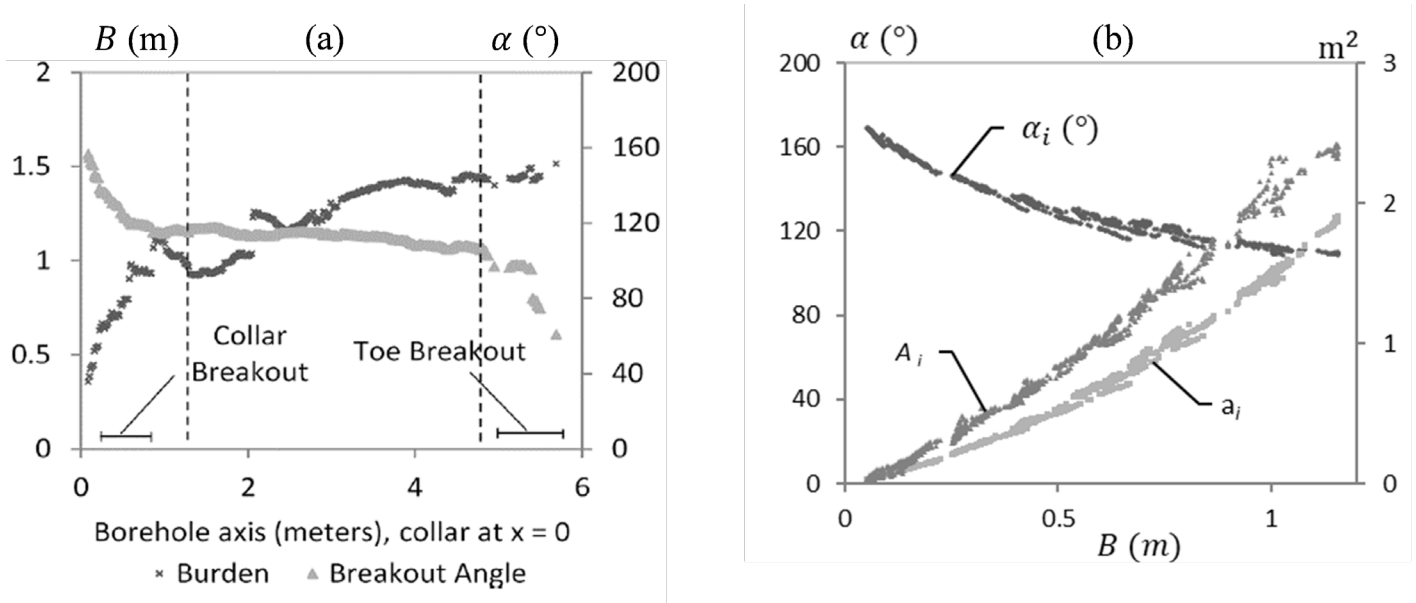


Figure 2: Sample results for SHB testing; (a) cross-sectional crater burden and breakout angle reported along the blasthole axis; (b) breakout angle α , crater area A and simplified crater area a with respect to burden (taken from Aubertin et al. 2021b).

SHOCKWAVE INTERACTION CRATERING

Rock blasting relies on two primary fracturing mechanisms: radial crack propagation from the borehole and tensile failure near a free surface, known as spalling. A third mechanism, cratering, may also occur when compressive waves from the blast interact constructively with reflected tensile waves at a free surface. This

interaction amplifies deviatoric (shear) stresses in localized zones near the blasthole, creating areas of high shear and low confinement. The resulting stress concentration follows an elliptical path influenced by the blast pulse seed length and the medium's impedance. Unlike traditional radial fractures, this mechanism produces a distinct breakout shape and is more prevalent in low-strength materials. It is typically triggered by longer, weaker pulse seeds from less efficient explosives. Understanding this third mechanism is crucial for optimizing blast designs, especially in softer rock types, as it highlights the complex wave interactions that contribute to effective burden removal.

FINDINGS, APPLICATIONS AND CONCLUSION

The research work summarized in this article aimed to define guiding principles for the design (and optimization) of blast patterns in rock salt considering the special geomechanical nature of salt. SHB tests were carried at three rock salt mines with distinctive features, to develop salt specific guidelines. The following contributions and findings arise from the presented research:

- A LiDAR assisted SHB testing protocol was developed to systematically quantify the response of rock salt during blasting event. The method is applicable to other rock types.
- The distinctive cratering profile of rock salt arises from the interaction between the emitted compressive wave and reflected tensile wave. The footprint of constructive wave interaction forms an elliptical zone, with a size that depends on blast wave attenuation, rock strength, burden dimension, and shape of the pressure pulse seed.
- The low mechanical strength of rock salt and the use of low VOD explosives with characteristically longer pressure pulse seeds tend to favor cratering by pressure wave interactions in salt and similar materials like potash bearing minerals.
- A cratering power law model of the form $Y = \psi b^{\epsilon^*}$ can capture characteristic breakout shape. In this equation, ϵ^* is a site specific constant while ψ is a burden dependent parameter. A specific charge to burden relationship can be derived from calibrated crater model.

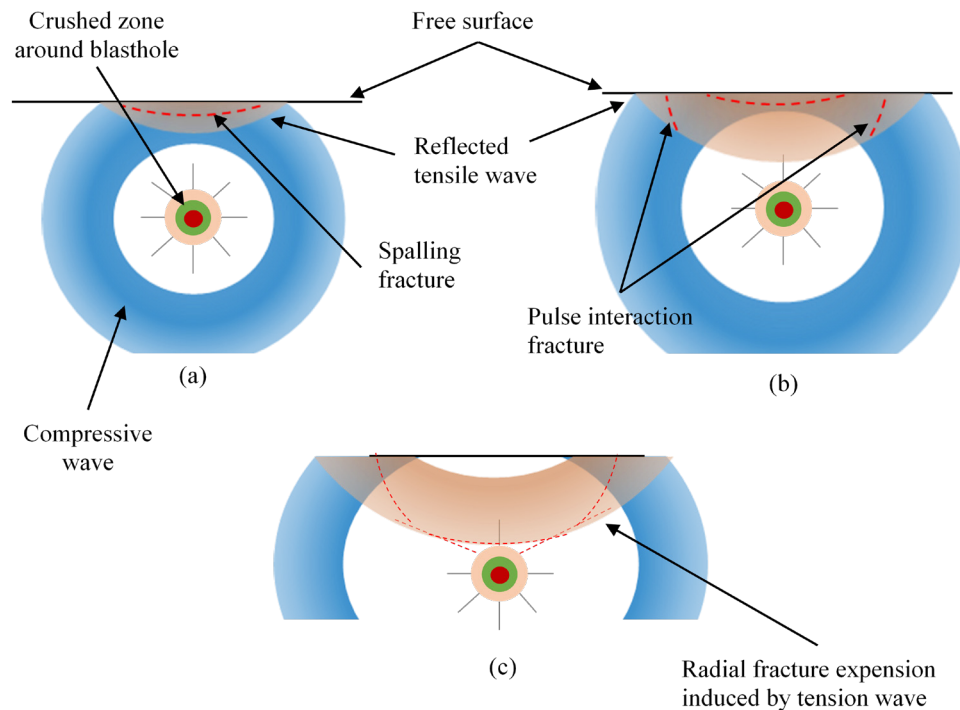


Figure 3: Conceptual representation of wave interaction cratering: the emitted compressive pressure wave is reflected at the free surface in tension; the two waves intersect and create zones of high deviatoric stresses that initiate failure (Aubertin 2021).

- Preferred explosives for rock salt are characterized by a less efficient chemical reaction generating low VOD (< 4500 m/s) and a long pressure pulse seed to maximise the footprint of constructive wave interaction. The predicted footprint of individual blastholes can be used to define a potential blast pattern layout by minimizing specific charge.

Two cratering mechanisms are traditionally considered in modern rock blasting techniques. Radial fracture extended by the reflected tensile wave, and spalling (failure in tension). A third cratering mechanism is prevalent in rock salt and similar material, arising from the interaction between emitted and reflected pressure waves. Table 1 summarizes key features of the three cratering mechanisms in their respective dominant form.

Table 1: Descriptive features of the three primary cratering mechanisms.

Key Factors	Radial fracture propagated in tension	Spalling	Pressure waves interaction
Geometry	Moderate to large burden	Near surface	Large ratio of pulse span to burden
Rock mass	Hard rock	Low - moderate T_o	Low porosity soft rocks
Explosive	High VOD	Any	Low VOD, long pressure seed pulse
Fracture origin	Blasthole	Free surface	High deviatoric stress zones
Failure type	Compression followed by tension	Tension	High deviatoric stress at low confinement
Crater shape	Prismatic (triangular)	Large radius (nearly planar)	Curved/Elliptical

ACKNOWLEDGMENTS

The present work was supported by the Natural Sciences and Engineering Council of Canada through its Industrial Partnership Scholarship (IPS) program, and the Discovery Grant program.

SELECTED BIBLIOGRAPHY

- Aubertin, J.D. 2021. The Special Nature of Rock Salt Blasting: Theory and Practice. In 48th annual conference on Explosives and Blasting Technique. International Society of Explosives Engineers (ISEE), Las Vegas.
- Aubertin, J.D., Hutchinson, D.J., and Diederichs, M. 2021a. Horizontal single hole blast testing – Part 1: Systematic measurements using TLS surveys. *Tunnelling and Underground Space Technology*, 114: 103985. Elsevier BV. doi:10.1016/j.tust.2021.103985.
- Aubertin, J.D., Hutchinson, D.J., and Diederichs, M. 2021b. Horizontal single hole blast testing – Part 2: Field observations and experimental trends from SHB campaigns at two underground salt mines. *Tunnelling and Underground Space Technology*, 114: 103984. Elsevier Ltd. doi:10.1016/j.tust.2021.103984.
- Langefors, U., and Kihlstrom, B. 1963. *The modern technique of rock blasting*. Wiley, New York.
- Ouchterlony, F., and Moser, P. 2012. Lessons from single-hole blasting in mortar, concrete and rocks. In *Rock Fragmentation by Blasting*. CRC Press, New Delhi. pp. 3–14.
- Rustan, A. 1995. *Controlled Fragmentation and Contours in Rock Blasting*. Doctoral Thesis, Lulea University of Technology, Lulea.
- Wimmer, M. 2007. *An experimental investigation of blastability* (SWEBREC Report 2007:1). Stockholm.
- Wimmer, M., Moser, P., and Ouchterlony, F. 2008. Experimental investigation of blastability. In *5th International conference and exhibition on Mass Mining*. Lulea University of Technology, Lulea.



ARMA N. G. W. Cook PhD Award Winner¹

Heterogeneous rockmass characterization for numerical rock engineering design

Day, J.J.¹, Clark, M.D., Rudderham, G.A., and Gagnon, É.

Geological Sciences and Geological Engineering, Queen's University, Kingston, Ontario, Canada

EXTENDED ABSTRACT

This keynote was invited because of my receipt of the N.G.W. Cook Doctoral Dissertation Award in 2017 from the American Rock Mechanics Association. As such, this abstract focuses on research themes that originated in my doctoral thesis (Day 2016) as well as related follow-up contributions by some of my graduate students: Matthew Clark, Gisèle Rudderham, and Émélie Gagnon.

Rockmass characterization is best conducted in the field and the laboratory with forward thinking toward what needs to be considered for numerical modelling inputs. Characterization benefits from using a combined lens of engineering geology and geomechanics to ensure geological details are captured and incorporated into rock engineering design. My research began with a focus on intrablock structures, which I define as meso-scale rockmass structures that occur within fracture-bounded blocks of rock. Intrablock structures influence rockmass shear and tensile strength, as well as deformability of the rockmass. Their geomechanical behaviours depend on their thickness, persistence, orientation, mineralization, and the wall rock material. Some examples of intrablock structures include hydrothermal veins, stockwork, fabric, defects, and sedimentary nodules. Their counterpart of rockmass structure, namely interblock structures, include fractures, joints, bedding, and faults.

Numerical rock engineering design involves three major steps: (i) site investigation, (ii) laboratory testing, and (iii) numerical modelling (Figure 1). When dealing with complex rockmasses, mineralogical identification and quantification becomes an important parallel process alongside geomechanical laboratory tests, as the geological insight is useful to assist with explaining any variability in geotechnical data. In the case of hydrothermal veins, for example, the vein characteristics including mineralogy and geometry, along with related numerical inputs, are important considerations for numerical modelling method selection.

Brittle overbreak in deep underground excavations under high ground stresses is an important consideration for ground support design and final excavation dimensions. Empirical prediction functions of brittle overbreak in heterogeneous rockmasses that contain hydrothermal veins and breccia, which can behave quite differently than homogeneous rockmasses, are provided by Day (2019). The overbreak functions are generalized to facilitate calibration in other heterogeneous rockmasses with inputs from overbreak mapping during construction and unconfined compressive strength (UCS) laboratory test data. Customization of the overbreak functions in a given project can facilitate extrapolation of expected brittle overbreak at later stages of the project.

Routine sample selection for geomechanical laboratory tests, per the ISRM Suggested Methods, exclude veined drill core (Bieniawski and Bernede 1978). Inclusion of veined samples in sample selection for UCS laboratory test

results in increased variability of stiffness, brittle damage thresholds, and peak strength properties. Depending on the vein and wall rock characteristics, the presence of veins in a UCS test specimen may either decrease or increase the geomechanical properties of the material. For example, Clark and Day (2021) demonstrated that calcite veins can weaken a host granodiorite wall rock but strengthen a host mudstone wall rock. Clark et al. (2019) provide guidance on measuring brittle damage thresholds of veined UCS specimens.

At the UCS specimen scale, we have investigated the influence of vein mineralogy, thickness, orientation, and microstructure on emergent UCS peak strength and failure behaviour using 2D Finite Element Method (FEM) numerical models. My first contribution to this research thread (Day et al. 2014a) produced calibrated stiffness and strength properties of individual joint elements in 2D FEM models of UCS tests against models with explicit vein geometries using material zones where the vein geometries were traced from petrographic thin sections. Fortunately, stiffness and strength properties of individual minerals are available in the literature. Rudderham and Day (2023) followed this work with a numerical investigation of the influence of vein thickness and orientation on the emergent UCS peak strength and failure modes. Part of that work involved the production of a rigorous model calibration framework against physical laboratory test data, which offers a useful way for practitioners to leverage numerical models to extrapolate laboratory test data into different vein geometries. Gagnon and Day (2022) mapped nine types of calcite vein microstructure geometries into 2D FEM models of UCS tests and showed that vein microstructure has significant impacts on the emergent peak strength of the specimen. The key takeaway here is that structural geology characterization data about vein types (e.g. antitaxial versus syntaxial vein microstructure) offers valuable supplementary information for geomechanical data analysis that can be used to extrapolate data from a small number of geomechanical laboratory tests across any related drill core.

At the rockmass scale, computation limitations require thoughtful optimization of scale versus detail of rockmass structure. The Composite Geological Strength Index (CGSI; Day et al. 2019, Day 2021) is a useful tool to facilitate the inclusion of veins in equivalent continuum rockmass model materials, where available inputs are limited to mineralogy and geometry. CGSI can be seamlessly integrated to numerical model material inputs by direct input replacing a GSI value in the Hoek-Brown shear strength criterion. CGSI offers an innovative solution to combine multiple suites or sets of disparate rockmass structures (i.e. any combination of fractures and/or veins) into a single useable value. Two calculation approaches based on different available site investigation data are available: (i) by block volumes of structure suites, or (ii) by spacing of structure sets. CGSI can also be used during geotechnical drill core logging to record intrablock structure data (Day et al. 2014b).

Models with discrete rockmass structures require input decisions concerning stiffness and strength of individual vein structures. An enhanced shear strength constitutive model for intrablock structures proposed by Day et al. (2015) and validated by Day et al. (2017) offers a solution for discrete modelling of veins as joint elements. The constitutive model expands the Mohr-Coulomb shear strength criterion into three states: (i) pre-peak “primary” state, (ii) post-peak “secondary” state, and (iii) ultimate “tertiary” state. Mohr-Coulomb facilitates tensile and cohesive components of strength which are important for intact veins. The primary state is before shear yield where stiffness and strength are related to the intact properties of the vein material. The secondary state represents the structure directly after yield where an initial, rough fracture surface has formed through the vein, and the fracture surface is akin to the peak strength of a clean, unsheared joint surface. The tertiary state occurs after shear when the surface is smoother and is akin to the residual strength of a joint.

Observation and measurement of geomechanical properties and geology in the field and laboratory are needed to anchor numerical models to reality. In conclusion, the combination of methods presented here offers a complete toolkit for the inclusion of intrablock structures in rock engineering design through all steps of geomechanical site investigation, laboratory testing, and numerical modelling.

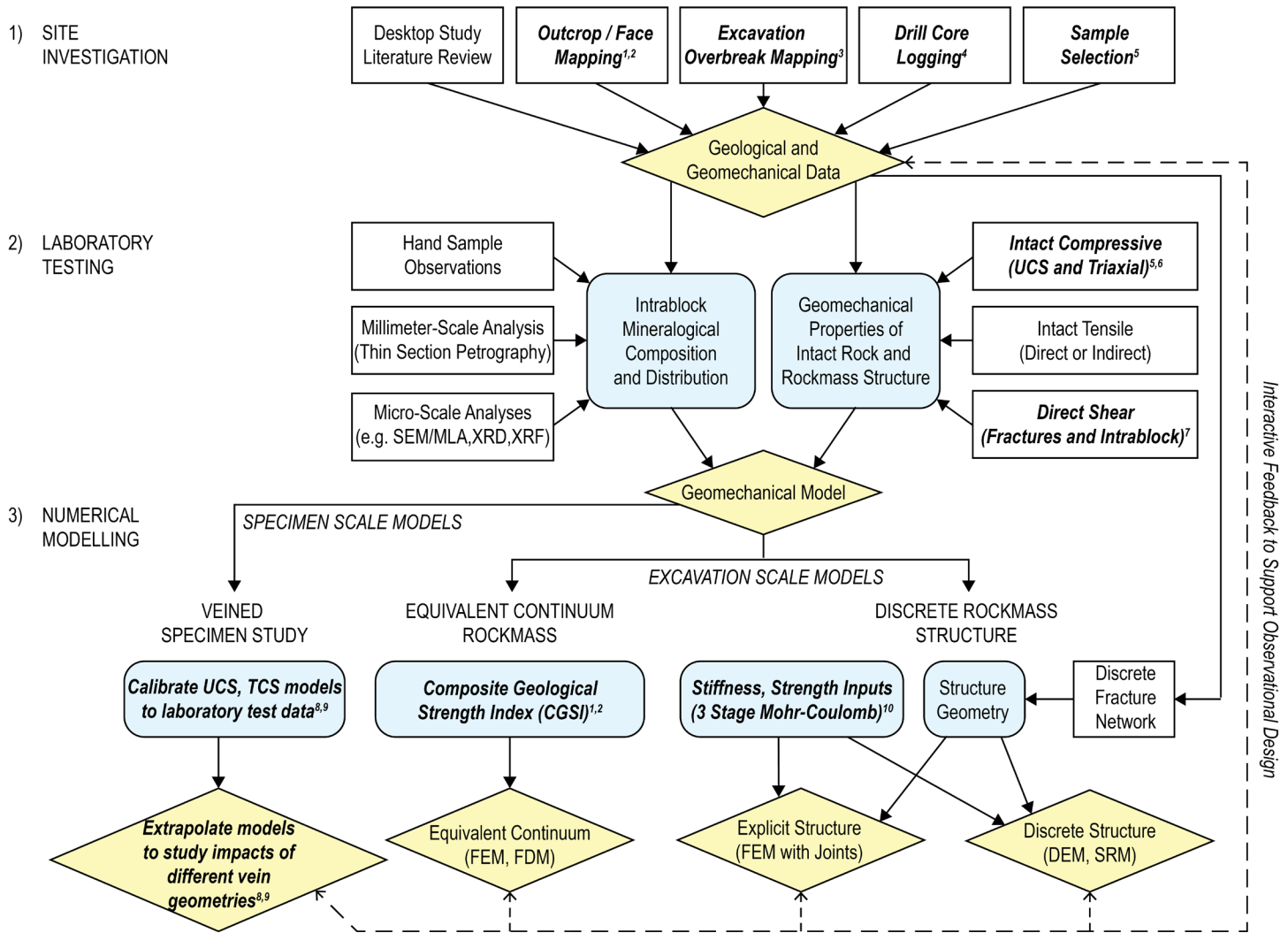


Figure 1: Rock engineering framework for heterogeneous rockmasses with intrablock structures, showing contributions by the authors (1: Day et al. 2019; 2: Day 2021; 3: Day 2019; 4: Day et al. 2014b; 5: Clark and Day 2021; 6: Clark et al. 2019; 7: Day et al. 2017; 8: Rudderham and Day 2023; 9: Gagnon and Day 2022; 10: Day et al. 2015)

REFERENCES

- Bieniawski, Z.T. and Bernede, M.J. 1978. Suggested methods for determining the uniaxial compressive strength and deformability of rock materials. *International Journal of Rock Mechanics and Mining Sciences and Geomechanics Abstracts*, 16(2):138–140. [https://doi.org/10.1016/0148-9062\(79\)91451-7](https://doi.org/10.1016/0148-9062(79)91451-7)
- Clark, M.D. and Day, J.J. 2021. Mineralogical and sample selection implications for geomechanical properties of intact heterogeneous and veined rocks from the Legacy skarn deposit. *Engineering Geology*, 285, 106067. <https://doi.org/10.1016/j.enggeo.2021.106067>
- Clark, M.D., Day, J.J., and Diederichs, M.S. 2019. Assessing the geomechanical behaviours of skarn-related hydrothermal veins in intact laboratory tests. In *Proc. 53rd US Rock Mechanics/Geomechanics Symposium*, New York, NY, USA, 23–26 June 2019; American Rock Mechanics Association (ARMA), 11p.
- Day, J.J. 2016. The influence of healed intrablock rockmass structure on the behaviour of deep excavations in complex rockmasses. PhD Thesis, Dept. Geological Sciences and Geological Engineering, Queen's University, Kingston, ON, Canada, 531p. <http://hdl.handle.net/1974/15306>
- Day, J.J. 2019. Brittle overbreak prediction in deep excavations for hydrothermally altered and heterogeneous rockmasses. *Bulletin of Engineering Geology and Environment*, 79: 1041–1060(2020). <https://doi.org/10.1007/s10064-019-01578-z>

- Day, J.J. 2021. How to incorporate variability of rockmass structures into equivalent continuum numerical models using Composite Geological Strength Index. In Proc. Rocscience International Conference, CRC Press/Balkema: 110–116.
- Day, J.J., Diederichs, M.S., and Hutchinson, D.J. 2014a. Component and system deformation properties of complex rockmasses with healed structure. In Proc. 48th US Rock Mechanics/Geomechanics Symposium, Minneapolis, MN, USA, 1–4 June 2014; American Rock Mechanics Association (ARMA), 11p.
- Day, J.J., Hutchinson, D.J., and Diederichs, M.S. 2014b. Challenges in characterization of complex rockmasses, using drill core, as input into geomechanical analysis for tunnel design. In Proc. World Tunnel Congress 2014, Foz do Iguaçu, Brazil, 9–15 May 2014, 10p.
- Day, J.J., Diederichs, M.S., and Hutchinson, D.J. 2015. Optimization of structural contact stiffness and strength for discrete simulation of progressive failure of healed structure. *Geomechanik und Tunnelbau (Geomechanics and Tunnelling)*, 8(5): 414–420. <https://doi.org/10.1002/geot.201500027>
- Day, J.J., Diederichs, M.S., and Hutchinson, D.J. 2017. New direct shear testing protocols and analyses for fractures and healed intrablock rockmass discontinuities. *Engineering Geology*, 229: 53–72. <https://doi.org/10.1016/j.enggeo.2017.08.027>
- Day, J.J., Diederichs, M.S., and Hutchinson, D.J. 2019. Composite Geological Strength Index approach with application to hydrothermal vein networks and other intrablock structures in complex rockmasses. *Geotechnical and Geological Engineering*, 37: 5285–5314. <https://doi.org/10.1007/s10706-019-00980-4>
- Gagnon, É. and Day, J.J. 2022. Vein genesis and the emergent geomechanical behaviour of numerically simulated intact veined rock specimens under uniaxial compression. In Proc. GeoCalgary, 75th Canadian Geotechnical Society Annual Conference, Calgary, AB, Canada, 10p.
- Rudderham, G.A. and Day, J.J. 2023. Veined rock performance under uniaxial and triaxial compression using calibrated finite element numerical models. *Geotechnics*, 3(4): 1219–1250. <https://doi.org/10.3390/geotechnics3040067>



GS-UK Glossop Medal Winner

Building slope process models considering engineering geology

Hutchinson, D.J.

Geological Sciences and Geological Engineering, Queen's University, Kingston, Ontario, Canada

EXTENDED ABSTRACT

The Glossop lecture was focussed on demonstrating the advances in remote sensing observation as applied to rock slope stability assessment, over three themes: Collecting, processing and interpreting remotely sensed data; Understanding, communicating and making decisions about rock slope instability; and Developing and calibrating slope process models to support instability forecasting.

Rock slope failure events are very often complex, involving several stages of activity and warning signs that cannot often be detected in advance, even with modern inspection and monitoring approaches. Observations of rock slope behaviour often show us that there are several stages to an instability, and that the rock material frequently fragments during the event. Remote sensing monitoring and the proliferation of videos of rockfall events provide us with a new level of understanding of these events.

More than a decade of remotely sensed data, collected at the White Canyon near Lytton in British Columbia, formed the basis for the work discussed in this presentation. At this site, the CN Railway tracks run along an embankment on the north side of the Thompson River, below several 100 m high slopes – both cut and natural slopes. Thousands of rockfalls occur on these slopes each year, largely managed by rock sheds erected over the tracks in several locations, and by the use of Slide Detector Fences in other locations which are intended to provide warning so the trains can stop outside the canyon should a rockfall occur. The key questions being asked include:

- How do we identify which features may generate failing rocks, next?
- How do we observe and measure the potential source zones / failure volume?
- Can we forecast potential failure?
- Once we have identified a potential source zone, what is the risk to the rail infrastructure?

The new methods developed to work with primarily terrestrial LiDAR data, and the development of a rockfall database including rockfall volume, shape and lithology, are discussed. Analysis of the data includes frequency and magnitude of the rockfalls, divided by rock type; discussion of the identification of pre-cursor events prior to larger instabilities; and assessment of the displacement rate, direction and relationship with the rockmass structure, to support deeper understanding of these processes.

Several case histories of the processes observed on these rock slopes are included in the presentation, demonstrating the effect of weather processes on the events and the deformations occurring before failure, including rockfalls from cut slopes and debris channel behaviour. As the processes are better understood and process models representing their behaviour can be developed, the ability to forecast these events increases.

The presentation concludes with recommendations regarding ongoing development of the tools, analysis and process models, and the linkage between the data collected and simulation of the rock slope behaviour.



CGS Franklin Award Winner

The role of rock mechanics in the geological storage of CO₂ through the lens of the Aquistore CO₂ Storage Project

Chalaturnyk, R.J.

University of Alberta, Edmonton, Alberta, Canada

EXTENDED ABSTRACT

Continuous monitoring of field conditions over 5 years of intermittent cold CO₂ injection at the Aquistore storage site suggests a general increase in well injectivity performance with time. The injectivity-relevant field observations and operational data, collected from the two highly instrumented injection and observation wells at Aquistore which were specifically drilled for CO₂ storage demonstrate that hydro-thermo-mechanical (THM) processes are involved in the noted variation of injectivity. Interpreting injection data in the context of injectivity index, the temporal evolution of CO₂ injectivity behaviour could most likely be explained through stress-dependent thermal mechanisms associated with semi-reversible effective permeability in the near-wellbore region. This region experiences sufficiently negative minimum effective stress that overcomes the tensile strength of the host rock leading to aseismic non-isothermal pore deformation, tensile micro-cracks, and/or opening of pre-existing critically stressed fractures. Events such as CO₂/brine chemical interaction (e.g. salt precipitation), rate-dependent pore flow (e.g. high-velocity laminar/turbulent) and CO₂ phase behaviour (e.g. kinematic fluidity) are not anticipated to positively contribute to the injectivity performance. Although semi-reversible stress-dependent changes in effective permeability are speculated to improve CO₂ injectivity performance, the non-isothermal induced stresses could also create new, localized, flow pathways through low-permeability non-reservoir formations, including caprock units. Understanding this thermal phenomenon is a critical consideration on long-term containment and conformance of the host aquifers and it needs to be further investigated.

CARBON CAPTURE AND STORAGE – CCS

“Carbon Capture and Storage” or “CCS” is a term that refers to technologies that capture the greenhouse gas carbon dioxide (CO₂) and store it safely underground (i.e. geological storage of CO₂), so that it does not contribute to climate change. CCS includes both capturing CO₂ from large emission sources (referred to as point-source capture) and also directly from the atmosphere (Figure 1). Point-source capture is when a large emission source, like an industrial facility, is equipped with technology allowing the capture and diversion to storage of CO₂, preventing it from being emitted. It is also possible to remove historical CO₂ emissions, those that are already in the atmosphere, through direct air capture and storage (DACCS) or bioenergy with capture and storage (BECCS). CCS can be applied across sectors vital to our economy, including cement, steel, fertilizers, power generation and natural gas processing, and can be used in the production of clean hydrogen (GCCSI, 2022).

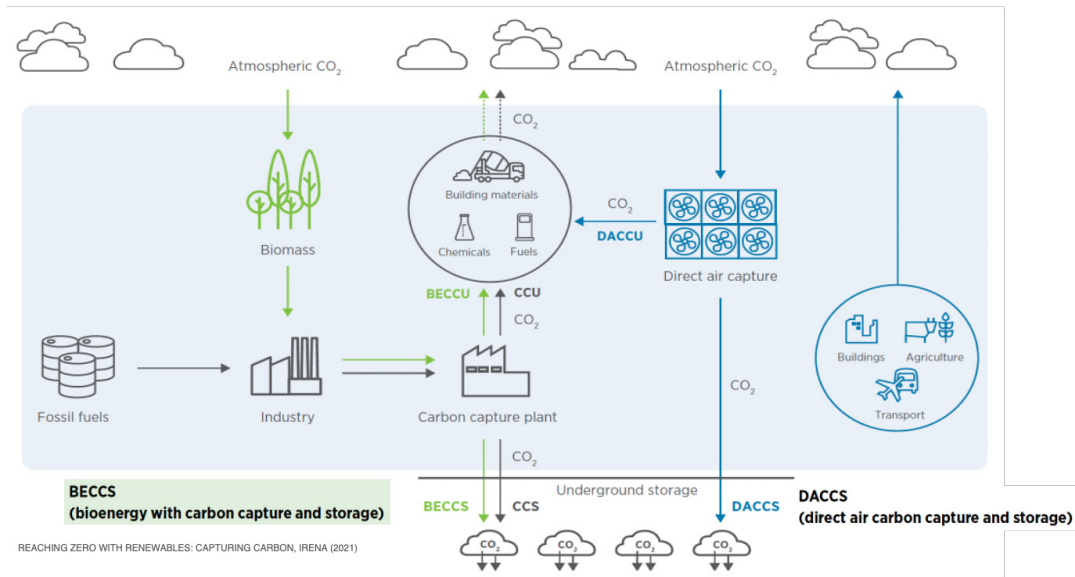


Figure 1: Overview of CCS Value Chain

GEOLOGICAL STORAGE OF CO₂

The geological storage of CO₂ involves injection of captured CO₂ into a deep underground geological reservoir of porous rock overlain by an impermeable layer of rocks, which seals the reservoir and prevents upward migration of CO₂ and escape into the atmosphere. Several types of reservoirs are suitable for CO₂ storage (Figure 2), with deep saline formations and depleted oil and gas reservoirs having the largest capacity. A geological site suitable for CO₂ storage must have:

- Sufficient injectivity to receive CO₂ at rate at which it is to be supplied;
- Secure containment (and conformance) of CO₂ for the long-term; and
- Sufficient capacity to store delivered CO₂ over lifetime of injection operations.

However, if CCS is implemented on the scale needed to make noticeable reductions in atmospheric CO₂, a billion metric tons or more, globally, must be stored annually, with the largest injection operations in regions with the highest CO₂ emissions. Securing such a large volume will require a solid scientific foundation that defines the coupled thermal-hydrologic-geochemical-geomechanical processes that govern the long-term fate of CO₂ in the subsurface. Also needed are methods to characterize and select sequestration sites, subsurface engineering to optimize performance and cost, approaches for ensuring safe operation, monitoring technology, remediation methods, regulatory overview, and approaches for managing long-term liability (Benson and Cole, 2008).

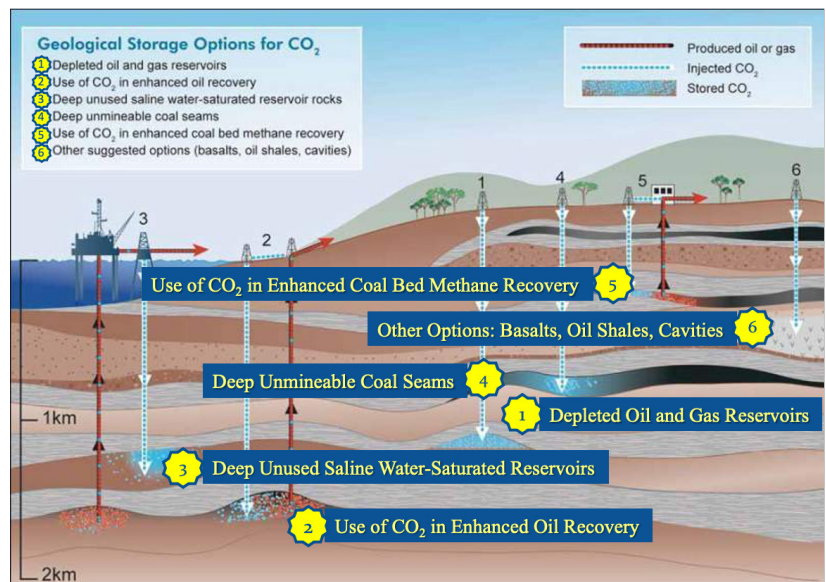


Figure 2: Subsurface options for geological storage of CO₂

ROCK MECHANICS ISSUES RELATED TO GEOLOGICAL STORAGE

Rutqvist (2012) provides a superb graphical overview (Figure 3) of the key geomechanical, and technical issues associated with geological storage. As with many rock engineering problems, these issues arise from the complex thermo-hydro-mechanical (THM) processes resulting from temperature and pressure changes within heterogeneous rock masses. For geological storage, the unique physical properties of CO₂ provide an additional complexity in understanding how reservoirs and surrounding seals react to CO₂ injection. Amongst the many risks that must be assessed for any geological storage site, one of particular importance is the maximum overpressure that can be safely applied without causing any geomechanical changes that would jeopardize the containment of the injected CO₂. For CCS, in situ stress determination using hydraulic fracturing techniques (i.e. minifrac, DFIT) and log-based techniques based on dipole sonic have all been applied to assess maximum injectivity limits. Assessment of the maximum injection is further complicated by cooling induced stress reductions that occur during CO₂ injection. Understanding the rock mechanical implications of temperature and pressure changes during CO₂ injection has been a focus of the continuous monitoring of field conditions over 5 years of intermittent cold CO₂ injection at the Aquistore storage site, a Canadian CCS demonstration project, where the data suggests a general increase in well injectivity performance with time that can be linked to the thermo-hydro-mechanical (THM) processes occurring within the injection horizon.

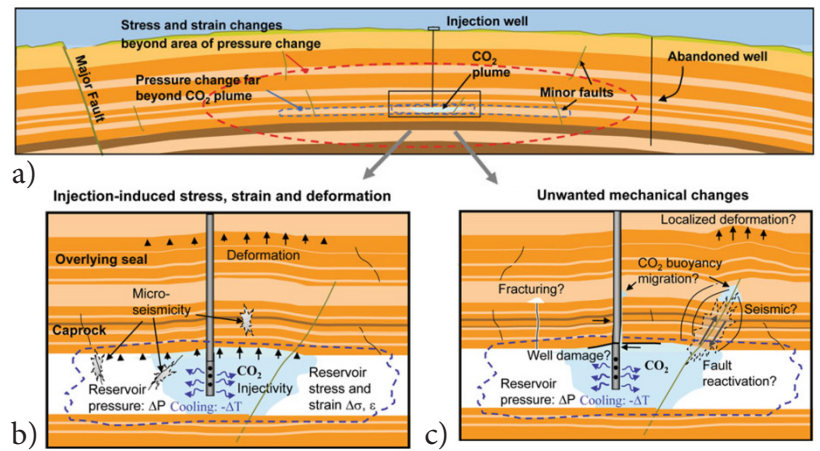


Figure 3: a) different regions of influence for a CO₂ plume, reservoir pressure changes, and geomechanical changes in a multilayered system with minor and major faults. b) injection induced stress, strain, deformations and potential microseismic events as a result of changes in reservoir pressure and temperature, and c) unwanted inelastic changes that might reduce sequestration efficiency and cause concerns in the local community.

OVERVIEW OF AQUISTORE CO₂ INJECTION SITE AND WELL PERFORMANCE

The Aquistore injection site is the geological storage component of the Boundary Dam Integrated Carbon Capture and Storage (CCS) demonstration project, owned by SaskPower and operated by Petroleum Technology Research Centre (PTRC) in Saskatchewan, Canada. The CO₂ is captured from the flue gas of a coal-fired power generation station where the excess amount, not being sold for EOR, is transported through an underground pipeline to a 3400 m deep well for injection (Movahedzadeh et al. 2021). A cumulative injected mass of over 450 ktonnes of CO₂ has been achieved by July 2022 with varying injection rate of up to 2400 tonnes/day of CO₂, through four perforation zones, over an interval of 200 m.

Interpreting injection data in the context of injectivity index, the temporal evolution of CO₂ injectivity behaviour could most likely be explained through stress-dependent thermal mechanisms associated with semi-reversible effective permeability in the near-wellbore region. This region experiences sufficiently negative minimum effective stress that overcomes the tensile strength of the host rock leading to aseismic non-isothermal pore deformation, tensile micro-cracks, and/or opening of pre-existing critically stressed fractures. Events such as CO₂/brine chemical interaction (e.g. salt precipitation), rate-dependent pore flow (e.g. high-velocity laminar/turbulent) and CO₂ phase behaviour (e.g. kinematic fluidity) are not anticipated to positively contribute to the injectivity performance.

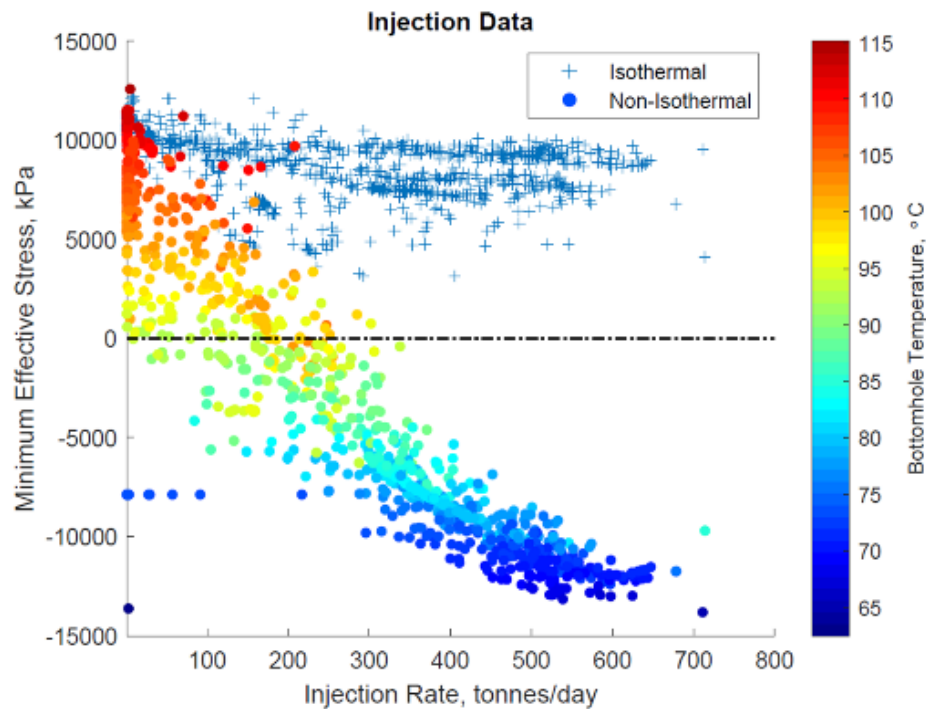


Figure 4: Relation between minimum effective stress and injection rate, with and without non-isothermal assumption.

SUMMARY

Observations support the conclusion that the temporal evolution of CO₂ injectivity behaviour is most likely caused through non-isothermal mechanisms associated with effective permeability. Thermo-hydro-mechanical interpretation from field data indicates that during cold CO₂ injection, the near-wellbore region would experience sufficiently negative minimum effective stress to overcome sandstone tensile strength and lead to non-isothermal aseismic pore deformation, induce tensile micro-cracks, or open the pre-existing critically stressed fractures (Figure 4).

ACKNOWLEDGEMENTS

The Petroleum Technology and Research Centre (PTRC) has been key organization leading the support for CCS since the early days of the IEAGHG Weyburn Project and now with the Aquistore Project. Their support is gratefully acknowledged as well as my colleagues on the Scientific and Engineering Research Committee (SERC). Dr. Alireza Rangriz Shokri is the key technical individual behind the reservoir geomechanical simulations for the Aquistore Project – much of this work is due to his talent and expertise. I would also like to acknowledge the efforts of Dr. Gonzalo Zambrano for his expertise in the monitoring programs at Aquistore.

REFERENCES

- GCSSI, 2022. Understanding CCS – Carbon Capture and Storage (CCS) Factsheet, 2p.
- Lyons, M., P. Durrant and K. Kochhar (2021), Reaching Zero with Renewables: Capturing Carbon, International Renewable Energy Agency (IRENA), Abu Dhabi, 108 p.
- Rutqvist, J. 2012. The geomechanics of CO₂ storage in deep sedimentary formations. *Int. J. Geotech. Geol. Eng.* 50, 525–551.
- Benson S.M. and D.R. Cole 2008. CO₂ sequestration in deep sedimentary formations. *Elements*, 4, 325–331.
- Movahedzadeh, Z., Rangriz Shokri, A., Chalaturnyk, R.J., Nickel, E., Sacuta, N. 2021. Measurement, Monitoring, Verification and Modelling at the Aquistore CO₂ Storage Site, *EAGE First Break* 39(2):69–75 DOI: 10.3997/1365-2397.fb2021013



CGS Thomas Roy Award Winner¹

Is it really necessary to quantify GSI?

Elmo, D.¹ and Yang, B.²

¹*Keevil Institute of Mining Engineering, The University of British Columbia, Vancouver, British Columbia, Canada*

²*The University of British Columbia, Vancouver, British Columbia, Canada*

EXTENDED ABSTRACT

Rules of thumbs and practical solutions are often invoked in engineering design practice. When considering the field of rock engineering, there is an abundance of qualitative and semi-quantitative classification scheme, some of which are elevated to the rank of industry standard for no reasons other than personal preferences of individual engineers. This thought-provoking statement agrees with the notion expressed by the physicist Max Planck that the success of a theory depends more on the reluctance to challenging the status quo rather than its actual scientific validity. One apt example is the problem of insisting to quantify what are essentially qualitative rock mass conditions as if the quantification process could add the experience factor for inexperienced engineers. This short paper proposes an opposite interpretation to the compulsive search for a quantified GSI Table that has characterised the rock engineering literature since 1995.

INTRODUCTION

The Geological Strength Index (GSI) was introduced by Hoek (1994), who postulated that the Bieniawski's 1976 version of RMR (Rock Mass Rating) could be used to estimate GSI (assuming a rating of 10 for dry conditions). The GSI Table engineers are more familiar with did not appear until 1995 (Hoek et al., 1995). In it, both the description of rock mass structure and surface conditions (joints surfaces) belong to the nominal category of measurements scale (Stevens, 1946), and accordingly the nature of the GSI Table is inherently qualitative. This should not be a cause of concerns amongst engineers since the original intent of the GSI Table was indeed to create an essentially qualitative classification system (Marinos et al., 2005). Nonetheless, the literature abounds of attempts to quantify the GSI table (e.g., Sönmez and Ulusay, 1999; Cai et al., 2004; Russo, 2009), as if the quantification process could somehow add the experience factor for inexperienced engineers. Furthermore, many of these attempts use parameters that are themselves qualitative assessments or even parameters that are non-directly measurable in the field (e.g., persistence factor), and therefore the proposed quantified GSI tables do not actually provide a less subjective estimate of GSI. Because the spatial distribution of structures in rock and their surface conditions are not constant, engineers have to accept that rock mass quality ratings should be reported as a range of conditions. Bertuzzi et al. (2016) showed that quantified GSI values and qualitative assessment of GSI fall in a range of ± 10 relative to each other, which would undermine the benefit of using a quantified approach.

The problem, as explained by Elmo et al. (2022a), is that engineers are so used to work with measurable quantities that they may perceive variability as a lack of certainty, and therefore as a lack of knowledge. In an epistemological perspective these quantification attempts can be explained as an effort to switch from rules of thumbs to rule of science. To this day we often invoke the continuous use of practical methods as evidence of

their validity (Yang et al., 2021). Continuous use represents a form of correlation, but to claim a causation would require proper scientific validation. It is impossible not to ask the rather provocative question as to whether some of the empirical systems we use in our design practice today have undergone truly scientific validation processes, including scientific replicability. What we propose departs from the GSI quantification trend, to recognize that the notion of assigning accurate numbers to represent rock mass quality is not meaningful. The scope of rock mass classification systems should be to classify rock masses based on their qualities rather than assigning accurate values to qualitative descriptions as if they were representing measurable mathematical variables.

REVERSING THE QUANTIFICATION PROCESS

What follows next is a concept initially presented in Elmo et al. (2022a, 2022b). Let us consider a system in which rock mass structure is measured along the Y-axis (vertical axis) and the characteristics of the fractures surfaces is measured along the X-axis (Figure 1). We could use a decreasing scale of 10 to 1 on the Y-axis, and similarly a decreasing scale of 10 to 1 on the X-axis. Table A assumes the calculated rock mass quality is equal to the ratio of the parameter Y to the parameter X. Conversely, for Table B the rock mass quality is calculated as the product of the parameters Y and X. It is apparent that Table A has very distinct ratings. On the contrary, Table B has a clear symmetric pattern, and equivalent ratings are repeated for different combinations of the parameters X and Y.

There is an “irreversibility bias” that affects Table B, in which the same emerging value can be obtained using different combinations of $[Y_i, X_j]$. Figure 1 compares Tables A and B with the GSI Table (Hoek et al, 1995). The underlying structure of the GSI Table bear a resemblance to Table B, in which, given an emerging value, it is not possible to identify the corresponding unique combination (e.g. $[Y_3, X_1]$ and $[Y_1, X_3]$) which created it. By superimposing rock types from actual field studies (data from Marinos and Carter, 2018), a geological trend becomes apparent (Figure 2) which agrees with the trend of Table A, in which the diagonal (red line) acts as a divider between two distinct regions in which different ratings are assigned to different cells. Using this approach, Elmo et al. (2022b) have derived a modified GSI Table (Figure 3) in which the emerging property (GSI) is unique to distinct combinations of the parameters $[Y_i, X_j]$. The revised GSI Table forces engineers to embrace the idea of rock masses as materials whose mechanical behaviour should be defined in the form of a potential stability envelope, defined by the minimum and maximum of the assigned $N \pm 5$ range.

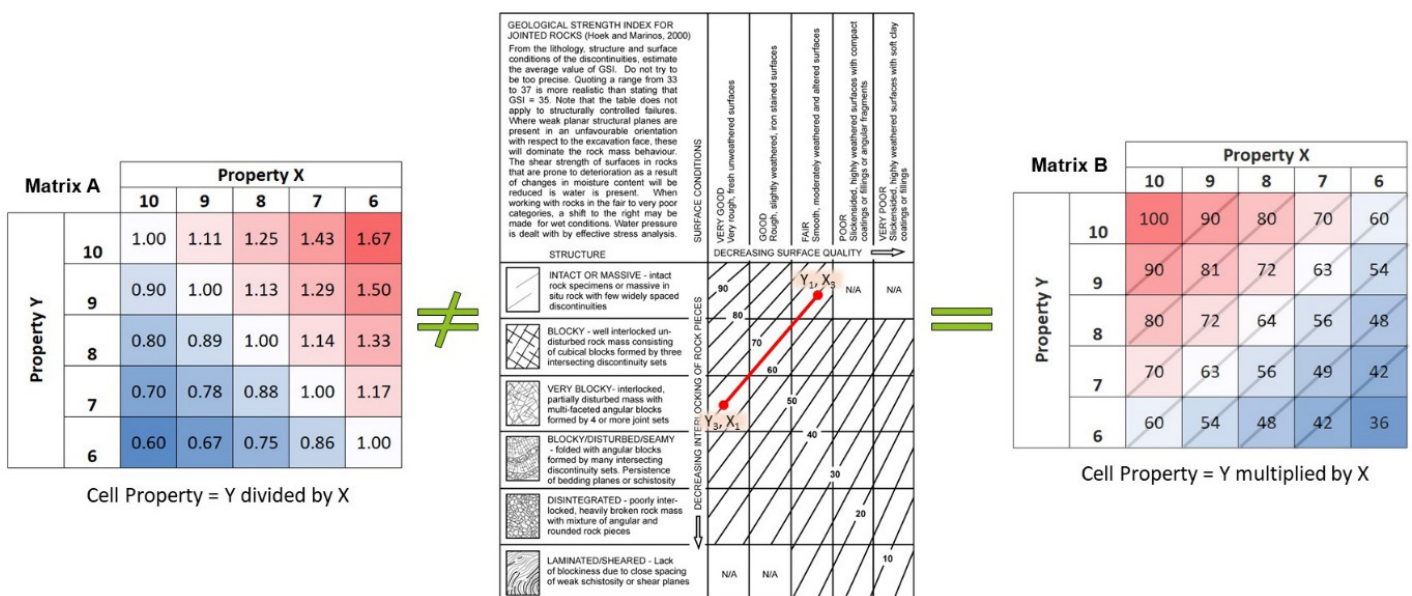


Figure 1: Comparison between Matrix A and Matrix B approach with the matrix format of the GSI system. Figure modified from Elmo et al. (2022a).

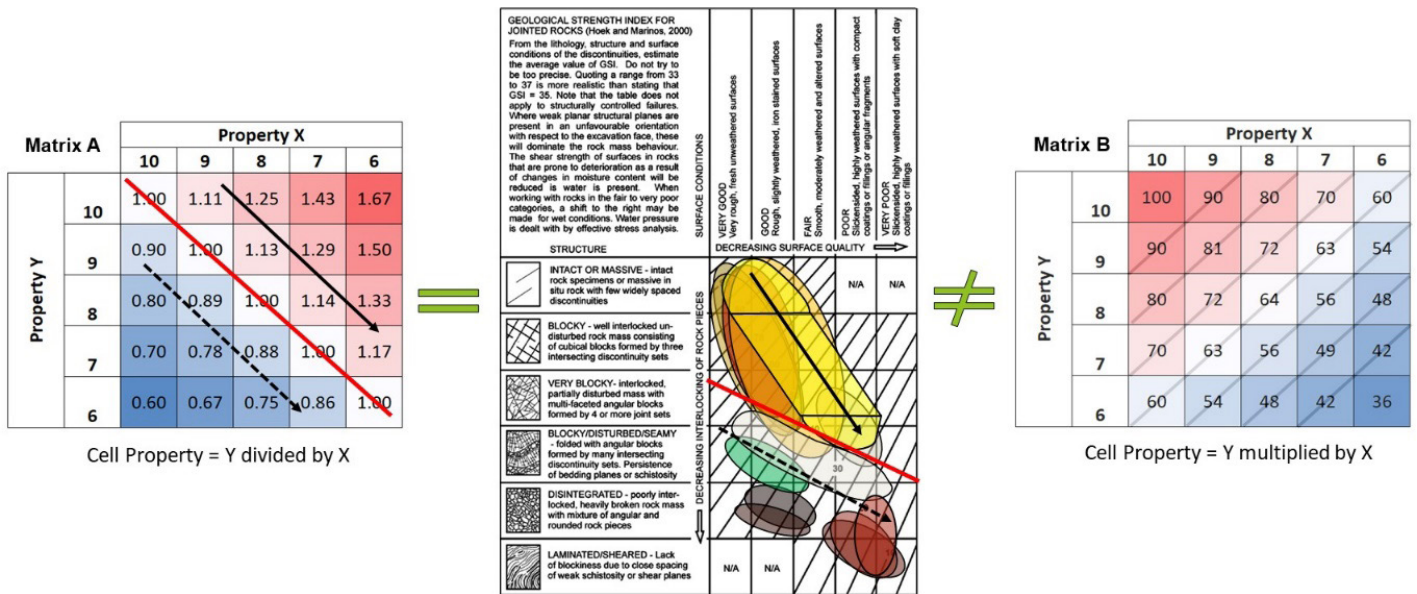


Figure 2: Comparison between Matrix A and Matrix B the matrix format of the GSI system including added geological data by Marinos and Carter (2018). Figure modified from Elmo et al. (2022a).

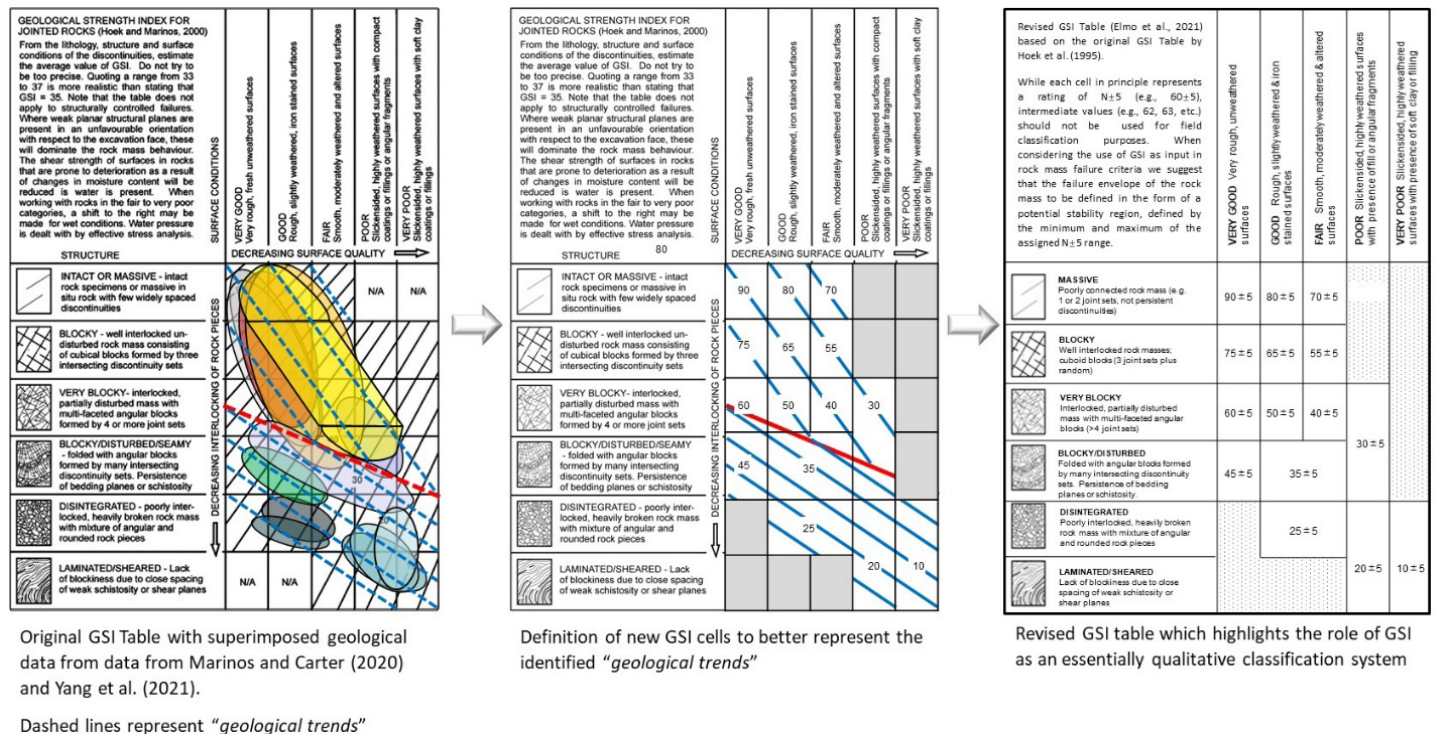


Figure 3: Evolution of the original GSI table to better account for geology and the irreversibility bias described in the text above. Adapted from Elmo et al. (2022b).

SUMMARY

In this short paper we have offered an opposite view to the common trend of GSI quantification. The quest by engineers to quantify what ultimate are qualitative (and therefore subjective) data creates an illusion of accuracy. We have proposed an updated GSI Table which better capture the need to move towards the adoption of a scenario-based design approach, whereby stability conditions are to be investigated considering a potential stability envelope defined by a range of GSI ratings. This approach places more emphasis on understanding

geology and mechanisms rather than on identifying accurate input for empirical failure criteria and numerical models. Whether we want to continue to rely on the original GSI Table, or any of the published modified versions, there remains the challenge of approximating the mechanical behaviour of jointed rock masses to that of isotropic equivalent continuum media. This echoes Barton (2021), who commented that more realistic design of slopes, mines and tunnels could be achieved using discontinuum models.

ACKNOWLEDGEMENTS

We would like to acknowledge that the work presented in this short paper is a condensed version of two articles published in 2022 (Elmo et al., 2022a and Elmo et al., 2022b). Full references to those articles are provided below.

REFERENCES

- Barton N. 2021. Continuum or discontinuum: GSI or JRC. Invited keynote lecture. In Proceedings of the Geotechnical Challenges in Mining, Tunnelling and Underground Structures (ICGCMTU2021), Malaysia (On-Line Conference), 20–21 December 2021.
- Bertuzzi R., Douglas K., Mostyn G. 2016. Comparison of quantified and chart GSI for four rock masses. *Engineering Geology*. 202. 10.1016/j.enggeo.2016.01.002.
- Bieniawski Z.T. 1976. Rock mass classification in rock engineering. In: Bieniawski Z.T. (ed.) *Proceedings of the Symposium on Exploration for Rock Engineering*, Cape Town, Volume 1. Balkema, Rotterdam, The Netherlands, 97–106.
- Cai M., Kaiser P.K., Uno H., Tasaka Y, Minami M. 2004. Estimation of rock mass deformation modulus and strength of joint-ed hard rock masses using the GSI system. *International Journal of Rock Mechanics and Mining Sciences*. 41(1): 3-19.
- Elmo D., A. Mitelman, B. Yang. 2022a. An Examination of rock engineering knowledge through a philosophical lens. *Geosciences*, 12, 174. doi.org/10.3390/geosciences12040174.
- Elmo D., B. Yang, T. Shapka-Fels, R. Tsai. 2022b. The Allegory of the Rock Engineering Cave. *Proceedings of the Eurock 2022 conference*, Finland.
- Hoek E, Kaiser PK, Bawden WF. 1995. *Support of underground excavations in hard rock*, Rotterdam, Balkema.
- Hoek E. Strength of rock and rock masses. *ISRM News Journal*, 2(2), 1994, 4–16.
- Hoek, E. and Brown, E.T. 1997. Practical estimates of rock mass strength. *International Journal of Rock Mechanics and Mining Sciences*. Vol 34, issue 8, pp 1165–1186.
- Marinos V., Carter T.G. 2018. Maintaining geological reality in application of GSI for design of engineering structures in rock. *Engineering Geology*, 248, 357–360, doi.org/10.1016/j.enggeo.2018.03.022.
- Marinos V., Marinos P., Hoek E. 2005. The geological strength index: applications and limitations. *Bull Eng Geol Environ*, 64: 55–65, 10.1007/s10064-004-0270-5.
- Russo G. 2009. A new rational method for calculating the GSI. *Technical Note. Tunneling and Underground Space Technology*. Vol 24, pp. 103–111.
- Sönmez H., and Ulusay R. 1999. Modifications to the geological strength index (GSI) and their applicability to stability of slopes. *Int. J. Rock Mech. & Min. Sci*, 36: 743–760.
- Stevens S.S. 1946. On the theory of scales of measurement. *Science*, 103, 677–680, <https://doi.org/10.1126/science.103.2684.677>.
- Yang B., Mitelman A, Elmo D., Stead D. 2021. Why the future of rock mass classification systems requires revisiting its empirical past. *Quarterly Journal of Engineering Geology and Hydrogeology*. 10.1144/qjegh2021-039.



CGS Hardy Lecture

Underground construction in complex rock environments: promises and pitfalls of observational design

Diederichs, M.S.

Department of Geological Sciences and Geological Engineering, Queen's University, Kingston, Ontario, Canada

EXTENDED ABSTRACT

The Observational Approach for geotechnical design and construction was discussed by Bjerrum and Terzaghi in the early 1960's as a means to cope with the uncertainty of working with Earth materials. Rather than defining, a priori, all underground conditions, the project team conducts exploration to define the nature, pattern and range of properties, assess the most probable deviation from these conditions, establish a design based on most probable condition, with a toolbox of modifications to the design should there be a foreseeable deviation. Measurable quantities during construction are to be determined and monitored. The as-built design is then verified or modified to suit actual conditions. This method served geotechnical engineering well, but as Peck observes:

"It is essential that the quantities to be observed should reflect the phenomena that will actually govern the behaviour of the works to be constructed....A mistaken preconception of the nature of the problem may lead to omission of observations of types that would have disclosed the real reasons for concern."

It is critical to understand the unique failure modes that may occur in isolation or in combination and tailor, not only the support and excavation design to these modes, but also the monitoring and response to change. "What indications of instability are given by each failure mode and what should be the response?" is a question that should be asked well before construction begins.

Rather than utilizing a codified classification scheme for conditions, or relying on standard measurements such as closure, conditions to be recorded, quantities to be observed, and triggers for response, must be relevant to the instability mechanisms anticipated. In this paper, the site investigation, design and monitoring cycle for tunnelling and cavern construction projects are explored using case histories from Canada, Europe, Chile and Australia. Analyses has evolved from 2D to 3D continuum to discontinuum code with discrete support representation. Conventional site investigation is now augmented to support the needs for this complex stability analysis focussed on the relevant ground mechanics in complex ground conditions. Both ground conditions as well as ground performance are integrated into an innovative observational design cycle with design, monitoring, re-analysis and response tailored to specific deformation and instability modes identified during investigation and pre-construction modelling.

The process of observational design is not "design as you go" but rather "learn as you go and select the correct pre-design along with toolbox options. As noted by Peck in 1969:

"The essential ingredient is the visualization of all possible eventualities and the preparation in advance of courses of action to meet whatever situation develops."

CGS Thomas Roy Award Winner¹

Rock mass characterization using DFNs, LiDAR and distributed optical sensing

Vlachopoulos, N.¹, Vazaios, I.², and Forbes, B.³

¹Royal Military College of Canada, Kingston, Ontario, Canada

²ARUP, London, England

³BGC Engineering Inc., Kingston, Ontario Canada

EXTENDED ABSTRACT

Underground projects require a realistic understanding of geological, structural and mechanical characteristics of the rock mass. This includes a comprehensive rock mass characterization, assessment to all existing site information and an accurate geological model. However, due to the lack of truly three-dimensional subsurface fracture geometry data, this reality is rendered difficult. Thus, the use of Discrete Fracture Networks (DFNs) arises as an interesting tool. DFN models are statistically generated from discontinuity features mapped in situ. These deterministic data can be obtained by employing various techniques, and more specifically with the use of laser scanning (i.e. Light Detection and Ranging— LiDAR). Complimentary discontinuity data can be obtained through fiber optic sensors coupled to tendon rock support elements, adding structural information from within the rock mass to the DFN model. This presentation will discuss the methodology associated with the implementation of LiDAR data into DFN models for the purpose of application in underground projects and the use of optical sensors to capture three-dimensional (3D) loading of tendon support and, in turn, identify intersecting discontinuity planes. The Distributed Optical Strain Sensing technology is demonstrated through double shear laboratory tests, as well as through an in situ application to monitor rock mass movement during a tunnel excavation.

BACKGROUND

In underground excavation projects the understanding of the rock mass conditions is fundamentally required to ensure safe engineering standards. The importance of an appropriate in-depth site investigation during the design stage of underground works is well documented and conventional techniques used to this purpose are based on heuristic structural classification systems. A modern investigation approach that is gaining ground, particularly for underground projects such as tunnels, is the generation of Discrete Fracture Networks (DFNs). A DFN model is a 3D computer rendering of the rock mass based on the geometrical features of discontinuities observed in the field and posteriorly extrapolated through statistical or deterministic approaches (Fekete and Diederichs, 2012). This technique utilizes discontinuity data that can be obtained from field mapping and can serve as input parameters for the geometrical modelling of the natural fractures that are present.

Accurate calibration of a DFN model so that it can be representative of the investigated geological conditions depends on two significant factors: a) the selection of appropriate input discontinuity parameters and b) the model generation methodology (deterministic or statistical approaches). Input parameters consist in mean discontinuity orientation, persistence, and intensity for each set determined in the analysis. Furthermore, those

parameters have to correspond to the geometric distribution of the discontinuities observed and mapped in the field. Regarding the model generation methodology, mapping of exposed rock mass areas can be conducted by applying various techniques, including manual mapping and virtual mapping through laser scanning (i.e. Light Detection and Ranging—LiDAR) and photogrammetric techniques. However, the aforementioned techniques are subjected to various limitations including limited access to the exposed rock, small rock mass exposures, etc. (Palleske et al., 2013). This highlights the importance of matching the most appropriate mapping method to specific site conditions.

LiDAR technology has been widely adopted in many industry sectors due to its capability of rapid and accurate 3D spatial mapping. In underground projects, like tunnels, LiDAR technology can be used to scan the excavated area in order to generate detailed 3D surface models. This can provide information regarding structural features of the rock mass, as the discontinuities intersecting the tunnel perimeter. For the purposes of this presentation, LiDAR extracted data from the Brockville Railway Tunnel (Diederichs et al., 2013) was used in order to determine discontinuity orientation, length and density from the 3D surface model and use them as input parameters for the DFN generation and update process.

Furthermore, DFN models can be combined with other numerical codes in order to assess specific rock mass properties, such as deformability and strength (Kulatilake et al., 2004; Farahmand et al., 2015) and to investigate the rock mass response during the excavation process, hence improving the accuracy of the geological model, analysis and thus, the overall design process. However, DFN models can only be useful if they are representative and correspond to the in situ conditions. Therefore, it is important to continually update the DFN geometry as the excavation advances, and new in situ data should be added to the existent data pool as part of an observational approach. Obtaining deterministic in situ discontinuity data during the excavation advance can be a challenge, especially those located past the excavation face. Within this context, a new technique using Distributed Optical Strain Sensing (DOS) was utilized to monitor strain along tendon support elements (Forbes et al., 2017, 2018a, b) and proved to be a good option to detect mobilized discontinuities crossing the support element. This technology captures strain with a spatial resolution of 0.65 mm. Accordingly, any rock mass movements, including discontinuities, can be detected around the support, their data can be added to the DFN data pool and the model can be validated and updated.

This presentation will demonstrate how laser scanning can be used as part of a methodology of generating DFN models in order to make an estimate of the rock mass conditions further within the excavation. Moreover, the capability of fine spatial resolution optical sensors (i.e. submillimeter spacing between measurement points) to monitor strain along tendon support elements is presented through selected results from laboratory double shear tests, as well as through a field application of tunnel support monitoring in order to demonstrate their potential to assist in the DFN generation and in the model update.

METHODOLOGY

This invited talk presentation focuses on the methodology and workflow that was utilized in producing validated and high-quality, refined DFN models. This methodology is highlighted in Vlachopoulos et al. (2020). The coarse steps of the methodology can be seen in Figures 1 and 2. A well-established methodology (that includes calibration and validated at all stages) for processing data from LiDAR in order to generate realistic input parameters for the DFN model is essential. The DOS technology can be complimentary in terms of characterizing the rock mass. The DFN model can predict the discontinuities beyond the face and a fiber optic sensor or probe can be installed past the face in order to validate the DFN predictions as well as determine other discontinuities or zones of interest within the rockmass.

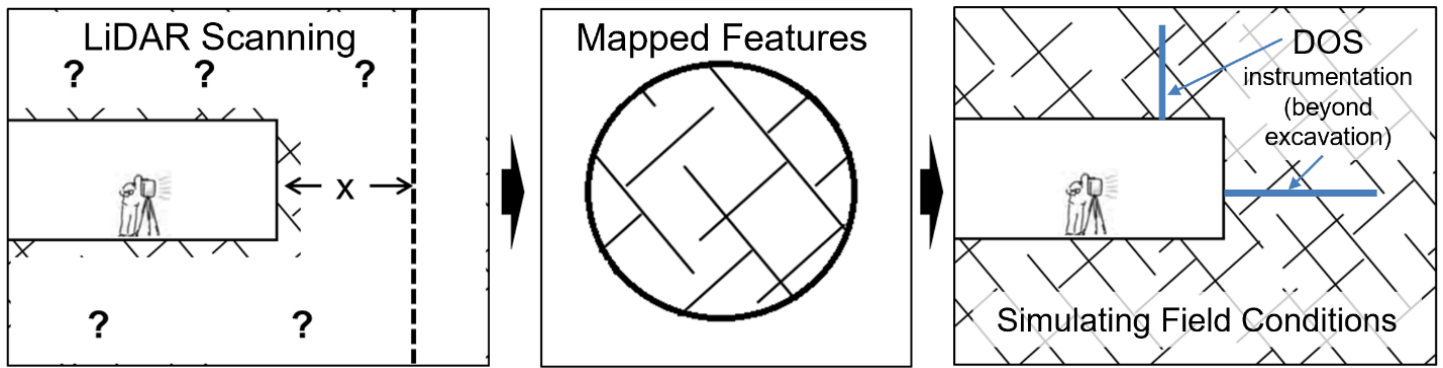


Figure 1: Depicting LiDAR as input for DFNs as well as DOS for proving the ground.

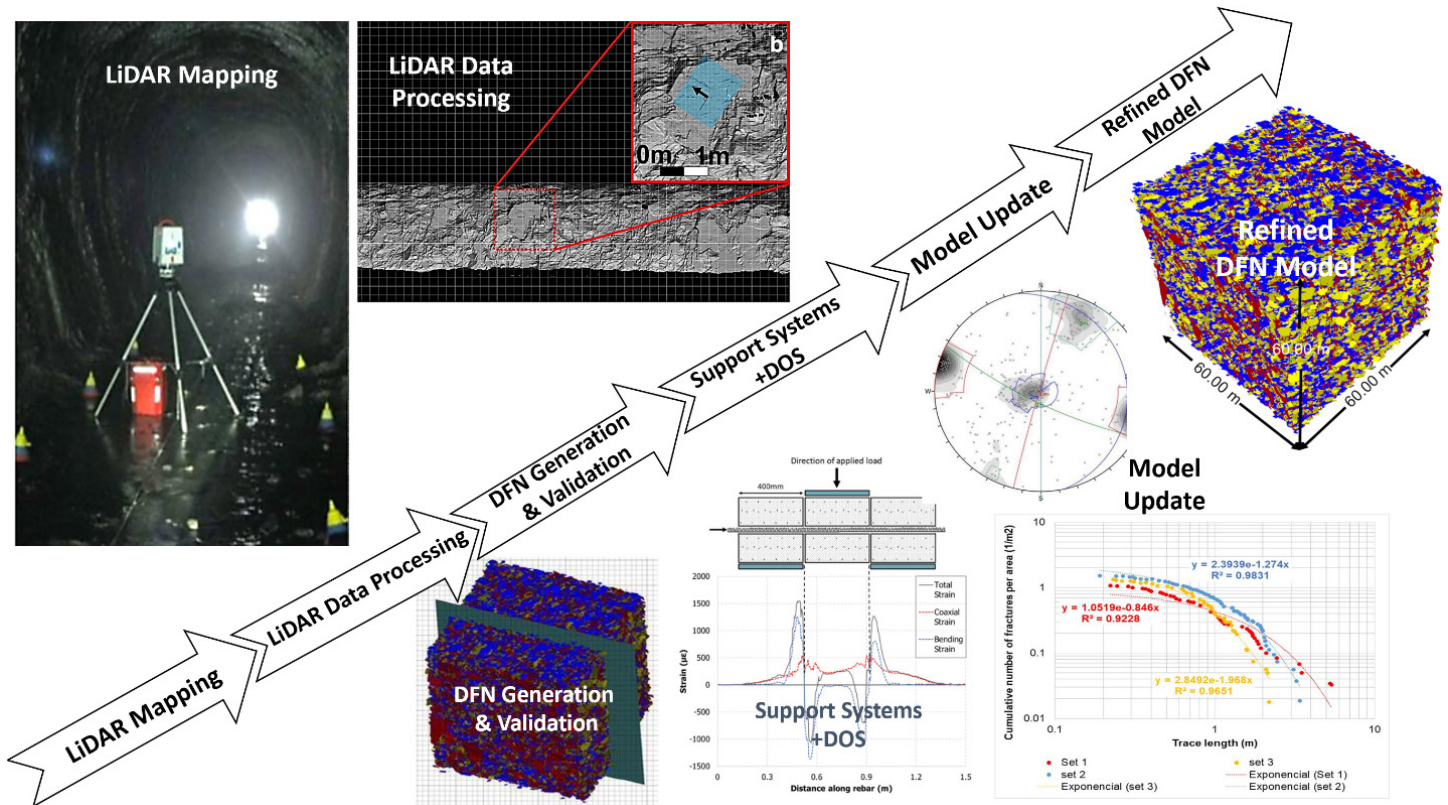


Figure 2: The main methodology and workflow that was conducted as part of this study.

SUMMARY

Predicting rock mass structural features is challenging due to the discontinuous nature that is intrinsically related to the rock material and to the rock mass geological history. Rock structure can have an important effect on the response of a rock mass to engineering operations, and more specifically to underground excavations. In order to improve rock mass characterization, statistic methods are being used to generate discrete fracture network models based on deterministic discontinuities mapped in situ. Accurate calibration of these models depends on the quality of mapping, on appropriate model input properties, on model update and on its validation by comparisons to the observed in situ conditions. Technologies for mapping, such as LiDAR, provide the means to collect reliable discontinuity data that can be used for a DFN generation and update process. Furthermore, laser scanning can be integrated efficiently in the excavation works taking place during tunnelling without leading to delays. Subsequent scans can also assist in updating the DFN model in order to improve the estimation of the rock mass conditions. DOS technology coupled to tendon support elements can be used to access information from within the rock mass and precisely locate movement across discontinuities. These data can be used to

validate the generated DFN model and/or to update it making it more accurate. Laboratory testing and in situ application showed the DOS technology potential of being integrated into a rock mass characterization methodology, aiming to enhance design and construction process.

A well-established methodology for processing data from LiDAR in order to generate realistic input parameters for the DFN model is the focus of the presentation. The DOS technology presented in this abstract can be complimentary in terms of characterizing the rock mass. The DFN model can predict the discontinuities beyond the face and a fiber optic sensor or probe can be installed past the face in order to validate the DFN predictions and determine other discontinuities or zones of interest within the rock mass.

ACKNOWLEDGEMENTS

The authors would like to thank the Natural Sciences and Engineering Council of Canada (NSERC), the Canadian Department of National Defence, Yield Point Inc., Geomechanica Inc., support provided by Dr. Mark Diederichs, and The Royal Military College (RMC) Green Team.

REFERENCES

- Diederichs MS, Carter MA, Lato MJ, Bennett JB, Hutchinson DJ (2013) LiDAR surveying for liner condition, rock stability and reconditioning assessment of Canada's oldest railway tunnel in Brockville. In: Proceedings of GeoMontreal 2013, Montreal.
- Farahmand K, Vazaios I, Diederichs M S, Vlachopoulos N (2015) Generation of a synthetic rock mass (SRM) model for simulation of strength crystalline rock using a hybrid DFN–DEM approach. In: ISRM regional symposium Eurock 2015 & 64th geomechanics colloquium, Salzburg, Austria.
- Fekete S, Diederichs MS (2012) Integration of 3-dimensional laser scanning with discontinuum modelling for stability analysis of tunnels in blocky rockmasses. *Int J Rock Mech Min Sci* 57:11–23.
- Forbes B, Vlachopoulos N, Hyett AJ, Diederichs MS (2017) A new optical sensing technique for monitoring shear of rock bolts. *Tunn Undergr Space Technol* 66:34–46. <https://doi.org/10.1016/j.tust.2017.03.007>.
- Forbes B, Vlachopoulos N, Hyett AJ (2018a) The application of distributed optical strain sensing to measure the strain distribution of ground support members. *FACETS* 3(1):195–226.
- Forbes B, Vlachopoulos N, Diederichs MS (2018b) Spile support performance monitored in a shallow urban tunnel using distributed optical strain sensing. In: 52nd US rock mechanics/geomechanics symposium, Seattle, USA.
- Kulatilake P, Park J, Um JG (2004) Estimation of rock mass strength and deformability in 3-D for a 30 m cube at a depth of 485 m at Aspo hard rock laboratory. *Geotech Geol Eng* 22:313–330.
- Palleske C, Lato MJ, Hutchinson DJ, Elmo D, Diederichs MS (2013) Impacts of limited spacing and persistence data on DFN modelling of rockmasses. In: Proceedings of the Canadian geotechnical society GeoMontreal conference, 2013.
- Vlachopoulos, N., Vazaios, I., Forbes, B. et al. (2020) Rock Mass Structural Characterization Through DFN–LiDAR–DOS Methodology. *Geotech Geol Eng* 38, 6231–6244. <https://doi.org/10.1007/s10706-020-01431-1>



Theme 1

Rock Mechanics and Rock Testing



Damage during stress relaxation in brittle rocks – recent findings from laboratory experiments

Walton, G.¹, Shirole, D.², Hedayat, A.¹, Paraskevopoulou, C.³, Perras, M.A.⁴

¹Colorado School of Mines, Golden, Colorado, USA

²IIT Delhi, Delhi, India

³University of Leeds, Leeds, UK

⁴York University, Toronto, Ontario, Canada

EXTENDED ABSTRACT

Relaxation is the process of stress reduction under a constant strain boundary condition, and represents one end-member of the range of time-dependent rock deformation processes that occur in nature. For rocks that are initially loaded to a sufficiently high stress, the relaxation process is associated with progressive damage development. In this presentation, findings from analysis of laboratory relaxation test data on two rocks, Stanstead Granite and Jurassic Limestone, are presented. A method for separately quantifying micromechanical tensile and shear damage is presented based on Digital Image Correlation (DIC).

EXPERIMENTAL PROGRAM

A total five single-stage relaxation tests were performed on Stanstead Granite, with two tests initiating relaxation at stresses between the crack initiation (CI) and crack damage (CD) thresholds, and three tests initiating relaxation at a driving stress just above CD. DIC and active ultrasonic monitoring data were collected during these tests. Additionally, relaxation test data from a cylindrical specimen of a low-porosity Jurassic Limestone with a driving stress just above CD were re-analyzed to evaluate trends in dilatancy.

SUMMARY

Analysis of Stanstead Granite data demonstrates that the degree of shear damage that occurs during relaxation is minimal relative to that experienced under comparable monotonic loading conditions (Figure 1), and the transition from primary to secondary relaxation is associated with a decrease in the proportion of damage associated with shear mechanisms. As an associated finding, relaxation damage is found to be more dilatant than damage under monotonic loading conditions, and this is attributed to relaxation-induced damage being more diffuse than that induced by monotonic loading. However, the overall trends in dilatancy as a function of damage evolution during relaxation are consistent with those expected under monotonic loading conditions, as demonstrated using Jurassic Limestone test data (Figure 2).

REFERENCES

- Shirole, D., Walton, G., and Hedayat, A. Characteristics of tensile and shear damage evolution during primary and secondary relaxation of Stanstead granite. Submitted to International Journal of Rock Mechanics and Mining Sciences May 2022.
- Walton, G., Paraskevopoulou, C., and Perras, M.A. Time-dependent volume change of brittle limestone during stress-relaxation. In preparation.

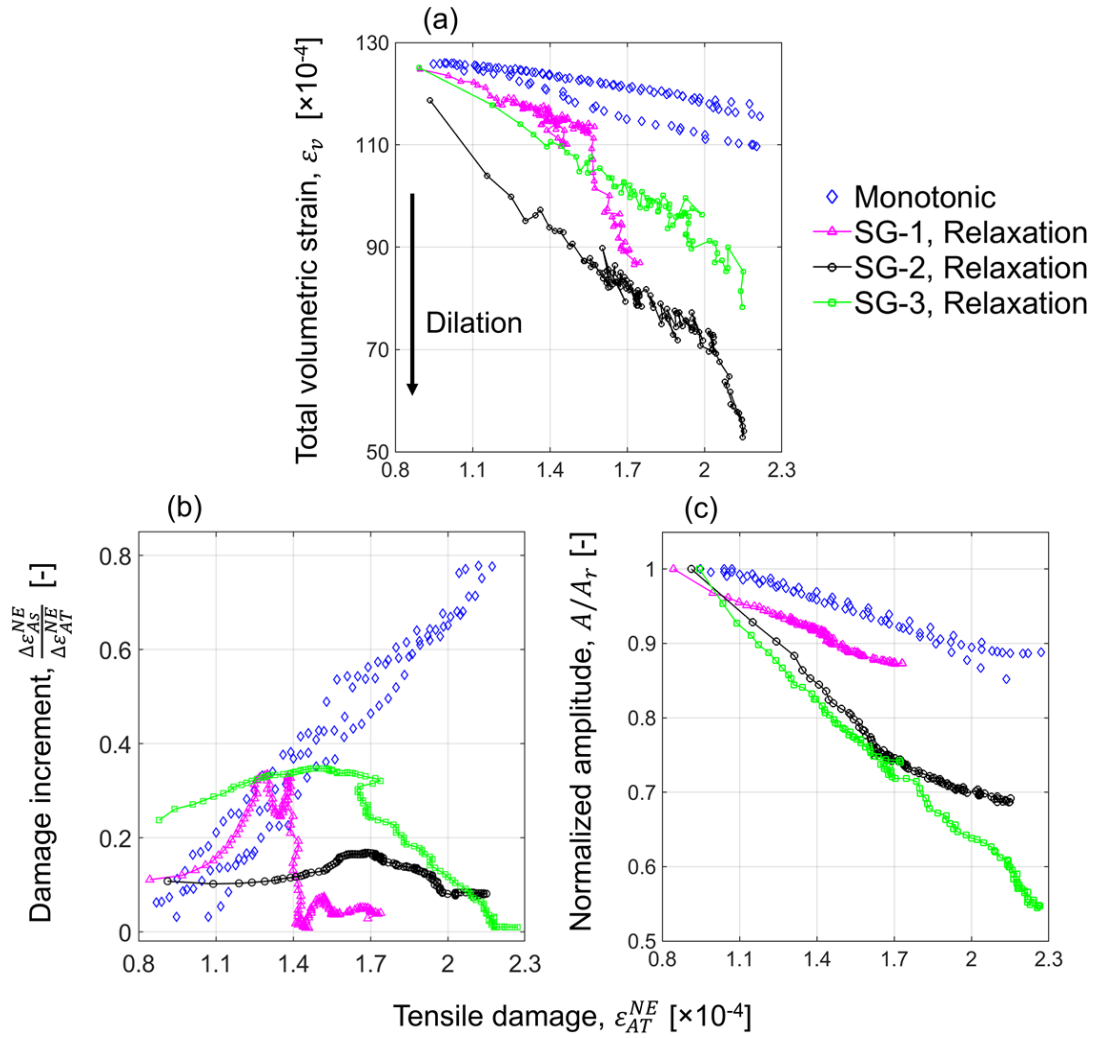


Figure 1: Comparison of rock behavior during monotonic UCS loading and stress relaxation having equivalent tensile damage: (a) evolution of total volumetric strains (normalized); (b) evolution of the ratio of the incremental change in tensile damage to incremental change in shear damage; and (c) modulation in ultrasonic wave amplitude (normalized) (Shirole et al., under review).

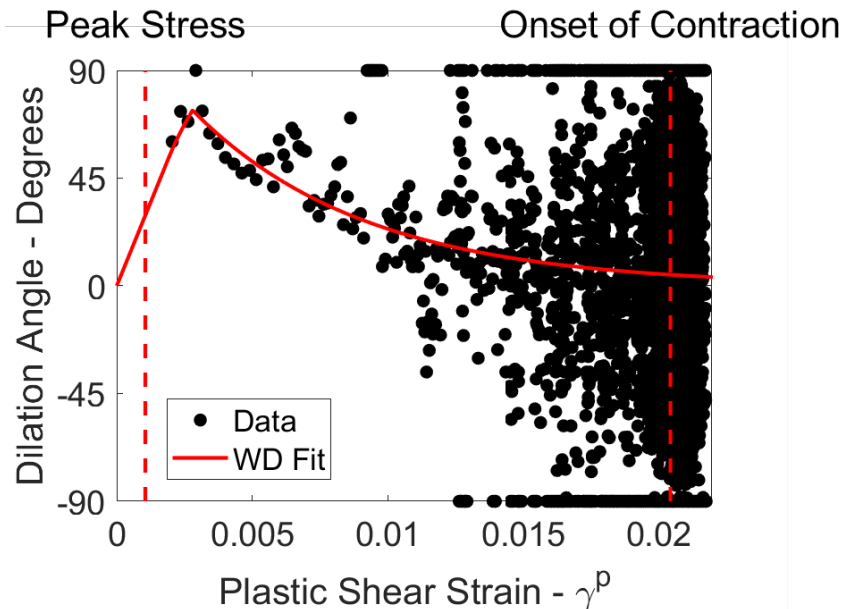


Figure 2: Trend in dilation angle for a Jurassic Limestone specimen under relaxation conditions with a driving stress just above the crack damage threshold (Walton et al., under review).



Micro-mechanical modelling of core damage

Bahrani, N.

Civil and Resource Engineering, Dalhousie University, Halifax, Nova Scotia, Canada

EXTENDED ABSTRACT

This paper presents the results of two numerical modeling approaches developed to simulate drilling-induced core damage. In the first method, the coring stress path obtained from a 3D elastic continuum model was applied to a calibrated 2D discontinuum model to create damage in the form of micro-cracks. In the second method, the core drilling process and core damage were explicitly simulated using a 3D discontinuum model. The damage mechanism during overcoring in high-stress environments is also discussed in this paper.

INTRODUCTION

The Unconfined Compressive Strength (UCS) and Young's modulus (E) of intact rock are two fundamental parameters required for the design of deep underground excavations. These parameters are usually determined from laboratory unconfined compression tests on cored samples. It is known that the process of core drilling from deep boreholes may induce damage to the cored samples in the form of micro-cracks (Figure 1a). This is caused by stress concentration at the rock-drill bit contact points and tensile stresses generated inside the core during drilling. Drilling-induced core damage may affect the mechanical properties of rock specimens, including strength and deformation properties. Figure 1b presents the stress-strain curves of undamaged and damaged Lac du Bonnet (LdB) granite. It is evident from this figure that the strength and Young's modulus of the damaged specimen are lower than those of the undamaged specimen. A clear indicator of core damage is the strong nonlinearity in the stress-strain curve of the damaged specimen, caused by the closure of micro-cracks during the initial stage of uniaxial loading. Another consequence of core damage which could lead to design errors is the incorrect estimation of in situ stress magnitudes determined from techniques based on elastic properties, such as overcoring.

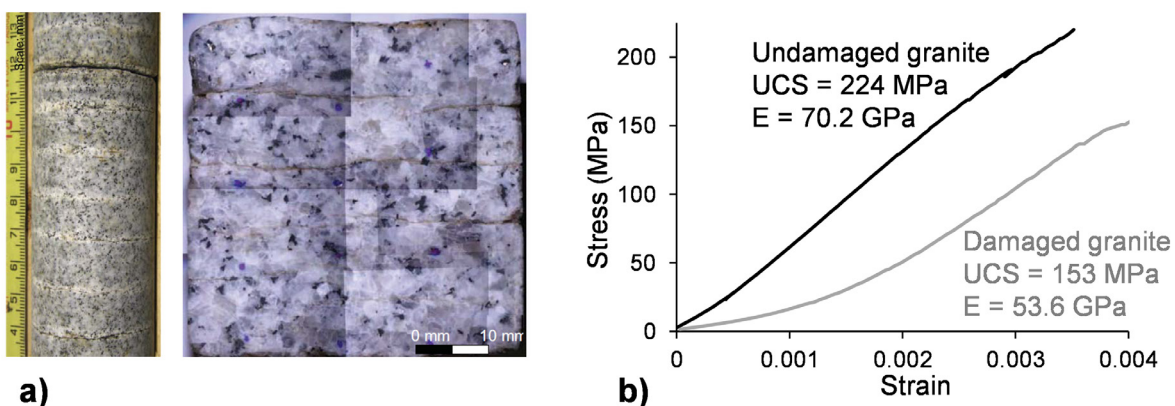


Figure 1: a) Examples of partial core disk and drilling-induced micro-cracks (Lim and Martin, 2010); b) stress-strain curves of undamaged and damaged Lac de Bonnet granite (courtesy of Derek Martin and Erik Eberhardt).

This paper summarizes the results of over a decade of research on drilling-induced core damage, utilizing two numerical modeling programs based on the Distinct Element Method (PFC and 3DEC by Itasca). The numerical simulations were conducted to reproduce the results of laboratory tests on LdB granite from Canada's Underground Research Laboratory (URL), considering the in situ stress state at its 420 level ($\sigma_1 = 60$ MPa; $\sigma_2 = 45$ MPa; $\sigma_3 = 11$ MPa).

INDIRECT MODELING OF DRILLING-INDUCED CORE DAMAGE

Several researchers have used continuum and discontinuum numerical methods to simulate drilling-induced core damage and dinking (e.g., Corthésy and Leite, 2008; Wu et al., 2018). Bahrani et al. (2015) developed an indirect approach to simulate core damage. This approach differs from other studies in that instead of explicitly simulating core drilling using a 2D axisymmetric or a 3D model, they obtained the coring stress path from a 3D elastic continuum model (i.e., black curve in Figure 2a) and applied it to a calibrated 2D discontinuum model. The clump logic in PFC was adopted to simulate a rock specimen with irregular shaped grains. First, the clumped specimen was calibrated to the properties of undamaged LdB granite (UCS = 213 MPa, $E = 65$ GPa). Next, an approximate coring stress path for a vertical borehole (i.e., gray arrows in Figure 2a) was applied to the calibrated undamaged clumped specimen to introduce damage in the form of micro-cracks. As shown in Figure 2b, the micro-cracks are nearly horizontal (i.e., subparallel to σ_1 direction) and randomly located within the specimen, although some signs of localization (i.e., incipient dinking) can be observed. In the next step, a UCS test was simulated on the damaged clumped specimen to match the properties of damaged LdB granite (Figure 2c).

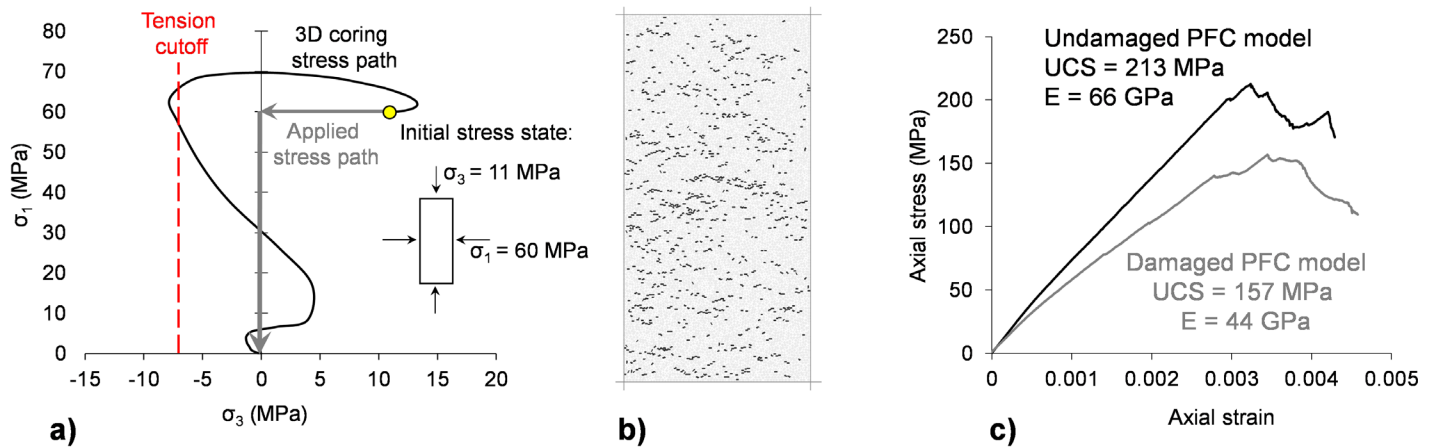


Figure 2: a) 3D coring stress path obtained from a finite element model and its approximate path applied to a calibrated PFC model; b) damaged PFC model; and c) stress-strain curves of undamaged and damaged PFC models (after Bahrani et al., 2015).

The stress-strain curves of the clumped specimens shown in Figure 2c indicate that the damaged specimen has a lower peak strength and elastic modulus than the undamaged specimen. However, the initial nonlinearity in the stress-strain response of damaged LdB granite is not captured by this model, suggesting that the simulated micro-cracks were not open. This could be due to the applied stress path, which only covered the reduction of the σ_3 magnitude in the compression zone (applied stress path in gray in Figure 2a). It is postulated that the application of tensile stresses to the clumped specimen to better match the 3D coring stress path, which exceeds the tension cutoff (black curve in Figure 2a), could have resulted in micro-crack opening during unloading, and subsequently micro-crack closure during loading and nonlinear stress-strain response.

DIRECT MODELING OF DRILLING-INDUCED CORE DAMAGE

To overcome the limitations of the indirect modeling approach described above, Bahrani and Valley (2020) used 3DEC to simulate drilling-induced core damage. The simulated core consisted of several tetrahedral blocks

bonded together at their triangular faces (contacts). This model is referred to as the Bonded Block Model (BBM). In the BBM, the blocks representing mineral grains were simulated as an elastic material forcing the failure to occur at the grain boundaries. The numerical simulations consisted of three main steps: 1) a 3D BBM representing a laboratory-scale rock specimen was first developed in 3DEC and calibrated to the laboratory properties of undamaged LdB granite; 2) a larger 3DEC model consisting of continuum and discontinuum domains was constructed to explicitly simulate core drilling from a vertical borehole (Figure 3a & b) and associated core damage (Figure 3c); and 3) the continuum domain was deleted and the damaged BBM was loaded uniaxially to match the properties of damaged LdB granite. After several calibration attempts, it was found that although the damaged BBM exhibits a lower peak strength and Young's modulus compared to the undamaged BBM (Figure 3d), it is not possible to match both parameters in a single model, meaning that either the peak strength or the elastic modulus of the BBM could be matched with those of damaged LdB granite. As a possible solution, Bahrani and Valley (2020) suggested using a BBM with 3D Voronoi blocks. An important finding from this research is the ability to capture the nonlinearity in the stress-strain response (Figure 3d), which is interpreted to be caused by the closure of micro-cracks opened due to tensile stresses generated inside the core during drilling.

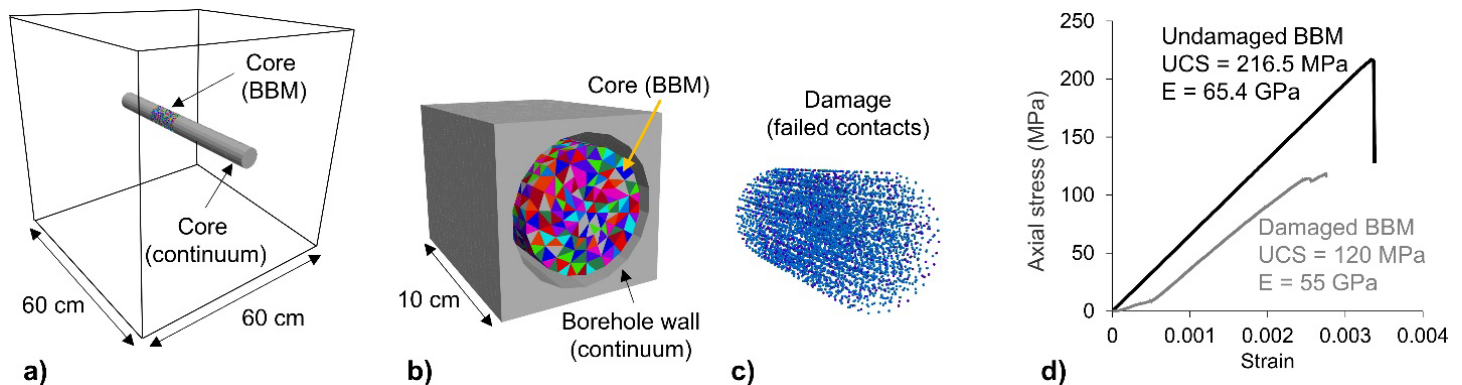


Figure 3: a) 3DEC model showing the core in the continuum and discontinuum (i.e., BBM) domains; b) close view of the BBM representing the core after drilling; c) simulated damaged core (failed contacts in BBM) from a vertical borehole at the 420 level of the URL; and d) stress-strain curves of undamaged and damaged BBMs.

DAMAGE MECHANISMS DURING OVERCORING

Overcoring is one of the most common in situ stress measurement techniques. The overcoring process involves drilling a small diameter pilot hole far from an excavation, installing a strain cell inside the hole (top image in Figure 4a), and overcoring the cell while continuously monitoring the strain response (top image in Figure 4b). The overcored sample is then loaded and unloaded biaxially in the field immediately following recovery to obtain its elastic properties (i.e., E and ν). In high-stress environments, it is expected that overcored samples from boreholes drilled at angles nearly perpendicular to the σ_1 direction exhibit the greatest amount of stress-induced micro-cracking, potentially creating anisotropy in the overcore (Martin and Christiansson, 1991). In such situations, the overcore is also loaded axially and the response of axial and diagonal strain gauges is checked for potential nonlinearity.

Two mechanisms could lead to damage to the overcore: 1. borehole wall damage during pilot hole drilling; and 2) core damage during overcoring. The stress path near the wall of the pilot hole is similar to that of a tunnel (black curve in Figure 4c). Therefore, if the induced compressive stresses exceed the crack initiation threshold, damage near the pilot hole wall occurs prior to the strain cell installation (bottom image in Figure 4a). The stress path within the overcore during overcoring is similar to that of a core during drilling (grey curve in Figure 4c). This means that if the tensile stresses exceed the tensile strength, further damage to the overcore may occur following the strain cell installation (bottom image in Figure 4b). These two mechanisms could result in a highly damaged overcore, leading to erroneous estimates of stress magnitudes.

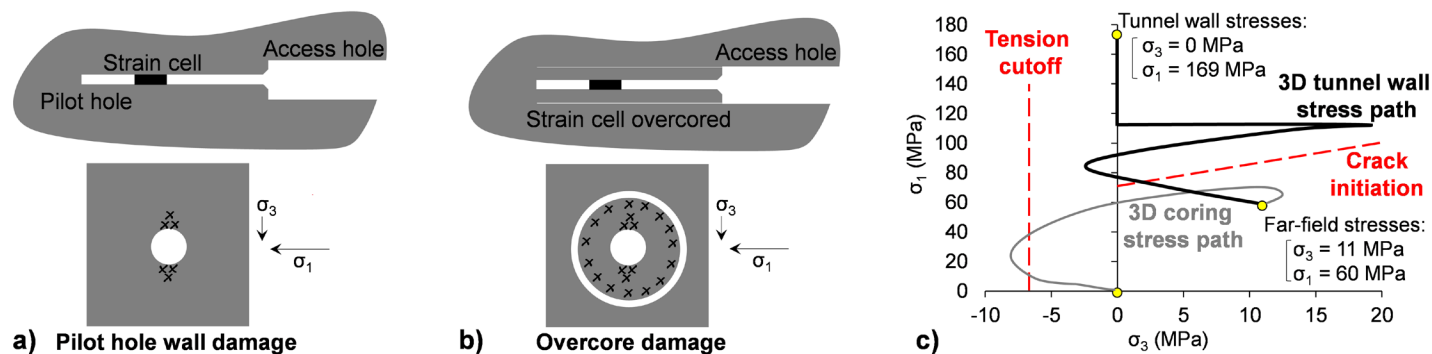


Figure 4: Schematic of overcoring process and associated damage: a) strain cell installed in a pilot hole; b) cell overcored using a thin-walled core barrel; c) comparison of 3D stress paths in the roof of a tunnel driven parallel to σ_2 direction and for a point inside a core from a horizontal borehole parallel to σ_2 direction (after Bahrani et al., 2019).

PATH FORWARD

Research is ongoing to investigate the influence of 3D coring and overcoring stress paths on micro-cracking and associated reduction in strength and deformation modulus. In this regard, 3D models will be used to simulate the overcoring process and better understand micro-cracking mechanisms. The objective is to develop tools that can reliably predict the level of core damage and associated changes to the properties of rock and account for their impact on stress magnitudes estimated using various measurement techniques.

ACKNOWLEDGEMENTS

The author wishes to thank Drs. Peter Kaiser and Benoît Valley for many years of collaboration and their contributions to this research. The financial support by NSERC and Rio Tinto is acknowledged.

REFERENCES

- Bahrani, N., and Valley, B. 2020. Capturing non-linear stress-strain response of brittle rocks due to closure of coring-induced micro-cracks using 3D bonded block model. In Proceedings of 54th US Rock Mechanics/Geomechanics Symposium, Golden, Colorado, USA, paper 1471, 9p.
- Bahrani, N., Valley, B., and Kaiser, P.K. 2015. Numerical simulation of drilling-induced core damage and its influence on mechanical properties of rocks under unconfined condition. *International Journal of Rock Mechanics and Mining Sciences*, 80: 40–50.
- Bahrani, N., Valley, B., and Kaiser, P.K. 2019. Influence of stress path on stress memory and stress fracturing in brittle rocks. *Canadian Geotechnical Journal*, 56(6): 852–867.
- Corthésy, R., and Leite, M.H. 2008. A strain-softening numerical model of core discing and damage. *International Journal of Rock Mechanics and Mining Sciences*, 45: 329–50.
- Lim, S.S., and Martin, C.D. 2010. Core discing and its relationship with stress magnitude for Lac du Bonnet granite. *International Journal of Rock Mechanics and Mining Sciences*, 47: 254–264.
- Martin, C.D., and Christiansson, R. 1991. Overcoring in highly stressed granite – the influence of microcracking. *International Journal of Rock Mechanics and Mining Sciences & Geomechanics Abstract*, 28: 53–70.
- Wu, S., Wu, H., and Kemeny, J. 2018. Three-dimensional discrete element method simulation of core discing. *Acta Geophysica*, 66: 267–282.



The Leeb Hardness Test for use in rock engineering practice

Corkum, A.G.

Dalhousie University, Halifax, Nova Scotia, Canada

EXTENDED ABSTRACT

The Leeb Hardness test (LHT with test value of L_D) is a rebound hardness test, originally developed for metals, that has been correlated to the Unconfined Compressive Strength (UCS with test value σ_c) of rock. The test is rapid, convenient, and non-destructive and can be carried out on drill core, block specimens or on rock outcrops. The low impact energy of the device makes it sensitive to surface conditions which makes it effective for determination of rock joint surface hardness. This makes the highly portable LHT device convenient for field testing and rock characterization.

LEEBS HARDNESS TEST FOR ROCK STRENGTH ESTIMATION

A standard methodology, (e.g., ISRM-SM) for the LHT in rock engineering has not yet been developed and various authors have explored different test methods (e.g., Asef 1995, Meulenkamp 1997, Verwaal and Mulder 1993, Corkum et al. 2018 and Desarnaud et al. 2019). Several main methodology issues were identified and investigated at Dalhousie over the course of multiple studies, specifically focused on the following.

1. Specimen size (scale effects) for core or block specimens to produce a repeatable test value (L_D)
2. Specimen surface conditions and roughness for test impacts.
3. The number of impacts that should comprise an average “test result” (L_D) and how L_D should be calculated from multiple readings (e.g., mean, average, trimmed mean).
4. Whether repeated impacts should be made at single point or over a specified specimen surface area.
5. Development of a robust correlation of L_D to σ_c .

A recommended methodology was proposed by Corkum et al. (2018) which addressed the issues described above. A large data set was compiled and used to develop a general L_D to σ_c correlation (shown in Figure 1) with additional correlations for specific rock types (sedimentary, metamorphic, and igneous). A current limitation of the data set is the limited data in the R1 range. The data set is available via an online repository (Corkum et al. 2021) and has been recently updated (Séguin et al. 2022). With the proposed methodology and L_D to σ_c correlation, the LHT provides an objective method of estimating rock σ_c that is improved over the ISRM field estimation method (ISRM 1981) which utilizes more qualitative means such as blows from geological hammer.

It has not been verified if the LHT provides a ‘better’ estimate of σ_c than the Schmidt hammer or other index tests (e.g., point load test); however, the LHT has been reported by Aoki and Matsukura (2007) to be applicable over a wider range of rock hardness than other index tests. Figure 2, modified after Aoki and Matsukura (2007), shows the range of applicability of the LHT relative to several other index tests. One key difference between the Schmidt and the LHT is that the LHT impact imparts a fraction of the energy of the Schmidt hammer (11 Nmm vs 0.74 Nm, respectively) and is thus more sensitive to local surface conditions. It is this sensitivity to local conditions that make the LHT a good option to evaluate joint surface hardness, particularly for graded or coated ‘composite’ surfaces such as weathered or altered joint surfaces.

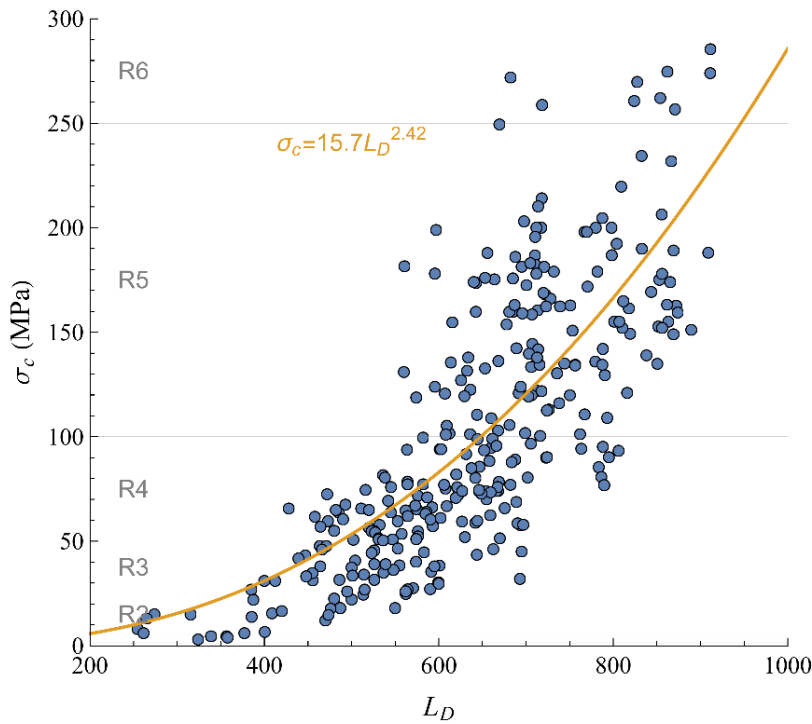


Figure 1: LHT data set and the L_D to σ_c general correlation.

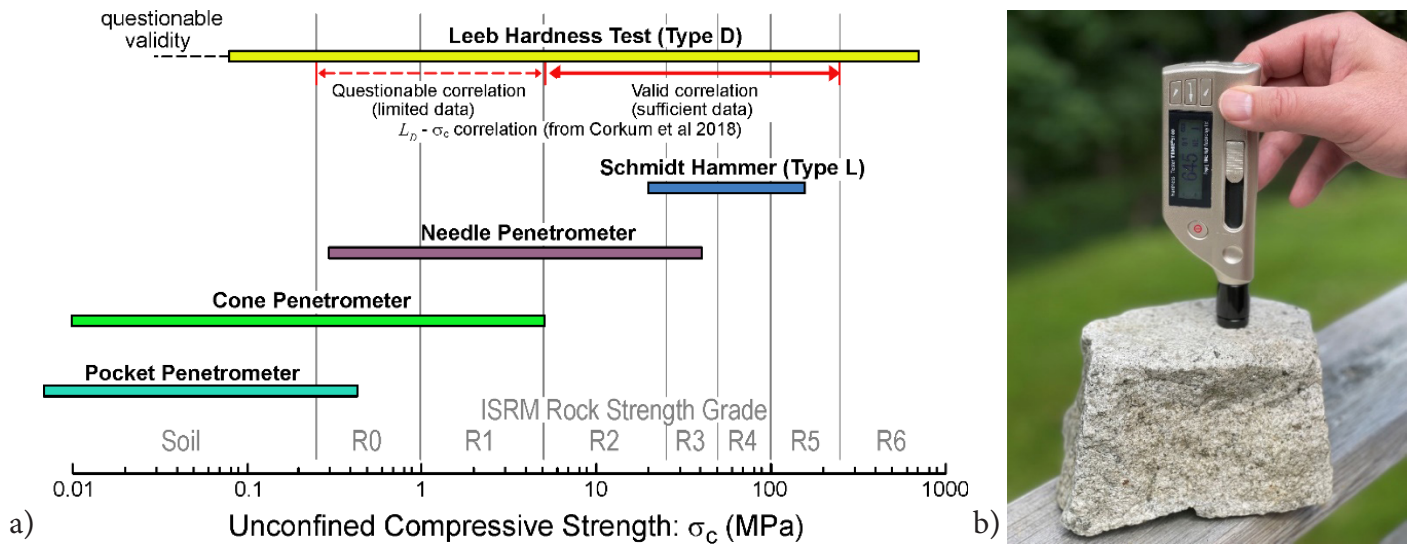


Figure 2: Leeb Hardness test is a convenient and effective tool for rock engineering; a) Range of applicability of the LHT (after Aoki and Matsukura 2007); b) The Leeb hardness test device.

LEEB HARDNESS TEST FOR JOINT WALL COMPRESSIVE STRENGTH DETERMINATION

Hack et al. (1993) generated an L_D profile of a weathered rock surface by sequentially gridding the surface and conducting LHT on each subsequent surface. They observed a zone where the surface ('Secondary' material) readings were influenced by the underlying harder, unweathered intact rock ('Primary' material). When combined with the L_D to σ_c correlations, the sensitive LHT offers a good option for objective quantifiable prediction of Joint Wall Compressive Strength (JCS) for the widely used Barton-Bandis (1990) joint shear strength criterion. However, for application of the LHT to JCS determination, an important issue is to determine what thickness of material below the surface affects the surface L_D reading. This is particularly important for joints surfaces with coatings and graded hardness (e.g., weathering and alteration).

The ‘Influence Zone’ thickness (t_{iz}) was investigated using artificial plaster composite specimens of contrasting but known hardness. The composite specimens comprised a plaster mixture (soft) and Wallace sandstone (hard) adhered during curing to form 50 mm diameter cylindrical composite specimens. The composite specimens were then ground down in sequential thin layers and LHTs were conducted on each surface to create an L_D profile. The exercise was conducted both for cases of grinding the plaster end and then with grinding the sandstone end. The L_D profiles revealed that t_{iz} is approximately 2 mm or less in both cases and L_D measured a distance (d_s) greater than t_{iz} from the contact between materials is unaffected by the underlying material hardness.

To gain further insight into JCS determination with the LHT, a series of L_D profiles were obtained on natural rock specimens. A series of natural rock surfaces containing material contacts (composite rock surfaces) and weathered surfaces with hardness gradients were used in the study. The rock block specimens were collected from various locations in Nova Scotia and Prince Edward Island. At the laboratory, various block samples were saw-cut to form prismatic block specimens. These specimens were ground down in sequential thin layers and LHTs were conducted on each surface to create L_D profiles for each natural rock block specimen. The L_D to σ_c correlation in Figure 1 was then used to provide JCS_L (Leeb correlation determined value) as a profile into the rock surface, as shown in Figure 3. The LHT JCS determination study was documented by Jeans (2021) and has been submitted for journal publication (Corkum et al. 2022).

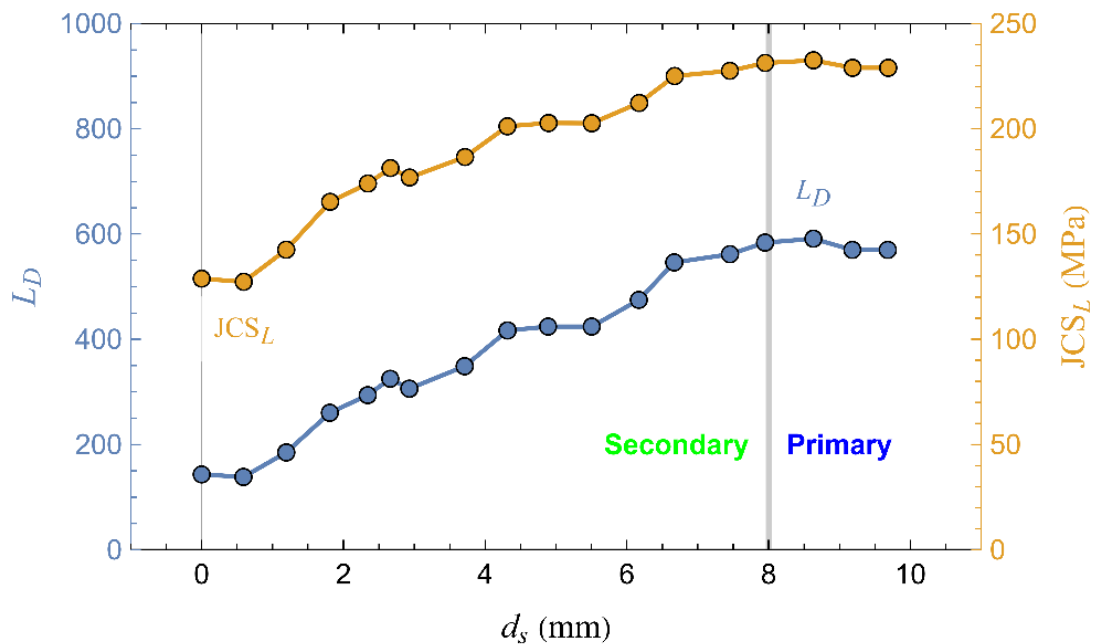


Figure 3: Typical profile of L_D for a graded surface along with JCS_L from the L_D to σ_c correlation.

Further study is needed to evaluate the most suitable means of utilizing profile, such as the one in Figure 3, for JCS determination. Should L_D measure at the surface be sufficient, or should the profile of measurements be averaged over a certain depth into the rock joint surface? The joint roughness, normal stress range and other factors may also warrant consideration and future study.

ACKNOWLEDGEMENTS

The author wishes to acknowledge BGC Engineering Inc (especially Derek Kinakin) and SKB (especially Diego Mas Ivars) for funding support and technical contributions. The work presented in this abstract is based on research conducted in two MASc programs by Yassir Asiri and Brock Jeans.

REFERENCES

- Aoki H, Matsukura Y (2007) A new technique for non-destructive field measurement of rock-surface strength: an application of the Equotip hardness tester to weathering studies. *Earth Surf Proc Land* 32:1759–1769. <https://doi.org/10.1002/esp.1492>
- Asef MR (1995) Equotip as an index test for rock strength properties. PhD thesis
- Barton NR, Bandis SC (1990) Review of predictive capabilities of JRC-JCS model in engineering practice. In: *Rock Joints, Proc Int Symp on Rock Joints, Loen, Norway* (eds N. Barton and O. Stephenson). pp 603–610
- Corkum A, Ghasemi M, Asiri Y, Kinakin D (2021) Leeb Hardness Test and UCS Correlation Data for Rock (V1), <https://doi.org/10.5683/SP2/O52YXA>
- Corkum A, Asiri Y, El Naggar H, Kinakin D (2018) The Leeb Hardness Test for rock: An updated methodology and UCS correlation. *Rock Mech Rock Eng* 51:665–675. <https://doi.org/10.1007/s00603-017-1372-2>
- Corkum A, Jeans B, Mas Ivars D (2022) Leeb Hardness Test as a Tool for Joint Wall Compressive Strength (JCS) Evaluation. *International Journal of Rock Mechanics and Mining Sciences* (Submitted)
- Desarnaud J, Kiriya K, Bicer Simsir B, et al (2019) A laboratory study of Equotip surface hardness measurements on a range of sandstones: What influences the values and what do they mean? *Earth Surf Proc Land* 44:1419–1429. <https://doi.org/10.1002/esp.4584>
- Hack H, Hingira J, Verwaal W (1993) Determination of discontinuity wall strength by Equotip and ball rebound tests. *Int J Rock Mech Min* 30:151–155. [https://doi.org/10.1016/0148-9062\(93\)90707-K](https://doi.org/10.1016/0148-9062(93)90707-K)
- ISRM (1981) Rock characterization, testing and monitoring: ISRM suggested methods. In: Brown T (ed) *ISRM Yellow Book*. Pergamon Press, Oxford
- Jeans B (2021) Leeb Hardness Test for Rock Joint Wall Compressive Strength Evaluation. MSc, Dalhousie University
- Meulenkamp F (1997) Improving the prediction of the UCS by Equotip readings using statistical and neural network models. *Memoirs of the Centre for Engineering Geology in the Netherlands* 162:85–101
- Séguin K, Kinakin D, Corkum A (2022) An Updated Database and UCS-Leeb Hardness Correlation. In *Proceedings: RockEng22, 22nd Canadian Rock Mechanics Symposium, Kingston, Ontario*.
- Verwaal W, Mulder A (1993) Estimating rock strength with the Equotip hardness tester. *Int J Rock Mech Min* 30:659–662. [https://doi.org/10.1016/0148-9062\(93\)91226-9](https://doi.org/10.1016/0148-9062(93)91226-9)



The Wild and Wonderful Adventures of Applying Rock Mechanics to Volcanology

Villeneuve, M.C.

Montanuniversität Leoben, Leoben, Austria

EXTENDED ABSTRACT

The study of volcanology is traditionally covered by experimental volcanology, field volcanology, geochemistry, rheology, geophysics and analytical modelling. Recent developments have consisted of applying rock mechanics and rock engineering techniques to volcanology, including field, laboratory and numerical modelling techniques. This abstract highlights how laboratory experiments focussing on strength, stiffness and permeability have demonstrated the complexity of volcanic rocks. This abstract also presents how these laboratory results have been used to develop conceptual models of volcanic processes, which can help with decision making regarding volcano monitoring and hazard assessment.

EFFECT OF POROSITY, TEXTURE AND ALTERATION ON PHYSICAL AND MECHANICAL PROPERTIES

Volcanoes are spatially and temporally complex rock environments due to the dynamic processes which form, deform and destroy them (Figure 1). This presents a considerable challenge for characterising the rock masses in volcanic environments, while also presenting the opportunity to use rock mechanics and rock engineering tools to help better understand volcanic processes. The key geological characteristics that differentiate volcanic rocks are the texture and mineralogy, linked to the emplacement and subsequent alteration and weathering history.

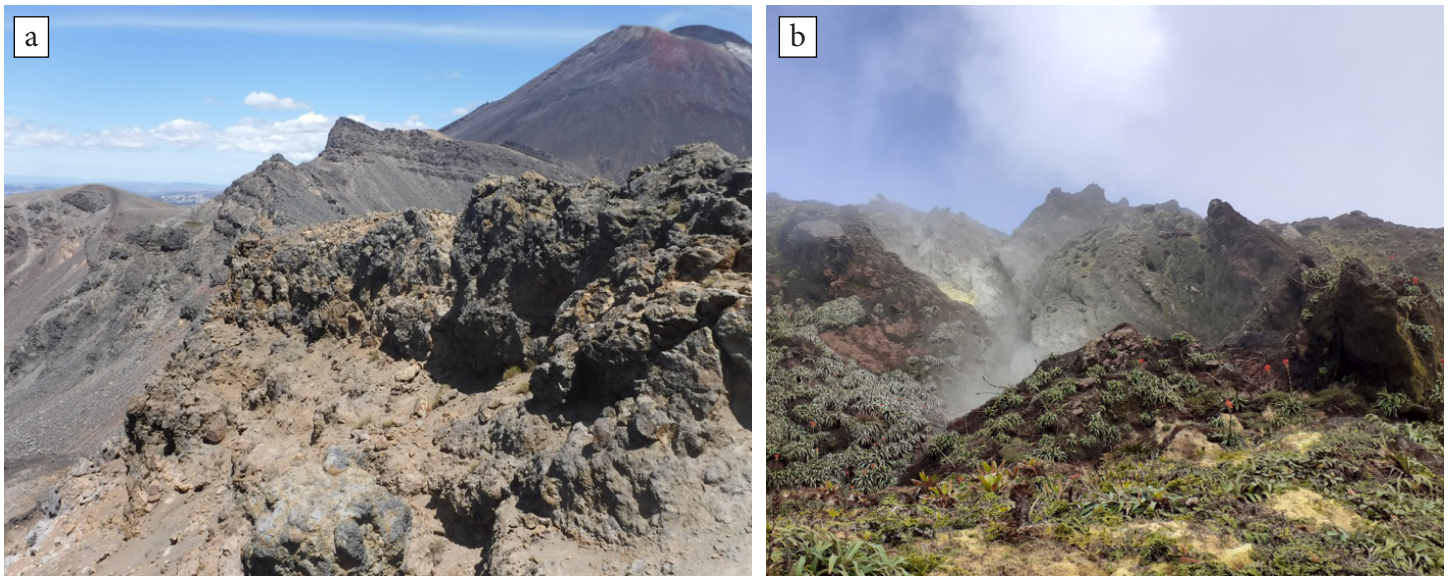


Figure 1: Highly variable rock masses in dynamic volcanic environments (a) lavas with variable texture and alteration on Tongariro volcano (New Zealand), with Ngauruhoe volcano in the background; (b) sulfuric fumarole on the lava dome of La Soufrière de Guadeloupe.

With a focus on andesite, which is an intermediate extrusive volcanic rock that forms many volcanic complexes, considerable laboratory experimentation has established that the physical and mechanical properties are affected by porosity, texture and alteration, as seen in Figures 2–4. Porosity consistently reduces strength and elastic stiffness (see reviews by Heap et al. 2020 and Heap and Violay, 2021), while increasing permeability (e.g. Villeneuve et al., 2019). Texture and alteration interact together to both increase and decrease strength, stiffness and permeability by concurrently reducing porosity through precipitation, increasing porosity through dissolution and changing the mineralogy by replacing primary minerals with higher porosity, lower strength and lower stiffness secondary minerals (e.g. Mordensky et al., 2019; Mordensky et al., 2022). Porosity, texture and mineralogy also affect the brittle to ductile transition, where rocks with higher porosity, such as brecciated lava, as well as more intensely altered dense lava transition to ductile behaviour at lower confinement than low porosity, unaltered lava (e.g. Mordensky et al., 2022).

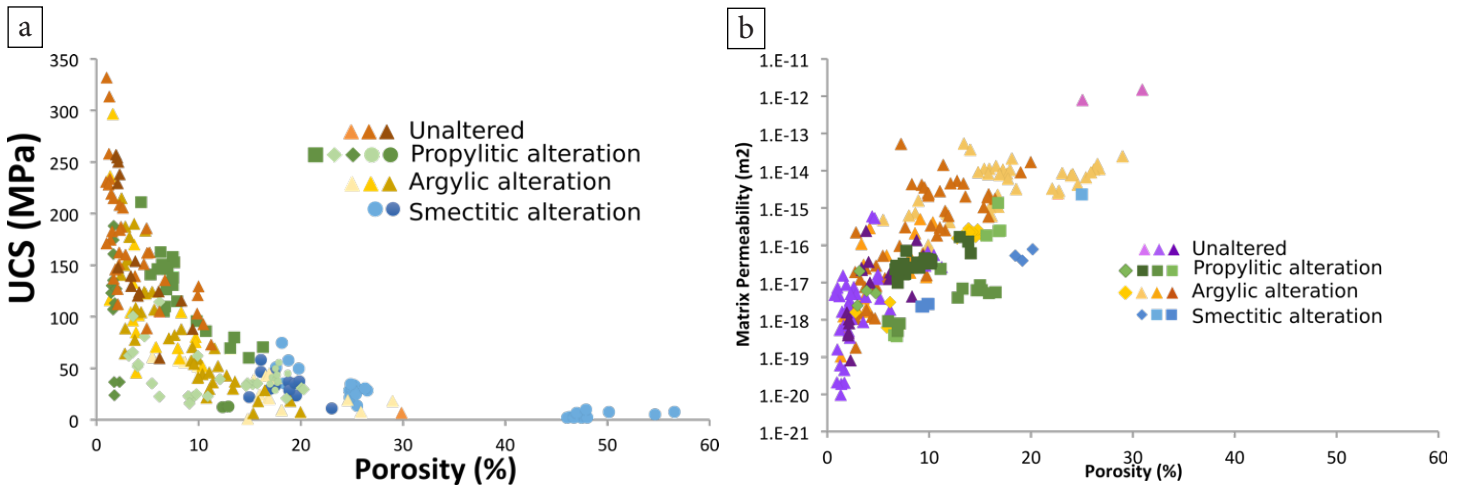


Figure 2: Effect of porosity, texture and alteration on strength (a) and permeability (b). (modified from Villeneuve et al., 2019).

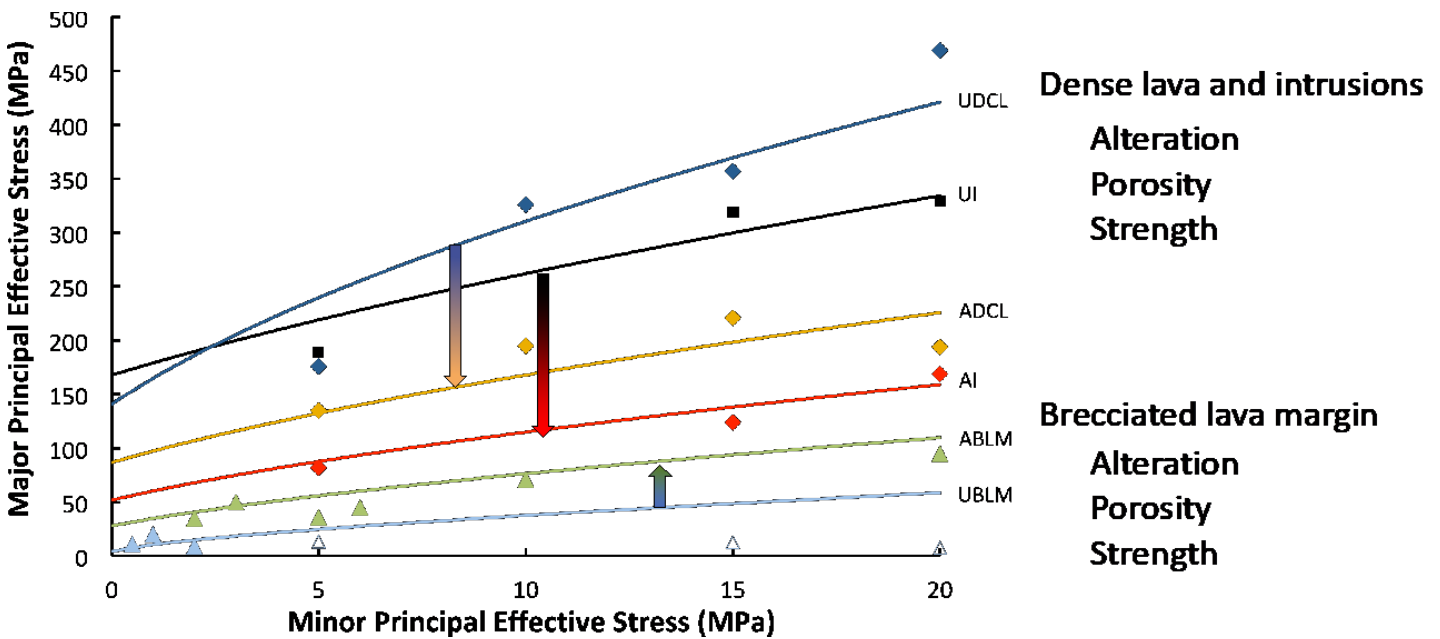


Figure 3: Effect of porosity, texture and alteration on failure criterion (modified from Mordensky et al., 2022).

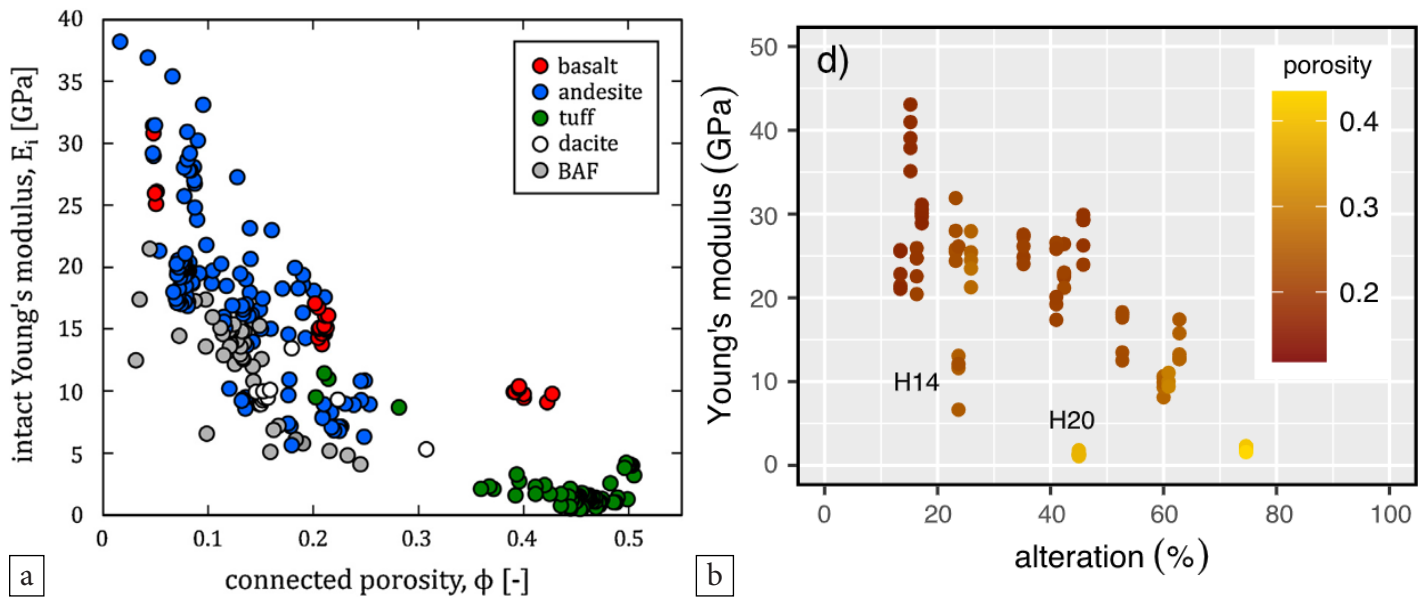


Figure 4: Effect of porosity and texture and alteration on elastic stiffness (a) (Heap et al., 2020), and effect of porosity and alteration on elastic stiffness (b) (Heap et al., 2021).

ROCK MECHANICS HELPING TO UNDERSTAND VOLCANOLOGICAL PROCESSES

The laboratory strength experiments on variably altered dense and brecciated andesite lava from Ruapehu volcano (New Zealand) provided evidence that altered lava behaves in a ductile manner at moderate confining pressures corresponding to 500 m to 1–2 km depth, and an explanation for the lack of pre-eruption seismicity in some altered volcanoes (Figure 5, a), like Ruapehu (Mordensky et al, 2019). Laboratory permeability experiments on intact and tensile fractured specimens demonstrated that altered, higher porosity andesite collected from the conduit at Whakaari volcano (New Zealand) have higher matrix permeability than unaltered, lower porosity andesite, however the tensile fractures for both rock types have similar permeability (Kennedy et al., 2020). In addition, the permeability of the tensile fractures in the altered andesite has a larger decrease with increasing confinement than those in the unaltered andesite. These findings were used to generate a conceptual model of opening and closing of fluid flow pathways related to dissolution, precipitation, tensile fracturing and crack closure within the rock mass comprising and surrounding the conduit at Whakaari volcano (Figure 5, b). Pressure builds up when flow pathways are closed, then is rapidly released as a phreatic eruption, followed by quiescence and renewed precipitation and crack closure (Kennedy et al., 2020).

SUMMARY

A large number of physical and mechanical experiments on a variety of volcanic rocks has provided the basis for developing evidence-based conceptual models of volcanic processes. There remain many volcanic processes that will benefit from combining traditional volcanology with rock mechanics and rock engineering, and the generation of good quality data that reflects volcanic rocks' unique challenges will enable the development of well-supported conceptual models. Physical characteristics, such as porosity, primary and secondary texture, primary and secondary mineralogy, as well as alteration, are key to making rock mechanics data meaningful in complex, heterogenous and dynamic volcanic rock masses.

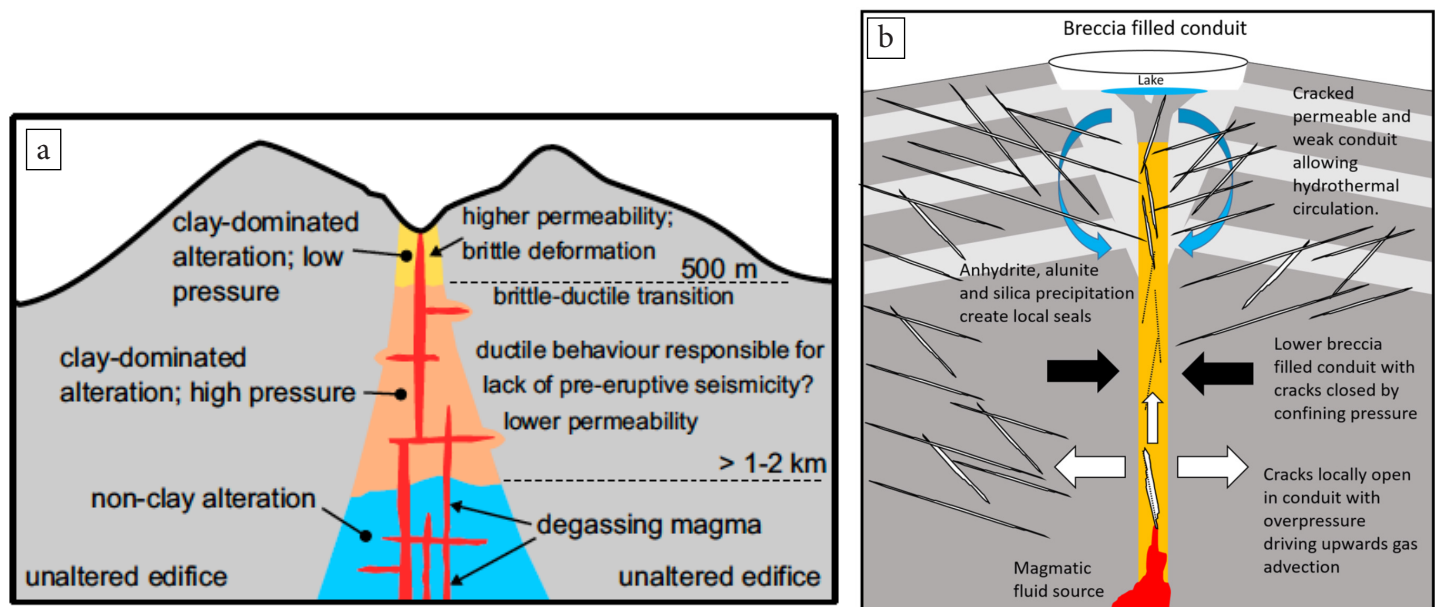


Figure 5: Conceptual models relating physical and mechanical parameters to volcanic processes. a) low seismicity at moderate depths in Ruapehu volcano resulting from ductile altered volcanic rocks at moderate confinement (Mordensky et al., 2019); b) over pressurisation in Whakaari volcano due to fluid flow pathway closure by precipitation in pores and fracture closure of soft altered rocks (Kennedy et al., 2020).

ACKNOWLEDGEMENTS

The author wishes to acknowledge students and collaborators Latasha Wyering, Paul Siratovich, Jonathan Mukhtar, Stefan Cook, Stan Mordensky, Elodie Saubin, Robin Hilderman, Lauren Schaefer, Marcos Rosetti, Cory Wallace, Theresa Maier, Mike Heap, Ben Kennedy, Hugh Tuffen, Marina Rosas-Carbajal for fantastic work in the lab and in the field, and working on fascinating volcanology issues.

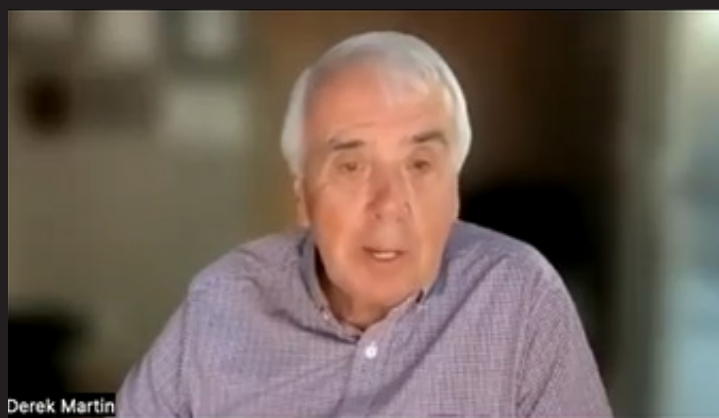
REFERENCES

- Heap, M.J., Villeneuve, M., Albino, F., Farquharson, J.I., Brothelande, E., Amelung, F., Got, J.-L., Baud, P. 2020. Towards more realistic values of elastic moduli for volcano modelling. *J Volcanol Geoth Res* 390, 106684. <https://doi.org/10.1016/j.jvolgeores.2019.106684>
- Heap, M.J., Baumann, T.S., Rosas-Carbajal, M., Komorowski, J., Gilg, H.A., Villeneuve, M., Moretti, R., Baud, P., Carbillat, L., Harnett, C., Reuschlé, T. 2021. Alteration-induced volcano instability at La Soufrière de Guadeloupe (Eastern Caribbean). *J Geophys Res Solid Earth*. <https://doi.org/10.1029/2021jb022514>
- Heap, M.J., Violay, M.E.S. 2021. The mechanical behaviour and failure modes of volcanic rocks: a review. *B Volcanol* 83. <https://doi.org/10.1007/s00445-021-01447-2>
- Kennedy, B.M., Farquhar, A., Hilderman, R., Villeneuve, M.C., Heap, M.J., Mordensky, S., Kilgour, G., Jolly, A., Christenson, B., Reuschlé, T. 2020. Pressure Controlled Permeability in a Conduit Filled with Fractured Hydrothermal Breccia Reconstructed from Ballistics from Whakaari (White Island), New Zealand. *Geosciences* 10(138). <https://doi.org/10.3390/geosciences10040138>
- Mordensky, S.P., Heap, M.J., Kennedy, B.M., Gilg, H.A., Villeneuve, M.C., Farquharson, J.I., Gravley, D.M. 2019. Influence of alteration on the mechanical behaviour and failure mode of andesite: implications for shallow seismicity and volcano monitoring. *Bulleting of Volcanology* 81(44). <https://doi.org/10.1007/s00445-019-1306-9>
- Mordensky, S.P., Villeneuve, M.C., Kennedy, B.M., Struthers, J.D. 2022. Hydrothermally induced edifice destabilisation: The mechanical behaviour of rock mass surrounding a shallow intrusion in andesitic lavas, Pinnacle Ridge, Ruapehu, New Zealand. *Eng Geol* 305, 106696. <https://doi.org/10.1016/j.enggeo.2022.106696>
- Villeneuve, M., Kennedy, B., Gravley, D., Mordensky, S., Heap, M., Siratovich, P., Wyering, L., Cant, J. 2020. Characteristics of altered volcanic rocks in geothermal reservoirs. In *International Society of Rock Mechanics Congress Foz do Iguasu, Brazil, 13–18 September 2019*.



Theme 2

Rockmass Mechanics and Structure Networks



Influence of joint stiffness on a shale slope behaviour

Martin, C.D.¹, Rafiei Renani, H.², Stevenson, G.², and Watson, A.³

¹*University of Alberta, Edmonton, Alberta, Canada*

²*Klohn Crippen Berger, Vancouver, British Columbia, Canada*

³*BC Hydro, Vancouver, British Columbia, Canada*

EXTENDED ABSTRACT

Unloading of the ground is an inevitable outcome of tunnel and slope excavations and the induced ground behaviour is controlled by this unloading stress path. Deformation analyses of this unloading process uses input parameters that are obtained from loading tests carried out in either the laboratory or in situ. Seldom in rock engineering do we have opportunities to monitor in situ ground behaviour as we unload and reload a rock slope. In this paper we describe the observations made during the excavation unloading of a shale slope. We simulated the unload process using finite element analysis in RS2 and checked the results using discrete element analysis with UDEC. We started the numerical analysis using conventional input parameters that were measured at the site from extensive investigations. In trying to history match the results from the numerical analysis with the measured displacements, it became obvious that input parameters in the numerical modelling had to be changed significantly from those determined during the site investigations. In this paper we describe the changes that had to be made to the input parameters in the RS2 model to history match the measured displacements.

GEOLOGY AND SLOPE EXCAVATION

The Site C Clean Energy Project is currently being constructed on the Peace River near Fort St. John, British Columbia. An overview of the Site C design is given by Watson et al. (2019) and Heidstra et al. (2017) which required (1V:1.6H) slope excavations in the Shaftesbury shales for the roller compacted concrete (RCC) buttresses. As each excavation phase was completed, the removed rock was to be replaced with RCC forming the foundation for the spillway and powerhouse structures before the next phase of excavation would be started. This incremental excavation and replacement approach would limit ground movements and the risks of exposing all of the rock slopes at once. This staged approach would also allow the instrumentation responses to be reconciled with the geological model in a step-wise process. Figure 1 shows an excavated slope and an RCC buttress.

The Shaftesbury shales at Site C contain two prominent features that are characteristic of valleys found in the interior plains of Western Canada: 1) bedding plane shears (BP, see Figure 1) and, 2) subvertical relaxations joints that strike subparallel to the river valley (see Figure 2). These features were described by Cornish and Moore (1985) and Imrie (1991), and are thought to be related to the high horizontal stresses measured at the site and the unloading associated with deglaciation and river valley formation. Matheson and Thomson (1973) and Patton and Hendron (1974) described the valley formation processes that can create these features.

Imrie (1991) described the in situ stresses at the site based on stress measurements performed using over-coring techniques in drill holes from exploratory adits. These measurements were located about 250 m in the left bank and 100 m in the right bank from the valley slopes. The testing identified a distinct increase in horizontal stresses below BP25, a bedding plane shear at approximately the bedrock level in the river. Above BP25 river downcutting had relieved much of the horizontal stresses perpendicular to the valley slopes.

The relaxation joints that strike subparallel to the valley wall are “open” near the face of the valley slopes, with partial infilling of silty clay and shale fragments. Beyond a horizontal depth of about 35 m the joints were mapped as tight with negligible apertures. The RCC Buttress slope excavation removed these open relaxation joints. The relaxation joints were readily observed in the slope excavations. The excavated rock mass near the original rock surface contained relaxation joints with trace lengths which often exceeded 10 m as shown in Figure 2. However, as the excavation started and advanced about 30 m into the abutment the trace lengths and frequency of the joints decreased significantly. The histogram in Figure 2 shows the trace lengths of the relaxation joints mapped on the final spillway buttress slope. Of the 2710 mapped joints only 400 (~15%) had trace lengths exceeding 5 m. Based on the joint mapping the rock mass is classified as massive.

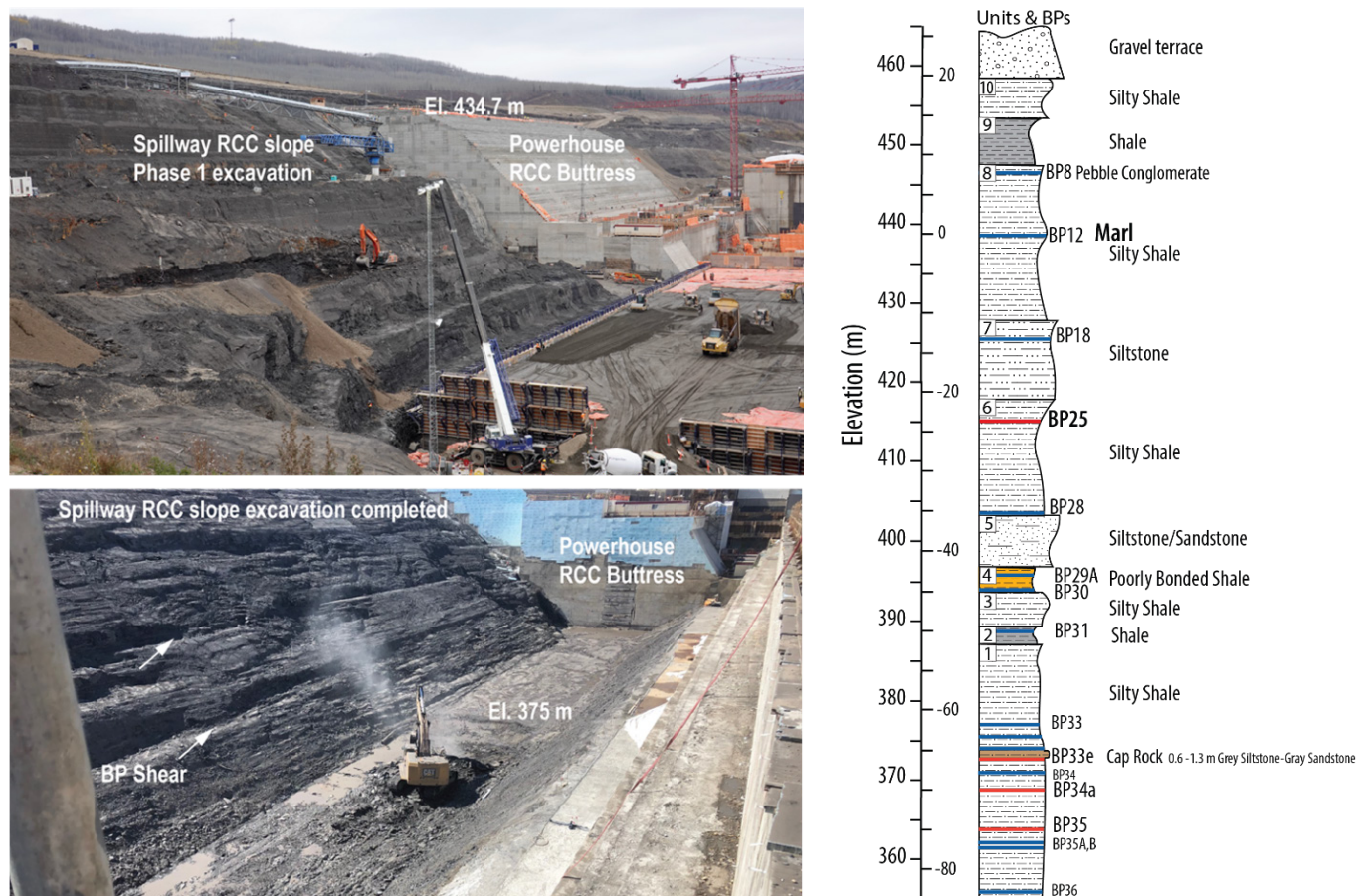


Figure 1: Powerhouse buttress and excavated slope for the spillway RCC buttress. The geological rock units 1 to 10, and bedding planes (BP) are shown on the stratigraphic column on the right.

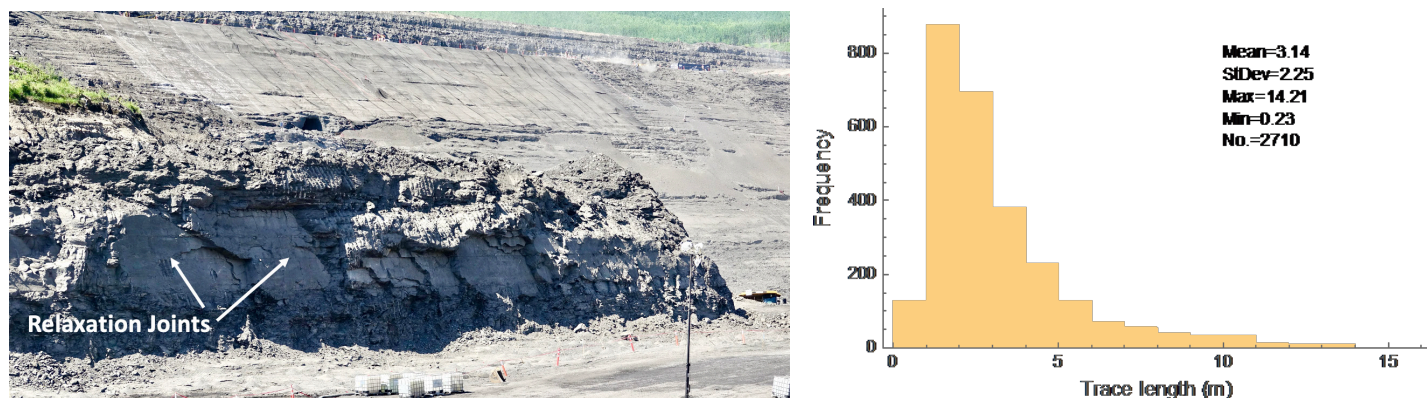


Figure 2: Photo of the subvertical relaxation joints observed in the slope excavation near the valley wall, and the histogram for the relaxation joints mapped at the final spillway slope.

DEFORMATION MODELLING AND HISTORY MATCHING

The initial finite element RS2 model used to predict the slope deformations contained homogeneous elastic shale with the bedding plane shears and input parameters shown in Figure 3. The bedding planes were elastic perfectly plastic with the friction angles that were measured in the laboratory (Cornish and Moore 1985). The normal and shear stiffness values of the bedding planes were $k_n = k_s = 4 \text{ GPa/m}$ based on laboratory and in situ tests. The objective of the deformation modelling was to simulate the Phase 1 excavations for the spillway buttress. Three slope inclinometers were installed at the crest of the slope and used to guide the history matching for the Phase 1 excavation. The Phase 1 excavation was simulated in 4 steps and the initial results for inclinometer M1A are shown in Figure 3. It is clear from Figure 3 that the calculated results were not in agreement with the measurements. Similar results were obtained for inclinometers M1B and M5. The modelling was repeated using different in situ stress ratios, different moduli and a modulus increasing with depth. None of these models provided results that were in agreement with the measurements.

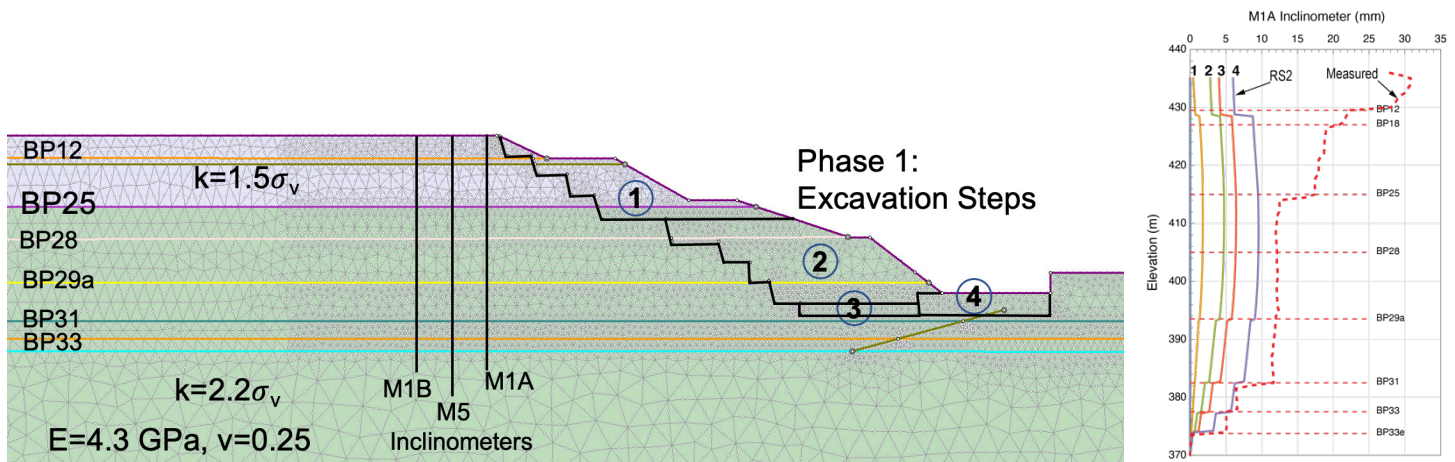


Figure 3: The RS2 model used to simulate the excavation sequence and examine the displacements at the inclinometers at the crest of the slope.

The relaxation joints were added to the RS2 model approximating the trace lengths, dip and mapping frequency (Figure 4). The evidence on site from tunnels, boreholes and mapping showed that these joints were tight and spaced 1 to 1.5 m apart. The stiffness of these relaxation joints was assigned the same value as that used for the bedding plane shears, because these shears and joints are very similar in nature, mainly a break in the rock with no mineralogical difference with the intact shale. Despite the addition of the relaxation joints the deformation pattern at the inclinometers remained essentially the same. Agreement with the measurements was finally achieved by reducing the k_n of the relaxation joints to 50 MPa/m compared to the measured k_n of 4 GPa/m.

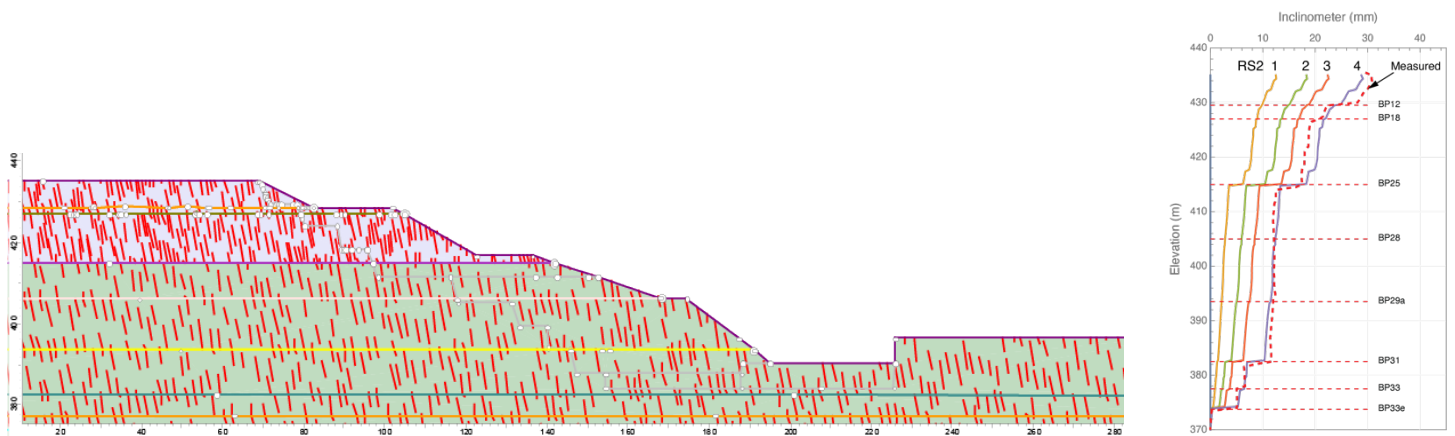


Figure 4: Simulation of the relaxation joints in the RS2 model. The inclinometer on the right shows the agreement obtained by reducing the relaxation joint k_n to 50 MPa/m.

Despite the massive nature of the rock mass at the location of the inclinometers, the relaxation joints and their unloading stiffness are clearly playing a role in the slope deformation pattern. Various sensitivity analyses were carried out but, in all cases, the low unloading stiffness of the relaxation joints was the primary parameter controlling the deformation pattern. The findings were also checked using the distinct element formulation in UDEC, with essentially identical results.

SUMMARY

The unique opportunity during the excavation of the shale slopes and construction of the RCC buttress at the Site C Clean Energy Project demonstrated the challenges in predicting realistic deformation patterns and magnitudes in a rock mass and the importance of considering the unloading stress path in selecting model parameters. Despite the relatively simple and well characterized site geology the following input parameters in the deformation model had to be adjusted to history match the measurements:

- The sparse relaxation joints in the massive shale had to be included in the model to simulate the displacement patterns measured by the inclinometers. This induces the direction of stiffness and strength anisotropy.
- A reduction in the normal stiffness of the relaxation joints, by several orders of magnitude compared to the values measured using the laboratory and in situ loading tests was required to correctly predict the displacement magnitudes. This induces the magnitude of the anisotropic response. The shear stiffness and friction angle of the relaxation joints did not influence the deformation pattern.

Predicting the slope deformations requires the strength and stiffness of the rock and the discontinuities. For this case study the strength values obtained in conventional laboratory tests were adequate for the deformation analyses. However, the stiffness values obtained from laboratory and in situ tests required considerable adjustment for simulating the slope deformation response to unloading. Regardless of the measured in situ stresses, slope deformations were controlled by the gravitational and low horizontal stress regime, caused by the excavation-induced disturbance. These findings are likely applicable to slope excavations in many jointed rock masses.

ACKNOWLEDGEMENTS

The authors wish to acknowledge the efforts by the instrumentation team at Site C to collect the data used in these analyses. The authors also acknowledge the permission of BC Hydro to publish this paper.

REFERENCES

- Cornish, L. J., and Moore, D.P. 1985. Dam foundation investigations for a project on soft shale. In Proceedings 38th Canadian Geotechnical Conference, Edmonton, AB., 171–178.
- Imrie, A. S. 1991. Stress-induced response from both natural and construction-related processes in the deepening of the Peace River valley, B.C. Canadian Geotechnical Journal, 28(5), 719–728.
- Matheson, D. S., and Thomson, S. 1973. Geological implications of valley rebound. Canadian Journal of Earth Sciences, 10(6), 961–978.
- Patton, F. D., and Hendron Jr, A. J. 1974. General Report on Mass Movements. In Proceedings Second International Congress of the International Association of Engineering Geology, Sao Paulo, Brazil (Vol. II, pp. 1–57).
- Heidstra, N., Nunn, J., Watson, A., Dodman, K., Carter, R., and Burmeister, L. 2017. Roller Compacted Concrete Buttress at the Site C Clean Energy Project. Canadian Dam Association Bulletin, 12–23.
- Watson, A.D, Stevenson, G.W., and Hanna A. 2019. Site C Clean Energy Project, Design Overview, Proceedings of the 87th Annual Meeting of International Commission on Large Dams, Sustainable and Safe Dams Around the World, 2019 Canadian Dam Association, Ottawa, ON, Canada, 2: 598–612.



Managing scale with empirical and simple numerical analysis techniques

Milne, D.

University of Saskatchewan, Saskatoon, Saskatchewan, Canada

EXTENDED ABSTRACT

Scale is one of the most important and challenging factors to account for in rock mechanics. It is a major factor influencing rock mass strength and rock mass stress / deformation properties. It is a factor when measuring roughness/waviness on discontinuity surfaces, when designing stable drift and stope dimensions underground and when determining sample size for laboratory testing.

Many of our design approaches have assumptions concerning the influence of scale that are often not apparent to the rock mechanics practitioner. These assumptions can result in critical rock mass properties being poorly collected and documented, and a design which has ignored important rock mass properties.

BACKGROUND

Scale considerations for the rock mass can start with the laboratory scale. The ASTM standards for UCS tests state: “The diameter of rock test specimens shall be at least ten times the diameter of the largest mineral grain.” The logic behind the use of 10 as the minimum ratio between sample diameter to grain size diameter is not stated, but seems reasonable. In practice, a mineral grain in a rock sample may often have a much higher strength than a rock sample, such as a sandstone, composed of quartz grains in a weaker matrix. When the sample diameter is 10 or more times the grain size diameter, the guideline suggests sample strength has reached a value less than the quartz grain strength and will not continue to drop as the sample size increases. It should be noted that the sample size is specified on the plane normal to the maximum applied stress in the lab test.

Bieniawski has produced a well-known relationship between sample size and intact rock strength (Figure 1). The graph is based on testing conducted on samples of diorite, coal and iron ore. For these samples, the effect of sample size may not have been based on sample grain size, but on minor planes of weakness such as cleats in coal samples or microfractures / defects in the rock. This general idea concerning sample size and strength, as it pertains to a rock mass, is discussed in Hoek and Brown (1980).

Discontinuity surface condition is also often measured at a few different scales for rock classification; slickensided or polished surfaces effect roughness at a tactile scale, a profile comb gives a 10 cm roughness scale and waviness is often measured at a 1 metre scale. These scales of roughness are chosen mainly for ease of measurement. The appropriate scale of roughness for estimating rock mass strength can be expected to increase with the scale of the engineering structure being designed. Guidelines for the collection of appropriate data relative to the engineering structure, and relative to rock mass block size, are needed.

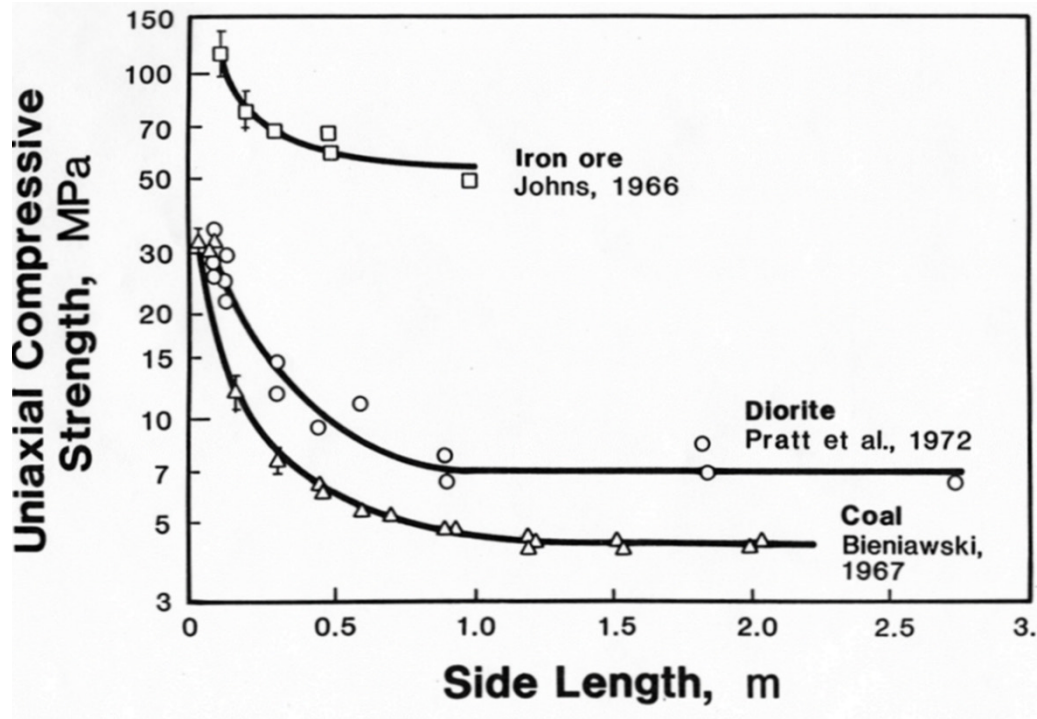


Figure 1: The effect of sample size on intact rock strength (after Bieniawski, 1984).

PROPOSED EFFECT OF DISCONTINUITY SPACING ON ROCK MASS STRENGTH

The idea behind grain size to sample size guidelines for lab testing can be applied to the average rock mass block size to the representative rock mass strength. Instead of considering the lab sample sizes, the scale of an engineering structure decides the volume of rock mass, and hence the number of intact blocks of rock, under loading. Also, the number of intact blocks of rock under loading increases as the average joint spacing decreases. As the size of an engineering structure increases, or the size of the intact blocks of rock decreases, the overall rock mass strength decreases with the number of intact blocks under loading. This change in strength is expressed as a percent of the intact unconfined compressive strength (UCS). Figure 2 shows the general idea between rock mass strength, as a per cent of the UCS, plotted against the average joint spacing at the engineering scale of a large open stope. For a very large average joint spacing (spacing of tens of metres), lab testing data may be adequate for estimating rock mass strength under compressive loading. For tight joint spacings in the order of centimetres, a design method which does not consider joint spacing, such as GSI, may work for estimating rock mass strength under compressive stresses. Between these two zones of average joint spacing (between about 10 metres and 10 centimetres), the spacing of jointing may be critical to estimating rock mass strength. Note that these spacing values can only be considered as conceptual limits.

As the size of the engineering structure under design changes, the average joint spacings which are critical to rock mass strength will also change. This is shown in Figure 3 where possible trends between joint spacing and rock mass strength are shown at the scale of boreholes, tunnels and open stopes. Hoek and Brown, (1988) comment on this issue as follows, “The Hoek-Brown failure criterion does not contain a parameter which depends upon the size of the opening or the spacing of the discontinuities. The user is left to decide upon the applicability of the criterion...”. Issues of scale are also discussed by Hoek et al. (2013) where an optional measure of RQD can be incorporated into the GSI calculation.

APPLICATION TO DESIGN

A good way to assess the site specific validity of a numerical or empirical design method is to consider factors that

may influence stability, and then determine if changing these values would influence the predicted behaviour. Consider the influence of joint spacing for a stope hanging wall. If three joint sets are present with joint spacings ranging between 0.3 to 1.0 metres, would hanging wall dilution be effected if joint spacing increased to between 1.0 to 3.0 metres? If it is felt that stability or dilution should decrease with the increase in joint spacing, or better yet, if case histories supports the assumption of decreased dilution, the effect of a change in joint spacing should be included in the design method. If the Stability Graph / Dilution Graph approach is used, joint spacing is only influenced by RQD which is 100% for both the close and more widely spaced joint spacing. The Stability Graph / Dilution Graph approach would not differentiate between the rock mass conditions.

For a 5 metre wide tunnel, the effect of a decrease in RQD from 50 to 25% (discontinuity spacing from about 6 cm to 4 cm), may decrease stability. For an assessment of stress based failure, the basic GSI system would not differentiate between these rock mass conditions.

SUMMARY

There is often a huge difference between intact rock strength and rock mass strength. When determining appropriate values for rock mass strength, the engineer cannot limit themselves to a lab value or a rock mass value without joint spacing data. There is a huge range of values that are partially governed by the size of the engineering structure under load relative to the size of the intact blocks of rock. If the rock mass properties are not carefully measured and documented, along with any errors in back analysis, advances in understanding the influence of scale will be challenging.

REFERENCES

- ASTM. ASTM D7012-10 Standard Test Method for Compressive Strength and Elastic Moduli of Intact Rock Core Specimens under Varying States of Stress and Temperatures. West Conshohocken: ASTM International, 2011.
- Bieniawski, Z.T., 1984. Rock Mechanics Design in Mining and Tunneling. Rotterdam: A.A. Balkema, 272 p.
- Hoek, E. and Brown, E.T., 1980. Underground Excavations in Rock, Institute of Mining and Metallurgy, London, 527 pp.
- Hoek, E. and Brown, E.T., 1988. The Hoek-Brown failure criterion – a 1988 update. Proc. 15th Canadian Rock Mech. Symp. (ed. J.H. Curran), pp. 31-38. Toronto: Civil Engineering Dept., University of Toronto.
- Hoek, E., Carter, T.G., Diederichs, M.S. 2013. Quantification of the Geological Strength Index chart, 47th US Rock Mechanics / Geomechanics Symposium, San Francisco: ARMA.

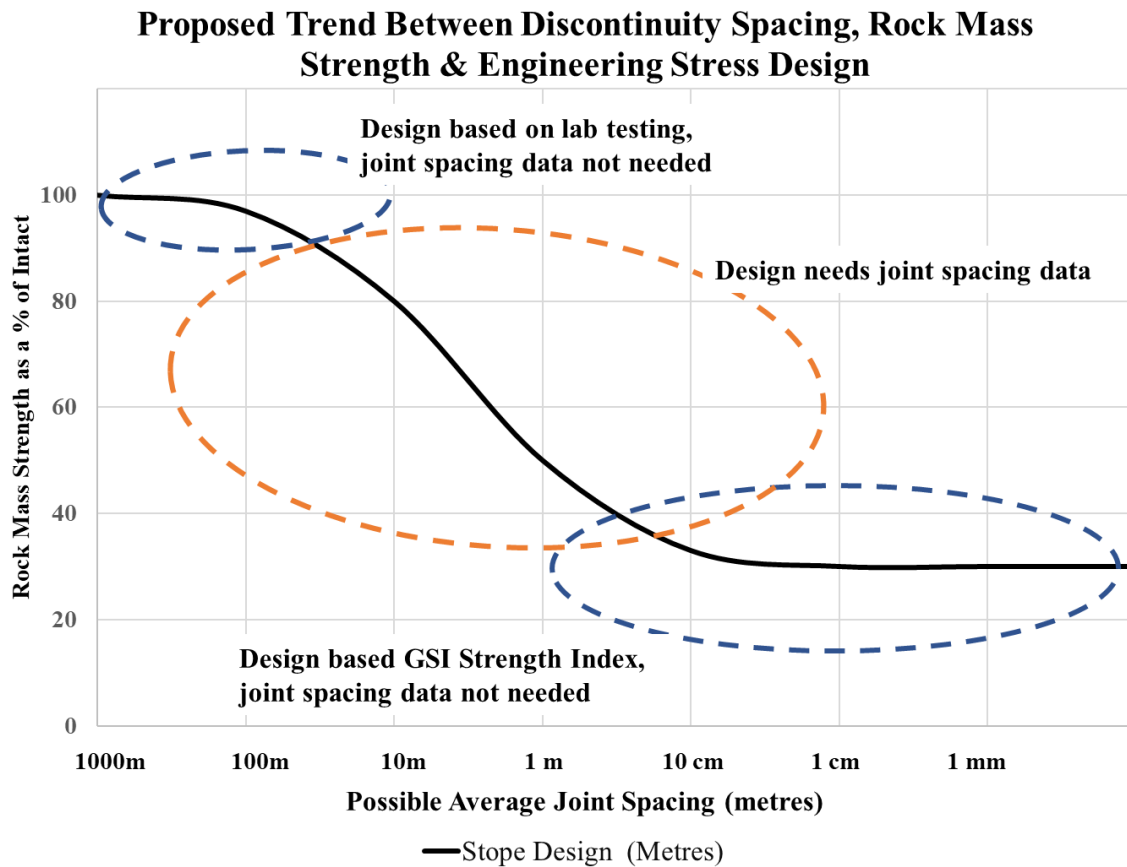


Figure 2: Possible influence of average joint spacing on rock mass strength for an open stope.

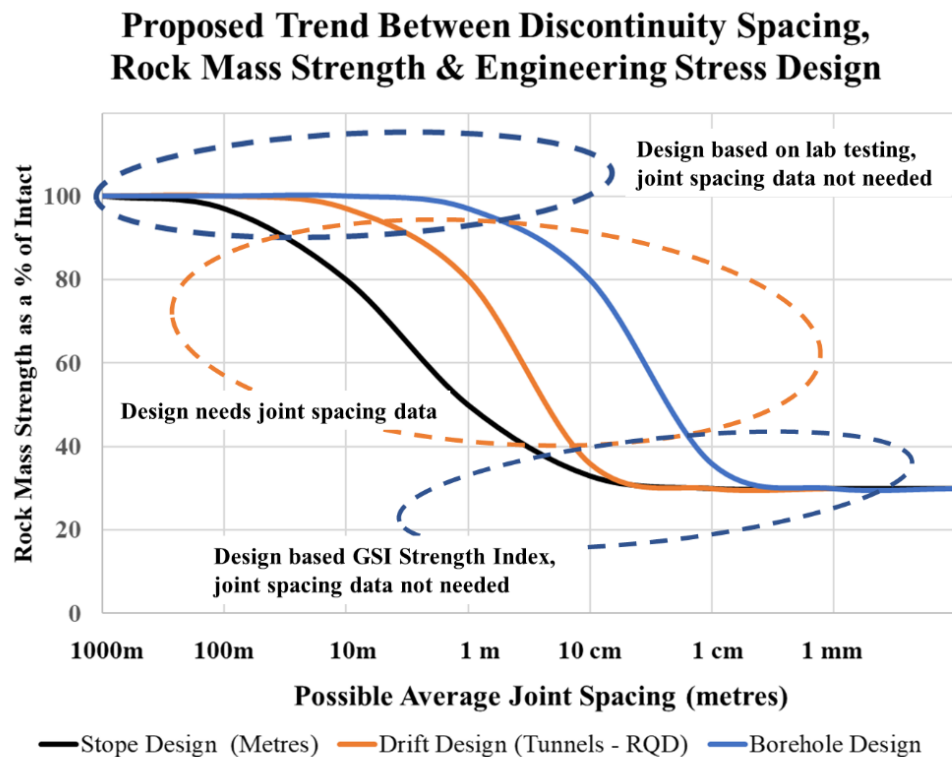


Figure 3: Possible influence of average joint spacing on rock mass strength at various scales.



Post-peak deformation behaviours of brittle rocks

Cai, M.

Laurentian University, Sudbury, Ontario, Canada

EXTENDED ABSTRACT

Using a super stiff rock mechanics test machine, which can obtain complete stress–strain curves of brittle hard rocks under axial- and lateral-strain-controlled loadings in the whole loading process, post-peak stress–strain curves of several brittle rocks are obtained. Compared with conventional test machines, the stiff machine does not cause explosive failure of the rock specimens, and the obtained stress–strain curves are all showing Class I type post-peak deformation behaviors under axial-strain-controlled loading. The machine also allows the stress–strain curves to reach the residual deformation stages and thus a proper assessment of the peak, plastic-strain-dependent post-peak, and residual strengths of brittle hard rocks.

INTRODUCTION

Despite more than six decades of research and development by numerous researchers, there are still many challenges in rock mechanics and rock engineering, such as determination of rock mass strength, prediction of rockburst, capturing accurate post-peak stress–strain curves of brittle hard rocks, amongst others. Rock strength and its post-peak deformation behavior affect the failure zone and failure modes of rock mass, which is of great importance for numerical modeling and rock engineering design.

To control failure in the post-peak deformation stage and obtain complete stress–strain curves of brittle hard rocks, a stiff test machine with an advanced servo-control system is needed. A few stiff test machines were developed in the period from 1960s to 1980s by some scholars (Cook and Hojem 1966; Bieniawski 1967; Wawersik 1968; Stavrogin et al. 1981). In some cases, it was possible to obtain Class I stress–strain curves of brittle hard rocks using axial-strain-controlled loading. However, as far as the author knows, currently none of those machines are in operation. Modern rock mechanics test machines such as Instron and MTS-815 use the structure of placing the rock specimen and the loading actuator in series. Because the stiffness of the hydraulic ram is low, it dominates the machine's loading system stiffness. When confinement is low, there is a risk of burst failure of the rock specimen when the test is conducted under axial-strain-controlled loading. To avoid damaging instrument and sensors, ISRM suggests that the specimens may not be conducive to post-peak testing in a uniaxial mode, and should be tested in a confined state. One way to control post-peak rock failure in modern conventional test machines was to use lateral-strain-controlled loading, and for most brittle hard rocks Class II stress–strain curves were obtained. This made some researchers believe that there is a type of rock called Class II rock.

Recently, Northeastern University (NEU) in China developed a rock testing machine called Stiffman with super high loading system stiffness (Figure 1). The machine can be controlled using either axial- or lateral-strain-controlled loading in the whole loading process to obtain complete stress–strain curves of brittle rocks. In this talk, some test results by Stiffman are presented to illustrate the capability of the new test machine.



Figure 1: Brittle hard rock testing system Stiffman (Cai et al. 2021).

POST-PEAK RESPONSES OF BRITTLE ROCK TESTED USING SOFT AND STIFF TEST MACHINES

Figure 2 presents the test results of Linghai granite using Rockman and Stiffman under axial-strain-controlled loading. Rockman is a conventional rock test machine developed by NEU, with a similar structure like MTS-815. Hence, its loading system stiffness is low. The test results of Rockman (Figure 2a) show that under axial-strain-controlled loading in uniaxial compression and triaxial compression at low confining pressures, the rock specimens fail violently in the post-peak deformation stage and it is not possible to obtain complete stress–strain curves of the rock. On the other hand, it is possible to load the rocks under axial-strain-controlled loading in a stable fashion using Stiffman and complete Class I stress–strain curves of the rock under uniaxial compression and triaxial compression at low confining pressures can be obtained (Figure 2b). This study clearly demonstrates that for the same rock and the same loading control, if we use different machines with different loading system stiffness we will get different post-peak responses. To capture complete stress–strain curves, real stiff machines are needed.

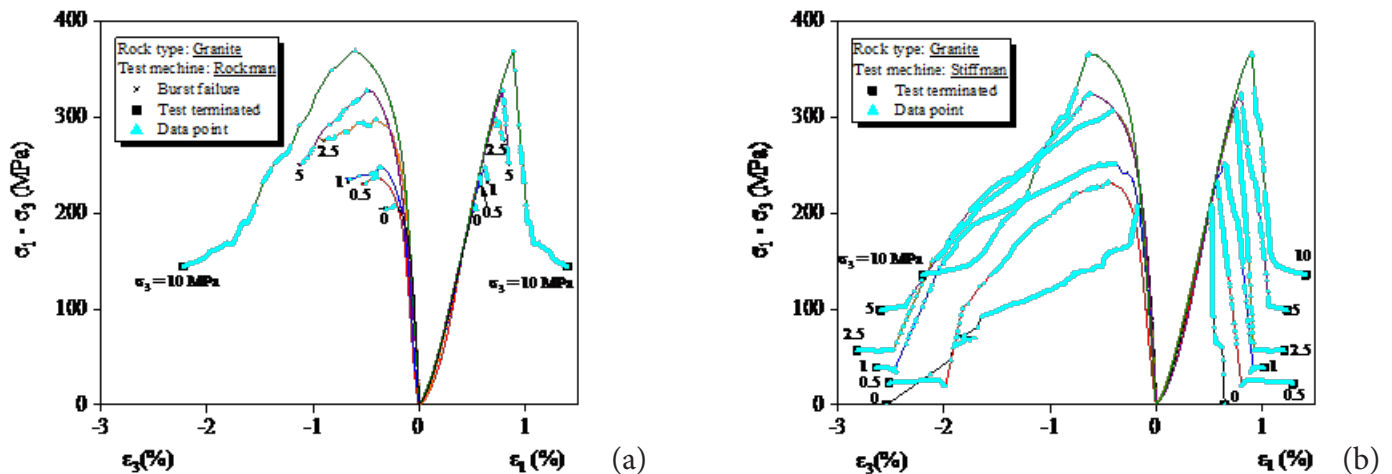


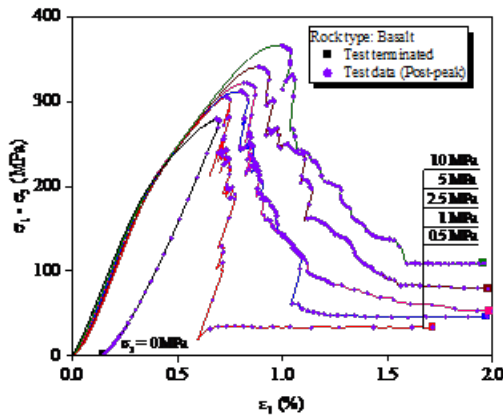
Figure 2: Stress–strain relations of granite obtained using (a) Rockman and (b) Stiffman (Cai et al. 2021).

POST-PEAK STRESS-STRAIN CURVES OF BRITTLE ROCK UNDER AXIAL- AND LATERAL-STRAIN-CONTROLLED LOADINGS

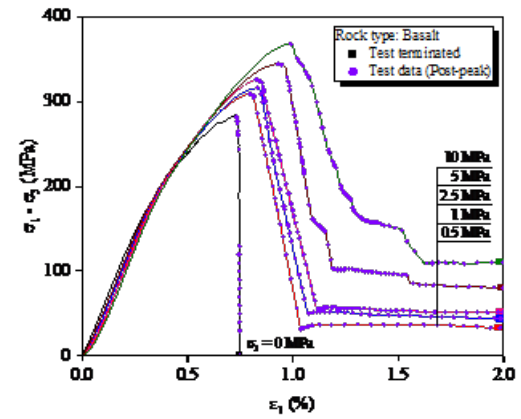
Figure 3a presents the stress–strain relations of basalt under lateral-strain-controlled loading. The rock is very brittle and strong with an UCS of 285 MPa. The failures of the rock specimens are stable and Class II stress–

strain curves are obtained. When there is no confinement or the confinement is low, rock dilation rate increases rapidly in the post-peak deformation stage, which leads to a sudden increase of the lateral strain rate. To keep the lateral strain rate at the set value in lateral-strain-controlled loading, the servo-control system must force the actuator to unload, which can result in Class II behavior. Under high confining pressures, the dilation of rock is restricted; this is the reason why the Class II behaviors under high confining pressures (e.g., $\sigma_3 = 5, 10$ MPa) are less obvious even under lateral-strain-controlled loading.

As can be seen from Figure 3b, for the same type of rock tested under axial-strain-controlled loading, the failures of the rock specimens are also stable and Class I stress–strain curves are obtained. This study clearly demonstrates that there is no such thing as Class II rock. Depending on the loading control mode used, a brittle hard rock specimen can exhibit either Class I or Class II post-peak stress–strain curves. Under lateral-strain-controlled loading, Class II behavior can be obtained when confinement is low; under axial-strain-controlled loading, Class I behavior is always obtained. However, to test brittle hard rock under axial-strain-controlled loading, stiff machines such as Stiffman are needed.



(a) Lateral-strain-controlled loading



(b) Axial-strain-controlled loading

Figure 3: Stress–strain relations of basalt obtained by Stiffman using (a) lateral- and (b) axial-strain-controlled loadings (Hou et al. 2022).

PLASTIC-STRAIN-DEPENDENT POST-PEAK STRENGTH

Figure 4 presents the stress–strain curves of Beishan granite obtained by Stiffman using axial-strain-controlled loading under cyclic and monotonic loadings. The confinement is zero in this case and the test machine can control the post-peak loading process stably. It is seen that the envelope of the cyclic loading corresponds well with the curve of monotonic loading. Similar cyclic loading tests with different confinements were conducted and based on the test results, the failure criterion covering peak, plastic-strain (ϵ_p) dependent post-peak, and residual strengths can be determined as

$$\sigma_1 = \sigma_3 + \left[m(\epsilon_p) \sigma_c \sigma_3 + s(\epsilon_p) \sigma_c^2 \right]^{0.5}$$

where

$$m(\epsilon_p) = 37.58e^{(-2.125\epsilon_p)} + 3.821 \quad (R^2 = 0.986), \quad s(\epsilon_p) = 2.192e^{(-16.71\epsilon_p)} \quad (R^2 = 0.999).$$

This type of failure criterion is based on test results without assumption and it can be used for numerical modeling to capture accurate depth of failure in brittle rock.

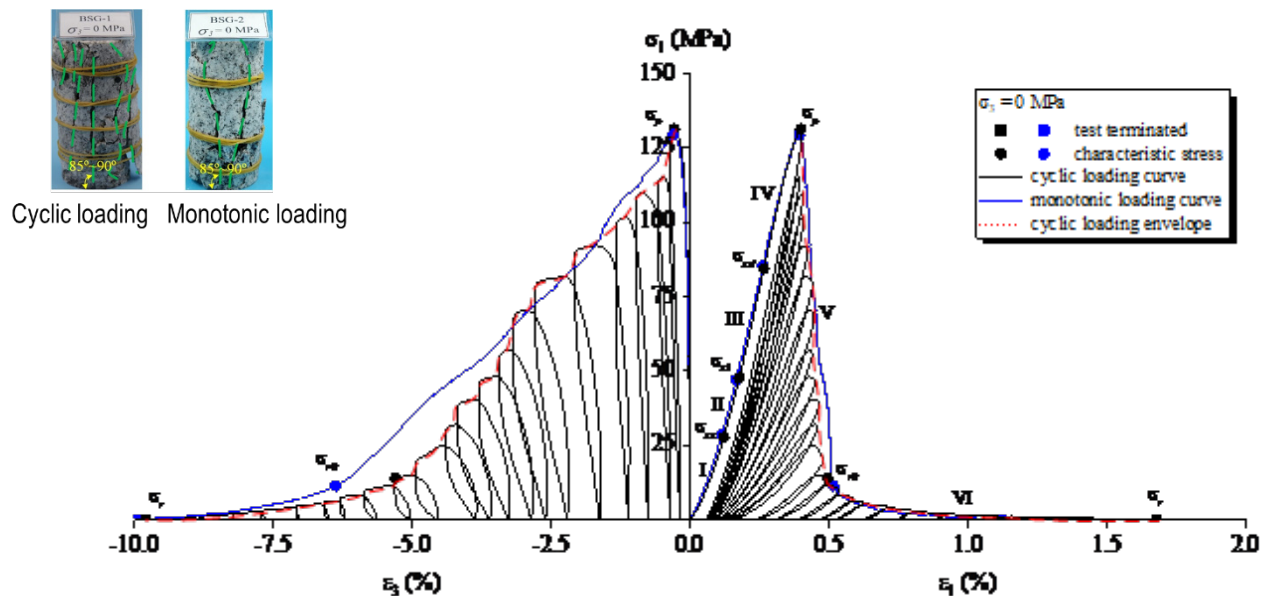


Figure 4: Stress–strain relations of granite obtained by Stiffman using axial-strain-controlled loading under cyclic and monotonic loadings.

SUMMARY

To capture useful Class I post-peak stress–strain curves for numerical modelling and mine design, it is advised to test rock using axial-strain-controlled loading. This can be conducted with axial-strain-controlled loading using stiff test machines such as Stiffman. For conventional test machine with insufficient machine stiffness, post-peak failure of brittle hard rocks can only be controlled using lateral-strain-controlled loading, and this often leads to Class II post-peak stress–strain curves. A brittle rock can exhibit either Class I or Class II post-peak deformation behaviors, depending on the control method used. Hence, it is not appropriate to classify brittle rocks into Class I and Class II rocks. Cyclic loading tests can be conducted to obtain plastic-strain-dependent post-peak strength.

ACKNOWLEDGEMENTS

The author wishes to thank NEU for granting access to Stiffman and P. Hou for conducting laboratory tests.

REFERENCES

- Bieniawski, Z. 1967. Mechanism of brittle fracture of rock. Part I, Part II, Part, III. *International Journal of Rock Mechanics and Mining Sciences* 4: 395-430.
- Cai, M., Hou, P., Zhang, X., and Feng, X. 2021. Post-peak stress–strain curves of brittle hard rocks under axial-strain-controlled loading. *International Journal of Rock Mechanics and Mining Sciences* 147: 104921.
- Cook, N., and Hojem, J. 1966. A rigid 50-ton compression and tension testing machine. *JS Afr Inst Mech Eng* 1: 89-92.
- Hou, P., Cai, M., Zhang, X., and Feng, X. 2022. Post-peak Stress–Strain Curves of Brittle Rocks Under Axial-and Lateral-Strain-Controlled Loadings. *Rock Mechanics and Rock Engineering* 55(2): 855-884.
- Stavrogin, A., Tarasov, B., Shirkes, O., and Pevzner, E. 1981. Strength and deformation of rocks before and after the breakdown point. *Soviet Mining* 17(6): 487-493.
- Wawersik, W.R. 1968. Detailed analysis of rock failure in laboratory compression tests. Ph.D. Thesis, University of Minnesota, Minneapolis, Minn. p. 165.



Challenges in rock engineering

Bewick, R.P.

WSP (Golder Associates Ltd.), Sudbury, Ontario, Canada

EXTENDED ABSTRACT

The rock mechanics community is undergoing a transition. The founders of the community are slowly transitioning. This is leaving a gap in fundamental details around several concepts. This gap has the risk of creating conditions where ‘mis-use’ becomes ‘best practice’. WSP Golder has had the opportunity to have great visibility of the global rock mechanics practice in mining. The visibility has provided evidence of systematic misuse of some rock mechanics aspects. Three consistent aspects are the concepts of: (1) support pressure; (2) intact rock strength; and (3) rock mass strength. In this presentation at RockEng2022, the three aspects are overview and some guidance provided. Due to space limitations, condensed wording is used to provide an overview of each item.

SUPPORT PRESSURE

Support pressure is an inconsistently used term and its application in design work is often seen to not be used appropriately (Figure 1). The term is used by Terzaghi (1946) and Barton et al (1974) to specify the required support load capacity to support the mass of material kinematically free to fall into an excavation. The term is also used to specify the feed back ‘pressure’ that an internal liner provides to an excavation that begins to converge.

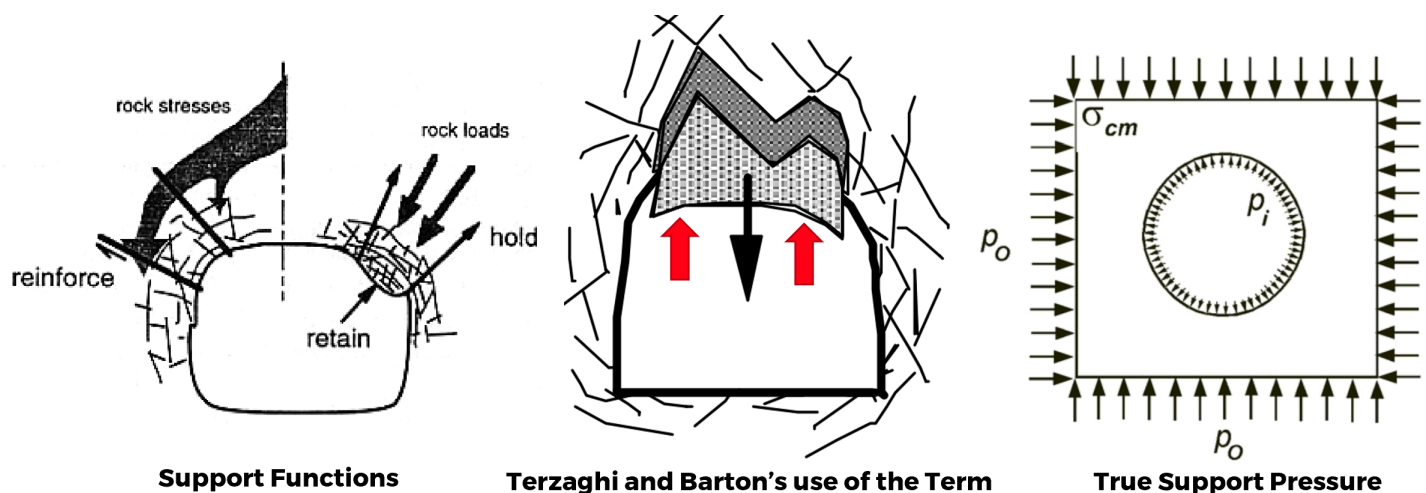


Figure 1: Support pressure term use and the support system functions.

Hoek (2001) outlines the use of support pressure for various support systems but with the following notes that are often not considered:

- The pressures stated are MAXIMUM support pressures (i.e., not achieved in practice) and these pressures assume:

- Circular geometry
- Closed rings
- Perfect symmetry
- Hydrostatic loading
- No bending moments
- Thinking practicality,
 - There is always asymmetric loading
 - Induced bending will occur
 - Support capacities are lower than provided
 - Mining geometries are not circular or closed ring systems
 - Drastic reduction in capacity and stiffness of support systems compared to those provided

Due to the above practical aspects, in mining, very few of the above needed assumptions for support pressure hold true. Thus, in mining, even for very heavy support systems (the heaviest practical), support pressures are limited and $\ll 1$ MPa and likely $\ll 300$ kPa. These low support pressures are seen in practice in underground mines that have installed some of the heaviest reinforce-retain-hold systems and monitored depth of failure evolution and bulking driven convergence during progressive mining induced loading.

INTACT ROCK STRENGTH

More time needs to be taken to understand the ‘variability’ of intact rock strength considering failure types, failure modes, alteration, vein intensity, and vein type (Figure 2). In complex rocks (heterogeneous), one of the main limitations of ASTM standards and ISRM suggested methods for intact rock strength determination is that they were predominately written for homogeneous rocks where failure is generally forced through the homogeneous rock matrix. When these standards and suggested methods (e.g., ISRM 1979 and ASTM D 2938-86) are applied to heterogeneous rocks, the reported strengths are highly variable (high standard deviation and coefficient of variation) and the test data frequently returns relatively low mean strengths. This is because the standards were designed with a focus on minimizing the influence of the testing procedure and testing apparatus on the test results. They were not written to provide guidance on the interpretation of rock strength (Bewick et al. 2015). This shortcoming becomes particularly evident in rocks that do not exhibit a consistent failure mode (i.e., axial splitting or single localized shear rupture) and failure type (i.e., failure through homogeneous rock, or influenced by a discrete defect). Thus, in many cases the variability in rock strength is not true variability but a mechanism dependent strength.

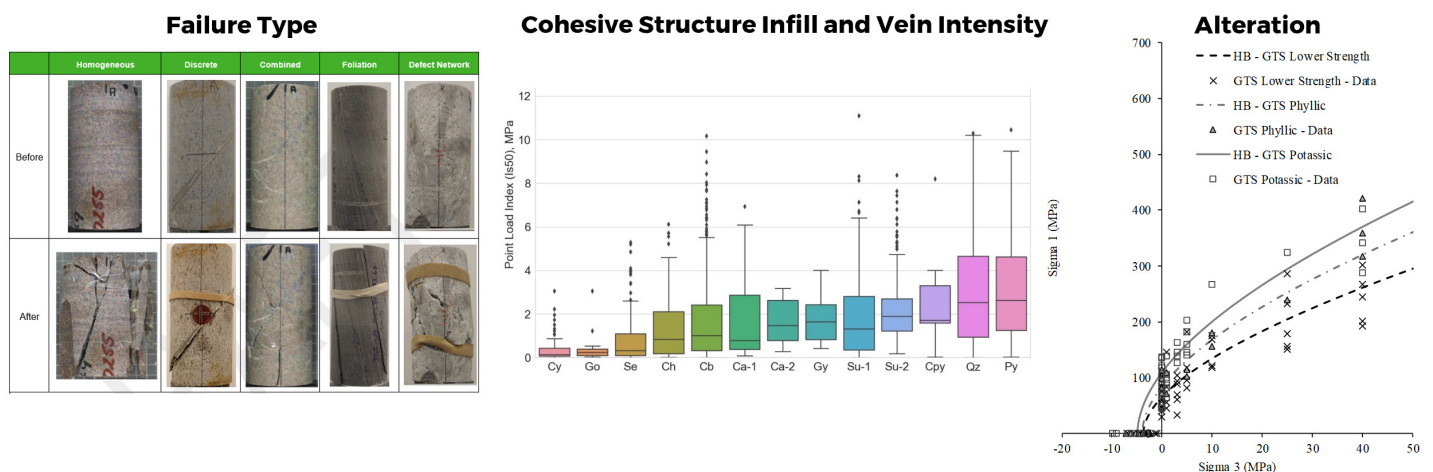


Figure 2: Some examples of rock character that generate variable rock strengths.

ROCK MASS STRENGTH

Rock mass strength estimation is often seen to focus on two approaches (Figure 3): (1) the GSI strength scaling equations; and (2) scale effects. Unfortunately, the GSI strength scaling approach is associated with a specific failure mechanism and scale effects are from a time when the rock engineering community did not understand as much as we do now about rock failure mechanics. A good example of rock mass strength is for rocks that stress fracture. For this failure mechanism (i.e., spalling), the rock mass strength is scale invariant and not related to the GSI strength scaling equation failure mechanism assumptions. This is shown in Figure 4 where the rock mass strength from actual field cases has been compiled up to about 35 m span. There is no scale dependency seen nor would a GSI strength estimation approach be appropriate. Rock mass strength is more failure mechanism dependent than due to scale effect (noting that scale may change the failure mechanism and thus relevant rock mass strength to consider. Rock mass failure mechanisms are dependent on the rock mass character and thus sufficient time and effort must be completed to understand what the rock mass looks like and how its feelings will be hurt under stress and strain.

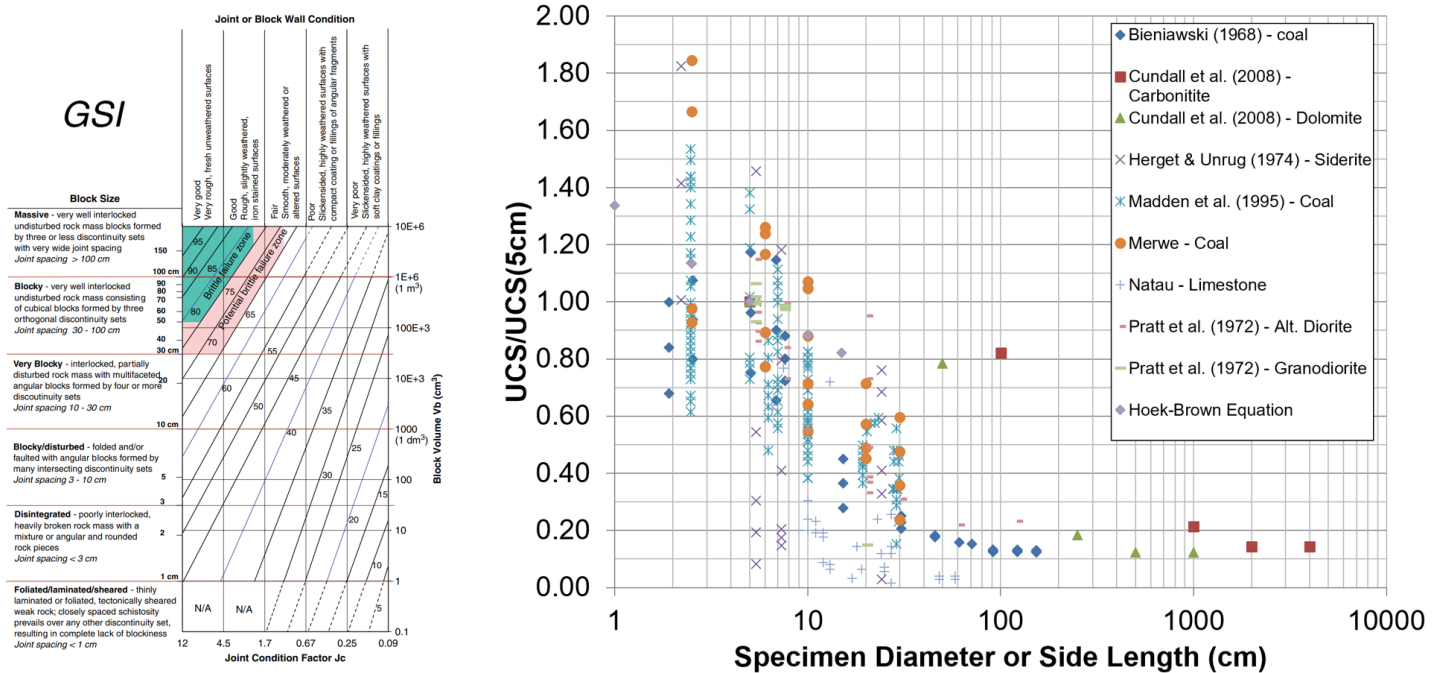


Figure 3: GSI chart (from Cai et al. 2004) and compiled scale effect data from the literature.

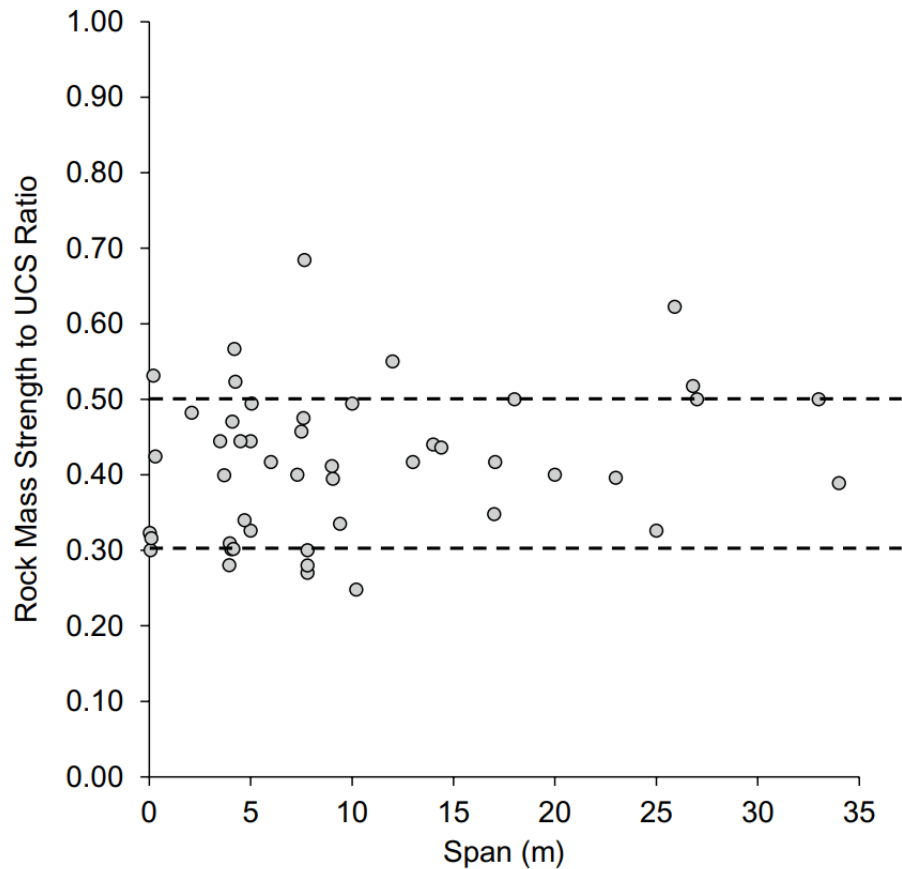


Figure 4: Spalling rock mass strength from constructed and back analyzed excavations including deep mines (from Bewick 2021).

REFERENCES

- ASTM D 2938-86 (1991) Standard test method for unconfined compressive strength of intact rock core specimens.
- Barton, N. R., Lien, R. and Lunde, J. 1974. Engineering classification of rock masses for the design of tunnel support. *Rock Mech.*, 6(4): 189-239.
- Bewick RP (2021) The Strength of Massive to Moderately Jointed Rock and its Application to Cave Mining. *Rock Mechanics and Rock Engineering*. DOI: 10.1007/s00603-021-02466-3. <https://rdcu.be/cj2Gn>.
- Bewick RP, Amann F, Kaiser PK, Martin CD (2015) Interpretation of UCS test results for engineering design. In: *Proceedings of the 13th International Congress on Rock Mechanics: ISRM Congress 2015 – Advances in Applied & Theoretical Rock Mechanics*. Montreal, Canada: International Society for Rock Mechanics and Rock Engineering. Paper 521.
- Cai M, Kaiser PK, Uno H, Tasaka Y, Minami M (2004) Estimation of rock mass strength and deformation modulus of jointed hard rock masses using the GSI system. *International Journal of Rock Mechanics and Mining Sciences*;41(1):3-19.
- Hoek E (2001) Big Tunnels in Bad Rock. *ASCE Journal of Geotechnical and Geoenvironmental Engineering*. 127(9), 726-740.
- Terzaghi, K. (1946). "Rock defects and loads in tunnel supports." *Rock tunneling with steel supports*. R.V. Proctor and T.L. White, eds., The Commercial Shearing and Stamping Co., Youngstown, Ohio, 17-99.



Theme 3

Innovations in Rock Mechanics Modelling



The evolution of factor of safety computation in slope stability analyses

Corkum, B.

Rocscience Ltd., Toronto, Ontario, Canada

EXTENDED ABSTRACT

Slope Stability Analyses of rock and soil slopes is an important component of the design of many mining and civil engineering projects. This is especially true for open pits, highway cuts, retaining structures, dams, levees and bridge abutments.

Limit Equilibrium methods for the calculation of stability have historically been the cornerstone of these analyses. Methods used to compute a factor of safety, such as Spencer (1967), Morgenstern and Price (1965), GLE (1981), Janbu (1956), Bishop (1955) have been used for over 50 years. However, these methods all require an a priori assumption as to the location and geometry of the failure surface. The most common assumption has historically been a circular failure surface. Using the center of rotation, contours of factors of safety are generated to give a spatial representation of the circular factor of safety (see Janbu 1956 for earliest example). The reason for the dominance of circular failure surfaces is simple – methods to find the minimum circular surface are well established and easy to run.

In many cases, failure surfaces are simply not circular. Any rock or soil slope with weak layers, anisotropy, spatial variability, or simply friction only materials, have noncircular global minimum failure surfaces. Several authors, and software products, have attempted to implement noncircular failure surface searching. Many of the very early methods in commercial software fell into two categories: (a) block search methods in which the user would define areas of a model in which surface polyline vertices would exist, and (b) path search methods in which surface polyline vertices would be randomly created with a convex constraint (Boutrup and Lovell, 1980). Both methods require enormous numbers of surfaces to be generated, often leading to inaccurate global minimum factors of safety. The 1980's and 1990's, with the advent of the personal computer, saw some preliminary attempts at finding the global minimum failure surface through trying to minimize the factor of safety through intelligent shifting of surface polyline vertices (Celestino & Duncan 1981, Greco 1996) or dynamic programming (Baker 1980). However, these methods were generally prone to getting trapped in local minima, requiring some guidance by the user to properly locate the failure surface.

Finding the global minimum noncircular failure surface can be classified as an NP hard problem. A problem in which there is no method to solve it in polynomial time and no method to verify that the solution is the true minimum in polynomial time. Basically, there are infinite possible surfaces with many local minima. During the 1980's and 1990's, an exciting development in the field of optimization was the pioneering work on metaheuristic optimization. Nature-inspired algorithms are an example, which draw from nature's ability to optimize complicated processes or problems. These problems also have infinite solutions with many minima. These algorithms are stochastic in nature and avoid getting trapped in local minima. An example of these types of algorithms includes Simulated Annealing (Kirkpatrick 1983), the metal annealing process where metal particles arrange themselves in a minimum potential energy state during cooling after subjection to high heat. The Particle Swarm Optimization was introduced by Kennedy and Eberhart (1995) and is a bio-inspired algorithm where a school of fish or a flock of birds can search for food using swarm intelligence. The Cuckoo Search (Yang and Deb

2009) is based on the aggressive brooding parasitism of some cuckoo bird species and their egg-laying strategy. There are many other examples, including ant colony, bee algorithms, harmony search, firefly algorithm, and multiverse optimization. Metaheuristic optimization techniques continue to be a thriving area of research with constantly new variations being released (Gandomi 2021).

Metaheuristic optimization applied to slope stability problems revolutionized the hunt for the global minimum failure surface. Early researchers such as Cheng (2003) used Simulated Annealing to try and locate both circular and noncircular failure surfaces. In the mid- to late-2000's, Rocscience developed a hybrid simulated annealing method (Xiao 2008,2009) which combined Very Fast Simulated Annealing (Ingber 1989) with a local Monte-Carlo optimizer (Greco 1996). This became the first instance of metaheuristic global optimization being combined with local optimization for finding a global minimum failure surface. As described in Xiao (2009), metaheuristic methods perform well in finding the approximate location of the global minimum failure surface but require a great deal of computational time to refine this surface to the true global minimum. In this case, it is much more efficient to take the approximate failure surface from metaheuristic optimization and switch to a local optimization technique to refine the solution.

In 2010, version 6.0 of Slide2 was released with Hybrid Simulated Annealing, becoming the first commercial product to use hybrid metaheuristic optimization to locate the global minimum failure surface. A research group at Rocscience continues to work on ways to improve the computation on global minimum failure surfaces in both 2D and 3D. Some of these improvements include: Particle Swarm Optimization, Cuckoo Search optimization (Wu 2012), Multiverse Optimization (Mishra et al. 2020), Surface Altering optimization (Mafi et al. 2021), 3D NURBS based optimization (Ma et al. 2022; Chan 2021; Cheng & Lau 2008), multimodal optimization (Li et al. 2020; Li et al. 2017; Li 2007), binary optimization for weak layer handling (Crawford et al. 2017).

Another method commonly used to compute the factor of safety of slopes is the shear strength reduction (SSR) method (Zienkiewicz et al. 1975, Dawson et al. 1999, Hammah et al. 2004; 2005a; 2005b; 2007). Numerical modeling methods such as the finite-element method are systematically used to determine the shear strength reduction factor (SRF) that brings the slope to the brink of failure. The concept is quite simple and is best explained with a Mohr-Coulomb material. The initial shear strength of the material is given by:

$$\tau = c' + \sigma'_n \tan \varphi'$$

The shear strength is then factored by a factor F:

$$\tau = \frac{c'}{F} + \frac{\sigma'_n \tan \varphi'}{F}$$

The new shear strength is then used to determine whether the slope is stable or unstable:

$$c'_{SRF} = \frac{c'}{F}; \varphi'_{SRF} = \tan^{-1} \left(\frac{\tan \varphi'}{F} \right)$$

Stable is defined as the state of finite-element solution convergence, whereas unstable is defined as the state of non-convergence. The value of F is then iterated on until a value is determined that is on the cusp of stability and instability. Many of the above references explain this in detail.

The advantages of the SSR method are 1) no assumption on mode of failure, 2) no assumption on the global minimum failure surface, 3) better physics when it comes to the constitutive relations and compatibility equations. Note that the limit equilibrium method calculates a factor of safety for shear failure along a pre-defined failure

surface utilizing force and moment equilibrium equations.

The disadvantages of the SSR method are 1) excessive computational times, 2) more input properties 3) finite-element expertise is generally required 4) due to the excessive compute times, sensitivity and probability analyses are difficult. Note that the limit equilibrium method is extremely fast (orders of magnitude faster than SSR in 3D), making parametric, sensitivity and probabilistic analyses both quick and easy. This is an extremely important requirement when variability in material properties and subsurface conditions exist.

Even with these limitations, SSR analyses have proven extremely useful in determining the stability of slopes. When used in conjunction with limit equilibrium analyses, they often provide validation as to the mode of failure and the factor of safety of the slope. In two-dimensions, they can run in under 5 minutes. If using Rocscience tools, the Slide2 model can be directly imported into RS2 and run with no extra work. All the Slide2 material models, including anisotropic models, can be used in RS2. More importantly, modes of failure that cannot be analyzed in Slide2, such as toppling, progressive failure, high horizontal stress failure, can be analysed with SSR.

In summary, the methods used to compute the factor of safety of a slope have evolved significantly in the last 70 years. Although uncertainty in the variability of input parameters and subsurface conditions remain, our ability to accurately compute the global minimum factor of safety has improved greatly. Now, with combinations of limit equilibrium and finite element methods, the tools for engineers to locate the global minimum failure surface and compute a global minimum factor of safety have never been better. However, polling done by Rocscience indicates that at least 40% of customers still rely on circular grid searching as their primary search method. Circular grid searches are known to overestimate the factor of safety by 10–20% (Gregory 2022) and in some cases, this difference can be much higher. A conundrum now faces practitioners when it comes to choosing search methods. This is highlighted by the many technical support queries the author has received as to the validity of noncircular results and whether they should be used for design.

Civil engineering slopes have generally been designed to exceed 1.5 as the factor of safety for permanent slopes, 1.3 for temporary slopes, 1.0 to 1.1 for seismic and rapid drawdown conditions. Although not universal, these are the most common numbers the author has seen. Little is known about the history of the 1.5 value, as any Google search on the internet is futile. The little the author knows is that personal communications (Wright 2022) would indicate that it originates with Arthur Casagrande and his work with the Army Corp. of Engineers. Regardless, it certainly dates back more than 50 years ago, when searching techniques were quite crude and SSR analyses did not exist. In essence, the state of the art when this number was conceived, was circular searching using limit equilibrium analyses. So, the question becomes, with our current state of noncircular searching and SSR analyses, should we still be using 1.5 as the design value? Another topic for a future talk, is how 3D factors of safety affect design compared to 2D.

REFERENCES

- Baker, R. (1980). Determination of the critical slip surface in slope stability computations. *Int. J. Numer. Anal. Methods Geomech.* 4, No. 4, 333–359
- Bishop, A. W. (1955). The use of the slip circle in the stability analysis of slopes. *Geotechnique* 5, No. 1, 7–17
- Boutrup, E. & Lovell, C. W. (1980). Searching techniques in slope stability analysis. *Engng Geol.* 16, No. 1–2, 51–61
- Celestino, T. B. & Duncan, J. M. (1981). Simplified search for noncircular slip surfaces. *Proc. 10th Int. Conf. Soil Mech. Found. Engng, Stockholm* 3, 391–394
- Chan N. (2021). Slide3 Searching with NURBS. Rocscience Internal report.
- Cheng, Y. M. (2003). Location of critical failure surface and some further studies on slope stability analysis. *Comput. Geotech.* 30, No. 3, 255–267
- Cheng, Y.M. & Lau C., (2008). *Slope Stability Analysis and Stabilization – New methods and insight*, Routledge.
- Crawford, B., Soto, R, Astorga, G, Garcia, J., Castro, C., Paredes, F. (2017), *Putting Continuous Metaheuristics to Work in*

- Binary Search Spaces, Complexity (2) 1–19.
- Dawson, E.M., Roth, W.H. & Drescher, A. (1999). Slope Stability Analysis by Strength Reduction, *Geotechnique*, vol. 49, no. 6, pp. 835–840.
- Fredlund, D.G., Krahn, J., and Pufahl, D. (1981). The relationship between limit equilibrium slope stability methods. *Proc. 10th Int. Conf. Soil Mech. Found. Eng. (Stockholm, Sweden)*, Vol. 3, 409–416.
- Gandomi (2021). Aquila Optimizer: A novel meta-heuristic optimization algorithm, *Computers & Industrial Engineering*, No. 157.
- Greco, V. R. (1996). Efficient Monte Carlo technique for locating critical slip surface. *J. Geotech. Engng* 122, No. 7, 517–525
- Gregory G. (2022). Extended Abstract – The paradigm shift in non-circular searching techniques and evolution of limit equilibrium factors of safety in slope stability analyses. For *Geocongress 2022 (special session)*.
- Hammah, R.E., J.H. Curran, T.E. Yacoub, and B. Corkum. (2004). Stability analysis of rock slopes using the Finite Element Method. In *Proceedings of the ISRM Regional Symposium EUROCK 2004 and the 53rd Geomechanics Colloquy*, Salzburg, Austria.
- Hammah, R.E., Yacoub, T.E. and Corkum, B., (2005), The Shear Strength Reduction Method for the Generalized Hoek-Brown Criterion,. In *Proceedings of the 40th U.S. Symposium on Rock Mechanics, Alaska Rocks 2005*, Anchorage, Alaska.
- Hammah, R.E., Yacoub, T.E., Corkum, B., Curran, J.H. (2005). A comparison of finite element slope stability analysis with conventional limit-equilibrium investigation, *Proceedings of the 58th Canadian Geotechnical and 6th Joint IAH-CNC and CGS Groundwater Specialty Conferences – GeoSask 2005*, Saskatoon, Canada.
- Hammah, R.E., Yacoub, T.E., Corkum, B., Wibowo, F., Curran, J.H. (2007), Analysis of blocky rock slopes with finite element shear strength reduction analysis. 1st Canada – U.S. Rock Mechanics Symposium, Vancouver, ARMA-07-040
- Ingber, L. (1989). Very fast simulated re-annealing. *Mathematical and Computer Modelling*, 12(8):967–973.
- Janbu, N. (1954). Application of composite slip surface for stability analysis. *Proceedings of the European conference on stability of earth slopes*, Stockholm, pp. 43–49.
- Li, S., Cami, B., Javankhosdel, S., Corkum, B., Yacoub, T., (2020). Considering multiple failure modes in limit equilibrium slope stability analysis: two methods., *GeoCalgary 2020*.
- Li, X. 2007a. Niching Without Niching Parameters: Particle Swarm Optimization Using a Ring Topology, *IEEE Transactions on Evolutionary Computation*, 14(1): 150–169.
- Li X. 2007b. A multimodal particle swarm optimizer based on fitness Euclidean-distance ratio. *Proceedings of the 9th annual conference on Genetic and evolutionary computation (GECCO '07)*, New York, NY, USA, 78–85
- Li, X. Epitropakis, G. M. Deb, K. and Engelbrecht, A. 2017. Seeking Multiple Solutions: An Updated Survey on Niching Methods and Their Applications, *IEEE Transactions on Evolutionary Computation*, 22(4): 518–538
- Ma, T., Mafi, R., Cami, B., Javankhosdel, S., Gandomi, A. (2022), NURBS surface optimization for identifying critical slip surfaces in 3D slopes, *ASCE Int. J. Geomech.* 22(9).
- Mafi, R., S. Javankhosdel, B. Cami, R. J. Chenari, and A. H. Gandomi. (2021). Surface altering optimization in slope stability analysis with non-circular failure for random limit equilibrium method. *Georisk: Assess. Manage. Risk Eng. Syst. Geohazards* 15 (4): 260–286.
- Mishra M., Ramana G.V., Maity D. (2020). Multiverse optimisation algorithm for capturing the critical slip surface in slope stability analysis. *Geotech. Geol. Eng.* 38:459–474.
- Morgenstern, N. R. & Price, V. E. (1965). Analysis of stability of general slip surfaces. *Geotechnique* 15, No. 1, 79–93.
- Spencer, E. (1967). Method of analysis of stability of embankments assuming parallel inter-slice forces. *Geotechnique* 17, No. 1, 11–26.
- Wright S. (2002). Personal Communication.
- Wu A., (2012). Locating general failure surfaces I slope analysis via cuckoo search. Rocscience internal report.
- Xiao Su. (2008). “Global Optimization in Slope Analysis by Simulated Annealing” Internal Rocscience Work Term Report.
- Xiao Su. (2009). “Global Optimization of General Failure Surfaces in Slope Analysis by Hybrid Simulated Annealing” Internal Report.
- Zienkiewicz, O.C., Humpheson, C., Lewis, R.W (1975). Associated and nonassociated. Visco-plasticity and plasticity in soil mechanics. *Geotechnique* 25(4), 671–689.



Challenges in the modelling of ground support

Karampinos, E.¹ and Hadjigeorgiou, J.²

¹*Université Laval, Québec City, Québec, Canada*

²*University of Toronto, Toronto, Ontario, Canada*

EXTENDED ABSTRACT

A wide range of numerical modelling approaches are used to model the mechanical interaction between ground support and a rock mass. Although continuum stress analysis approaches, in the modelling of ground support can allow for material deformation and yield, they cannot fully reproduce the prevalent discontinuous failure mechanisms of jointed rock masses. This paper employs three numerical case studies, from field and laboratory investigations, to highlight challenges in the modelling of ground support. Emphasis is given on the importance of adequately reproducing the failure mechanisms of both the rock and the ground support elements to successfully capture ground support performance. It is demonstrated that discontinuum stress analysis approaches can successfully model the failure mechanism of anisotropic rock masses, rock reinforcement, and welded wire mesh surface support.

INTRODUCTION

Stress analysis modelling is a valuable tool in the investigation of ground support requirements and performance in rock engineering. A wide range of stress analysis approaches are used to model ground support. Continuum modelling approaches are more widespread for multiple reasons including relative ease of use. These approaches can reproduce the displacement and yield in the rock mass but cannot fully capture the associated failure mechanisms in anisotropic rock mass behaviour. When the aim is to investigate the performance or the residual capacity of individual ground support elements, or a system, for the purposes of design specifications, explicit modelling of ground support is necessary. In this case, it is critical to capture the loading and failure mechanisms in both the rock and the ground support. This paper focuses on the challenges associated with modelling ground support using three examples that reproduced the mechanical behaviour and failure mechanisms of anisotropic rock masses, rock reinforcement and welded wire mesh.

REPRODUCTION OF THE BUCKLING SQUEEZING MECHANISM IN HARD ROCK MINES

Structurally defined squeezing mechanism in hard rock mines often results in a buckling failure mode and large rock deformation. The buckling mechanism is driven by relatively high stress and the presence of foliation and can result in detachment and rotation of rock slabs. Continuum stress analysis approaches have modelled the deformation and damage in the walls under these conditions (Kalenchuk et al. 2017). However, they cannot capture the structurally controlled buckling failure mechanism. It is only discontinuum approaches that can potentially reproduce the complex anisotropic rock mass behaviour including block deformation rotation and relative movement of blocks. Figure 1 shows the modelled squeezing mechanism at the LaRonde mine using the 3D discrete element method (DEM). This model reproduced the level of deformation as observed underground and allowed for rotation of blocks, opening of fractures and block detachment that would have not been possible with a continuum modelling approach. The stress redistribution around the excavation, the development of the plastic zone and the slip in the structures agreed well with field observations.

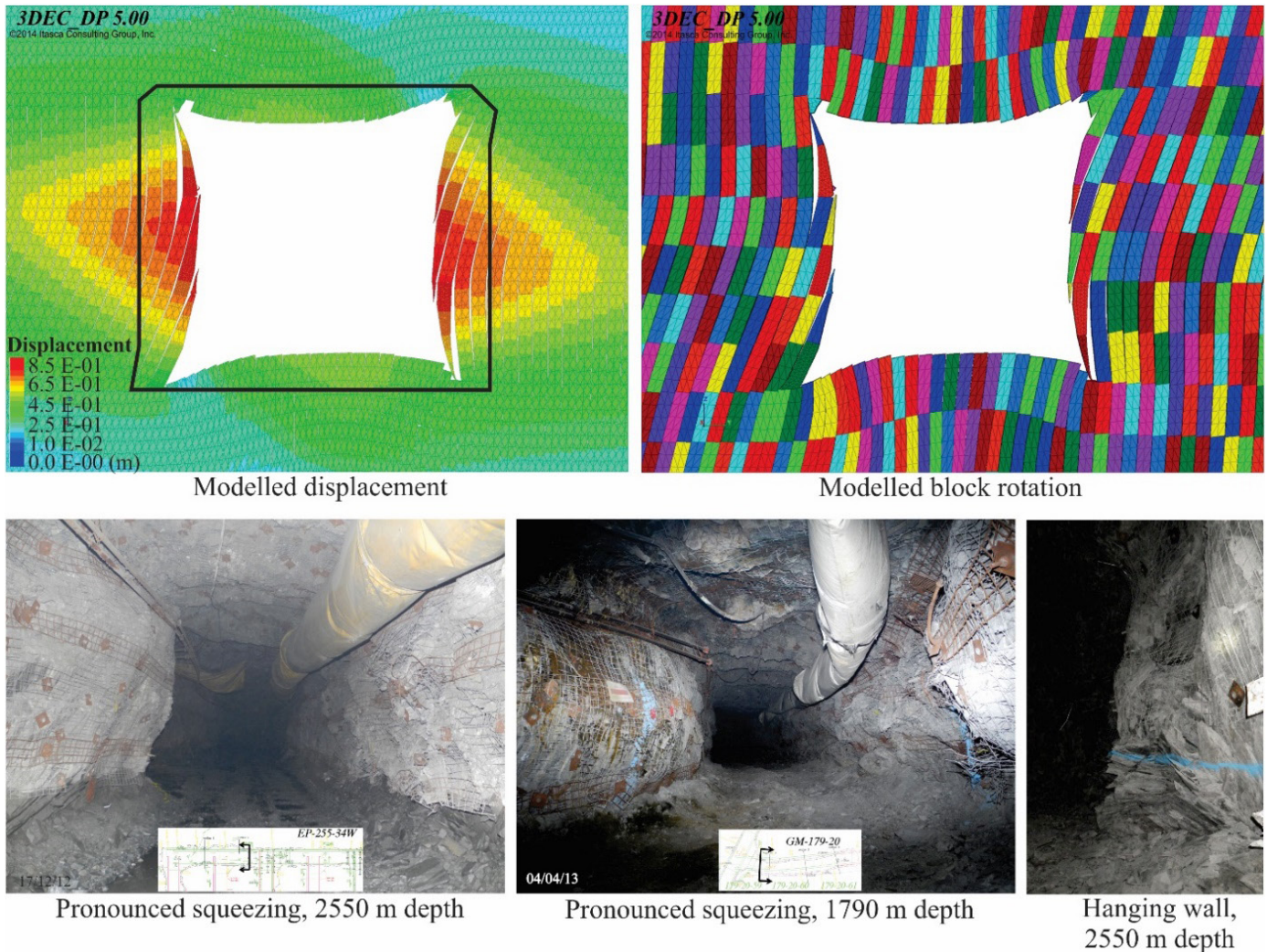


Figure 1: Modelled squeezing mechanism in LaRonde Mine (Karampinos et al., 2015).

The reproduction of the failure mechanism in discontinuum stress analysis approaches requires the explicit representation of discontinuity geometry and a relatively more extensive calibration process. It is the first step for adequately modelling ground support under the observed discontinuous failure mechanisms.

REPRODUCTION OF THE FAILURE MECHANISM OF ROCK REINFORCEMENT

Continuum modelling approaches can model rock deformation but cannot fully capture the role of the various ground support elements in anisotropic rock mass behaviour. Limitations of continuum approaches consist of difficulties in capturing load response and rupture potential of reinforcement crossing discontinuities, inability to capture localized strain and difficulties in interpreting numerical results (Pierce et al. 2018). Figure 2 shows an example of modelling of ground support in structurally controlled deformation at LaRonde mine. The rock reinforcement elements were modelled explicitly using structural elements in the 3D DEM. An extensive calibration process of the material properties of the structural elements was first necessary to capture the mechanical behaviour of the different rock bolt types. Modelling of in situ pull-out tests on the rock reinforcement elements was used to reproduce the load-displacement response and the failure mechanism of the bolts. The calibrated structural elements were subsequently introduced in the model, at different deformation stages in the same sequence as installed in the field. The model reproduced the mechanical behaviour of ground support observed in the field.

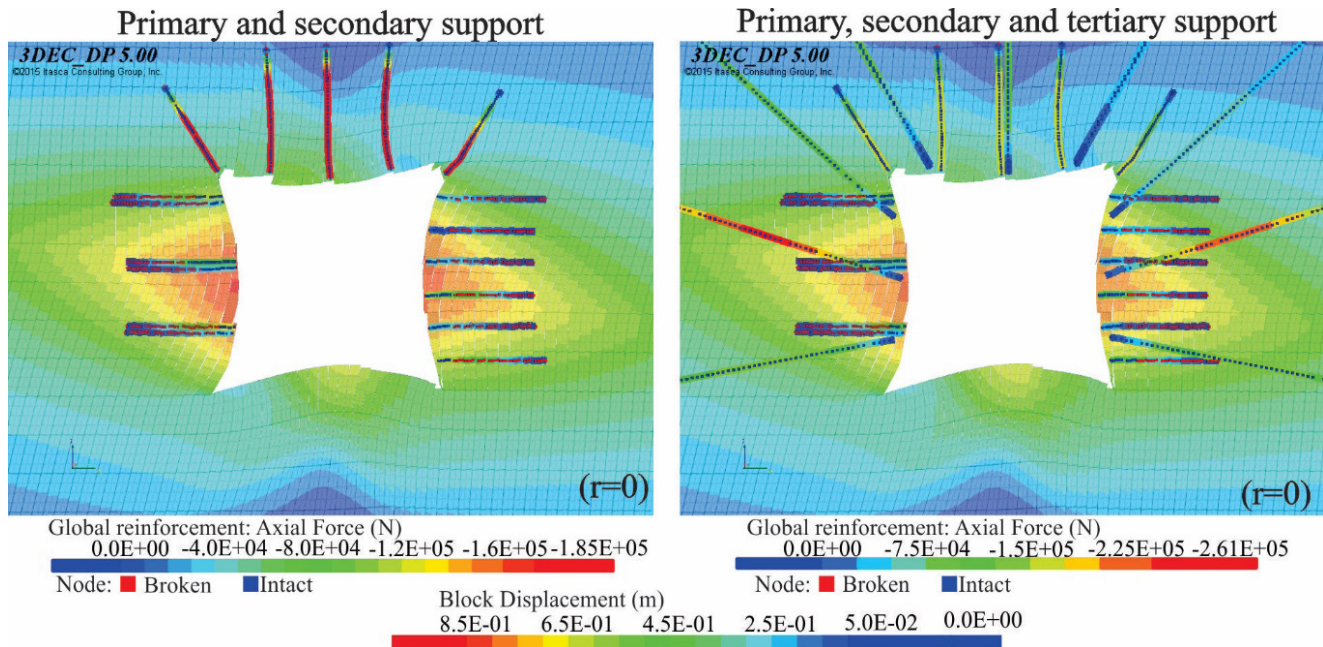


Figure 2: Modelled performance of rock reinforcement elements in squeezing ground (after Karampinos et al., 2016).

Explicit modelling of rock reinforcement was necessary to capture the sliding failure mechanism of friction rock stabilizers and hybrid bolts in the walls, the high axial load of rebars in the back and the impact of the different reinforcement elements on the displacement. The use of a discontinuum approach, although more challenging than a continuum approach, reproduced the performance of bolts in anisotropic rock mass behaviour. The numerical results agreed with field measurements and observations at the mine. This is a prerequisite for subsequent investigation of the impact of different reinforcement scenarios using numerical modelling.

REPRODUCTION OF THE MECHANICAL BEHAVIOUR OF WELDED WIRE MESH

The mechanical behaviour of mesh as a surface support is controlled by multiple parameters including the type of the mesh, the loading and restraining conditions and the interaction with other ground support elements that are difficult to quantify. Laboratory tests provide valuable information on the mechanical behaviour of mesh under specific testing configurations. Numerical modelling experiments can complement laboratory investigations and provide significant insight into the mechanical behaviour of mesh under different testing configurations.

The main challenge of numerical models is reproducing the interaction between the plates and the steel wires, the redistribution of the load to the steel wires, the displacement of the mesh and resulting failure mechanisms under a range of loading conditions. This has not been fully demonstrated in continuum modelling approaches. The discrete element method (DEM) can be used to reproduce the mechanical behaviour of mesh reported in laboratory investigations. A multi-stage calibration process was followed to overcome difficulties in reproducing explicitly the failure mechanisms of the mesh. The developed models successfully reproduced the load, displacement and failure of the mesh as observed in two different testing configurations. Figure 3 shows the captured difference in the axial load and the failure mechanism in the mesh between a diamond and a square bolting pattern.

The results agreed with the reported laboratory results and demonstrated the importance of reproducing the load redistribution in the steel wires for capturing the mechanical behaviour of the mesh. The developed models can be subsequently extended to investigate the impact of additional loading and restraining conditions on the performance of mesh. These are necessary steps to establish confidence in the numerical modelling of surface support.

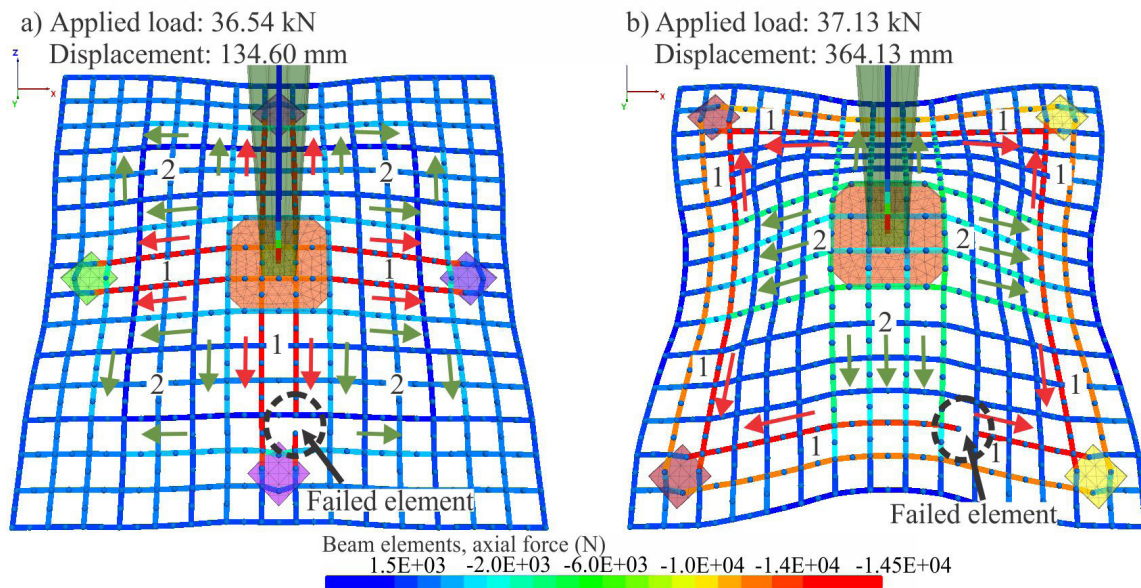


Figure 3: 3D DEM modelling of the mechanical behaviour of welded wire mesh using structural elements; a) diamond bolting pattern; and b) square bolting pattern (after Karampinos and Hadjigeorgiou, 2021).

CONCLUSIONS

The choice of a numerical model should be dictated by the objectives of a problem and what is considered acceptable performance. Continuum modelling approaches are extremely useful and can provide valuable information for a multitude of rock engineering problems. Continuum models, however, have significant limitations in capturing ground support performance. For these purposes, discontinuum modelling may be of greater value. Discontinuum stress analysis approaches can explicitly reproduce the failure mechanisms of anisotropic rock masses and the rock reinforcement, the interaction between the rock reinforcement and the rock mass and the mechanical behaviour of mesh.

ACKNOWLEDGEMENTS

The authors wish to acknowledge the financial support of the Natural Sciences and Engineering Research Council of Canada and several industrial partners. Dr. Jim Hazzard of Itasca Consulting Group, Inc. provided significant technical input in various parts of this work, and his support is greatly acknowledged.

REFERENCES

- Kalenchuk, K.S., Mercer, R. and Williams, E. 2017. Large-magnitude seismicity at the Westwood mine, Quebec, Canada. In *Deep Mining 2017: Proceedings of the Eighth International Conference on Deep and High Stress Mining*, Perth, Australia, 89–101.
- Karampinos, E., Hadjigeorgiou, J. 2021. Quantifying the impact of bolting patterns on the performance of welded wire mesh. *Geotechnical and Geological Engineering*, 39(1), 359–376.
- Karampinos, E., Hadjigeorgiou, J. and Turcotte, P. 2016. Discrete element modelling of the influence of reinforcement in structurally controlled squeezing mechanisms in a hard rock mine. *Rock Mech Rock Eng.* 49(12), 4869–4892.
- Karampinos, E., Hadjigeorgiou, J., Hazzard, J. and Turcotte, P. 2015. Discrete element modelling of the buckling phenomenon in deep hard rock mines. *Int J Rock Mech Min Sci*, 80, 346–356.
- Pierce, M., Hadjigeorgiou, J. and Furtney, J. 2018. Standalone rock reinforcement models as an aid to advanced ground support analysis. In *52nd US Rock Mechanics/Geomechanics Symposium*.



Incorporating probability in modelling – from DFN to numerical modelling

Carvalho, J.L.

WSP (Golder Associates Ltd.), Toronto, Ontario, Canada

EXTENDED ABSTRACT

Probabilistic methods in ground engineering have grown acceptance in the design process over the last few decades. While deterministic approaches are still widely used, the increase in computing power and advances in statistical treatment of geological materials has promoted the use of probabilistic methods. This presentation covers two basic aspects of probability in modelling, namely, characterization of the data and the application of statistical data in analysis and development of tools.

STATISTICAL DATA TREATMENT

One of the most important aspects of modelling is the acquisition and understanding of the input data. This cannot be emphasized enough, especially if probabilistic analyses are the objective. This starts with a comprehensive geological model which will provide the framework to how the acquired data fits together; this data includes not only material behaviour and geological structures, but also regional stresses and hydrogeology.

BLOCK MODELS AND DISCRETE FRACTURE NETWORKS (DFN)

There are a number of very well-developed tools to handle complex geology and represent it in the form of a block model. A block model is a simplified representation of the geology in the form of ‘blocks’ or ‘bricks’ containing estimates of data, such as grade, density, rock type or any other geological and engineering entity values. Although these tools were originally developed to produce estimates of ore grades and reserves, they are now routinely used to provide spatial geotechnical information, which feeds numerical analyses.

Another tool that has been developed and advanced over the last 30 years is the Discrete Fracture Network (DFN). DFN models are built from field data in the form one-dimensional data (e.g., borehole logs or scanlines), two-dimensional data (e.g., wall or cell mapping, outcrop mapping or tunnel mapping), and three-dimensional data (e.g., seismic data). Ideally, these data are acquired in sufficiently large populations to provide reliable statistical representations.

DFN models use a stochastic process, allowing multiple realisations to help constrain the range of outcomes. A technique known as ‘simulated sampling’ compares a sample of the model corresponding to a field data set (e.g., a borehole or traces on a plane) and adjusts the model property distributions until the actual and simulated sampling populations agree.

Discrete Fracture Network modelling is only the start. Accurate definition of the rock mass fabric is the critical starting point for many rock mass characterisation activities. DFN models can be used in their own right for analyses, exported as discrete geometries for use in Discrete Element Methods (DEM, PFC) or upscaled for use in continuum models (e.g., FEM).

LABORATORY AND FIELD DATA

When dealing with measured data, we are faced with uncertainty associated with the parameters we are trying to quantify. This uncertainty can be generally assigned to one of two types, epistemic or aleatory. Epistemic uncertainty (reducible uncertainty) is due to limited knowledge, and one should make all efforts to eliminate it through more sampling, measurements, testing, etc. Aleatory uncertainty (irreducible uncertainty) is due to the natural randomness or variability of the data and needs to be addressed statistically. Strength estimates of rock units rely on intact strength from laboratory testing, rock mass quality from field mapping and drilling, and strength of discontinuities. A convenient way to represent the rock mass quality distribution (e.g., GSI, RMR, etc.) is to use a block model. The advantage of a block model for rock mass quality is that it provides not only the pdf, but it also represents the spatial distribution, which allows one to sample from the correct range of the curve for specific locations in the model (see Figure 1b). Strength data, for intact rock or discontinuities, can be characterized using frequentist (classical) approaches or with Bayesian approaches. The fundamental difference between the two approaches is that in the frequentist approach, the parameters are considered unknown, but fixed, i.e., probability is defined as the limit of the relative frequency of an event after many trials; in the Bayesian approach, the parameters are considered random variables and probability is defined as the degree of belief in an event. The degree of belief is based on prior knowledge about the event, such as the results of previous experiments and probabilities are updated after obtaining new data. Figure 1a shows the results of 10,000 realizations of the intact Hoek-Brown envelope using a Markov chain Monte Carlo (MCMC) technique.

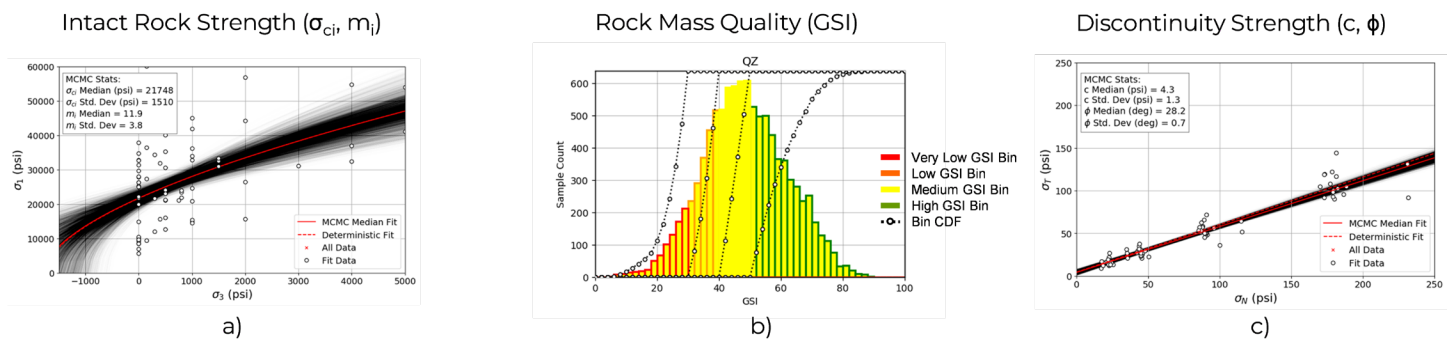


Figure 1: Sampled strength parameters: a) intact rock envelope, b) GSI; c) discontinuity shear strength.

DFN AS AN ANALYSIS TOOL

DFN models can be used directly in the analyses of surface or underground wedges. The ability to cut a slope or a tunnel in a block model to provide a daylighting surface allows stability analyses of wedges. The analyses of wedges/blocks in a DFN setting present significant advantages over conventional wedge analyses. Traditionally, conventional methods consider only 3 fracture sets, assume fractures are ubiquitous and infinite, and wedges sizes are based on maximum possible wedges. They also do not provide size or spatial distribution of wedges, making the probability of failure conditional on the probability of occurrence. On the other hand, DFN analyses of wedges consider both simple and composite blocks, provide spatial and size distributions for a given area of a slope or length of tunnel, thus calculating probability of occurrence and probability of failure. The ability to analyse composite blocks makes DFN an ideal tool to analyse and design inter-ramp (multi-bench) pit walls. Algorithms have been developed to assess the stability of non-daylighting wedges by considering failure through rock mass sections of the sliding surface of large multi-bench wedges, which may have enough drive to break through an intact toe.

Another application of DFN models is the estimation of the rock bridge percentage in a potential sliding surface for large slopes. The rock bridge percentage distribution in a rock mass is generated by sampling multiple

realizations of the DFN model and tracing potential failure paths to obtain the distribution. This distribution can be sampled in conjunction with the procedures outlined in the previous section to use in limit equilibrium slope stability analyses (e.g., Spencer method). Today, it is feasible to use Monte Carlo methods with upwards of 1000's of realizations in limit equilibrium tools. The availability of rock bridge percentages allows the user to define anisotropy in the models by comparing the sliding surface orientation with respect to the fracture sets, and considering the combined strength of the rock mass and the discontinuities, according to their pro-rated strengths:

$$c_{\text{weighted}} = (\% \text{ } rb) \times c_{\text{rm}}^i + (1 - \% \text{ } rb) \times c_{\text{flt}}$$

$$\phi_{\text{weighted}} = \tan^{-1}[(\% \text{ } rb) \times \tan \phi_{\text{rm}}^i + (1 - \% \text{ } rb) \times \tan \phi_{\text{flt}}]$$

The instantaneous cohesion and friction angle, c_{rm}^i and ϕ_{rm}^i , of the rock mass bridges can be determined from the sampled Hoek-Brown envelopes for the correct confinement at the base of the slices.

Numerical Analyses

All the rock mass characterization procedures presented in the previous sections are applicable to numerical models (e.g., FEM, FDM, DEM, etc.). The challenge for numerical models lies in the required time to solve them, which makes it prohibitive to employ a Monte Carlo approach. Also, numerical models provide a much larger set of results than limit equilibrium methods (e.g., displacements, bearing capacity, convergence, extent of failure, SRF, etc.). It is necessary to determine what defines success and failure in order to interpret the outcomes. For instance, in the design of foundations, one may be interested in the probability of the settlement exceeding a threshold; therefore, that should be the parameter that will define the probability of success. In most cases, stability is the outcome of interest, and it is usually measured through the Shear Strength Reduction (SSR) method and the estimation of a Stress Reduction Factor (SRF), which is akin to a factor of safety. This process is very time consuming, even for two-dimensional models. Numerical modellers have employed point estimate methods to overcome these time limitations. This method consists in sampling each parameter at two discrete points, mean minus one standard deviation and the mean plus one standard deviation; the model is then solved for all combinations of the sampled parameters, therefore requiring 2^n realizations. This is feasible when the number of parameters to be sampled is relatively small, as the number of realizations grows exponentially; for instance, if we have 5 materials, each represented by 2 variables (e.g., c and ϕ), the number of realizations is equal to $2^{10} = 1024$, which offers no advantage over the Monte Carlo method.

A better approach that renders the problem more tractable is the Response Surface Method. In this approach, the key parameters impacting the stability of the model are varied independently. The SRF is first computed using the best estimates for all parameters, producing the result for a base case. SRF values are then computed for the same model using credible lower bound and upper bound values for each parameter, k , while keeping all other parameters at their most likely value. A normalized response ($\eta^k = f(x^k)$) is then built for each parameter, k , by fitting the lower bound ($\eta_{\text{LB}}^k = \text{SRF}_{\text{LB}}^k / \text{SRF}_{\text{BC}}$) and upper bound ($\eta_{\text{UB}}^k = \text{SRF}_{\text{UB}}^k / \text{SRF}_{\text{BC}}$) SRFs, normalized by the base SRF_{BC} . The response function for each realization, i , is then approximated as the product of all the normalized responses for each sampled parameter:

$$\text{SRF}_i = \text{SRF}_{\text{BC}} * \prod_{k=1}^n \eta_i^k, \quad i = \text{realization number}; \quad n = \text{number of parameters}$$

The distribution of the response is then derived via Monte Carlo simulations to provide a probability distribution for the SRF. Note this is all conducted outside of the numerical model (in Excel or Python, so it is efficient). Considering our previous example of a model with 5 materials, each with 2 parameters, the number of times the model needs to be solved is equal to 1 (base case) + $2 \times n$ parameters = 21.

This is a much more reasonable number of combinations to solve, and it is feasible with today's available computing power, even for 3-dimensional models. However, the following assumptions need to be observed for the method to be valid:

1. All properties are independent (correlated properties should be sampled together)
2. Impact of all properties is multiplicative, i.e., the product of the ratio of SRF^k to the base SRF_{BC} , η , for two or more sampled parameters is equal to the SRF resulting from direct application of same sampled parameters in a single realization
3. Distributions for the sampled parameters should be limited or truncated by the credible lower bound and upper bound (response function is only valid for this interval)
4. The failure mechanism must be consistent for all realizations

ACKNOWLEDGEMENTS

The author wishes to acknowledge the WSP Golder team who have led, implemented, and advanced the methodologies presented in this publication, namely, Karen Moffitt, Steve Rogers, Karl Lawrence, Mark Nelson, Marisol Valerio, Tina Darakjian, Anna Kate Miller, Rodrigo Ortiz, Paul Matlashewski, and Mike Yetisir, among others.

REFERENCES

- Contreras, L.F., Brown, T. E., and Ruest, M. 2018. Bayesian data analysis to quantify the uncertainty of intact rock strength. *Journal of Rock Mechanics and Geotechnical Engineering*. p. 11–31.
- Golder Associates Inc. 2019, FracMan, version 7.8, computer software, Golder Associates Inc, Redmond, <https://www.golder.com/fracman/>
- Harr, M.E. 1987. *Reliability-based Design in Civil Engineering*. McGraw-Hill Inc., New York.
- Hoek, E., Rippere, K.H., and Stacey, P.F. 2000. Large -Scale Slope Designs – A Review of the State of the Art. In *Slope Stability in Surface Mining*, Hustrulid, McCarter & Van Zyl (eds), SME, Colorado, pp. 3–10.
- Lawrence, K.P., Nelson, M., Yetisir, M. and Matlashewski, P. 2020, 'Kinematic assessment of composite failure mechanisms in pit slopes: a novel slip surface identification algorithm for DFN models', *Proceedings of the 54th US Rock Mechanics Symposium*, American Rock Mechanics Association.
- Rogers, S., Moffitt, K.M. & Kennard, D. 2006, 'Probabilistic tunnel and slope block stability using realistic fracture network models', *Proceedings of the 41st US Rock Mechanics Symposium*, American Rock Mechanics Association.
- Rogers, S.F., Elmo, D., Beddoes, R. and Dershowitz, B. 2009, 'Mine scale DFN modelling and rapid upscaling in geomechanical simulations of large open pits', in JR Read (ed.), *Proceedings of the International Symposium on Rock Slope Stability in Open Pit Mining and Civil Engineering*, University de los Andes, Santiago, CD-ROM only.
- Rogers, S., D'Ambra, S., Dershowitz, W.S. and Turnbull, R. 2018, 'Probabilistic bench scale slope designs based upon realistic discrete fracture network models', *Proceedings of the 2018 International Symposium on Slope Stability in Open Pit Mining and Civil Engineering*, BCO Congressos, Barcelona.
- Rogers, S., Hamdi, P., Moffitt, K.M. & Dershowitz, W.S. 2018, 'DFN based analysis of step path failure pathways for improved slope stability analysis', *Proceedings of the 2018 International Symposium on Slope Stability in Open Pit Mining and Civil Engineering*, BCO Congressos, Barcelona.
- Rosenblueth, E. 1981. Two-point estimates in probabilities, *Appl. Math. Modelling* 5 (1981), p. 329–335.
- Spencer, E. 1967. A method of analysis of the stability of embankments assuming parallel inter-slice forces. *Geotechnique*, 17, p. 11–26.



Recent advances in discrete element modelling

Hazzard, J.F., Potyondy, D.O., Purvance, M.

Itasca Consulting Group Inc., Minneapolis, Minnesota, USA

EXTENDED ABSTRACT

The paper describes recent developments in application of Discrete Element Modelling (DEM) approaches to solving field-scale engineering problems. Current shortcomings and possible solutions are outlined.

Introduction

Cundall (2001) suggested that “the future trend for numerical modelling in soil and rock may consist of the replacement of continuum methods by particle methods.” While Discrete Element Methods (DEM) have become more popular as computer power has increased, they are clearly not replacing continuum methods for engineering applications — especially for field-scale problems.

Three issues with DEM methods are hindering its widespread use in rock engineering:

1. model run times are too long;
2. macroscopic rock behavior is difficult to capture; and
3. micro property calibration is difficult.

This paper describes recent developments aimed at overcoming these obstacles.

ROCK BEHAVIOUR: SPHERICAL GRAINS

From the earliest days of DEM, particles could be circular/spherical or polygonal (Cundall, 1971). The advantage of circular/spherical particles is that the contact detection and force calculations are simple, and the computational demands are therefore reduced. These approaches are very popular in both granular mechanics and rock mechanics; however, there is much evidence that spherical particles cannot accurately capture the micromechanical behaviour of rock — especially those with a crystalline microstructure (Potyondy and Cundall, 2004). This is evident in the well-known inability of these models to reproduce realistic ratios of compressive to tensile strength (≥ 10). Various attempts have been made to overcome this problem including inhibiting particle rotations, clumping together grains into irregular shapes (Cho et al., 2007), providing a grain-based model consisting of a parallel-bonded base material overlain with a polygonal grain structure (Potyondy, 2010; Bahrani et al., 2011), and the flat-joint contact model (Potyondy, 2012; 2018). Each of these approaches has met with some success, but the fundamental problem of unrealistic microstructure remains. For this reason, models of rock are often created with polygonal-shaped grains using the DEM programs UDEC (Itasca, 2019) or 3DEC (Itasca, 2020). Polygonal grains can produce realistic rock-like behavior (Figure 1) but the computational cost can be significant. In 3DEC, every face of a polygon is triangulated, and contact force and displacement calculations are performed at every vertex of every face.

Various researchers have investigated the effect of particle shape, in particular, Voronoi polyhedra versus tetrahedra. While Voronoi grain shapes seem intuitively to be more representative of actual rock microstructure, these models tend to show unrealistic macro behavior (Figure 2). The Voronoi grain shapes may be more realistic, but since the grains themselves do not break, the tortuous path required for a fracture to propagate inhibits macro failure, whereas tetrahedral grains provide a clearer path for failure to occur (see Ghazvinian et al., 2014 and Figure 2). Rasmussen (2022) describes a method for simulation of breakable Voronoi grains and obtains very impressive results in two dimensions.

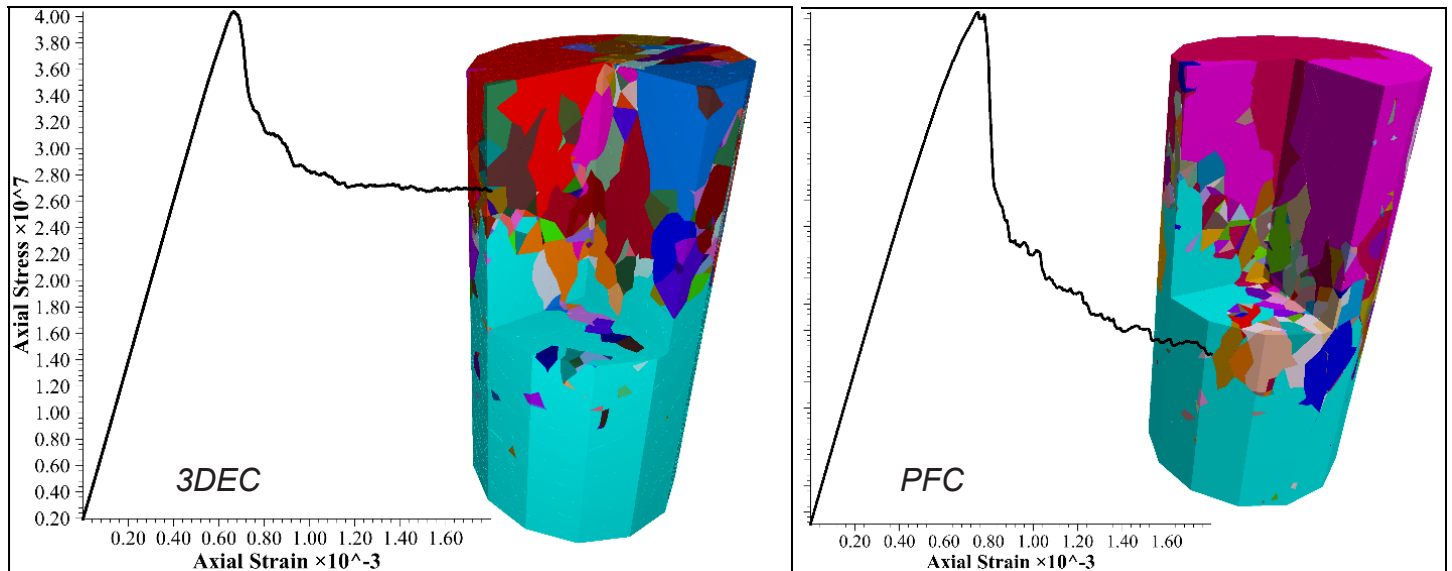


Figure 1: Stress-strain curve and fragmentation in an Unconfined Compressive test in a 3DEC model composed of bonded tetrahedra (left) and a similar PFC model (right).

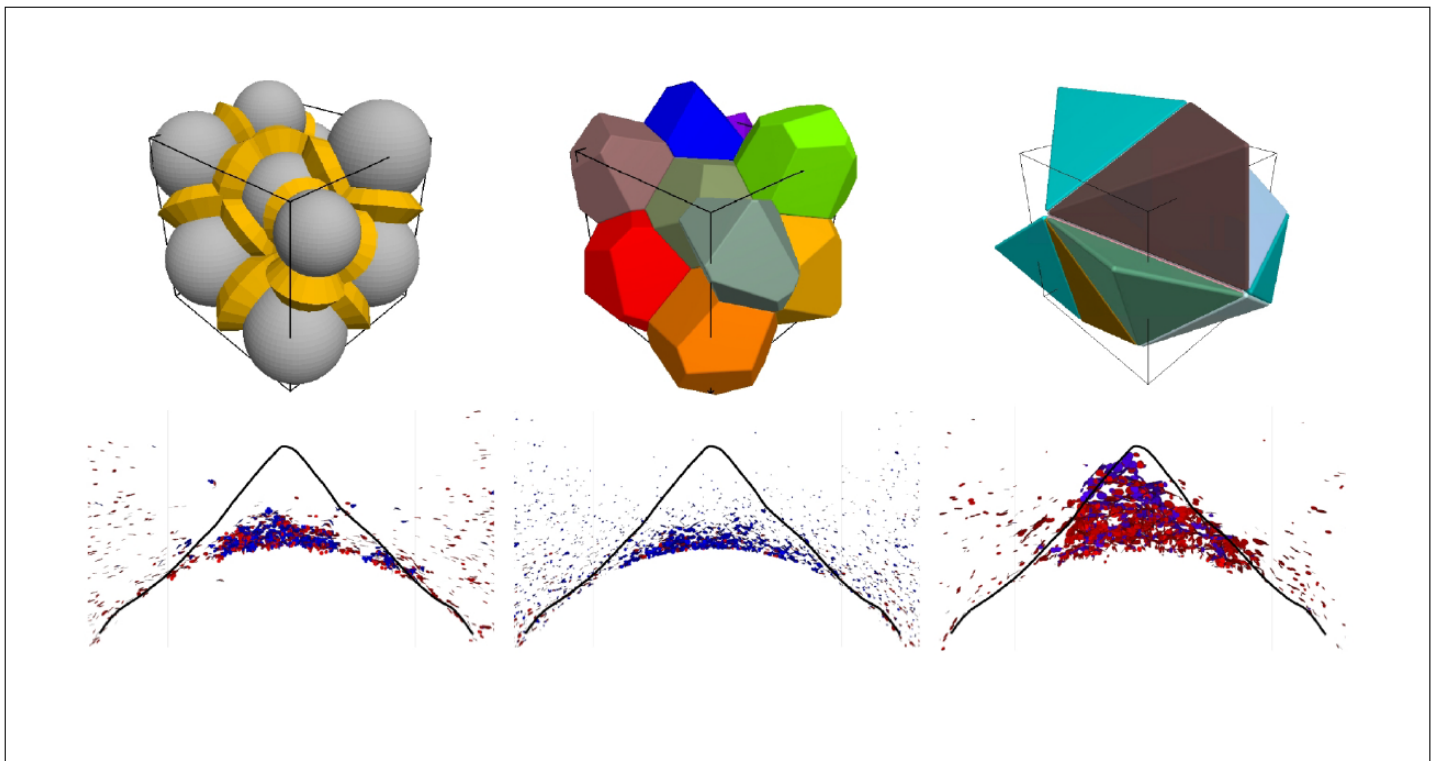


Figure 2: Simulation of notch formation in a tunnel with different grain microstructures. The notch from the Mine-by Experiment test tunnel is shown as a black line. Red and blue disks represent tensile and shear cracks, respectively (from Potyondy et al., 2020).

SPEED

Polygonal blocks in PFC do not produce a subcontact at every vertex. Instead, the Gilbert–Johnson–Keerthi (GJK) algorithm (Gilbert, 1988) is used to determine the overlap state of rigid blocks. With this method, there is only a single contact between blocks, and an iterative approach is used to work out the overlaps between vertices and contacting faces. Figure 1 (right) shows the 3DEC model run with PFC. Results are similar but the calculation time was approximately five times faster.

Another development that enables the possibility of using DEM in field-scale models is easy coupling between a continuum model and DEM model. In this way, the area of interest (with high stress gradients) can be modelled as DEM and the surrounding area can be modelled as a much more efficient continuum with seamless transition of stress and displacements across the boundary (see for example Potyondy et al., 2020).

Finally, the explicit nature of DEM calculations lends itself to distributed memory parallel processing. The easy access to clusters on the cloud makes this a realistic possibility for the average engineer. Recent developments with PFC3D run on an AWS cluster show that significant speed-ups are possible with this approach.

CALIBRATION

Some problems inherent in micromechanical modeling of rock are: (1) the need to calibrate micro properties to achieve the desired macrobehaviour; (2) highly heterogeneous stress distributions leading to unrealistic cracking patterns; and (3) difficulty in matching both compressive and tensile strength. These problems can be overcome with a Spring Network type contact model (Rasmussen, 2021). In this model, the Young's modulus and Poisson's ratio are specified for a bonded specimen, and the elastic response is quite close to the values set, regardless of the rigid block geometry used. This is accomplished using a theoretical method to set the contact stiffnesses based on a lattice with zero Poisson's ratio. Poisson's effect is simulated by applying an elastic correction to the contact forces.

With this approach, it is possible to create a DEM model composed of rigid blocks that comes close to results that would be obtained with an equivalent continuum or hybrid model (continuum with a limited number of fractures). Figure 3 shows a tunnel network with extensive jointing that is modeled only with rigid blocks. Using sufficient blocks with the Spring Network model, a field-scale model can be run in a reasonable amount of time that closely resembles a continuum with the advantage of possible slipping and separation on joints and faults.

SUMMARY

There is clearly still work to be done before Cundall's prediction of a discontinuous future for numerical modelling in geomechanics becomes a reality, but continued advances in algorithms, methodologies and computer systems are bringing the possibility of field-scale DEM modelling closer to reality.

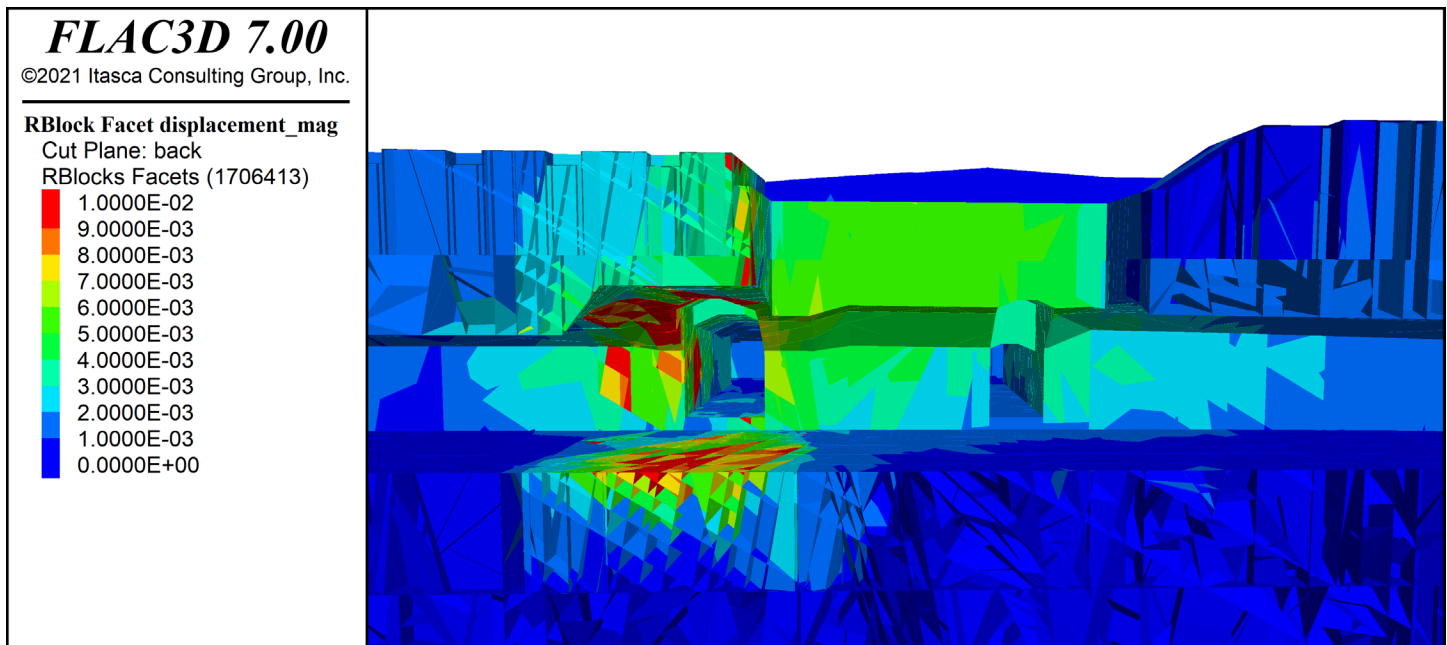


Figure 3: PFC model of 250,000 rigid blocks with many joints showing displacements around tunnels.

REFERENCES

- Bahrani, N., Valley, B., Kaiser, P.K. and Pierce, M. 2011. Evaluation of PFC2D Grain-Based Model for Simulation of Confinement-Dependent Rock Strength Degradation and Failure Processes, in Proceedings of the 45th US Rock Mechanics / Geomechanics Symposium, San Francisco, CA, June 26–29.
- Cho, N., Martin, C.D. and Sego, D.C. 2007. A Clumped Particle Model for Rock, *Int. J. Rock Mech. Min. Sci.*, 44, 997–1010.
- Cundall, P.A. 2001. A discontinuous future for numerical modeling in geomechanics? *Geotechnical Engineering*, 149(1), 41–47.
- Cundall, P.A. and Strack, O.L. 1979. A discrete numerical model for granular assemblies, *Geotechnique*, 29, 47–65.
- Ghazvinian, E., Diedrichs M.S. and Quey, R. 2014. 3D Random Voronoi Grain-Based Models for Simulation of Brittle Rock Damage and Fabric-Guided Micro-fracturing, *Journal of Rock Mechanics and Geotechnical Engineering*, 6, 506–521.
- Gilbert, E.G., Johnson, D.W. and Keerthi, S.S. 1988. “A fast procedure for computing the distance between convex objects in three-dimensional space,” *IEEE Journal of Robotics and Automation*, 4(2), 193–203.
- Itasca Consulting Group, Inc. 2020. 3DEC — Three-Dimensional Distinct Element Code, Ver. 7.0. Minneapolis: Itasca.
- Itasca Consulting Group, Inc. 2021. PFC — Particle Flow Code, Ver. 7.0. Minneapolis: Itasca.
- Itasca Consulting Group, Inc. 2019. UDEC — Universal Distinct Element Code, Ver. 7.0. Minneapolis: Itasca.
- Potyondy, D.O. 2018. A Flat-Jointed Bonded-Particle Model for Rock, paper ARMA 18-1208 in Proceedings of 52nd U.S. Rock Mechanics/Geomechanics Symposium, Seattle, USA, 17–20 June 2018.
- Potyondy, D. 2012. A Flat-Jointed Bonded-Particle Material for Hard Rock, in the 46th US Rock Mechanics / Geomechanics Symposium, Chicago, IL, USA, 24–27 June.
- Potyondy, D.O. 2010. A Grain-Based Model for Rock: Approaching the True Microstructure, in *Rock Mechanics in the Nordic Countries 2010* (Proceedings of Bergmekanikk i Norden 2010, Kongsberg, Norway, June 9–12, 2010), pp. 225–234. C.C. Li, et al., Eds. Kongsberg: Norwegian Group for Rock Mechanics.
- Potyondy, D., and Cundall, P. 2004. A bonded-particle model for rock, *Int. J. Rock Mech. Min. Sci.*, 41, 1329–1364.
- Potyondy, D., Vatcher, J. and Emam, S. 2020. “Modeling of Spalling with PFC3D: A Quantitative Assessment,” Itasca Consulting Group, Inc., Report to Svensk Kärnbränslehantering AB (SKB), Stockholm, Sweden, Ref. 2-5732-02:20R50, October 22, 2020, Minneapolis, Minnesota.
- Rasmussen, L.L. 2021. Hybrid Lattice/discrete Element Method for Bonded Block Modeling of Rocks, *Computers and Geotechnics*, 130, article 103907.
- Rasmussen, L.L. 2022. A breakable grain-based model for bi-modular rocks, *Int. J. Rock Mech. Min. Sci.*, 151, article 105028.



Application of strain-softening in analysis of underground mining

Ghazvinian, E.¹, Fuenzalida, M.¹, Garza-Cruz, T.¹, Cancino, C.¹, and Pierce, M.²

¹*Itasca Consulting Group, Minneapolis, Minnesota, USA*

²*Pierce Engineering, Minneapolis, USA*

EXTENDED ABSTRACT

A numerical model that represents the damage induced by stress or large deformation around an excavation, slope or caving process must account for the progressive failure and disintegration of the rock mass from an intact/jointed condition to a bulked material. Four critical factors that control the overall behavior of the rock mass matrix during this process are as follows:

- **Cohesion and Tension Weakening and Frictional Strengthening:** As the rock mass deforms, it undergoes a reduction in strength from its peak in situ value to a lower residual value. In general, massive to moderately jointed rock masses weaken by fracturing and the associated loss of cohesion and tensile strength but also have the ability to strengthen when even lightly confined due to a combination of friction mobilization and dilation resulting from bulking — the spatial rearrangement of blocks and increasing porosity — of the fractured rock. These mechanisms largely occur in sequence.
- **Post-Peak Brittleness:** The rate at which the strength drops from peak to residual as the loaded material accumulates plastic deformation is referred to as brittleness. Rocks that maintain their peak strength with continued loading are referred to as perfectly plastic (ductile). Rock masses that instantaneously drop to residual strength properties when they exceed their peak strength are referred to as perfectly brittle. In consequence, the brittleness controls how fast or slow the stresses are shed away from the yielded rock mass with accumulated strain.
- **Modulus Softening:** The rock mass increases in volume as intact rock blocks fracture, separate, and rotate during the yielding and mobilization process. As the rock mass bulks, a reduction in modulus is expected to occur. Representing this decrease in stiffness is crucial for assessing the evolving stress state around the cave and underground openings because, as a rock mass dilates/bulks, its ability to carry stress (for a given amount of elastic deformation) decreases.
- **Dilational Behavior:** Dilation is the change in volume of a rock that occurs with shear distortion. An accurate assessment and representation of the dilational behavior of a jointed rock mass is essential to predict the correct volume increase during plastic deformation. This will impact the confinement-dependent strength of the rock mass.

This overall process — loading the rock mass to its peak strength, followed by a post-peak reduction in strength to some residual level with increasing strain — often is termed a “strain-softening” process. The Itasca Constitutive Model for Advanced Strain Softening (IMASS) has been developed to represent the rock mass response to stress changes using strain-dependent properties that are adjusted to reflect the impacts of dilation and bulking as a rock mass undergoes plastic deformation (Ghazvinian et al., 2020).

In IMASS, damage, disturbance and the associated loss of strength (i.e., “softening/weakening”) is captured in two phases delineated by three Hoek-Brown strength envelopes (Figure 1):

- During Phase 1:
 - Damage is the result of fracturing of intact rock due to stress changes. This causes only small (negligible) increases in porosity and permeability.
 - Loss of strength results from small strain processes.
 - The numerical assessment of damage is dependent on the accumulation of plastic shear strain. Phase 1 ends once the rock mass has reached the “critical plastic shear strain” and its strength equals the post-peak strength.
- During Phase 2:
 - Additional straining and disturbance are the result of rearrangement of rock blocks and cause a significant increase in porosity (up to 40%) and permeability.
 - Loss of strength results from large-strain processes.
 - The numerical assessment of disturbance is dependent on the accumulation of volumetric strain (bulking). Phase 2 ends once the rock mass has reached its maximum bulking potential. At this point, the rock mass has reached its ultimate residual strength and its strength will not evolve further with additional straining.

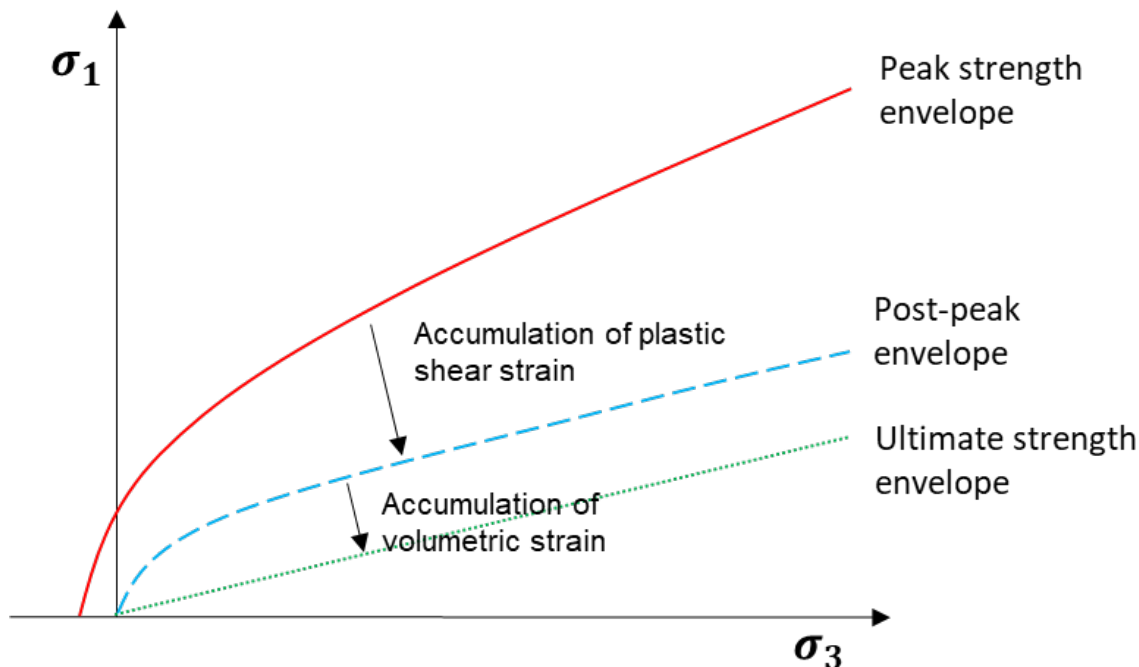


Figure 1: Yield surfaces in IMASS constitutive model.

The ability of a numerical model to simulate key aspects of rock mass strain-softening behavior is critical in capturing the correct ground response when subjected to stress changes as well as large deformations that are expected in various mining applications.

REFERENCES

- Ghazvinian, E., Garza-Cruz, T., Bouzeran, L., Fuenzalida, M., Cheng, Z., Cancino, C., and Pierce, M. 2020, ‘Theory and Implementation of the Itasca Constitutive Model for Advanced Strain Softening (IMASS)’ in R Castro, F Báez & K, Suzuki (eds), Proceedings of the Eight International Conference & Exhibition on Mass Mining (MASSMIN 2020), pp 451–461.



Geotechnical domain determination and characterization – what assumptions have you inherited?

Palleske, C.K.

RockEng Inc., Kingston, Ontario, Canada

EXTENDED ABSTRACT

The concept of geotechnical domaining is implicated in nearly all aspects of geological engineering practice. During the data collection phase, information is grouped into “domains” which are often defined (spatially or geologically) by the interval being logged or mapped. Geological boundaries are frequently defined prior to geotechnical investigations with a different application in mind (lithologies grouped into “ore” and “waste”, for instance) and these same boundaries are then adopted for the domains used in the geotechnical work. Any geotechnical design tool, whether empirical, numeric or analytical, rely on explicitly defined domains where representative parameters are applied. Despite the critical importance of having appropriately defined domains, there are no widely used standards to guide domaining and the domain definition process relies on the experience of practitioner and their understanding of geological controls on ground reaction. Some of the factors to consider in the data collection, domain delineation and domain characterization portions of a geotechnical study and the assumptions that are often made or inherited throughout these project stages are presented here.

DATA COLLECTION – CAMPAIGN PLANNING

Typically, geotechnical data collection campaigns primarily consider the geometry of a project with limited attention to site geology. Data collection targets generally focus on ensuring good spatial coverage, and, particularly if structural data is being collected, reducing orientation bias. In some cases, data collection may target critical geological features, such as major faults. If the site geology is relatively simple this approach is adequate, though not necessarily comprehensive. When a site is geologically more complicated, the limitations of a geometry-based data collection campaign introduce geotechnical project risks as there is far greater impact should critical sampling zones be overlooked.

For sound planning of data collection, regardless of site complexity, all available relevant information should be reviewed to determine or conceptualize conditions that are likely to be encountered, with a particular focus on identifying zones or features that may create significant ground control challenges. It should be noted that at this stage, assumptions are made about what domains exist and therefore require sampling. For this reason, a good understanding of the geology of the site and of similar systems, as well as the associated ground behaviours should be relied on to minimize risks associated with characterization blind spots – effectively recognizing the assumptions that are being made when choosing where to collect information.

Subsequent data collection should then aim to provide sufficient sampling (in type, quantity and spatial distribution) of these domains of interest (based on perceived hazard), as well as the main bulk of the rock mass, to increase confidence (i.e., data uncertainty is reduced) in their characterization for design applications. Planning an adequate data collection campaign requires examining the data that is already available regarding the structural and geological history of the site and conceptualizing the ground conditions that will be encountered

(with significant relevance to engineering design). For example, when planning a laboratory testing program, focus should be placed on specific mechanical properties that are most relevant to the expected ground reaction based on the geological conditions and the specifics of the project (for instance shear strength rather than UCS values for relatively shallow slopes in strong rock) (Kalenchuk et al., 2020). The data to be collected should serve to prove (or disprove) the assumed model.

DATA COLLECTION – CAMPAIGN EXECUTION

Standard geotechnical campaigns will collect parameters from commonly used classification systems that assume a certain range of ground conditions and associated behaviour; however, if the conditions or expected behaviours for a project fall outside the usual range(s) of these systems, then the factors relevant to these outlier conditions must also be collected. A good understanding of the geological setting allows loggers or mappers to know what to expect and enables the data collection campaign to adapt accordingly. This may include assessing slaking potential in soft or clay-rich rocks or defining intensity of diskings in burst-prone ground.

The factors most relevant to domain definition often fall outside of the geotechnical database as geomechanical domains are controlled by geological factors that must be identified at the data collection stage (if not before). As such, the geological factors that are associated with changes in geomechanical parameters (e.g., alteration types - if these are known or suspected) must be logged in a systematic way that allows associated data to be easily filtered and grouped. While this may be relatively straightforward during the geotechnical campaign for a logger or mapper familiar with the site lithologies, significant database limitations can be introduced when geotechnical and geological database are inherently incompatible. A geotechnical dataset is far more powerful if it can be directly linked with information in the geology database, which is usually far more extensive. However, it is often the case that the geology database predates geotechnical considerations, the information of interest to the geotechnical practitioner has not been collected, and/or the loggers/keepers of the geology database are not amenable to change. This illustrates the importance of incorporating geotechnical data objectives early in a project to enable adaptation of geological data collection before it becomes too onerous to adjust. In all cases where a separate geology database exists, the geotechnical practitioner should become familiar with geological data collection procedures and practices and note areas where discrepancies may occur (for instance ignoring narrow intrusions in a host rock that are unimportant to an orebody model, but are associated with alteration that changes ground behaviour).

DOMAIN DELINEATION

Geotechnical domains can be grouped into two broad categories: design domains that are defined by the excavation geometry (typically scale and orientation), and geomechanical domains that are defined by geological controls and ground reaction modes or mechanisms. As optimising excavation geometry is often one of the goals of a geotechnical study, and therefore at least partially determined by the practitioner, design domains are not discussed further here.

Delineation of appropriate geomechanical domains may be an iterative process – starting with the domain conceptualization from the initial assessment of the site geology and merging or sub-dividing these domains if additional information indicates this is appropriate.

Geomechanical domains group volumes with similar parameters and expected behaviours; thus, a domain with a wide range of data variability should be treated as a flag and reviewed rigorously to evaluate underlying assumptions. Specifically, this should include:

- Is the design/analysis sensitive to the variable parameter(s)?
- Are the data reliable? (i.e., are the values “correct”?)
- What is the cause of the variability?
- How is this variability spatially distributed?

Once these aspects of data are understood, the appropriateness of the domain limits should be reevaluated. The level of refinement of domains depends on the variability of the ground and the type of study or analyses being undertaken.

The rock quality distribution curves shown in Figure 1 demonstrate variable ground conditions within several lithology domains. For high-level characterization (e.g., estimating required ground support levels during a pre-feasibility study) these groupings may suffice. However, as the level of detail applied to geotechnical analyses increases, these domains become too broad and determination of representative parameters becomes impossible. A better understanding of the source of the variability and its spatial distribution is required to create more appropriate geomechanical domains. In the case of Figure 1, domaining has been assigned by rock type and the presence of alteration zones has been overlooked. Altered rock mass volumes have been grouped with the unaltered volumes because the underlying lithology types are the same. The inadequate domaining is evidenced by the shape of the curves; for most units, the curves up to about the 40th percentile cover a wide range of rock quality (in this case, based on site specific knowledge, this is known to be associated with a range of alteration types and/or intensity). Above the 40th percentile the rock mass quality is more consistent, and representative of conditions in the unaltered volumes.

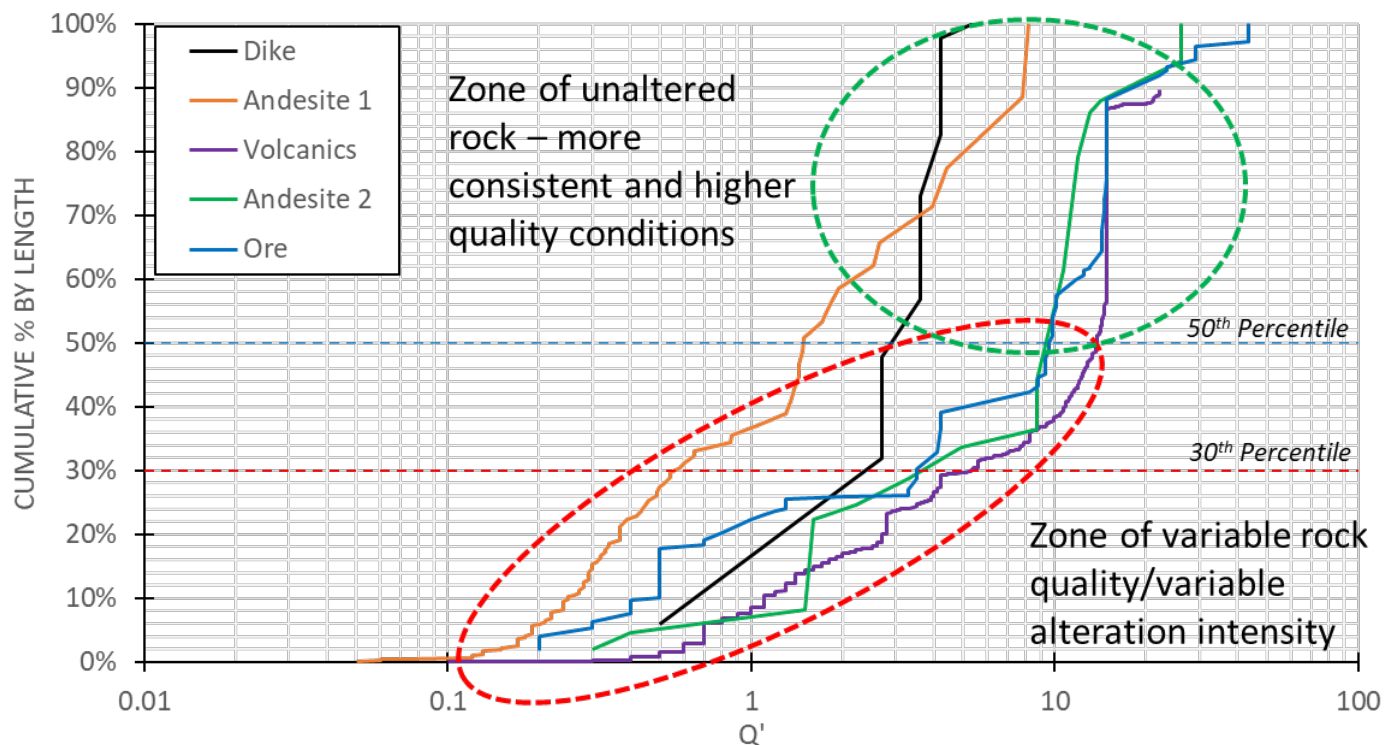


Figure 1: Distribution curves grouped by lithology for a project site.

DOMAIN CHARACTERIZATION AND/OR PARAMETERIZATION

When conducting geotechnical design, it is common to do sensitivity testing on a range of input parameters, especially when the geomechanical domains are identified as highly variable or uncertain. However, it is much

less common to evaluate the validity of the assumed domains over which those parameters are applied (i.e., has the smearing of variable data caused the model outputs to be out of line with observations). The rock quality distributions shown in Figure 1 illustrate the difficulty of parameterizing a variable domain. It is common to use “average” and/or “lower-bound” conditions (e.g., the 50th percentile and 30th percentiles indicated in Figure 1) as these are inferred to be appropriate, and reasonably conservative design inputs. However, as demonstrated by the case described above, these values are not actually representative of the altered ground or of the fresh rocks. Further, as it is more likely that the poorer quality rock will be located in spatially limited zones around controlling structures and not randomly distributed throughout the domain, using “average” values may prevent a model or design from capturing the behaviours and conditions that are the most critical to a project.

In the author’s experience there is a tendency to respond to data variability by collecting more data but rarely by re-evaluating the appropriateness of the geological model to which existing data has been applied. The root of this may lie with the geotechnical practitioner not feeling capable, qualified or entitled to adjust a site’s geology model to create new domains or because the practitioner has not recognized that the assumptions and simplifications that are appropriate for the geology model are not the same for a geomechanical model.

The technique/skills/budget required to collect and analyse geotechnical data are often an inherent limitation to geotechnical design. This is particularly true for advanced modelling techniques which depend on an increased number of input parameters. In instances where the input parameters can be collected (extensive laboratory testing, for instance), model outputs are still dependent on these parameters being assigned in an appropriate way to appropriate volumes. For many projects, developing a good understanding of the site geology and how geological controls impact ground behaviour is more useful than collecting large amounts of information to add precision to flawed assumptions.

SUMMARY

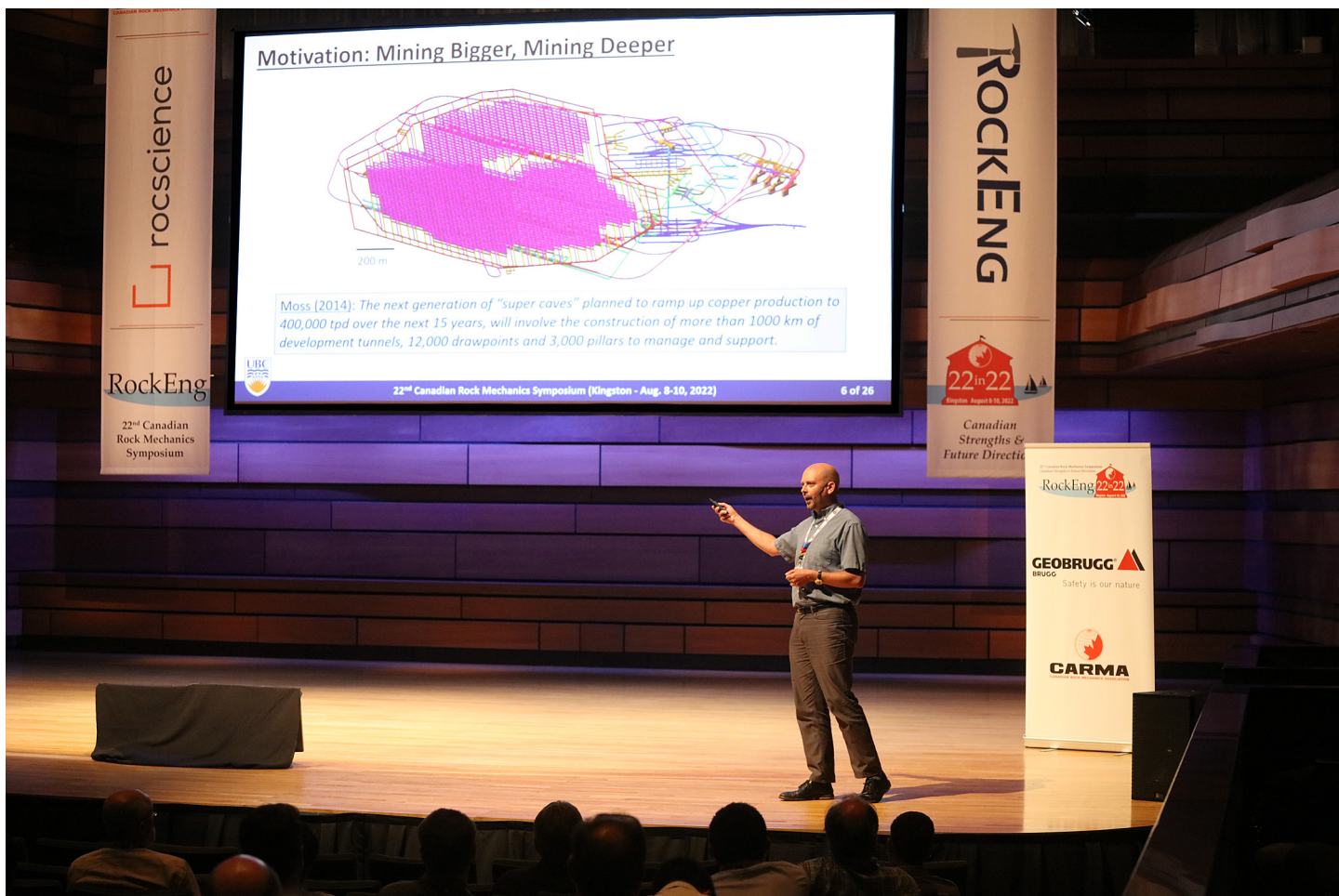
Geotechnical analyses and designs rely on domain definition; however, all stages of site characterization (planning data collection, conducting data collection and data analyses) often rely on inherited models that are typically built for non-geotechnical purposes using geological and geometric assumptions and simplifications that may or may not be appropriate for geotechnical efforts. Because practitioners inherit geological and geometric assumptions, it is critical that geotechnical practitioners:

- Be, or become, familiar with relevant geology
- Give critical thought to potential geological controls on design outcomes at all site characterization stages (starting at data collection planning)
- Analyse data with consideration for both geometric domains and geomechanical domains

Improving the quality of geotechnical analyses and designs often does not require more advanced techniques or even the collection of more data but rather a sound understanding of the geological setting of a project and how to apply what is known in the most meaningful way for a given project stage.

REFERENCES

Kalenchuk, K., Palleske, C., Hume, C. and Oke, J., 2020, June. Support Design and Implementation in Difficult Ground Conditions-Managing the Expected and the Unexpected. In ISRM International Symposium-EUROCK 2020. OnePetro.



Mining deeper: The need for new numerical tools for brittle rock failure

Eberhardt, E., Rahjoo, M., Lavoie, T., Roy, J., and McMillan, R.

The University of British Columbia, Vancouver, British Columbia, Canada

EXTENDED ABSTRACT

Stress-induced brittle failure in the form of spalling and strain bursting can lead to significant safety hazards and costly delays through required repairs to installed support systems. Arising from these experiences is that commonly used design tools are proving to be insufficient for robust prediction and can be dangerously misleading. What must be recognized is that these have been developed based on experiences dominated by shear failure, whereas brittle failure involves a component of extensile fracturing that introduces a higher sensitivity to confinement and a geometric dilation that is more directional in its development. Results are presented from recent research directed at developing new continuum- and discontinuum-based numerical tools tailored specifically to brittle failure and deformation-based support design. These are focused at two different scales to address mine footprint reliability and support vulnerability.

MOTIVATION AND BACKGROUND

The World Bank (2017) projects that the demand for copper will see a tenfold increase over the next 30 years in response to the transition towards electric cars and renewable energy sources. However, the ICSG (2019) identify several constraints on copper supply, which include the need to mine deeper as near surface resources are exhausted. Already the industry is seeing the transition of several large open pits to underground mass mining operations to access deeper low-grade porphyry copper deposits, with cave mining methods being favoured due to the tonnages and economics achievable (Eberhardt et al. 2015). Examples of cave mines proposed for British Columbia alone include the Kwanika, Red Chris, Kemess and KSM underground projects. These will add to the already operating New Afton cave mine.

With the need to mine deeper, comes several challenges that expose limitations in existing design tools. First, the new generation of caving projects are unprecedented with respect to their size and depths (see Eberhardt et al. 2015). Thus, the high stress environments and complex stress paths involved are outside the experience-base represented in the empirical design tools frequently relied upon for characterization and support design. Second, the rock behaviour models commonly used for numerical modelling (e.g., Mohr-Coulomb, Hoek-Brown) have been developed based on observations of shear failure in weak rock. Recent experiences in deep cave mining have demonstrated that these are insufficient for robust prediction and design where spalling and strainbursting are encountered. Missing is the consideration that these brittle failure modes are highly sensitive to confinement, experiencing extensional fracturing under low confinement and shear under high confinement (Diederichs 2007). Furthermore, brittle failure involves the generation of fractures sub-parallel to the maximum principal stress, with opening perpendicular to this (Figure 1). Therefore, bulking is directional in its impact on support design, whereas conventional rock behaviour models treat this as a volumetric attribute (Rahjoo et al. 2021). These limitations have significant implications with respect to the depth of failure and bulking displacement inputs required for a deformation-based support design approach as proposed by Kaiser (2016) to safely manage highly stressed brittle rock.

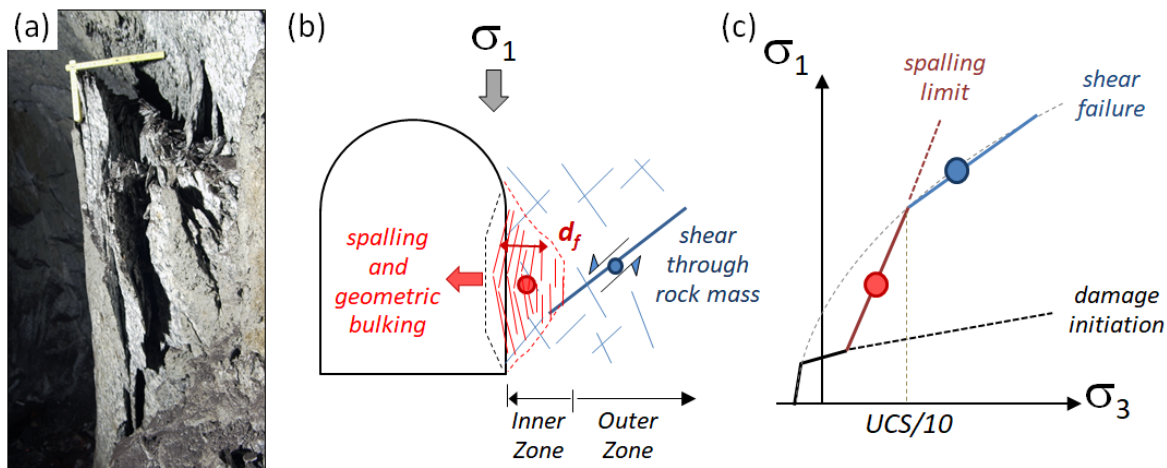


Figure 1: (a) Example of spalling and directional dilation in highly stressed rock. (b) Illustration of low-confinement inner zone dominated by extensile fracturing and high-confinement outer zone dominated by shear. (c) “S-shaped” failure envelope after Diederichs (2007) differentiating low and high confinement behaviours for a $UCS/10$ threshold.

To address these limitations, research has been conducted under the former Rio Tinto Centre for Underground Mine Construction and current International Caving Research Network (ICaRN). Highlighted here are recent results directed at developing numerical modelling procedures to assess both the depth of brittle failure and the corresponding bulking as a function of the cave mining stress path. These have been directed at the mine footprint scale using continuum modelling to better account for the influence of confinement on strength and depth of failure, and at the mine pillar scale using discontinuum modelling to explicitly model stress fracturing, geometric dilation/bulking, and rock support performance.

FOOTPRINT RELIABILITY: CONTINUUM MODELLING

Figure 2 shows the results from a Map3D analysis carried out for an operating panel cave mine using a 3-D confinement-dependent extensional-/shear-fracturing criteria developed by Rahjoo (2019). The analysis simulates an extraction level footprint subject to a post-undercutting sequencing strategy where the extraction level is developed in advance of the undercut. The key indicators used for the analysis include the stress path, strain path (negative principal strains indicate the formation of extensional fractures), and strength σ_2 -dependency. The results closely reproduce the depth of failure observed in borehole camera data as a function of distance to the undercut abutment stress (Figure 2c). Comparisons to the Hoek-Brown criterion calibrated to the crack initiation strength (Figure 2d) was found to significantly under-predict the distal extent (i.e., distance from the undercut) of stress fracturing, and the Mohr-Coulomb criterion calibrated to the crack initiation strength (Figure 2e) was found to vastly over-predict the depth of failure.

SUPPORT VULNERABILITY: DISCONTINUUM MODELLING

Figure 3 summarizes the results from a 3DEC bonded block model simulating a typical cave mining stress path. The key mining stages accounted for include the excavation of the extraction-level drifts (i.e., footprint development), followed by compression of the pillars simulating the abutment stress as the undercut passes over, and slow unloading of the model to simulate the subsequent stress shadowing. Several key learnings have emerged from the models as discussed in Lavoie et al. (2022). Two of the more important findings are: i) adding even a small support pressure (as uniformly as possible) can significantly improve the performance of the excavation; and ii) in a caving operation, it is crucial to install and maintain appropriate support before and ahead of the undercut abutment stress. The difference is mostly attributable to the extra confinement the support pressure provides to the failed skin, allowing it to carry more load and thus provide more confinement to the rock behind it limiting the depth of failure and subsequent rock mass bulking.

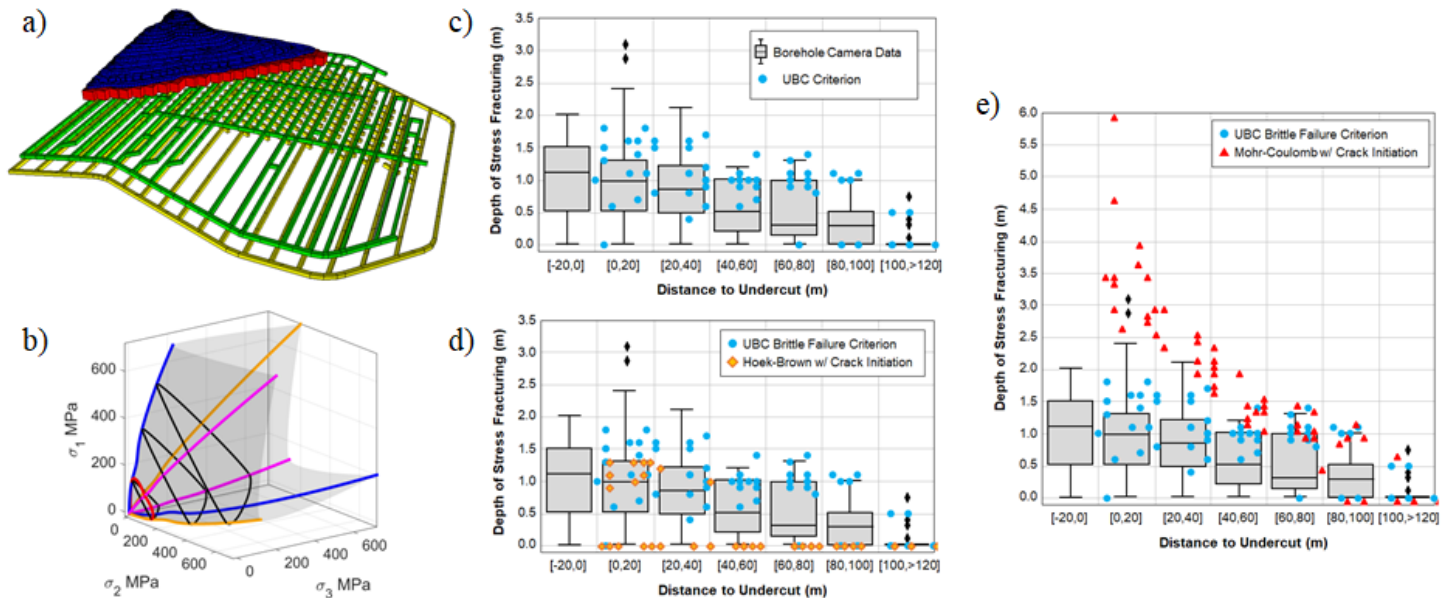


Figure 2: a) Footprint-scale continuum model of an operating panel cave mine, showing extraction level (gold), undercut level (green), advancing undercut (red), and growing cave (blue). b) 3-D confinement-dependent combined extensional-/shear-fracturing strength criterion (see Rahjoo 2019), and c) corresponding model results of depth of stress fracturing validated against measured values derived from borehole camera data (data courtesy of PT Freeport Indonesia). Comparison of model results with d) Hoek-Brown criterion calibrated to the crack initiation strength, which under predicts, and e) Mohr-Coulomb criterion with a crack initiation limit, which over predicts.

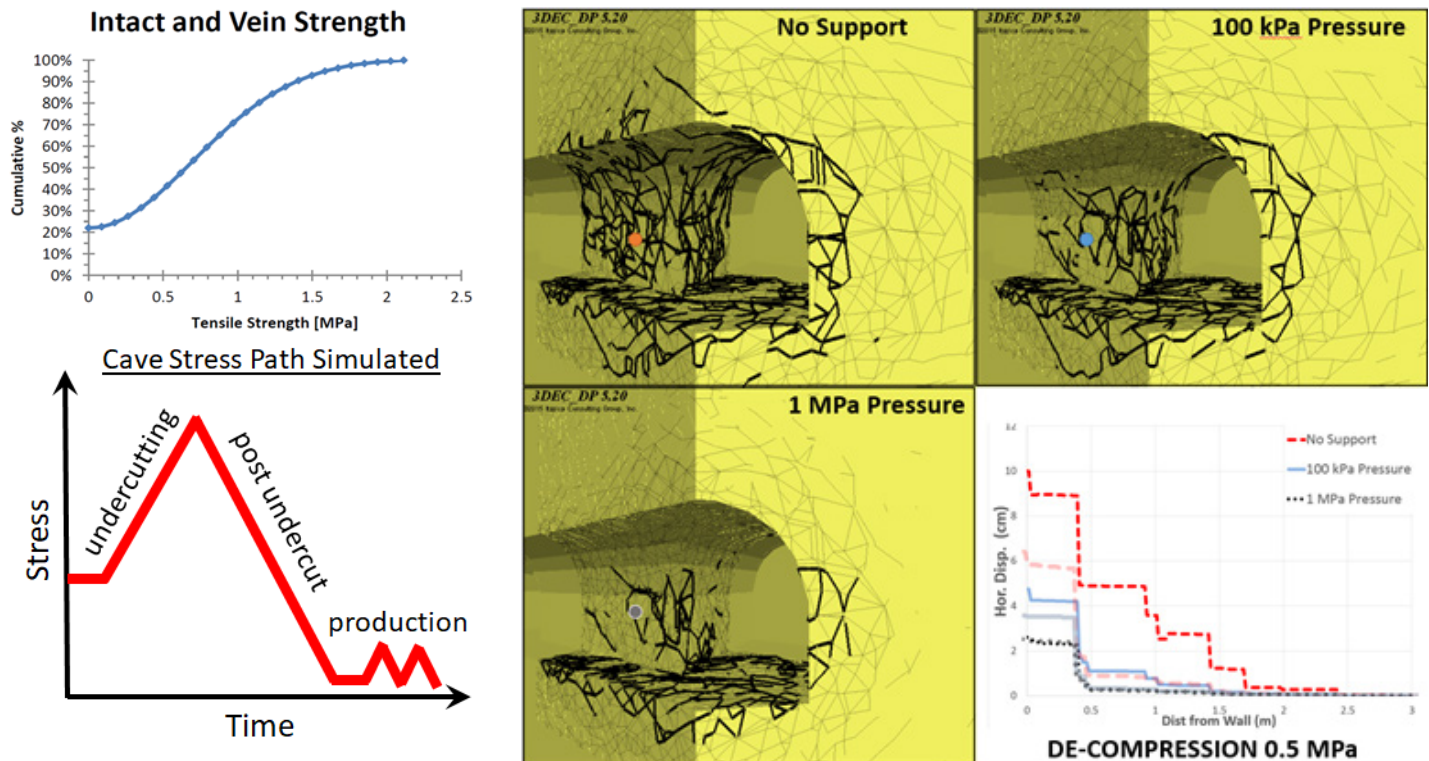


Figure 3: 3DEC-BBM modelling of pillar-scale spalling and support performance. Shown are the model inputs in the form of the distribution of contact strengths (upper left) and cave mine stress path (lower left). To the right, the results compare extent and depth of stress fracturing for 0, 100 kPa and 1 MPa support pressures. The modelled extensometer displacements (lower right) show those corresponding to the undercut abutment stress and maximum pillar compression (fainter traces), and those at the end of the simulated stress path (heavy lines). After Lavoie et al. (2022).

SUMMARY

As new cave mining projects extend to greater depths outside the current experience base, it is essential that they anticipate the rock mass behaviour correctly, requiring the development of new tools that account for stress-induced brittle failure and deformation. First, recognizing the need to model large-scale problems at the footprint scale, we have developed a 3-D confinement-dependent extensional strain-shear fracturing criteria. This accounts for extensional fracturing under low confinement and shear under high confinement to better predict the depth of failure around highly stressed excavations in massive brittle rock. Although not discussed here, we have also developed a corresponding 3-D dilation model to predict the bulking displacements relative to confinement, including an innovative focus on directional dilation (instead of volumetric dilation) to more correctly account for fracture opening during spalling (see Rahjoo & Eberhardt 2021). These have been developed for implementation into any continuum-based numerical code.

At the pillar scale, we have developed a 3-D bonded block modelling technique capable of explicitly modelling brittle failure and the subsequent rock mass bulking due to geometric incompatibilities when broken rock pieces move relative to each other as they are squeezed into the excavation, together with the performance of different support strategies (see Lavoie et al. 2022). The significance of this technique is that it addresses several challenges with respect to 3-D geometric controls on excavation performance, correct handling of the unidirectional bulking associated with brittle fracture damage, and careful consideration of the highly localized straining of support elements at discrete fractures that are both opening and shearing. The model results demonstrate the sensitivity of the brittle failure and bulking processes to confining stress and the effective role that a small amount of support pressure can have on improving excavation performance. This emphasizes the need for deformation-based support design principles, as well as the need to explicitly model the rock support system and its sequencing relative to the mining stress path.

ACKNOWLEDGEMENTS

This work was made possible through funding provided by the Rio Tinto Centre for Underground Mine Construction (RTC-UMC), NSERC, and PT Freeport Indonesia and Mitacs as part of the International Caving Research Network (ICaRN). The authors would like to thank Prof. Peter Kaiser, Dr. Matt Pierce, Allan Moss, Ryan Campbell and Dr. Terry Wiles for their valuable technical contributions to this work.

REFERENCES

- Diederichs, M.S. 2007. Mechanistic interpretation and practical application of damage and spalling prediction criteria for deep tunnelling. *Can. Geotech. J.*, 44(9): 1082–1116.
- Eberhardt, E., Woo, K., Stead, D. and Elmo, D. 2015. Keynote Paper – Transitioning from open pit to underground mass mining: meeting the rock engineering challenges of going deeper. In *Proc. 13th Int. Cong. on Rock Mechanics*, Montreal. ISBN 978-1-926872-25-4, Paper 896: 1–14.
- ICSG 2019. *The World Copper Factbook 2019*. Lisbon: International Copper Study Group.
- Kaiser, P.K. 2016. Ground support for constructability of deep underground excavations. Muirwood Lecture, International Tunnelling Association. ISBN: 978-2-9701013-8-3.
- Lavoie, T., Eberhardt, E. and Pierce, M.E. 2022. Numerical modelling of rock mass bulking and geometric dilation using a bonded block modelling approach to assist in support design for deep mining pillars. *Int. J. Rock Mech. Min. Sci.*, 156(105145): 1–18.
- Rahjoo, M. 2019. Directional and 3-D confinement-dependent fracturing, strength and dilation mobilization in brittle rocks. PhD thesis, Geological Engineering, The University of British Columbia.
- Rahjoo, M. and Eberhardt, E. 2021. Development of a 3-D confinement-dependent dilation model for brittle rocks. *Int. J. Rock Mech. Min. Sci.*, Part 1: 145(104668) and Part 2: 148(104773).
- World Bank 2017. *The Growing Role of Minerals and Metals for a Low Carbon Future*. Washington, DC: World Bank Publications.





Theme 4

In Situ Monitoring and Rock Engineering



Rock engineering innovations in mine design

Espley, S.J. and Larsen, S.

Stantec, Mining and Energy Consulting Engineering, Sudbury, Ontario, Canada

EXTENDED ABSTRACT

Mining methods in underground hardrock environments are slowly evolving to take advantage of the latest learnings in rock behaviour and to leverage new technology in the mining processes. A recent example is the Preliminary Economic Assessment of the Rockcliff Metals Rail and Tower Deposits in northern Manitoba with narrow and steeply dipping veins in competent host rocks. Given the low-grade nature of the copper (zinc, gold, silver) deposits there is an immediate challenge of achieving economic returns from traditional mining methods and designs in underground mining. Open stoping methods with ribs and sills for mine-wide stability are typically applied in this style of deposit with much of the deposit remaining unrecovered. An innovative approach using guiding principles achieves the required economics of these zones and, in turn, drives a new mine design using a selected suite of technologies to enhance safety, unit costs, and productivity – technologies such as automation, remote controls, electric mobile fleets, precise drilling, remote detonation, and mass blasting. The design leverages first-principles thinking for the ground stability assurances of the crown pillars, stopes, and development access headings. A modern shrinkage mining method is the outcome, allowing the hangingwall and footwall rocks to unravel in a controlled fashion and fill the open stope voids as the pull of the ore is extended to the bottom of each deposit. The approach requires innovative approaches in engineering, changing from traditional solutions. Other engineering design concepts and innovations to apply to mine designs are outlined.

GEOLOGY AND BACKGROUND OF RAIL AND TOWER DEPOSITS

Rockcliff Metal's Rail and Tower near surface deposits, and the Bucko Mill near Wabowden community, are located in the Flin Flon-Snow Lake region of northern Manitoba, Canada, as shown in Figure 1.



Figure 1: Mineral Deposit Location: Northern Manitoba, Canada.

The mining concept, as outlined in the Preliminary Economic Assessment, is to extract the Tower and Rail deposits sequentially with rapid development and high production tonnage rates. Mobile assets and core infrastructure are reused and redeployed from one site to the next. Run of mine ore is sorted on surface whereby high-grade ore is shipped and processed into saleable concentrates at the Bucko mill, in a hub-and-spoke arrangement. The sorter's rejects are backhauled and used with development rock as unconsolidated rockfill over top of the broken muck in shrinkage stopes and in AVOCA stopes.

The design of the mine is based on a step change approach in guiding the selection of mining method and technologies to achieve the overarching business goals of zero harm, low carbon, small footprint, engaged workforce, input of communities, and positive returns to shareholders. The required mining goals include high production and development rates using a Rail-Veyor™ with development LHDs and a continuous hagg-style ore loader, low ventilation with a battery-electric mobile fleet, no compressed air and recycled dewatering for process water, accurate drilling of up/down holes with emulsion loading and remote detonators for mass blasting of production stopes, underground communication and real time monitoring and location systems, and limited operational personnel underground by use of automation, process controls, and remote functionality for fans, dewatering, drilling, blasting, and mucking activities. Ventilation and material handling are upside benefits of the Rail-Veyor™ system with air flows in and out of the mine via the twin drift declines, i.e., fresh air pushed down the personnel/access heading and return air pushed up the haulage heading, while the material handling system is extended with the development progress with no schedule delays for infrastructure tie-ins once the ore is reached, as compared to other material movement systems involving crushers, hoists, skips and conveyors. Short stub vent raises are required to supplement air flows across the lateral expanse of each deposit and for winter heating. The twin ramps are laid out with maximum grade, switchbacks, and with level accesses that are widely spaced, vertically, for the footwall extraction Rail-Veyor™ drifts, and a series of transverse crosscuts, as opposed to longitudinal retreat drawpoints, for mucking onto the rail cars. Total footages are minimized from the top of each deposit to depth.

Figure 2 is an isometric view of the Tower Deposit showing the integration of the main design concepts, with additional advantages for setting up underground diamond drilling stations to further explore the deposits' extents to depth and laterally.

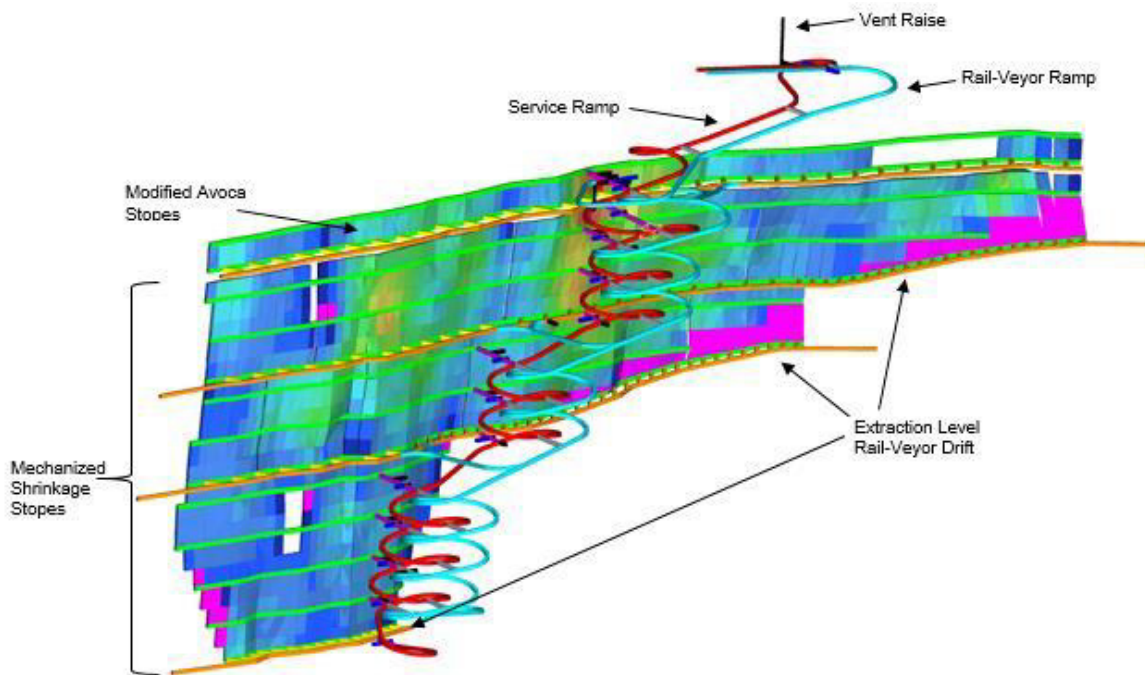


Figure 2: Mine Design, Tower Deposit (Isometric View).

ROCK MECHANICS DESIGN ELEMENTS

Innovative rock engineering solutions include the development of a first-principles approach to stope design to maximize recovery and minimize development, with a summary as follows:

- Rock engineering for modern shrinkage and AVOCA uses inputs/tools to support the mine design, including lithology domaining and geotech core logging, structural and rockmass characterization, stress/strain numerical modelling, and particle flow code modelling to understand ore flows, ore recovery and dilution, waste fill interaction, drawpoint locations.
- Traditional open stope design using Matthew's Method is not reflective of shrinkage design concepts, with controlled caving of the hangingwall and footwall for regional support. Open stope design uses extensive rib and sill pillars, resulting in approximately 50% extraction of these zones while shrinkage and AVOCA allows for +90% recovery. In shrinkage mining, 2 m rib pillars are centrally located to limit the closure of the hangingwall and footwall and extraction is done centre-out.
- A 10-m sill pillar (between AVOCA and shrinkage stopes) is needed for mine stability. Cemented rockfill is a trade-off to allow recovery of the 10 m sill pillar at the end of mine life. 15 m temporary rib pillars are required on all Rail-Veyor™ horizons; this ore is recovered by uppers mining on the next lower stoping horizon.
- Pulling ellipses are used to design drawpoints to maximize ore recovery and limit dilution via waste entrainment from the hangingwall, footwall and unconsolidated waste fill. Drawpoints, widely spaced vertically and horizontally, are staggered from horizon to horizon. This yields exceptional recovery and limits dilution from entrained waste and wall rocks in muck flows.
- A sand zone and regolith in the crown pillars require spiles and pre-grouting and the use of short development rounds with shotcrete to control ground water inflows.
- Box cuts are located according to surface conditions, for each cut's stability and for laydown areas with surface access roads/infrastructure and for mine access via the declines.
- A modified AVOCA mining method supplements the design with early ore, with stoping directly under the crown pillars. AVOCA allows for the extraction activity to be closely followed by filling to limit opening time, to prevent excess deformation and relaxation, to maintain crown stability.
- Short backfill raises on the AVOCA bottom sill are spaced along the strike length and used by LHDs for dumping the reject sorter waste and rock development waste onto the top of the shrinkage stopes as the muck is pulled down.
- Cable bolts are required along the mid-sills into the hangingwall and up into the crown pillars along with ground monitoring of the crowns throughout the mine's life.
- Ground support in development uses 1.8 m resin rebar on a 1 m spacing with screen. Poor ground conditions and drawpoints require 3 m inflatable or 4 m cables with an additional 75 mm shotcrete layer.

SUMMARY

The unique challenges of the modern shrinkage mine design are largely social, in gaining support from stakeholders when diverging from traditional methods to those that leverage innovation for improved safety, productivity, and sustainability. Technical teams can use a whole mine approach, including digital and innovative processes and technologies, to benefit every design and all stakeholders. Shrinkage, with controlled slough for ground support, is not a new mining method. What is new is the use of innovation within the mine design and a need for a first-principles approach in engineering design work. Mine designs can use a step change approach to create guiding principles to improve personnel health and safety, gain 10-100× improvement in production and productivity, and produce high economic yields compared to traditional designs. The shrinkage method is modernized with highly accurate drilling, remote detonation mass blasting technologies, automation, remote control, electric vehicles, and use of material handling via the Rail-Veyor™. Coupled with other technical and social solutions, optimization occurs.

Other mine design improvement opportunities include ore sorting, dry stacking and elimination of tails and waste rock in underground voids, recycling water, use of renewable green energy sources with battery storage, reducing energy use through efficiencies and controllers, and using electric mobile equipment (to replace diesels) with low ventilation requirements. Rock engineering innovations include:

- Stope and excavation cavity monitoring surveys using unmanned vehicles and drones
- Rock behaviour monitoring using wireless technologies for dams, pillars, hangingwall rocks
- Lidar and geo-referencing technologies for auto scanning and mapping of geological structural features in excavations/open cuts
- Automated core logging systems for lithology and geotechnical data and AI database cataloguing
- Traditional methods need to incorporate new thinking to evolve to Zero Harm and Low Carbon designs using modern material movement, process design, and monitoring technologies, challenging our paradigms:
- No shafts, ore/waste passes, and vent raises
- No underground crushers and large excavations (minimized drift heights/widths, dev footages)
- No conveyor belts, haulage trucks and diesel equipment

Stantec uses Prevention through Design and Net Zero in engineering practice – this means identifying hazards and carbon emissions, respectively, during the design phase to eliminate them and/or reduce them to as low as reasonable. This applies throughout the life cycle: exploration, construction, commissioning, operations, and closure. Safe and low carbon design concepts, coupled with economic considerations of maximizing mining intensity, improving operability, improving quality, and gaining high energy efficiency provide the step change in performance. The other critical element to be added is the social engagement – working together on solutions brings new designs to life.

ACKNOWLEDGEMENTS

The authors wish to acknowledge Rockcliff Metals Alistair Ross and Mike Romaniuk for leading the design of a new mining method using Alex Henderson's step change design approach. Geotechnical support by Dr. Mark Diederichs, Dr. Jean Hutchinson, Dr. Mike Yao, Dr. Doug Milne, Farid Malek, and Miguel Fuenzalida were invaluable, along with the oversight by Dr. Kathy Kalenchuk with RockEng and Itasca sub-consultants who completed the PEA geotechnical study elements. The mine design using novel technologies was completed by Stantec's Mickey Murphy and Matt Borraro using Prevention Through Design for the PEA engineering work.

REFERENCES

- Henderson, A. "Guiding Principles for a Step Change Process", 2019.
- Espley, S. "A Whole Mine Approach – Transformation of Mining", 2020.
- BESTECH, 2020, "Preliminary Economic Assessment, Rockcliff Metals Corp, Rail and Tower Deposits and Bucko Mill", NI 43-101 Technical Report.



Residential hillside development and rockfall mitigation

Tannant, D.D.

The University of British Columbia, Okanagan Campus, Kelowna, British Columbia, Canada

EXTENDED ABSTRACT

Residential development on steep bedrock-controlled hillsides is driven by population growth and the desire to exclude new developments from agricultural areas and flood-prone land on valley bottoms. While hillside development costs are typically high, the increased cost is offset by lower undeveloped property purchase costs and the higher price commanded by lots with views. These developments rely on cut and fill excavations for access roads and residential lots. The excavation cuts often create rockfall hazards, and natural rock bluffs are another source of rockfalls.

The Okanagan Valley in southern British Columbia is used to illustrate the rockfall hazards created via hillside developments and techniques used to mitigate the rockfall risk. The rock types in the area are dominated by intrusive igneous rocks, extrusive volcanic rocks, and metamorphic gneiss.

ROCK CUTS

Rock cuts for hillside developments are typically limited to heights less than 8 m for lots and less than 12 to 15 m for roads. However, some rock cuts can be higher. The design for rock cuts typically uses a planned slope of 0.25H:1V. Vertical cuts may be used if the cut height is less than 6 m. A 0.25H:1V cut slope is a practical compromise that maximizes the useable area (maximum for vertical cuts) while helping maintain the rock cut slope stability and minimizing the travel path length for rockfalls. For poor quality rock masses, the rock cut slope may be reduced to 0.5H:1V or even 1:1.

Controlled blasting using a closely spaced line of lightly charged pre-split blastholes is often used when the height of the rock cut exceeds ~6 m. For small rock cuts, a hydraulic hammer mounted on an excavator is used rather than explosives to create the excavation. Hydraulic hammering is also frequently used to trim loose rock from blasted rock faces.

ROCKFALL MITIGATION

Techniques that have been used to manage the rockfall risk are listed below.

- Recommendations to developers and their civil engineering design engineers early in the development process to minimize rock cut heights
- Eliminate lots where the hazard is deemed to be too great
- Locate roads beside the rock cuts rather than houses
- Trim blast or rock scale unstable rock faces
- Use walk-up house designs where the backyard is one floor higher than the street-level garage
- Implement no-build covenants for the rockfall hazard area
- Use small retaining wall landscaping along the toe of rock cuts

- Keep people away from the rockfall hazard zone with a fence and prevent parking near rock cuts
- Upgrade the fence to capture and retain small rockfalls or use purpose-built rockfall fences
- Use a rockfall catchment ditch and add an earth berm where space permits
- Install wire mesh drapery over the rock face
- Hold the rock in place with rockbolts, mesh or wire ropes

ROCKFALL CATCHMENT WIDTH

For some rockfall mitigation options, it is important to estimate the required rockfall catchment width at the base of the rock face. Sometimes it is possible to perform field tests to see how far rocks will travel before the mitigation is implemented. In many cases, months to years pass between a rock face excavation and the initiation of the house construction. This provides an opportunity to assess the rock face performance and response to freeze-thaw and wet-dry cycles. Field observations can indicate the width of the rockfall catchment zone and identify areas where rock scaling should be performed. Knowledge of the required rockfall catchment width is needed for mitigation options such as fences and no-build covenants. Figure 1 shows a chart of the recommended rockfall catchment width versus rock face height with or without a chain-link fence installed along the catchment boundary.

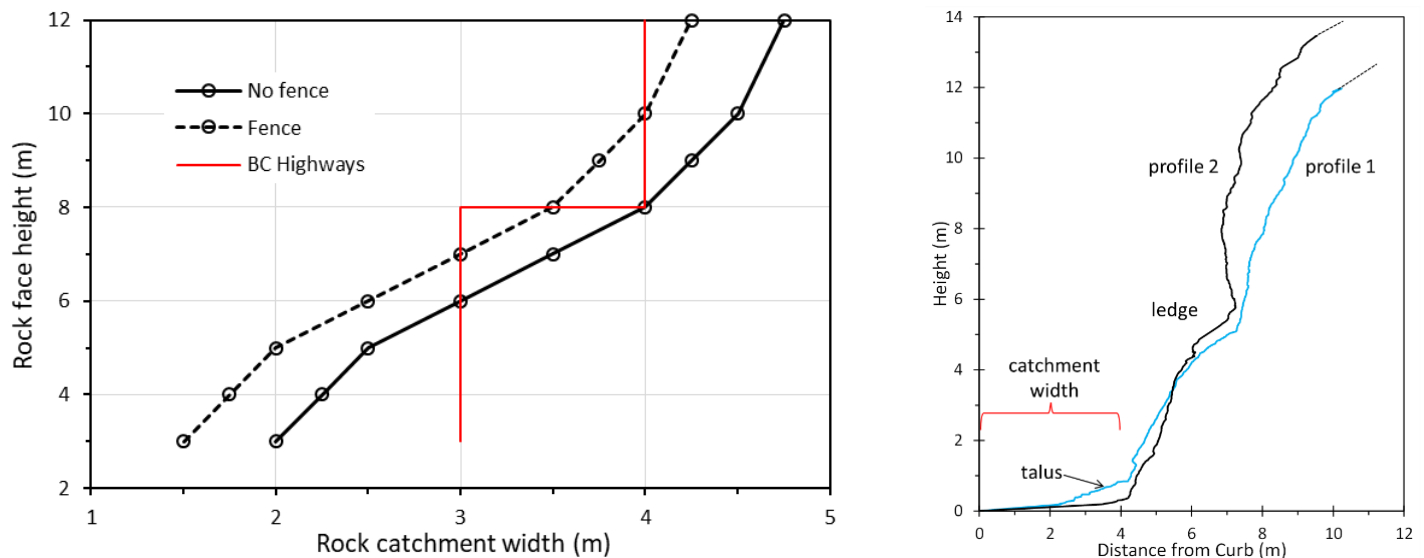


Figure 1: Recommended rockfall catchment width at the toe of a rock cut and two profile examples.

EXAMPLES

Some examples of rockfall mitigation measures are presented in the following photos. Figure 2 shows before and after photos of a trim blast to remove overhanging rock on a natural bluff above a new subdivision. The potential for bat habitat in the cliff delayed the blasting by six months.

The application of multiple rockfall mitigation techniques can be observed in Figure 3. The rock face was excavated using a pre-split blasting technique followed by hydraulic hammering to remove high spots. The rock face was manually scaled. A hybrid of a rockfall fence and wire mesh drapery was installed. Finally, the lots are designed for a walk-up house style to minimize the exposed rock face height (which is still high for a backyard). In Figure 4, a fence was installed in the backyards of stepped lots to keep people away from the rockfall hazard zone. A no-build covenant for the rockfall hazard zone was also placed on the land title for the lots. A fence above the rock cut prevents people and animals from falling over the edge. Access for future rock scaling, debris removal, and rock stabilization, if needed, is also incorporated into the subdivision layout.



Figure 2: Before and after view of overhanging rock removed by a trim blast (trees along the crest also removed).



Figure 3: Backyard rock cut implementing multiple rockfall mitigation solutions starting with pre-split blasting.



Figure 4: Commercial grade chain-link fences used to keep people away from backyard rockfall hazard zones.

Wire mesh drapery restricts the rockfall travel path, allowing for smaller catchment widths. Figure 5 shows examples of wire mesh drapery and the anchors used to hold the supporting wire rope.



Figure 5: High tensile strength wire mesh draped over a rock face and held by an upper wire rope; different techniques are used to anchor the wire rope and keep the wire mesh drapery close to the rock surface.



Characterizing complex seismicity in mines

Brown, L.¹, Carusone, O.², and Pelletier, D.²

¹BESTECH, Sudbury, Ontario, Canada

²Vale, Sudbury, Ontario, Canada

EXTENDED ABSTRACT

Dynamic rock mass failure in mines is a function of many factors, most notably: the three-dimensional stress field, rock mass properties, and mining practices. All of these factors vary significantly throughout a mining environment and over time, making it challenging to quantify and delineate complex seismic responses to mining. By characterizing seismic responses using the independent seismic source parameters time and location, particularly with respect to known mine blast times and locations, insights into the underlying energy sources and processes driving rock mass failure can be gained.

CHARACTERIZING MINE SEISMICITY IN SPACE AND TIME

The presence of diverse rock mass failure mechanisms throughout mining environments contributes to seismic responses with distinctive spatial and temporal characteristics. Induced seismicity is commonly synonymous with stress fracturing related seismic source mechanisms and occurs in close spatial and temporal proximity to mining-induced stress change. Consequently, the energy from induced seismic events is often proportional to the experienced stress change induced by a discrete mine blast (Gibowicz and Kijko, 1996; McGarr et al., 2002). On the contrary, the energy from triggered seismicity may be disproportional to the experienced stress change induced by a discrete blast (Gibowicz and Kijko, 1996; McGarr et al., 2002), and triggered seismic events are largely observed as spatially and temporally independent of discrete mining-induced stress change. This type of seismicity typically results from larger scale rock mass failure processes, such as geological features and high extraction ratios, making it challenging to attribute to individual mine blasts.

Complex seismic responses to mining contain components of both induced and triggered seismicity. These responses often pose a significant risk to mining operations as they represent a potential for disproportionate energy release in proximity to active mine workings. Areas where complex seismicity is observed have recently been blasted and consequently represent increased exposure as workers and/or equipment are likely to be advancing the mining cycle nearby.

Figure 1 depicts seismicity for roughly 12-hours following blasting at Creighton mine. Three distinct seismic responses are approximated by circles and corresponding magnitude time histories are shown. The development blast response (lower right) is relatively tightly spatially clustered with more than 80% of the 27 events occurring within two hours of the mine blast – induced seismicity. The production blast response (upper left) exhibits a strong response in close spatial proximity to the blast, but many seismic events continue to occur throughout the duration of the time window including the occurrence of a $M_w > 1$ event more than 4 hours after the blast – complex seismicity. A third seismic response occurs in a location remote from both mine blasts (lower left), with no clear temporal relation to either mine blast and a $M_w > 1$ event occurring more than 3 hours after the most recent blast – triggered seismicity.

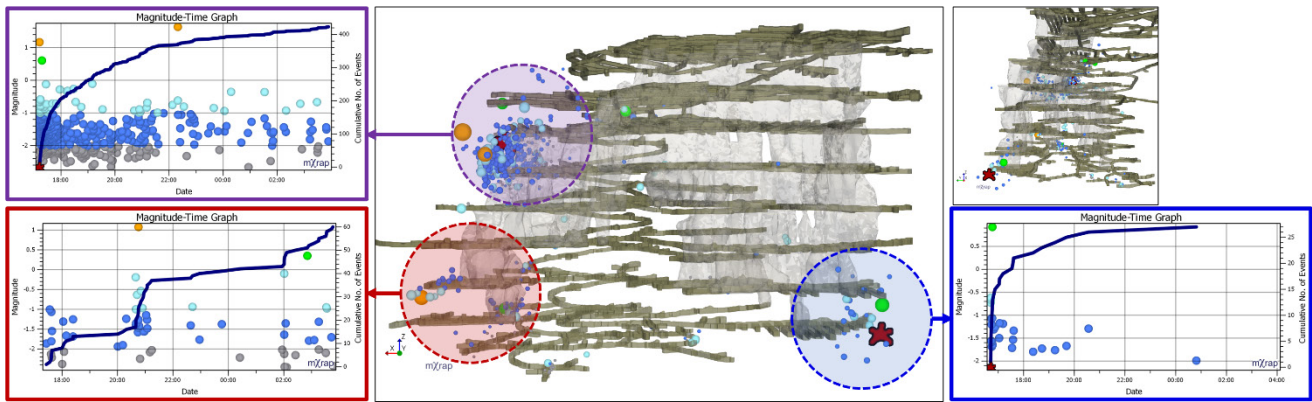


Figure 1: Seismicity occurring within approximately 12 hours of a production blast (upper left) and development blast (lower right) at Creighton mine. Magnitude time history charts for seismic responses approximated by circles are shown coloured in blue, purple, and red for induced, complex and triggered seismicity, respectively. Events are shown coloured according to moment magnitude and blasts are shown as red stars.

SEISMIC RESPONSE PARAMETERS

The proximity of event times to regular mine blasting can provide insights into the mechanisms driving rock mass failure. Time refers to the absolute time of occurrence of a seismic event and is commonly recorded as the GPS synched time of the occurrence of the event. Time After Blast (TAB) is the time difference between a seismic event and the associated mine blast. Time Between Events (TBE) is the time difference between a seismic event and the preceding event within the same seismic response. The upper and lower portions of Figure 2, respectively, depict the seismic responses shown in Figure 1 coloured according to TAB and TBE in hours.

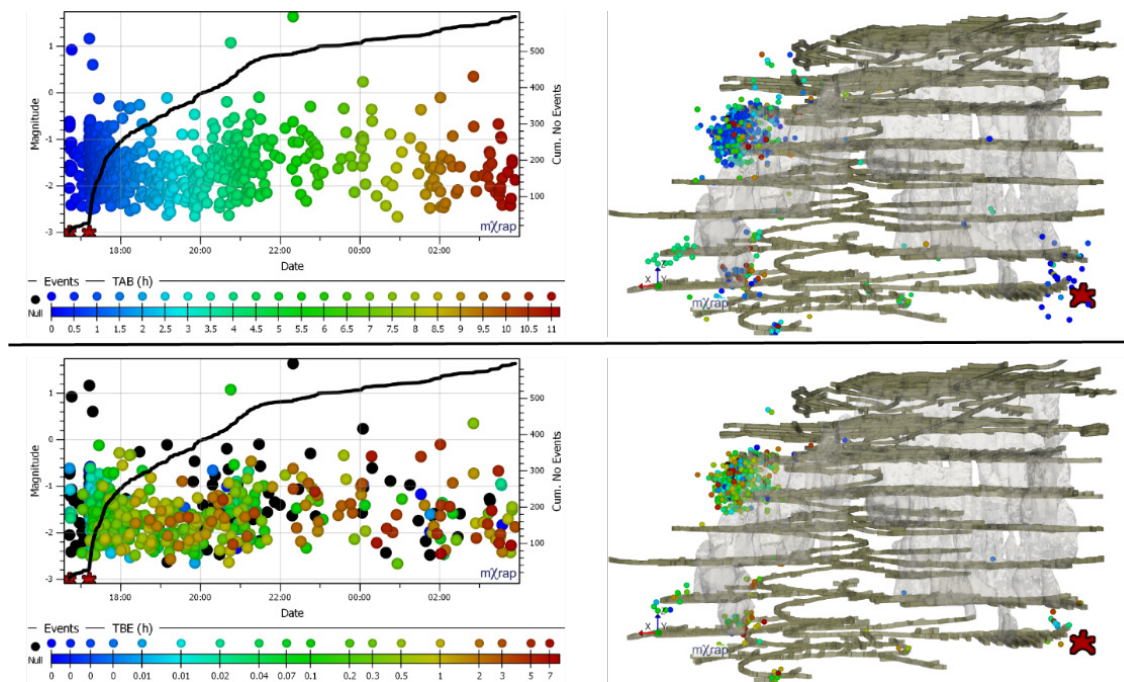


Figure 2: Seismic events occurring approximately 12 hours following mine blasting shown coloured by Time After Blast (upper) and Time Between Events (lower). Time Between Events values cannot be calculated for the first event in a seismic response and are null (black) on the magnitude-time chart and excluded from the spatial plot.

TAB, TBE, Distance To Blast (DTB), and Distance To Centroid (DTC), known as Seismic Response Parameters, work to quantify and delineate the space-time relation of seismic responses to mining and can be used to evaluate seismic source mechanisms, seismic hazard and seismic risk in mines (Brown, 2020).

SEISMIC RESPONSE RATING HAZARD MAPS

Spatial plots produced using Seismic Response Parameters, and sums of normalized parameters referred to as Seismic Response Rating (SRR), can provide insights into seismic source mechanisms and consequently seismic hazard throughout mining environments. Figure 3 (left) depicts two consecutive levels at Creighton mine coloured by Temporal SRR (Normalized TAB + Normalized TBE), calculated over approximately 3 months with no mine blasting. Overlaying these plots with mapped geological structures and all seismic events $MW \geq 1$ occurring in the 5 months following the resumption of regular mining activities (shown right), highlights the relation between geology, seismic hazard and high Temporal SRR values. These maps correlate well with high hazard seismically active structures known to release energy at times unrelated to mine blasting – complex seismicity.

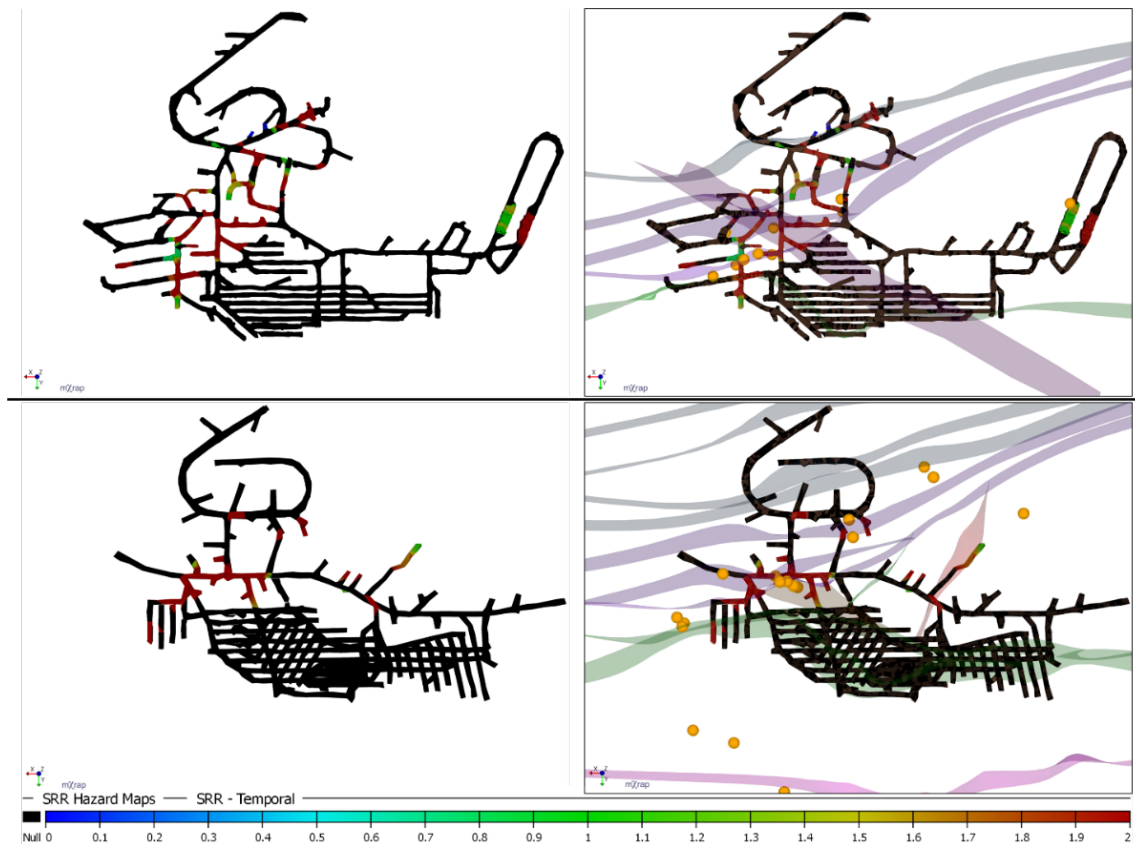


Figure 3: Temporal Seismic Response Rating (Normalized TAB + Normalized TBE) spatial plots calculated over approximately 3 months with no mine blast for two levels at Creighton Mine (left). Plots shown right include mapped geological features and all events $MW \geq 1$ occurring in the 5 months following resumption of regular mining activities.

Normalized Seismic Response Parameters consider both the occurrence and lack of occurrence of seismic events as characteristic of the seismic source mechanism. Consequently, they are well suited for application to short time periods and small datasets. This can be advantageous in active mining environments where rock mass conditions are continually changing due to regular mining activities. Figure 4 depicts a short term SRR spatial plot (the sum of Normalized TAB, TBE, DTB and DTC) considering one week of seismic data at Creighton mine. Grid points are shown coloured according to the 80th percentile of SRR for all seismic events within 50 ft. These values are also mapped to the closest minodes, representing the mine excavations, with null values shown in white. Induced, complex and triggered seismic responses are approximated in blue, purple and red, respectively. The inset image provides an alternate view of the prominent complex responses with the addition of local geological structures. As SRR does not consider event magnitude, only time and location, seismic events $MW \geq 0$ (large green circles) serve as an independent validation of potential disproportionate energy release – complex and triggered seismicity.

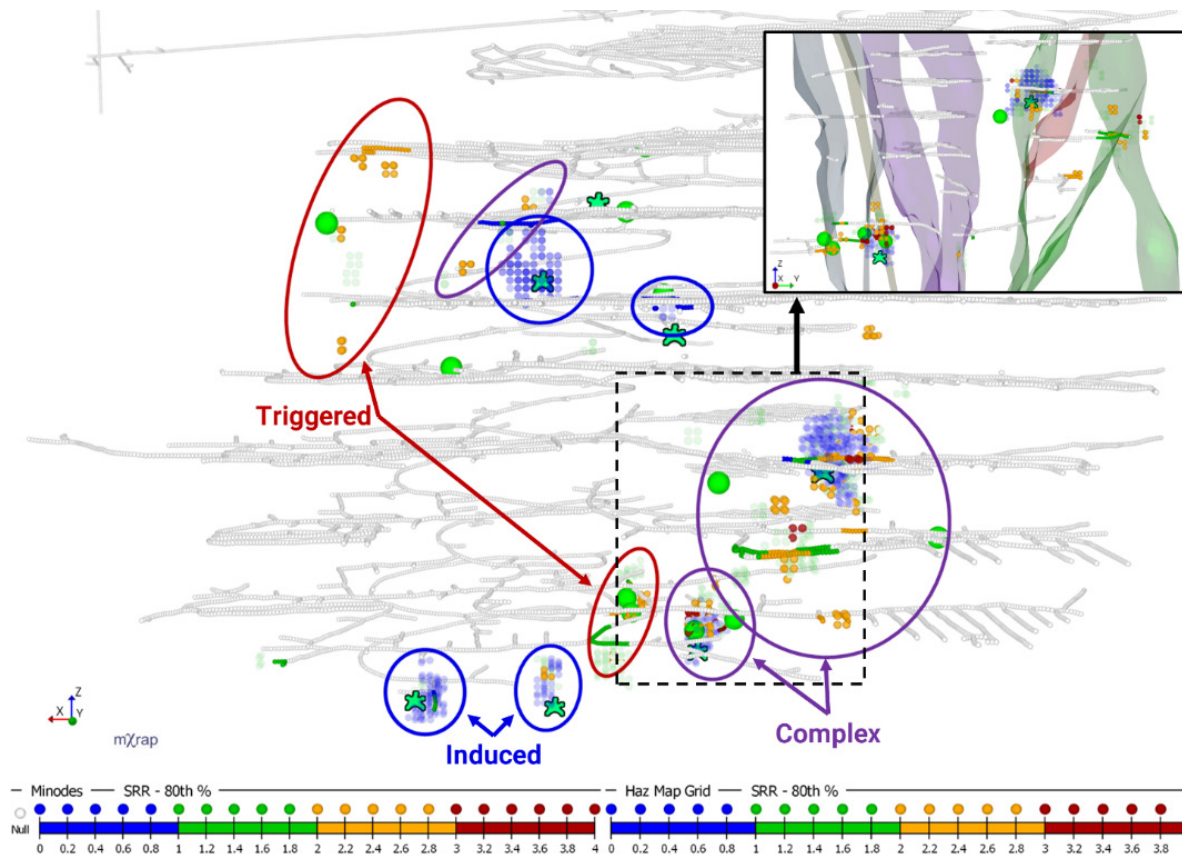


Figure 4: Seismic Response Rating (Normalized TAB + Normalized TBE + Normalized DTB + Normalized DTC) 80th percentile spatial plot of mine wide grid and minodes (representing excavations) calculated over one week at Creighton mine. Events $MW \geq 0$ are represented by large green circles and mine blasts are shown as green stars.

SUMMARY

Seismic source mechanisms which generate triggered seismic responses are relatively stationary, however, mine blasting migrates throughout mining environments over time. When blasting approaches triggered source mechanisms (e.g. geological features or highly stressed pillar), such that the mechanism is contained within proximity of the mining-induced stress change, it is possible to observe complex seismicity. Seismic Response Parameters and Ratings, such as TAB, TBE, and SRR, can be used to evaluate seismic source mechanisms and characterize complex seismicity in mines prior to the occurrence of large magnitude events.

ACKNOWLEDGEMENTS

The authors wish to acknowledge the ACG for use of their mXrap software (Harris and Wesseloo, 2015).

REFERENCES

- Brown, L. G. 2020. Quantifying discrete seismic responses to mining. *Canadian Geotechnical Journal*, 58(7), 1023–1035.
- Harris, P. H., and Wesseloo, J. 2015. mXrap software, version 5. Australian Centre for Geomechanics, The University of Western Australia, Perth, Western Australia.
- Kijko, A., and Funk, C. W. 1996. Space-time interaction amongst clusters of mining induced seismicity. *Pure and Applied Geophysics*, 174(2), 277–288.
- McGarr, A., Simpson, D., and Seeber, L. 2002. Case histories of induced and triggered seismicity. *International Handbook of Earthquake and Engineering Seismology Part A (International Geophysics)* (Editors: HK Williams, H Kanamori, PC Jennings, and C Kisslinger), Academic Press, International Geophysics, 81(A), 647–661.



The design of the tunnels & caverns for the Rozelle Interchange

Hunt, C.¹, Trim, M.², Bateman, J.², and Tepavac, D.³

¹McMillen Jacobs, Vancouver, British Columbia, Canada

²McMillen Jacobs, Sydney, Australia

³McMillen Jacobs, Melbourne, Australia

EXTENDED ABSTRACT

Rozelle Interchange is the most complicated and challenging road tunnel project ever attempted in Australian tunnelling history. This paper focuses on the technical challenges associated with the excavation of four caverns (numbered 3, 4, 11 and 12) and associated tunnels. This is considered a small but important part of the wider project. The presentation focuses on the technical challenges of designing these caverns within a heterogeneous, generally weak sandstone under high-stress conditions while providing a construction sequence that would align with the contractor's preferred techniques and schedule. The paper sets out the key design goals in terms of deformation, allowable strain in the rock mass and allowable shear along bedding and jointing. The paper outlines the numerical modelling work undertaken and the proposed sequence of excavation and support. The paper also highlights other challenges encountered during the excavation and the designed solutions to overcome these challenges.

INTRODUCTION

The Rozelle Interchange (RIC) and Western Harbor Tunnel Enabling Works, as part of Sydney's wider WestConnex Network, will provide a new underground motorway interchange to City West Link and provide an underground bypass of Victoria Road between the Iron Cove Bridge and the ANZAC Bridge, with links to the approved Western Harbor Tunnel. The Project is being designed and constructed by the John Holland CPB Contractors (JHCPB) Joint Venture with McMillen Jacobs as the designer of primary and secondary support.

CAVERN ARRANGEMENT

The caverns 3, 4, 11 and 12 are located in the northwest part of the wider project, where two or three lane highways bifurcate (refer to Figure 1). The excavated span of the caverns is between 26 to 29 m, with a height of 10 m.

GEOLOGY

The caverns were constructed predominantly in Hawkesbury Sandstone. This is a quartzose sandstone with medium to coarse grain minerology, deposited in beds or layers (Pells 2002). These layers, ranging in thickness from less than 0.5 m to greater than 5 m but generally occur between 1 and 3 m, form the macro rock fabric.

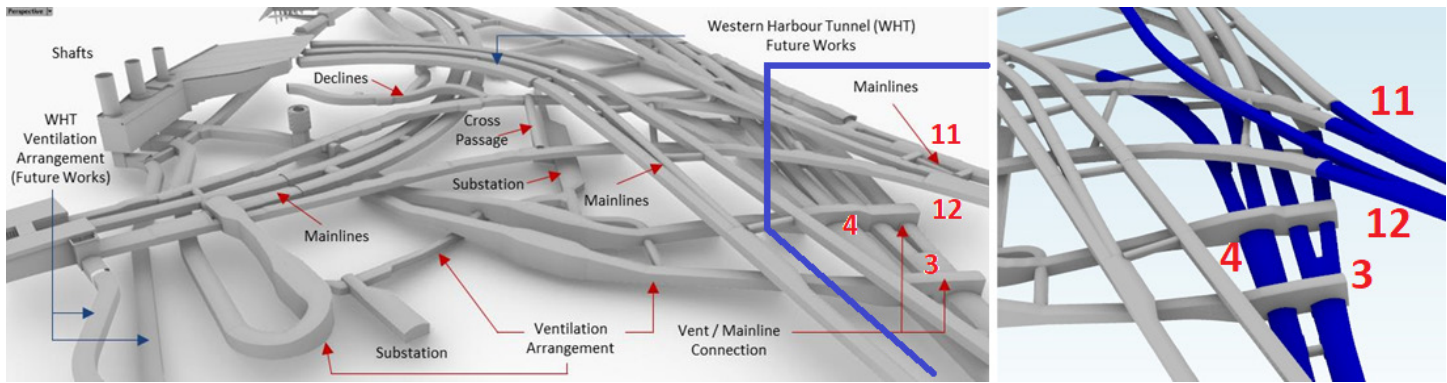


Figure 1: The location of the caverns 3, 4, 11 and 12 within the wider Rozelle Interchange complex.

Empirical and site-specific data suggested that expected sandstone joint sets were strongly dipping /subvertical joints with east-west to east-northeast - west-southwest orientation. Along with the dominant subvertical joint sets, random and subhorizontal joints were expected. Joint persistence is variable between 1 and 5 m but typically terminates between the primary bedding planes. The spacing of joints can range between 1 and 10 m.

The presence of a high in situ horizontal stress field in the Sydney Basin has been well publicized (McQueen 2004; Oliveira and Diederichs 2017). Predicted horizontal stresses are presented in Table 1. In the more competent rock conditions, for depths to crown of 40–50 m, the expectation for high in situ stress effects was an important consideration for the design given the well-recognized potential for consequences related to tunnelling under high in situ conditions as outlined in Tepavac et al. (2017).

Table 1. Approximations of in situ stress magnitude in the Sydney Basin

Horizontal Stress	Bertuzzi (2014)	Oliveira and Parker (2014)
Major Horizontal Stress, σ_H	$2 \sigma_v + (1.5-2.5) \text{ MPa}$	$(3.0-3.8) \sigma_v + (1.0-1.2) \text{ MPa}$
Minor Horizontal Stress, σ_h	$0.7 \sigma_H$	$0.61 \sigma_H$
Note: σ_v denotes vertical stress.		

The rock mass above the crown of the caverns exhibited jointing, shearing, and faulting beyond the expected typical range in Hawkesbury Sandstone. The location of the caverns was in a zone noted within the project specific Geotechnical Interpretation Report (GIR; prepared by PSM the project Geotechnical Engineer) as being structurally complex. One of the reasons for the structural complexity is that a large scale fault zone ends and anastomoses within the rock mass at this location. Furthermore, it was recognized that an extensive dyke intersected the caverns named as “Dyke C”, the exact position of which was unknown till excavation. Figure 2 presents the caverns and the location of the structurally complex zone.

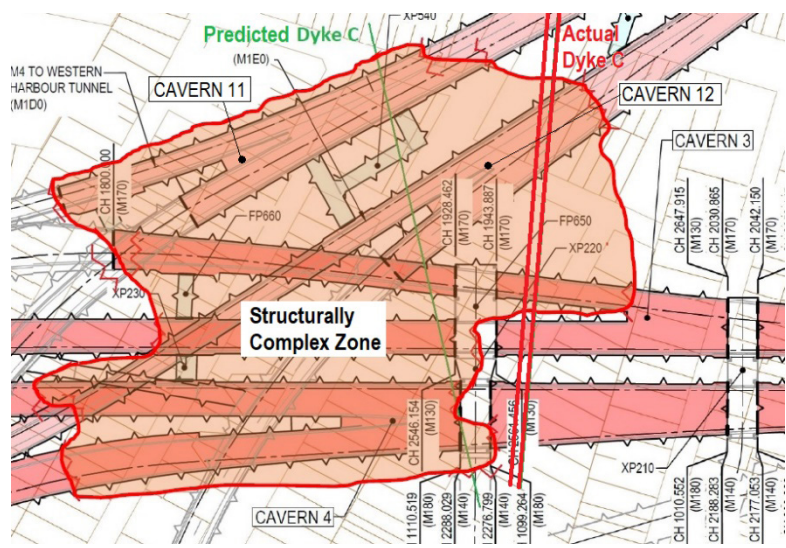


Figure 2: The location of the structurally complex zone and Dyke C in relation to the caverns.

The GIR also presented the anticipated sandstone design parameters which were used in the numerical analysis. The sandstone parameters were presented on differing scales (block size of 1 to 2 cubic metres and the tunnel scale).

KEY ISSUES FOR DESIGN EVALUATED THROUGH NUMERICAL ANALYSIS

The primary focus of the numerical analyses was to predict the ground movements induced by the excavation of the tunnels and caverns, the stability of the excavation, and the performance of primary support components of rock bolts and shotcrete lining. The models predict the loads that develop in the rock bolts and shotcrete lining, and these loads are compared against the specified respective design capacities for these support components to evaluate their performance. The following key issues for design were assessed through the numerical modelling.

1. Previous experience (including laboratory test data in various classes of sandstone) in the Sydney region indicates that critical axial strains for the Hawkesbury Sandstone are about 0.2%, beyond which failure in sandstone may occur. Design cases in UDEC are compared against this limiting value to confirm global stability of the tunnel.
2. Though isolated bolts may be allowed to exceed their allowable capacity, the global stability of the rock beam/arch may still be maintained (i.e. the group capacity of the design rock bolts is greater than the factored sum of calculated loads in the rock bolts). To verify the global stability of tunnels after bolt failure, bolts exceeding design capacity are deleted in a subsequent stage in the UDEC models. The new forces in the rock bolts after the redistribution of stresses are then plotted to show that progressive bolt failure does not occur.

In addition, the shear displacements of rock defects are assessed to compare with the limit of shear displacements for rock bolts to evaluate their performance. Maximum shear displacements after installation of rock reinforcement must not exceed 10 mm at the locations where rock reinforcement intersects any bedding planes or joints in the rock mass. The 10 mm limitation is with respect to the potential damage caused to the grout/sheathing protection surrounding a DCP rock bolt and the effect this has on the long-term durability of the rock bolt.

3. Crown sag in tunnels for spans greater than 20 m in length must not exceed a deflection of 35 mm (measured from the time of placement of the primary lining).
4. Shotcrete lining performance is mainly evaluated from FLAC and STRAND7 analyses. In the FLAC analyses, the forces (thrusts, shears, and bending moments) developed in shotcrete lining due to the ground movements were calculated. These forces are factored and compared against the shotcrete design capacity using the moment-thrust and shear-thrust interaction diagrams to assess the adequacy of shotcrete lining against ground-induced stresses. A load factor of 1.5 was used to assess the performance of the shotcrete lining for the characteristic ground parameters. Additional sensitivity analyses were conducted for each of the design sections to assess performance of the shotcrete lining with unfavourable ground conditions.

NUMERICAL MODELLING

Numerical modelling was generally undertaken using FLAC, FLAC3D and 3DEC in that sequence as the understanding of the potential behaviour of the rock mass developed and the design issues noted above were resolved. Within the numerical models the proposed excavation and support sequence was replicated with an empirically based ground relaxation model prepared for Hawkesbury sandstone on tunnelling projects from the Sydney area.

In terms of the 3DEC analysis, based on the geomechanical properties of 1 to 2m³ rock blocks and discontinuities provided by the Geotechnical Interpretive Report (GIR) Discrete Fracture Networks (DFN's) were developed. The DFN's were calibrated to the 1 to 2 m³ sized rock blocks, and then further re-sized and calibrated to the 'tunnel scale'. The 3DEC modelling complimented the FLAC3D models and assessed stress in pillars, overstressed bolts, strain in the rock mass, and bedding shear displacement.

In terms of the cavern excavation and construction sequence the modelling and input from the Contractors construction team combined to develop the preferred alternative. McMillen Jacobs prepared the sequence with specific limitations on the advancement of the individual three headings with respect to one another, the installation of primary rock bolts (DCP anchors) and secondary cable bolts, and the minimum strength grout in the primary bolts should achieve before commencement of the next heading or installation of secondary cable bolts. Figure 3 below sets out in overview the construction sequence for the caverns, as a note the 5th step was the excavation of the bench to the invert level.

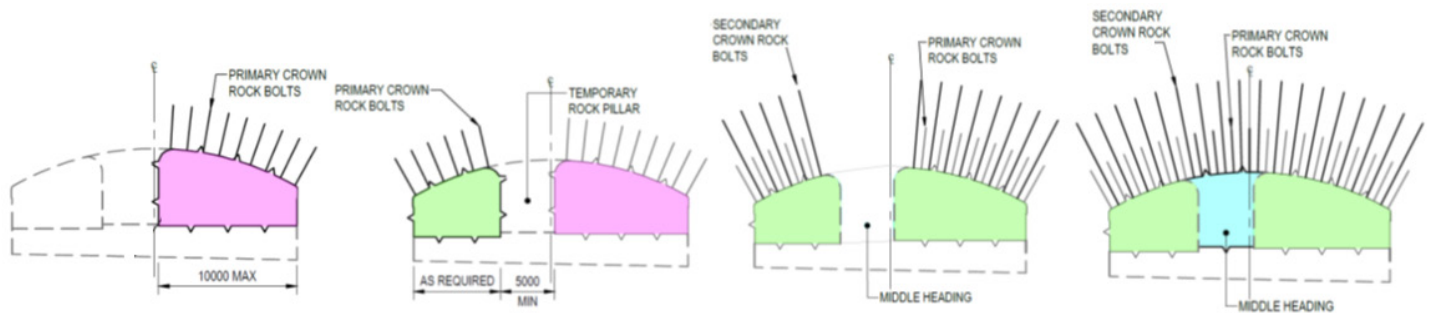


Figure 3: Overview the construction sequence for the caverns.

SUMMARY

The caverns were constructed successfully with final excavation in May of 2022.

ACKNOWLEDGEMENTS

The authors wish to acknowledge John Holland, CPB Contractors for giving their kind permission to present this paper, as well as specifically Rachael Price, Chris Grabham and PSM.

REFERENCES

- McQueen, L.B., Bewick, R.P., Sutton, J., and Morrow, A. 2017. Stress-induced brittle failure of the Hawkesbury Sandstone – Case study from crack initiation to tunnel support. Proceedings of the 16th Australasian Tunnelling Conference 2017.
- Oliveira, D., and Diederichs, M. 2017. Tunnel support for stress induced failures in Hawkesbury Sandstone. Tunnelling and Underground Space Technology. 64: 10–23.
- Oliveira, D.A.F., and Parker, C.J. 2014. An alternative approach for assessing in-situ stresses in Sydney. 15th Australasian Tunnelling Conference 2014.
- Pells, P.J.N. 2002. Developments in the design of tunnels and caverns in the Triassic rocks of the Sydney region. International Journal of Rock Mechanics and Mining Sciences 39: 569–587.
- Tepavac, D., Mok, P., Oliveira, D., Asche, H., Sun, Y., and Simmonds, S. 2017. High in-situ stress and its effects in tunnel design: An update based on recent project experience from WestConnex M4 East & New M5 Tunnels, Sydney, Australia. Proceedings of the 16th Australasian Tunnelling Conference, Sydney, Australia.



Making connections towards data driven underground excavation models

Perras, M.A., Morgenroth, J., Vasileiou, A., Alcaino-Olivares, R., Golabchi, Y., and Khan, U.T.

Department of Civil Engineering, Lassonde School of Engineering, York University, Toronto, Ontario, Canada

EXTENDED ABSTRACT

For underground excavations there has never been a better time to install instrumentation to monitor rock mass deformation and hazards. Instruments that can monitor the full spectrum of ground conditions are now more accessible and can live stream the data anywhere in the world. This provides an opportunity to use machine learning and new data-driven techniques to improve how we use the data, to improve operations, and our understanding of physical phenomenon driving deformations. In particular, the use of integrated machine learning and traditional models is a promising emerging avenue. Recent work, in collaboration with industry, has shown successful applications of various machine learning approaches, to integrate sensor data in underground design and operation. In addition to working with mining companies, ancient Egyptian tombs are also being monitored by the authors, along with environmental parameters, to understand complex influences on crack growth and rock mass deformations. Many opportunities exist, further case studies are needed to continue to validate these methods, increase confidence in the community, and ultimately improve our understanding of the complexities of underground excavation behaviour.

BACKGROUND

There is now a wealth of instrumentation data at the fingertips of underground excavation designers and mine planners. Integrating and extracting more value from instrument readings and other data sources to fit into a live workflow that aids in decision making is the real challenge: the sheer volume and complexity of the data can overwhelm the capabilities of the planning team. Machine learning can lend a hand in developing relationships between these data, e.g., input parameters such as excavation advance rate or excavation volume, and the resulting output parameters, such as underground excavation response. Although we have many analytical, empirical, and numerical methods that can aid in determining such design decisions, those methods are not always updated as new observations are acquired in a timely manner. This is where machine learning (ML) approaches could enhance our ability to make informed decisions by analyzing the relationships between instrument readings and production decisions, at a regular or even real-time basis, by making connections between them and our underground excavation models.

An exciting new area of research is in developing data driven modelling approaches that are known as integrated ML approaches, where a ML algorithm, such as an artificial neural network (ANN), approximates a complicated function which is then integrated into a well-established numerical method or physics-based models (Nature Editorial 2021). These integrated approaches offer the benefit of using high-performing ML predictive models, with more interpretable physics-based numerical models, and the potential to reveal new insights into the geomechanical system being modelled. For example, recent work by Morgenroth et al. (2022) used a Convolutional Neural Network (CNN) to predict tunnel liner yield at the Cigar Lake Mine and this could be put into an operational workflow by integrating the CNN into a geomechanical model, like FLAC, which could in turn be used to forecast yield when modelling different future production scenarios.

MAKING THE CONNECTIONS

For data-driven methods to be applied to underground excavations, instrumentation data is required in order to provide input on the rock mass response. The instruments are specific to the ground behaviour that is encountered, such as survey targets for squeezing ground conditions (Figure 1a) or micro-seismic sensors for rock bursting conditions (Figure 1b). In more recent work by the authors, environmental sensors have also been included to understand the impact of thermal and moisture fluctuations on deformations. This work started at a cliff in Egypt (Figure 1c) that threatens to collapse onto a tourist pathway near tomb KV42 (Alcaino-Olivares 2019) and has more recently progressed to the stability assessment of a near-surface tomb (Figure 1d) that could be influenced by the high thermal gradients from surface exposure at tomb TT95 (Ziegler et al. 2019).

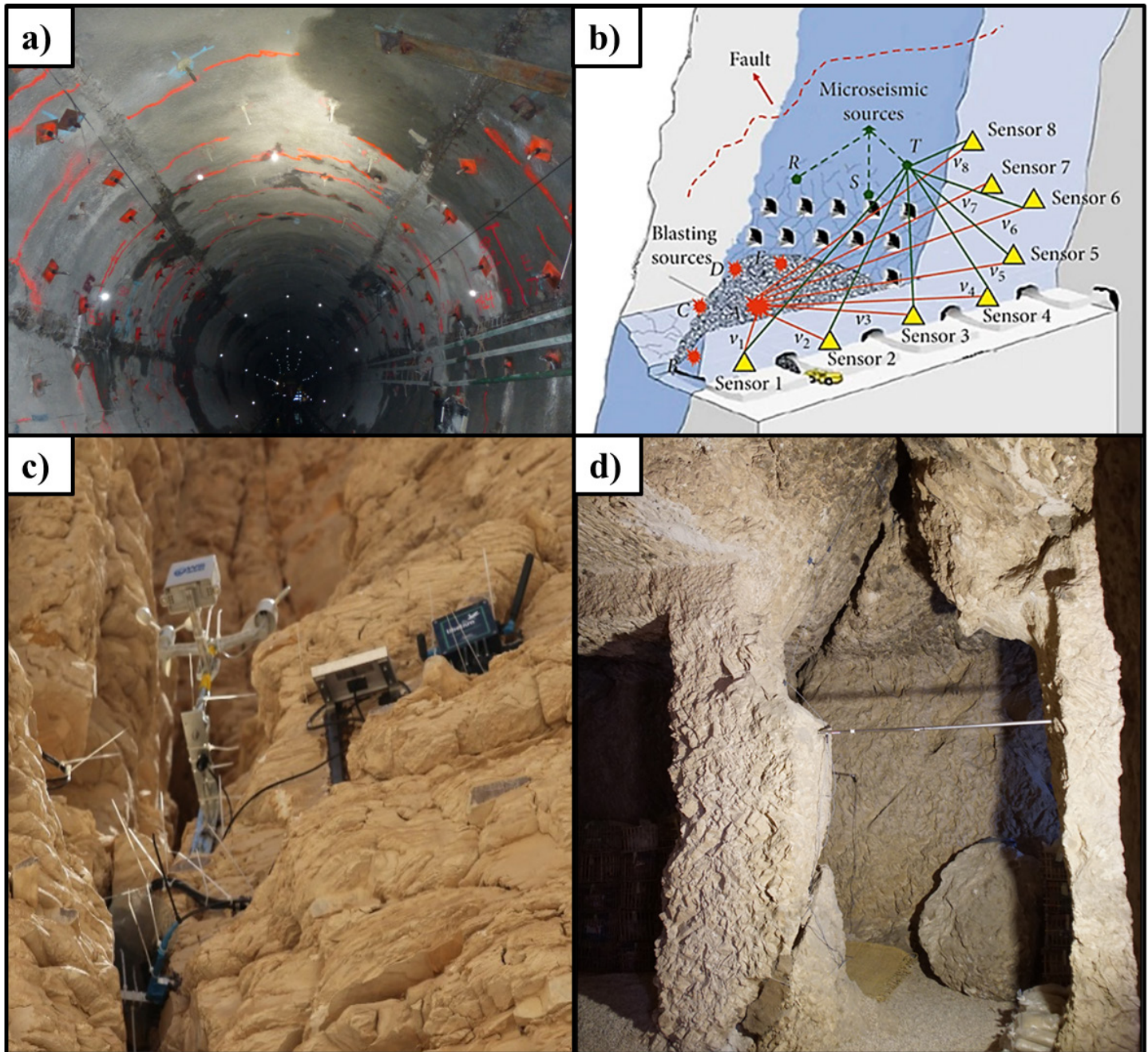


Figure 1: Various monitoring sensors for different geomechanical situations, including a) survey targets to measure radial squeezing, b) schematic of a mine's microseismic sensor array, c) measuring crack movement and environmental parameters near tomb KV42, and d) measuring pillar displacement in tomb TT95.

Monitoring and data collection are the first step in capturing the complex relationships between environmental parameters and rock deformation and as Potyondy (2007) noted, “Little relevant data are available” to validate models that deal with time-dependent deformation and environmental influences that, for example, contribute to stress corrosion. Advancing the rock mechanics toolbox with the aid of data-driven methods could help bridge gaps for which solutions have yet to be taken up by industry.

MACHINE LEARNING AND UNDERGROUND EXCAVATIONS

The primary focus of machine learning in the mining industry has been on autonomously driven vehicles and resource exploration and delineation with only more recent work focused on underground excavation behaviour, such as rock bursting, tunnel support performance, and time—dependent deformations (Morgenroth et al. 2019). Recent work by the authors with various mining, instrumentation and consulting companies has seen interest in exploring the opportunities for data-driven approaches. For example, work with Cameco used a CNN to predict tunnel linear yield (Figure 2a) using sigmoid error weighting scheme (Figure 2b) at the Cigar Lake Mine (Morgenroth et al. 2022). Work with Vale has been successful at predicting stress magnitudes at Garson Mine, where a microseismic events database was used in a Long-Short Term Memory (LSTM) network to demonstrate that a comparable stress magnitudes could be predicted (Figure 2c) as a manually calibrated numerical model (Figure 2d), but requiring less computational time and engineering hours (Morgenroth et al. 2021).

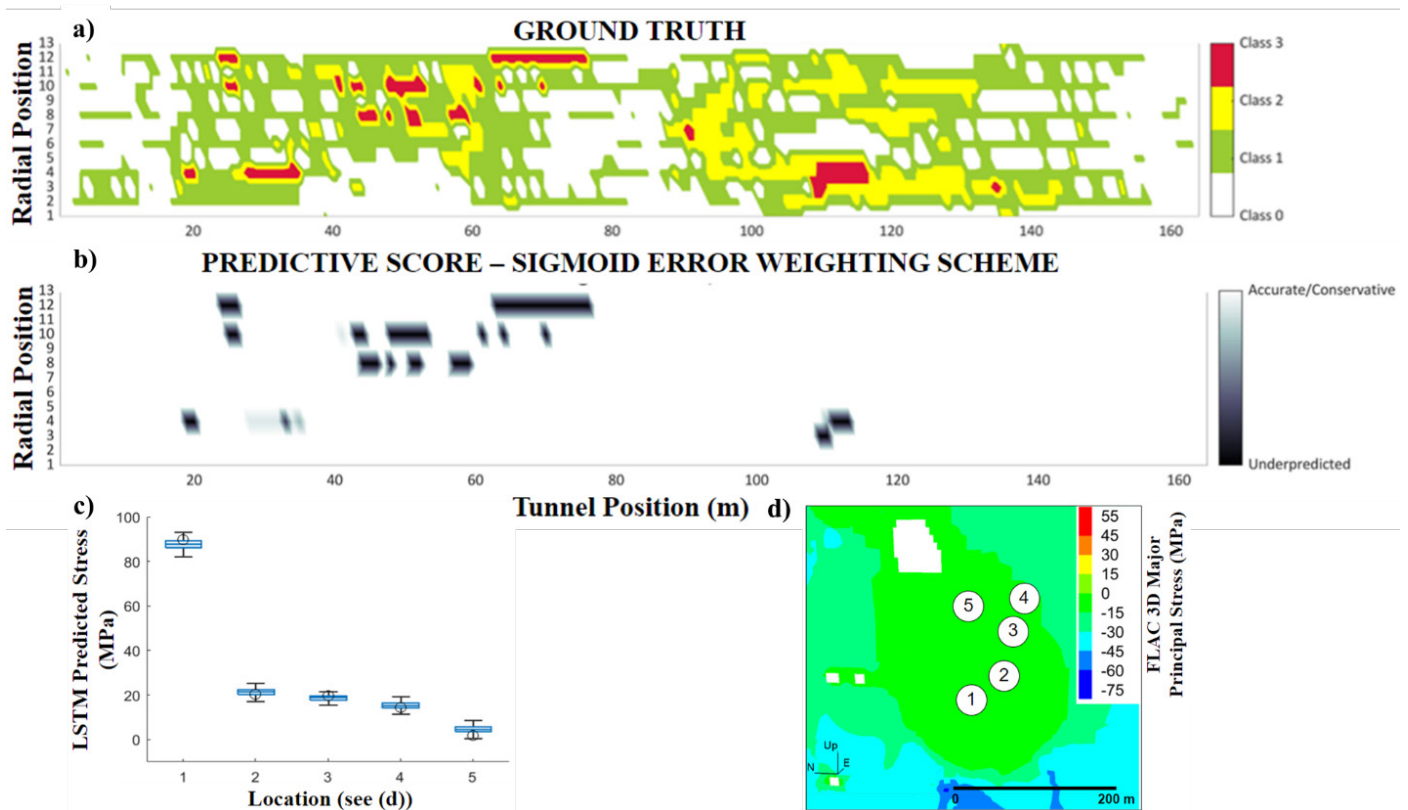


Figure 2: ML results comparing a) the ground truth support classes installed against b) a CNN sigmoid error weighting scheme predictions (Morgenroth et al. 2022), and c) LSTM Major Principal Stress magnitude predictions compared to d) a calibrated FLAC 3D numerical model stress concentration at 5 different locations (Morgenroth et al. 2021).

Such case studies are needed to demonstrate to industry the value of and what can be achieved with machine learning. It also provides an opportunity to investigate large data sets that industry partners can provide access to, but do not always have the time to utilize. Case studies on their own may not be enough to encourage uptake of emerging methods and approaches. Demonstrating the accuracy of various machine learning tools by replicating existing empirical prediction tools can also build confidence in these approaches (poster by Golabchi).

WHAT DOES THE FUTURE HOLD?

The rock mechanics research community is taking up the challenge of exploring data-driven modelling, among other machine learning methods. Industry is installing sensors more widely to aid in rock mass behaviour observation, monitoring at high temporal and spatial resolutions, which will allow near real-time predictions to aid in operational activities within active mining environments. Making connections between long-term sensor monitoring data sets and the rock mass behaviour to develop data-driven models is the direction that is emerging which could yield new developments in our understanding of complex influences on rock mass behaviour and also allow for more timely interventions for unstable ground. In addition to aiding the rock mechanics community, advances in ML techniques can also be made by using existing methods or creating new ones better suited to rock mechanics. To achieve these improvements in understanding and prediction tools will require case studies and data sets from extreme cases that record new influences on the rock mass that previously have seldom been recorded. This will lead to changes in our understanding of rock mass behaviour and ultimately the tools that industry takes up into their everyday workflows to improve underground excavation safety and productivity.

ACKNOWLEDGEMENTS

The authors wish to acknowledge the many partners that have contributed to this research, including Kathy Kalenchuk from RockEng, Lindsay Moreau-Verlan from RockEng (formerly Vale), Andrew Hyett from Yield Point, Chriss Twiggs from Cameco, Martin Ziegler from Swiss Topo and ETH Zurich, and Susanne Bickel and Andrea Loprieno-Gnirs from the University of Basel. We wish to thank them for their extensive discussions and partnerships on various grants, papers, and student thesis, that continue to shape this research direction. In addition to those individuals, we wish to thank the Permanent Committee of the Supreme Council of Antiquities in Cairo for granting permission to conduct research in Egypt. The authors also wish to acknowledge that this research has been in part funded by Natural Sciences and Engineering Research Council of Canada (NSERC) through Discovery Grant program [RGPIN-2018-05918] and in part by funding from Canada's New Frontiers in Research Fund (NFRF), [NFRF-2020-00893].

REFERENCES

- Alcaino-Olivares, R., Perras, M.A., Ziegler, M., Maissen, J. 2019. Cliff stability at tomb KV42 in the Valley of the Kings, Egypt: A first approach to numerical modelling and site investigation. Proceedings of the 53rd US Rock Mechanics/ Geomechanics Symposium, New York, USA.
- Morgenroth, J., Khan, U.T., Perras, M.A. 2019. An overview of opportunities for machine learning methods in underground rock engineering design. *Geosciences*, 9(12), 504–527.
- Morgenroth, J., Perras, M.A., Khan, U.T., Kalenchuk, K., Moreau-Verlaan, L. 2021. Forecasting principal stresses using microseismic data and a long-short term memory network at Garson Mine, Garson, ON. Proceedings of the Canadian Geotechnical Society Annual Conference, Niagara Falls, ON.
- Morgenroth, J., Perras, M.A., Khan, U.T. 2022. A convolutional neural network approach for predicting tunnel liner yield at Cigar Lake Mine. *Rock Mechanics and Rock Engineering*, 55, 2821–2843.
- Nature Editorial, 2021. The rise of data-driven modelling. *Nature Reviews Physics*, 3(383).
- Potyondy, D. 2007. Simulating stress corrosion with a bonded-particle model for rock. *International Journal of Rock Mechanics and Mining Science*, 44, 677–693.
- Ziegler, M., Colldeweih, R., Wolter, A., Loprieno-Gnirs, A. 2019. Rock mass quality and preliminary analysis of the stability of ancient rock-cut Theban tombs at Sheik 'Abd el-Qurna, Egypt. *Bulletin of Engineering Geology and the Environment*, 78, 6179–6205.



Transforming underground: A case study on the design of the Long Baseline Neutrino Facility Far Site

Stewart, H.¹ and Pollak, S.²

¹Arup, Toronto, Ontario, Canada

²Arup, New York, New York, USA

EXTENDED ABSTRACT

The Long Baseline Neutrino Facility (LBNF) Far Site Conventional Facilities are planned to be sited at the Sanford Underground Research Facility (SURF) located within the former Homestake Gold Mine in Lead, South Dakota. The project involves excavation and support of three large caverns which will house four 10 kT fiducial volume liquid argon (LAR) neutrino detectors and appurtenant support utilities, as well as numerous ancillary connecting drifts and chambers (see Figure 1). The North and South Caverns have an approximately 20 m span, are 28 m tall, and will be primarily supported with rock bolts and shotcrete. The central utility cavern has a similar span however is only approximately 11 m tall. The facilities will be constructed at the 4850 Level. The design uses permanent rock bolts and includes significant ground instrumentation, as there are no real benchmarks for similarly sized caverns at this depth.

GEOLOGY AND BACKGROUND

The SURF caverns will be constructed through the upper member of the Poorman Formation Schist, predominately comprised of planar to highly contorted foliated metasediments. The rock unit is intruded by rhyolite in the form

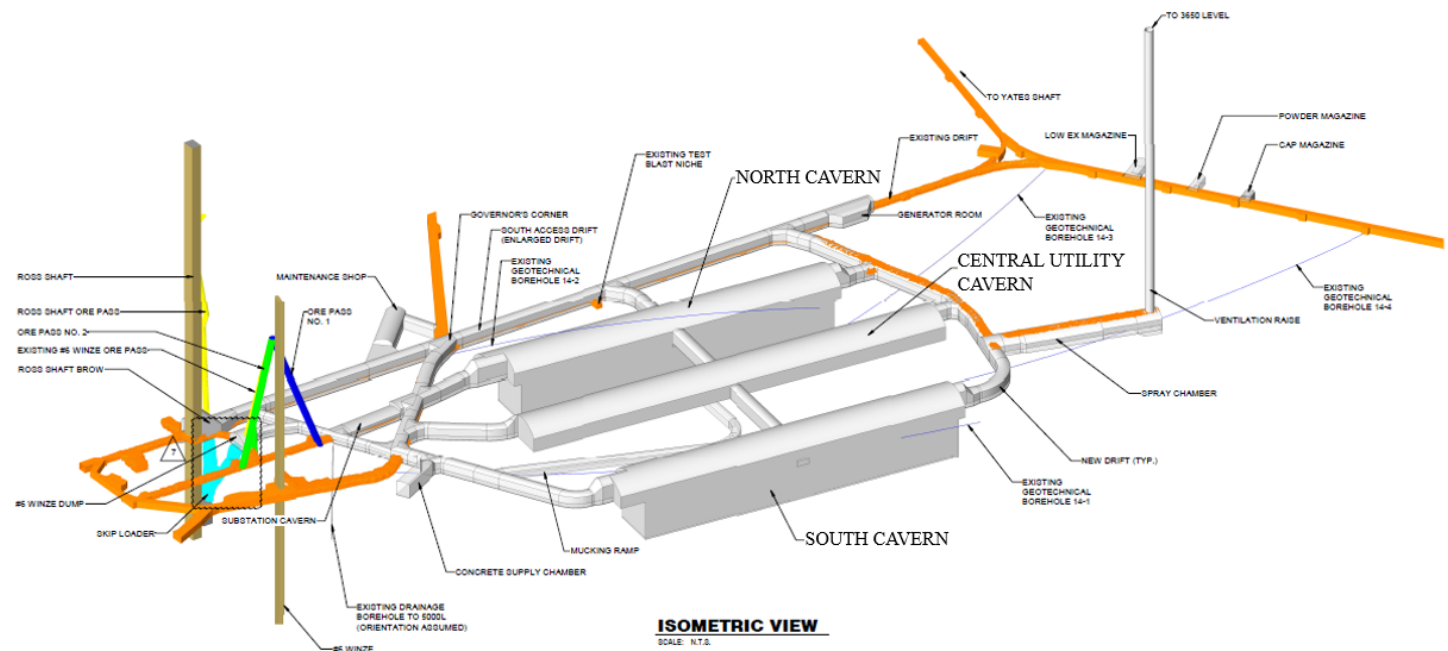


Figure 1: Isometric view of proposed LBNF excavation at the 4850 Level. Proposed excavations are in grey and existing drifts and shafts are in orange and brown.

of sub-vertical dikes. Historically, rhyolite dikes have performed poorly in drift and chamber sidewall excavations at the 4850 Level. This has resulted in minor spalling and rock support issues.

A two phased approach for project specific site investigations was adopted to determine if the proposed location was suitable for cavern construction. The site investigations included detailed geological mapping of existing mine drifts, drilling 4 sub-horizontal boreholes, in situ stress testing, and extensive lab testing of rock core. The rare access granted by the existing mine drifts, combined with the supplemental horizontal boreholes, allowed for a well-defined 3D rock mass model to emerge.

ROCK MECHANICS DESIGN

The design progressed based on the key ground behavior mechanisms anticipated from the rock mass characterization stage which included brittle spalling in rhyolite, wedges, slabbing along foliation, overbreak, and groundwater (see Figure 2). Design methodology included empirical, analytical (kinematic stability assessment), and 3D numerical analyses. Key design elements included a detailed back analysis to validate the proposed geotechnical design parameters and preparing detailed 3DEC distinct element modelling for caverns, including the use of a specific brittle-spall constitutive model to capture the rhyolite behavior in numerical models.

As part of the project's risk mitigation strategy, trigger action and response plan (TARP) is provided in the contract drawings and a pilot tunnel has been constructed through the central top heading of each cavern prior to enlargement. Numerous MPBXs are currently installed and providing valuable data for design validation as the caverns are sequentially enlarged to full size.

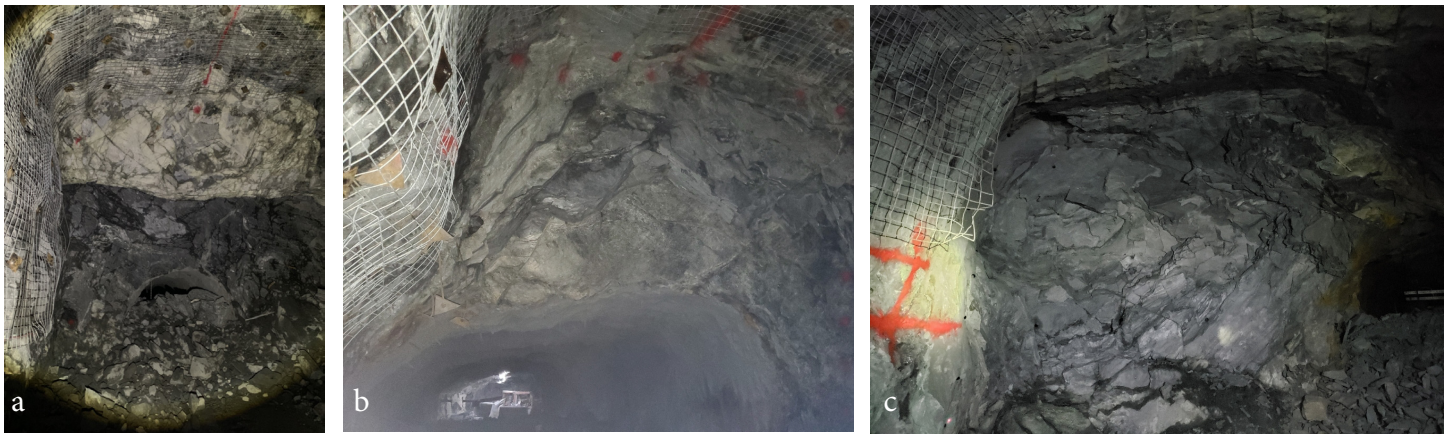


Figure 2: Observed rock mass behaviour: a. brittle spall of Rhyolite b. wedge/block formation c. slabbing off face.

SUMMARY

Constructing large span caverns deep underground for civil and scientific infrastructure has resulted in the need for extensive ground characterization and permanent rock support design. This presentation summarizes the site investigation, ground characterization, design approach, and key observations from construction to date.

ACKNOWLEDGEMENTS

The authors wish to acknowledge the Fermi National Accelerator Laboratory (FRA) for providing Arup the opportunity to present this work.



Making sense of geomechanical data in mine design or the good, the bad and the missing

Coulson, A.L.

Wood Environmental and Infrastructure Solutions Canada Ltd., Toronto, Ontario, Canada

EXTENDED ABSTRACT

This presentation hopes to convey that, although we do not always collect all or the correct information, we can still investigate the geomechanical data, with verification and calibration to often expand the dataset, to aid in the mine design of open pit and underground mining operations, and to optimise economics while maintaining stability and safety. We will review several different sources of data for rock mass characterization, discussing limitations, errors, and ways to investigate, from rock mass classification, structural interpretation, in situ stress determination and rock strength testing. The examples discussed come from the last 30 years of site investigation and mine design at some of the most interesting mining projects around the world.

OVERVIEW

Large open pit and underground mining projects often take anywhere from 5 to 30 years to develop, dependent on market conditions for the definition of an economic resource (Figure 1). During this time often multiple studies by various consultants and different mine developers result in collection of data to support the various levels of study from conceptual scoping studies, preliminary economic assessments, pre and feasibility level to detailed engineering studies, followed by operational ongoing design and mine closure studies. Ideally, consistency in data measurement and management would exist; however, there are generally holes in collection and loss of data requiring the geomechanical design engineer to perform detective work to verify and consolidate a functional dataset for the design requirement at hand.



Figure 1: A Typical Large Open Pit and Potential Underground Mine – Antamina, Peru.

The basis for mine design is rock mass characterization based on structural analysis and rock mass classifications, such as the Rock Mass Rating, RMR'89, (Bieniawski, 1989), the Q-System (Barton et al., 1974), and the Geological

Strength Index, GSI, (Hoek et al., 1985). It is our objective to collect the raw data during site investigations, so that data is determined separately for at least two classifications enabling comparison. Typically, RMR and GSI are used for open pit stability, while Q and Q' (modified Q) are predominantly used for underground design. An example of a fundamental difference in the parameters of each classification that creates confusion is the difference in the joint roughness categories between RMR'89 and Q, such that RMR'89 has a 5-scale small roughness category, while Q has 3 categories for small scale roughness and 2 larger scales based on shape. Ideally, the physical description of roughness is preferred: however, this is often not the case and roughness may be defined by the rating number only, which may often require verification logging to better understand. We have expanded the cross tabulation below in Table 1 (after Hutchinson and Diederichs, 1995) to aid in joint roughness, Jr, determination for Q, but based on the roughness descriptions for RMR'89.

Table 1: Assessment of Jr Based on Joint Roughness and Probable Large Scale Joint Undulation

Definition	Planar	Undulating / Curved	Discontinuous / Stepped / Irregular
K: Slickensided	0.5	1.5	2
SM: Smooth/Polished	1	1.75	2.5
SR: Slightly Rough	1.25	2	3
RO: Rough	1.5	2.5	3.5
VR: V. Rough	1.75	3	4
Go: Gouge filled > 5 mm	1	1	1

In addition, other parameters that have been found to be poorly recorded are joint infill, type and thickness and joint alteration, Ja, parameter, which is often recorded with very high values that are not representative of the actual conditions. The Ja parameter was found to be so poorly differentiated for hard infill and hard rock classification that Milne et al., (1992); Nickson et al., (2001), developed a field test for the assessment of Ja, for the condition of rock wall contact of the joint as in Table 2 for ranges of Ja from 0.75 to 4.0. Barton's original description is used for discontinuities that are separated due to thick, soft infill > 2 mm with no initial contact or any contact, using the range from 4 to 20. It should be recognised that the latter are generally applicable for faults or shears. Applying these steps has aided in the basic collection of data and has been used with success to determine comparisons between RMR'89 and Q when using Bieniawski's relationship for Q, while identifying issues in the data where large discrepancies exist.

Table 2: Assessment of Ja for Rock Joints after Barton et al. 1974 - Rock Wall Contact

Field Test	Joint Coating / Condition	Value
Very hard cannot be scratched easily with a knife	Tightly healed, hard, non-softening filling	0.75
Can be scratched with a knife	Unaltered, surface staining, or hard infilling	1.0
Can be gouged (deep scratch) with a knife	Unaltered, surface staining, or hard infilling	1.5
Can be scratched with a fingernail and feels slippery/soapy to touch	Slightly altered joint walls, non-softening mineral coatings	2.0
	Silty-, or sandy-clay coatings, small clay-fraction (non-softening < 2 mm)	3.0
Can be dented/gouged with a fingernail, feels slippery/soapy to touch	Low friction clay mineral coatings, i.e. kaolinite, mica, talc, gypsum, graphite, etc. (1–2 mm)	4.0

Another area that is essential for design of hard rock open pits and for understanding of underground opening stability is the structural joint fabric, which is required not only for the classification systems, but also for kinematic stability analysis of pit walls and open stope stability using the stability graph method (Potvin 1988, Nickson 1992, and Hadjigeorgiou et al., 1995) as an example for underground mining. With the advent of more site investigations using Acoustic and Optical televiewer (ATV/OTV) surveys, a plethora of structural data may exist to aid in design. However, it is essential to critically review the data, by either comparison to other forms of joint orientation information such as oriented core data or joint mapping campaigns as inappropriate processing without reconciliation back to the core photos and checks on sensitivity can result in significant errors in the distribution of joint sets. In the example below (Figure 2) the ATV dataset provided by the mine was easily observed to be in error. By plotting the data with the 'blind zone', i.e., cones of low joint intersection due to borehole orientation, it was observed that the main cluster plotted in the blind zone and would suggest that most of the jointing to be parallel to the core axis. As is noted in the core photos, this was not the case. Further comparison to the oriented core joint observations indicated a marked difference. After having the third party review the data again it was found that an error had occurred during input of the borehole size; following correction of this, the data was able to be reconciled to the observations in core, and a valid data set was used for design.

Other important considerations with ATV/OTV data are the resolution of the survey and sensitivity of the analyses. Poor resolution matched with over zealous sensitivity at the processing stage can result in ghost images that do not correlate to the actual structure. It is advisable to always think and question "does this make sense?" and not blindly process data.

Further, the amount of data to review relative to the opening or region should be taken into consideration during design. Grouping of holes within spatial regions or reducing the observation volume to 2 to 4 times the underground opening volume and relative to the orebody and lithology are techniques used to more clearly define the local joint fabric, rather than plotting everything and hoping for the best.

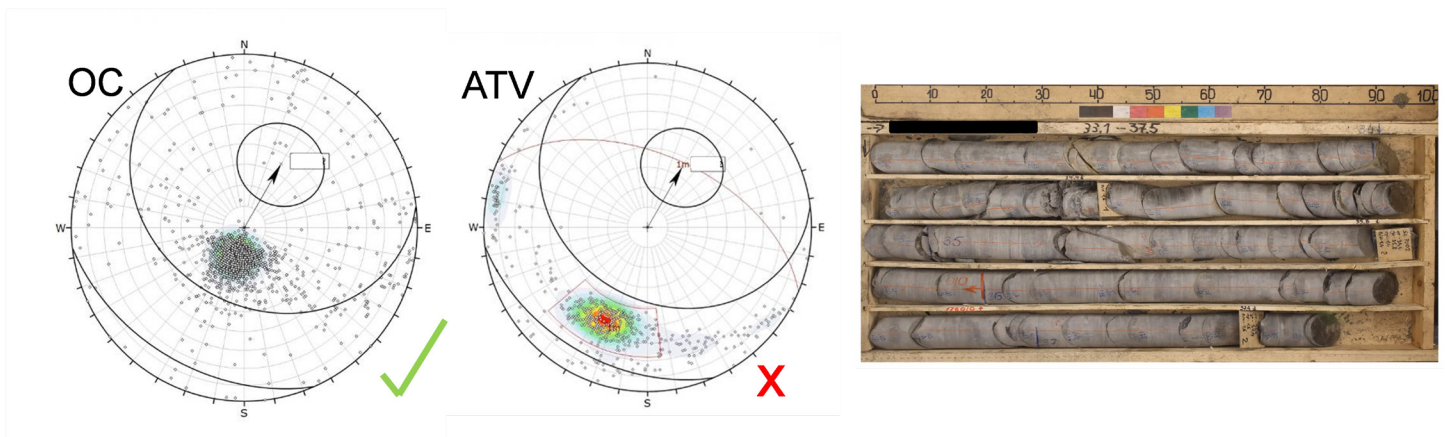


Figure 2: Comparison of Oriented Core (OC) versus Acoustic Televiewer (ATV) and Core Photos for a Single Borehole.

Further, the presentation will discuss the need to understand the in situ stress regime, and how a lot of projects outside of well defined mining zones require a structural geology approach and comparison to other regions to develop a preliminary stress regime as there is often a lack of testing data. Also, if time permits a discussion on the validity of rock strength testing with regards to errors in test setup and sample preparation will take place.

Geomechanical mine design, although not rocket science but actually rock science, needs to address fundamentally the quality and quantity of the data. If there are questions, then find methods to validate the dataset.

ACKNOWLEDGEMENTS

The author wishes to acknowledge the Rock Mechanics Team at Wood, James Tod, Marc Orman, Milton Teran, Cynthia Lane, David Ko, Blake Easby, Kellen Shenton, Blake Broadland and many more, whose attention to detail, hard work and inquisitive minds make working together on numerous projects the thing that keeps us going.

REFERENCES

- Barton, N., Lien, R. and Lunde, J. 1974. Engineering classification of rock masses for the design of tunnel support. *Rock Mechanics*, 6 May, pp. 186–236.
- Bieniawski, Z.T. 1989. *Engineering Rock mass Classification*. Wiley, New York. pp.251.
- Hadjigeorgiou, J., Leclair, J.G., Potvin, Y. 1995. An Update of the Stability Graph Method for Open Stope Design. 97th CIM-AGM, Rock Mechanics and Strata Control Session, Halifax, Nova Scotia.
- Hoek, E., Kaiser, P.K. and Bawden, W.F. (1995). *Support of Underground Excavations in Hard Rock Rotterdam*: Balkema. 215 pp.
- Hutchinson, D.J. and Diederichs, M. 1996. *Cable Bolting in Underground Mines*. BiTech Publishers.
- Milne, D., Germain, P., Potvin, Y. 1992. Measurement of rock mass properties for mine design. *Proceedings of the ISRM-Eurock Symposium on Rock Characterization* (Chester, U.K., September 14–17, 1992). A. A. Balkema.
- Nickson, S.D. 1992. *Cable Support Guidelines for underground Hard Rock Mine Operations*. M.A.Sc. Thesis. The University of British Columbia.
- Nickson, S., Coulson, A. and Hussey, J. (2000) Noranda's approach to evaluating a competent deposit for caving. *Proc. MassMin 2000*, Brisbane (ed. G. Chitombo), 367–83. Aust. Inst. Min. Metall.: Melbourne.
- Potvin, Y. 1988. *Empirical Open Stope Design in Canada*. Ph.D. Thesis. The University of British Columbia.



Seismic hazard metrics

Moreau-Verlaan, L.

RockEng Inc., Kingston, Ontario, Canada

EXTENDED ABSTRACT

Underground mine operators are increasingly aware of the important contributions of seismic risk management to achieving safe production. For this reason, the mining industry is placing greater emphasis on the development and implementation of seismic risk management programs. Critical elements to any seismic risk management program include: a) techniques to gauge seismic hazard levels, and; b) methodologies to mitigate seismic risks incurred. Integrating both of these critical elements, seismic risk management is hinged on the ability to identify and quantify seismic hazard, and subsequently enact a trigger-action-response-plan to guide hazard mitigation. In considering both critical elements to seismic risk management, the ability to gauge (or quantify) seismic hazard is crucial. As an input to seismic risk management, hazard assessments offer a comparative approach (spatially and/or temporally) to determine where and/or when (relative to mine extraction sequence) elevated seismic hazard is expected. Historically, seismic hazard assessment techniques have been centered on seismic data interpretations (Kijko and Funk, 1994). More recently, numerical stress model interpretations have been employed in seismic hazard estimations (Kalenchuk, 2022). Though both techniques are reasonable approaches to identifying high seismic hazard, their suitability in gauging effectiveness of hazard mitigation remains unvalidated.

Identification of high seismic hazard motivates the development and implementation of suitable hazard mitigation, with the goal of reducing seismic hazard in the areas of high-risk exposure. Approaches to seismic hazard mitigation include: strategic, design-based solutions, and; tactical, operationally-based techniques. Examples such as geomechanically-constrained mine sequencing and drift destress blasting have been readily adopted by the mining industry, however an engineered approach to design and/or gauge effectiveness in seismic hazard mitigation remains unresolved. In considering design approaches to seismic hazard mitigation, the absence of robust metrics to quantify seismic hazard constrain the iterative feedback loop applicable to engineered design. Subsequently, the effectiveness of mitigating controls remains questionable without quantifiable evidence on their hazard-reduction impact. Therefore, robust seismic hazard metrics are a base requirement in the development and implementation of engineered seismic hazard mitigation.

Focusing on seismic hazard metrics, the opportunity and suitability of existing geomechanical rock metrics and in situ rockmass monitoring technologies to quantitatively gauge seismic hazard potential and mitigation effectiveness is considered. Employing the idea that seismic hazard mitigation strategies are designed to impose a change to in situ conditions (either a reduction in stress load, or alteration of material behaviour in responding to stress load), a correlation between the in situ conditions, imposed change and the effectiveness of the mitigation strategy is suggested.

SEISMIC HAZARD

Seismic hazard is defined as the probability that a seismic event of a minimum intensity will occur within a defined ground volume and within a given window of time (Gibowicz and Kijko, 1994). Mining induced seismicity is a

response to the complex change in forces acting on a rockmass. As excavation are mined out, induced stresses are redistributed, altering the forces imposed on the surrounding rockmass in both direction and scale. If the internal forces exceed the internal strength of the rockmass, change in the rockmass itself occurs, damage is incurred and seismicity is generated (Verma et. al, 2022). Seismic hazard is the industry accepted metric to describe the probability of seismic occurrence. However, based on the concept that seismicity is a phenomenon linked to stress-induced rockmass change, can seismic hazard levels be correlated with rockmass parameters? If so, then quantifiable rockmass metrics capable of measuring variability in rockmass parameters may be useful in gauging variability in seismic hazard as well.

Historically, seismic hazard levels have been gauged on seismic data interpretation (Kijko and Funk, 1994; Wesseloo, 2020), employing a ‘rear-view mirror’ approach (based on past seismic data recorded) in quantifying potential future seismic hazard. As an example, Figure 1 depicts a typical frequency-magnitude chart, employing the Gutenberg-Richter distribution, where seismic data alone is used to establish future seismic hazard, based on the largest projected potential seismic event. An improvement to seismic hazard assessments for future-forecasting potential may be realized by integrating quantitative measures from seismic-influencing parameters. Aligned with the understanding that seismic event generation is linked with rockmass response to changes in stress state, there is a positive correlation between seismic hazard and impacting parameters (Mendecki, 2016). Seismic impacting parameters classified as in situ conditions include: in situ stress; depth of mining; mechanical strength and stiffness of rock and rock mass; degrees of homogeneity of the rock mass, including fabric as well as joint-and fault-scale structures. Additionally, induced conditions also impact seismic hazard levels: extraction ratio; extent of the mined-out area; mining rate and the spatial/temporal sequence of extraction; additional stress induced by the adjacent mining, and; continuity of the mine layout itself and in its relation to geological structures. Therefore, in the context of mine seismicity, seismic hazard assessments should include consideration of the impacting parameters, with engineered parameter-weighting based on established correlations between the in situ and induced factors and their influence on hazard levels.

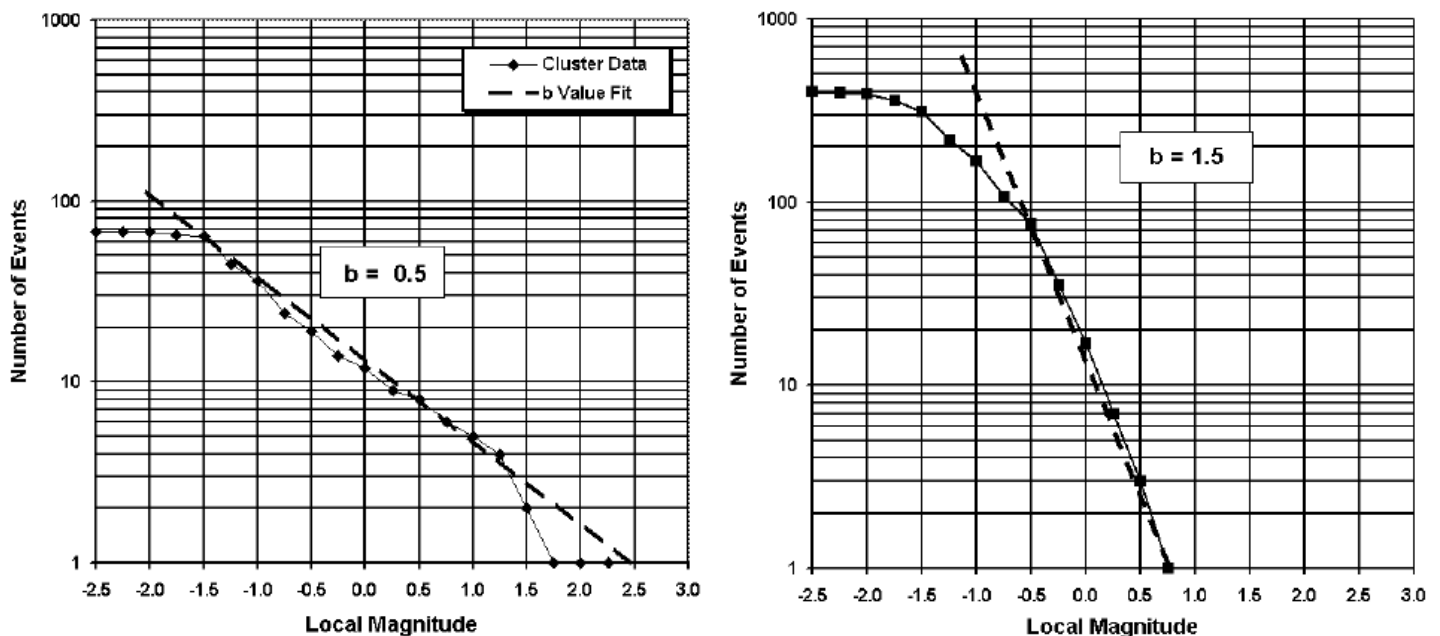


Figure 1: Typical frequency-magnitude chart (Hudyma et al., 2003).

Development of a seismic hazard metric that integrates all impacting parameters could offer enhanced seismic hazard assessments and may contribute to improved seismic hazard forecasting. However, these enhancements and improvements can only be realized with the extension of monitoring approaches and refinement of

measurement techniques specific to impacting parameters (rather than focusing solely on seismic data). Efforts to define the correlation between measurable impacting parameters and resulting seismic occurrence is warranted; offering an improved, over-arching opportunity towards seismic hazard assessments.

SEISMIC HAZARD MITIGATION

Seismic hazard mitigation is centered around preventative controls to mitigate adverse rockmass response to over-stressed loading conditions. With respect to seismic risk management, seismic hazard mitigation is complementary, but different from rockburst risk mitigation. Seismic hazard mitigation focuses on controls to prevent the occurrence of seismicity, typically through strategic design factors (i.e., rockmass preconditioning and/or high stress management with geomechanically-constrained stope sequencing). Alternatively, rockburst risk mitigation addresses tactical controls applicable to managing sudden destabilization of an excavation. An example of rockburst risk mitigation is dynamic ground support, whereby dynamic support is not expected to prevent the occurrence of seismicity, but rather is expected to retain and hold the deforming rockmass around an excavation with the goal of preserving overall excavation stability. Inclusion of both seismic hazard mitigation (i.e., trigger prevention) and rockburst risk mitigation (i.e., failure prevention) are critical elements to any seismic risk management program.

Development of an enhanced seismic hazard metric that integrates all impacting parameters not only provides an improved seismic hazard assessment approach, but offers the quantifiable measurements required for confidence in engineered design strategies to achieving hazard mitigation. Current hazard mitigation strategies are derived from theoretical principles on the basis that adjustment to the in situ and/or induced conditions will mitigate seismic hazard. As an example, seismic hazard mitigation for high stress development advance (typically through competent rockmass) often includes drift destress blasting (Figure 2). Theoretically, the drift destress blast layout is intended to weaken (or soften) the rockmass around the unconfined excavation boundary; thereby preventing brittle energy storage, redirecting stress concentration away from the unconfined excavation boundary, and ideally mitigating stress-induced violent failure.

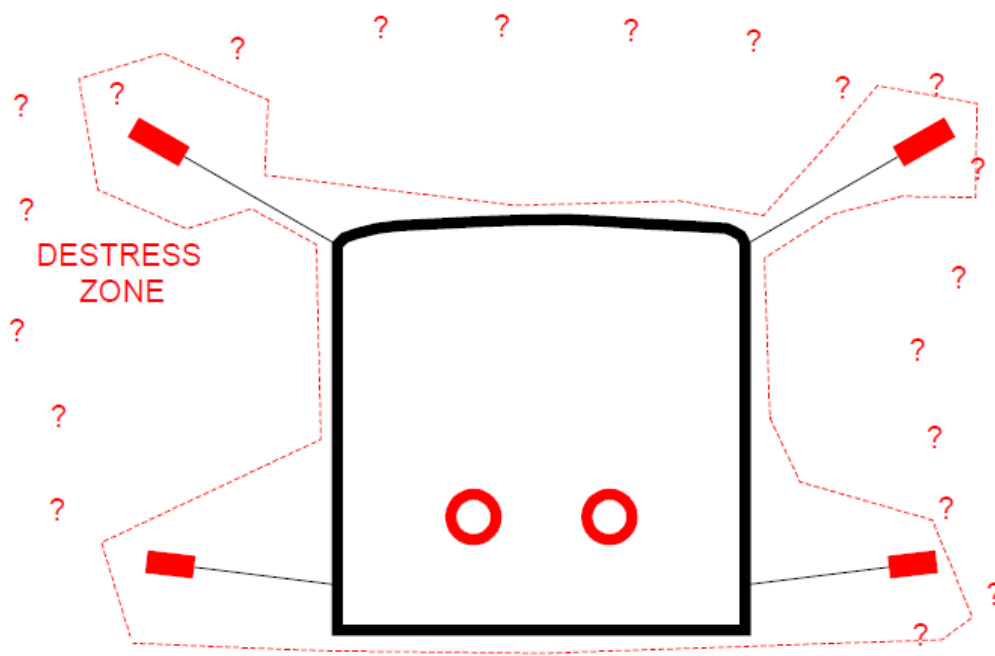


Figure 2: Typical drift destress layout (cross-section).

Unfortunately, establishing and designing for any hazard mitigation is not straight-forward. Which parameters can operationally be adjusted? How much adjustment is required? What is the technique to effectively achieve the adjustment? Was the adjustment effective? Resolution to these unanswered questions require on-going data collection and correlative analyses. In answering these questions, quantifiable measurements on the impacting parameters to seismic hazard mitigation are necessary for validation of the design. A holistic data collection program centered on rockmass metrics (and not just seismic data alone) will supply the quantifiable data necessary to guide engineered design strategies in achieving hazard mitigation, and will deliver the evidence necessary to gain acceptance of seismic hazard mitigation techniques.

SEISMIC HAZARD METRICS

Employing the positive correlation between impacting parameters and seismic hazard (suggested by Mendecki), data collection programs could be expanded to include all measurable impacting parameters. Currently, operating mine sites that are concerned with high stress seismic risk management focus considerable resources on seismic monitoring systems, seismic data collection and advanced seismic analyses. Tools and techniques centered on seismic data are important contributing metrics to seismic risk management. However, additional and complementary on-going, routine data collection, targeting quantitative rockmass metrics, predefined as impacting parameters correlated to seismic hazard, are strongly recommended. Directed at in situ conditions and coinciding with existing seismic data collection, spatially delineated geomechanical databases for mechanical rockmass properties, geological structures, and stress interpretation would refine the suite of characteristics available for correlation to seismic hazard levels. Subsequently, correlative spatial analyses between the geomechanical data and the seismic data can be used to identify those geomechanical characteristics that coincide with elevated levels of seismic activity.

SUMMARY

Improvements to seismic risk management are inherently linked to: 1) establishing robust seismic hazard assessment techniques and, 2) developing engineered methodologies for design of seismic hazard mitigation controls. An improved ability to quantify seismic hazard potential and gain confidence in mitigation strategies necessitates the advancement of correlative-based metrics, employing both in situ and induced impacting parameters. As a base requirement, seismic data collection and statistical analyses is appropriate, however correlative-based integration with quantifiable metrics from all impacting parameters enhances the risk management controls arising from seismic hazard mitigation.

REFERENCES

- Gibowicz S.J., and Kijko, A. 1994. An introduction to mining seismology. London: Academic Press Limited.
- Hudyma, M.R., Heal, D., and Mikula, P. 2003. Seismic Monitoring in Mines – Old Technology – New Applications. In Proceeding 1st Australasian Ground Control in Mining Conference, Sydney, 201–218.
- Kalenchuk, K. 2022. Predicting mine-wide seismogenic hazard with confidence using calibrated numerical models. RaSim10.
- Kijko, A. and Funk, C.W. 1994. The assessment of seismic hazard in mines. The Journal of the South African Institute of Mining and Metallurgy. 94(7), 179–185.
- Mendecki, A. 2016. Mine Seismology Reference Book: Seismic Hazard. Institute of Mine Seismology.
- Verma, A., Brown, L., Espley, S., Price, M., Moreau-Verlaan, L., and Sampson-Forsythe, A. 2022. Seismic hazard assessment and mapping: A comprehensive case study at Vale's Garson Mine, Sudbury, ON, Canada. RaSim10.
- Wesseloo, J. 2020 Addressing misconceptions regarding seismic hazard assessment in mines: b-value, Mmax, and space-time normalization. The Journal of the Southern African Institute of Mining and Metallurgy, Vol. 120, 67–80.



A few underground observations in deep mining: hard igneous rock

Simser, B.P.

Principal Ground Control Engineer, Glencore Sudbury Operations, Sudbury, Ontario, Canada

EXTENDED ABSTRACT

A critical portion of a mine design loop (initial data – design – execute – monitor – improve) comes from underground observations (the monitor stage). Many geological environments are inherently variable and difficult to put reliable design numbers to. The Glencore Sudbury operations are typical of contact deposits in the Sudbury Basin where high quality, strong igneous rock is the norm. In the context of shallow mining, the variability is often not as important: in situ or even mining induced stress usually does not exceed the rockmass strength. In intermediate or deep mining, even high quality rockmasses may experience yielding/stress fracturing around openings, but the depth of yield varies due to the variability of rockmass strength.

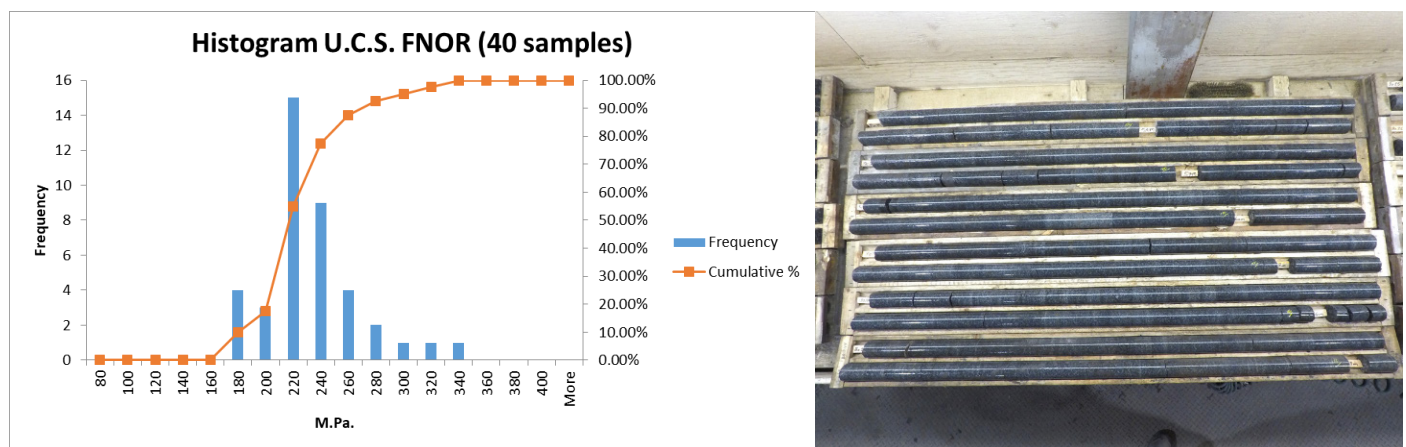


Figure 1: Example of Felsic Norite unconfined compressive strength testing results from one of Glencores' Sudbury Operations. Photo represents typical felsic norite from NQ core.

Figure 1 shows unconfined compressive strength testing from one of the more homogenous rocks found in the Glencore Sudbury mines, felsic norite. The intact strength has a wide band width, although even the low-end strengths are good or very good quality rock. The rockmass characteristics (jointing and other geological structure) vary in a similar manner, for example rock quality designation (RQD) is generally >75 except for fault zones or other anomalous areas. Although both intact and rockmass properties are consistent with high quality rockmasses, there is a significant difference in behaviour especially in the very high end rockmass strengths where strain bursting can become more pervasive in the deep mining context.

Underground observations become an essential part of the mines ground control program, as the inherent rockmass variability equates to limited accuracy when forecasting actual mining response. Numerical models for example, are great homogenizers of the rockmass strengths. Sensitivity analyses tend to dial properties up or down for the entire rock unit, whereas the full range of rock properties can be realized within the zone of

influence of a 5×5 m cross sectional area tunnel. Monte Carlo type simulations can give a range of potential responses; however, it can be prohibitively expensive to cater for the worst-case scenario 100% of the time.

The presentation gives examples of underground photos, seismic records, drill core and acoustic televiewer surveys from the Glencore Sudbury Operations. Many of the observations are related to stress/strength. For example, a near vertical drillhole at great depth with no breakouts (stress notching) in a high horizontal stress field means the rock is very strong and may be more prone to bursting than the adjacent area with breakouts. Severe borehole squeezing in a relatively weak copper vein occurs at lower stress levels than severe squeezing in the stronger host rocks.

Mechanical excavation (a deep raisebore example is shown) in the context of very strong rock induces relatively few flaws (blast fractures, blast gases infiltrating existing geological discontinuities...) and strain bursting/stress notching perpendicular to the principal stress direction should be expected. Conversely the more jointed/ altered portions of the rockmass have more degrees of freedom to relieve stress concentrations and can be less strainburst prone.

The influence of scaling on the near skin stresses around an opening is also discussed. In cycle shotcrete can be useful by deliberating keeping some of the fracture zone around an opening in place. The relatively small amount of shotcrete provides enough confinement to keep some of the stress fractures in place, which in turn adds more confinement to the rockmass around the skin of the opening. Removing the fractured material (normal practice of scaling to solid) can either propagate the process until a stable arch forms around the opening; or the removal of confinement may trigger a strain burst.

ACKNOWLEDGEMENTS

The author wishes to acknowledge the “boots on the ground” Glencore Sudbury Ground Control Team past and present: Alex Hall, Pranay Yadaz, Rick Deredin, Bleir Millions, Ed Deneka, Peter Raymond, Jared Lindsey, Chris O’Connor, Ali Jalbout, Chris Pritchard, Scott Carlisle, Graham Swan (in no particular order!).

REFERENCES

- Goodfellow, S., Simser, B., Drielsma, C, and Gerrie, V. 2017. In situ stress estimation using acoustic televiewer data. Underground Mining Technology. Australian Centre for Geomechanics, Perth, Australia.
- Hall, A., Simser, B. and Cai, M. 2021 Mechanisms of deterioration in a bored raise in brittle rock. International Journal of Rock Mechanics and Mining Sciences.
- Diederichs, M. 2014. When does brittle failure become violent? Spalling and rockburst characterization for deep tunneling projects. Proceedings of the World Tunnel Congress 2014, Brazil.



Evolution of seismic risk management strategies at Vale's Ontario Operations over the last decade

Yao, M., Chinnasane, D., Forsythe, A., and Landry, D.

Vale Canada Ltd., Sudbury, Ontario, Canada

EXTENDED ABSTRACT

Vale Canada Limited has been operating many underground mines in the Sudbury basin for over a century and all mines have experienced a significant increase in the number of major seismic events over the last decade. Various mitigation strategies have been developed at Vale's North Atlantic Operations in Ontario to manage and control the risks associated with seismicity and rockbursts over the last decade. Recent data analysis at all mines reveals that although the number of major seismic events has increased over time, the number of rockbursts has exhibited a decreasing trend in recent years.

This paper will focus on the evolution of Seismic Risk Management Strategies developed over the last decade, including both strategic and tactical control measures. Some examples will be presented in the paper to demonstrate increased effectiveness of the control measures over the last decade. Future research directions associated with the development of strategies to mitigate the seismicity and/or rock burst hazards will also be presented.

INTRODUCTION

Vale Canada has operated several underground mines in Sudbury for over a century, and currently five mines are active (Figure 1). Numerous mining methods, including open stoping, cut and fill and post pillar cut and fill, etc., are being used. Orebodies have a wide variety of varying geometries and many of these mines are at advanced stages of extraction. The primary geomechanics challenges are substantial with rock burst-prone ground conditions (Figure 2).

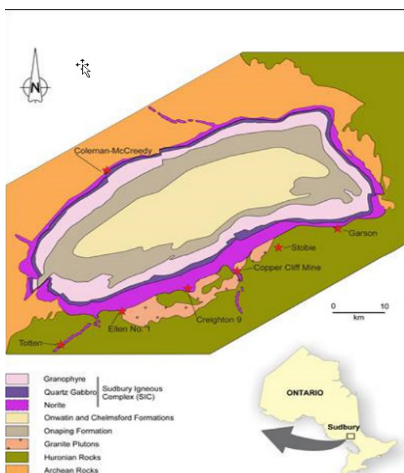


Figure 1: Vale's Sudbury mine operations.



Figure 2: Geomechanics challenges: seismicity and rock burst.

SEISMIC RISK MITIGATION STRATEGIES

Seismic Risk Mitigation Controls can be categorized as two types, i.e., strategic and tactical controls. Strategic controls focus on mine design/mining method/ mining sequence, such as pillarless /underhand mining, center-out and pushing stresses to abutment, mining away from geological structures, and using seismic hazard assessment tools. On the other hand, tactical controls may include seismic monitoring and data analyses, dynamic ground support systems, re-entry protocols, equipment mechanization (i.e., boom bolters), pillar destressing, face destressing, face support standards and ground control communication program.

Generally speaking; strategic controls are the most effective while tactical controls are the least effective.

EXAMPLES OF STRATEGIC CONTROLS

Mining method/sequence: change from ‘bottom-up’ to ‘top-down’ to eliminate sill pillars, which reflects the Creighton model with a pillar-less and top-down center-out sequence, that presents the least seismic risk, especially in wide orebodies due to de-stressing effects.

A few examples are given below on the evolution of the strategic controls being implemented in Figure3 (Copper Cliff Mine) and Figure 4 (Coleman Mine):

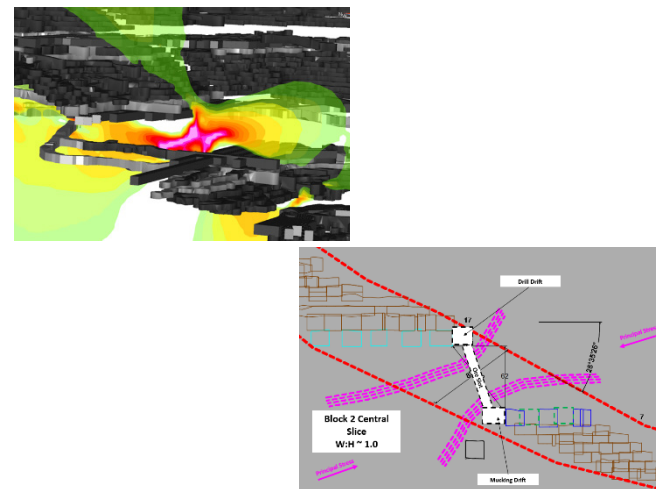
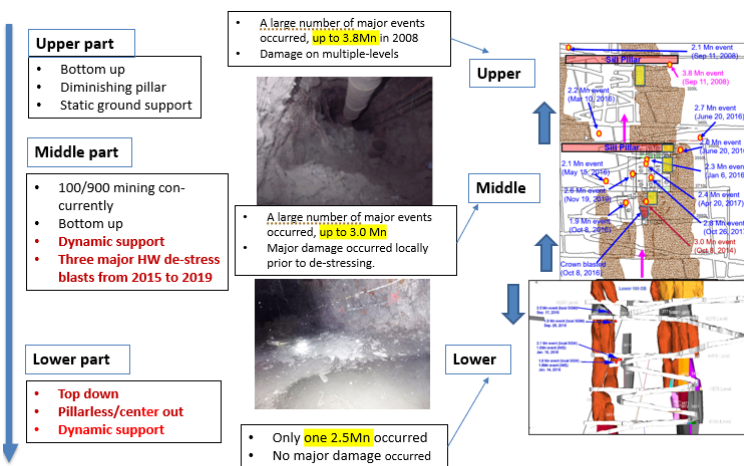


Figure 3: Mining sequence change from bottom up to top down.

Figure 4: Mining method change from cut and fill to bulk mining with a de-stress slot in the orebody.

EXAMPLES OF TACTICAL CONTROLS

Since 2013, face support has been implemented in all burst-prone ground conditions, and this strategy in conjunction with face de-stressing has been demonstrated to be very effective in controlling strain bursts in development headings (Figure 5).

Many de-stress blasts have been successfully executed in sill pillars at Copper Cliff Mine, Coleman and Garson (locally) from 2015. This de-stress blasting strategy has been demonstrated to be very effective in reducing: the magnitude of major events; the number of the larger magnitude (> 2.5 Mn) events and the high stress conditions in the Sill Pillars (Figures 6 and 7).

De-stress blasting needs to be carefully designed to understand stress redistribution, which could trigger seismicity in other areas.

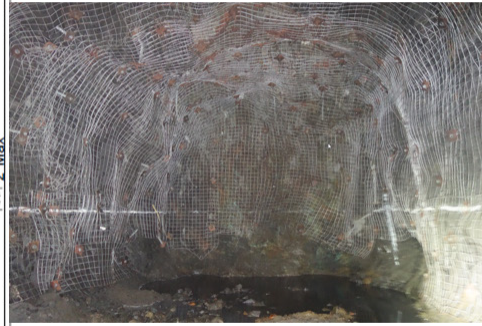
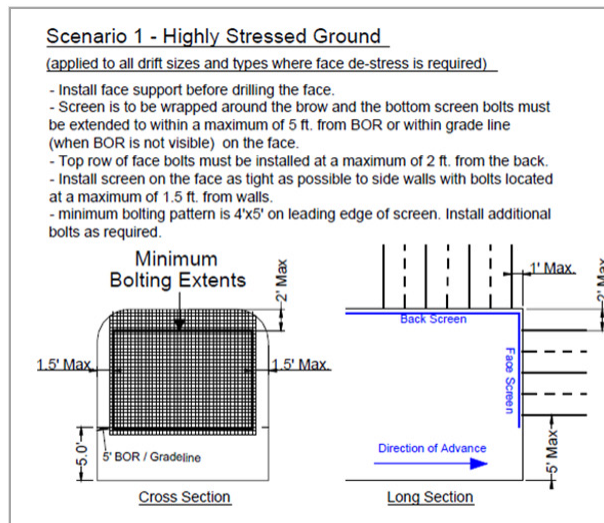


Figure 5: Face support has been introduced since 2013 to control strain bursts in development headings.

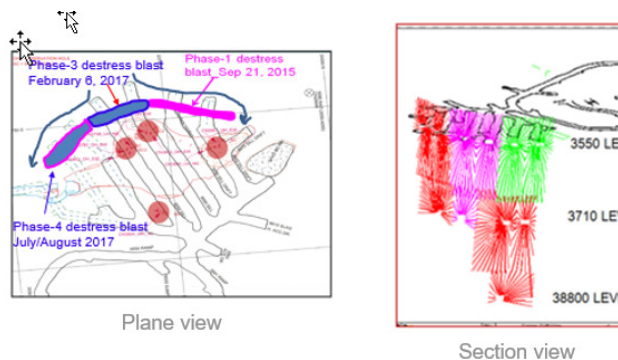


Figure 6: De-stressing design in 100/900 at CCM.

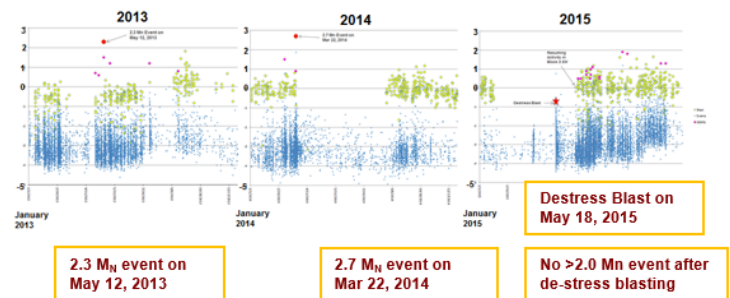


Figure 7: Reduction of the magnitude of major events at Coleman.

Figure 8 illustrates the evolution of ground support systems being implemented at Creighton Deep (at a depth greater than 2,500 m below surface) over the last decade. Significant surface support with mesh and straps have been introduced within the recent years.

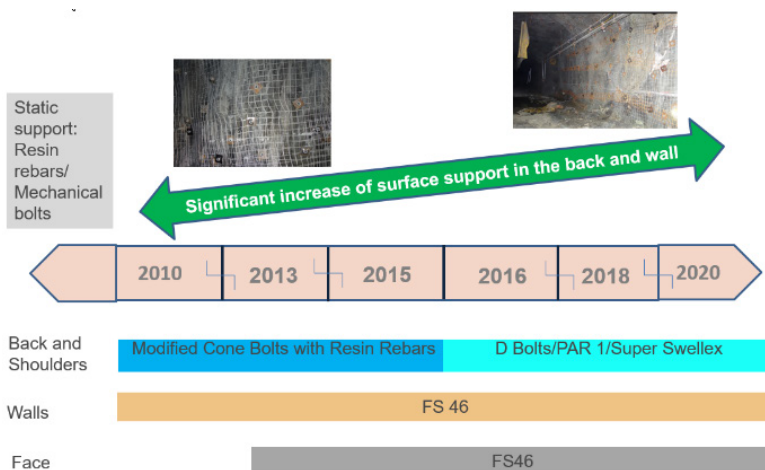


Figure 8: Evolution of dynamic support systems at Creighton.



Figure 9: Boom Bolter in narrow vein mining.

Mechanized equipment is being used instead of hand-held methods in high stress, narrow vein orebodies to limit exposure at Coleman mine (Figure 9). In addition, boom bolters are prioritized in areas of high seismic hazard for primary/enhanced support installation and face support.

THE RESULTS AND FUTURE RESEARCH DIRECTION

As shown in Figure 10, although the number of large seismic events (≥ 1.0 Mn) increased over successive years, the number of rockbursts displayed a decreasing trend since 2014.

In addition, seismic data analysis also reveals that:

1. The annual largest magnitude event at each mine remains similar.
2. There is no significant increase of magnitude for the largest magnitude event, and
3. The number of major seismic events (≥ 2.5 Mn) decreased from 2014.

As part of innovative seismic mitigation strategies, hydraulic preconditioning technology is being explored to manage the seismic risk in the future at Creighton Mine as well as other Vale Sudbury mine operations.

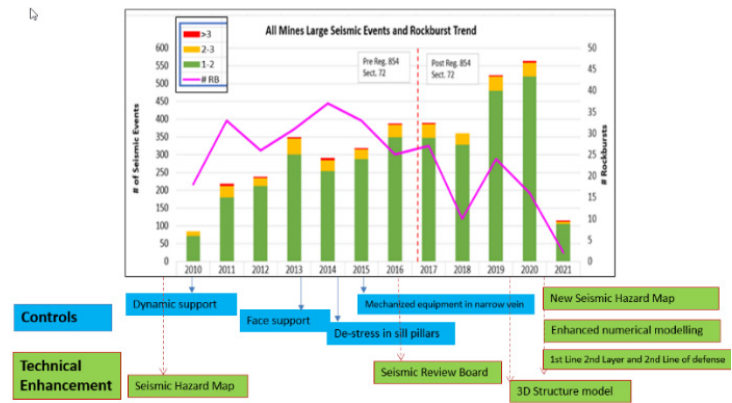


Figure 10: Seismicity and rock bursts trend with Controls and Technical Enhancement over the last decade.

SUMMARY

- Historical seismic and rockbursts data (2010 – 2020) reveals that trends are on the right track.
- Significant effort has been made to enhance strategic and tactical controls in the last decade.
- Strategic controls (most effective) are being applied to all new mining zones with high seismic risk at the design stage.
- All high seismic risk zones in the current mining areas have been identified, and critical work are being undertaken to address the risk.
- Future technologies need to be developed and introduced to reduce worker's exposure in highly burst-prone mining areas.
- Technical challenges: no standard and reliable tools are available in industry to accurately assess seismic hazards. New tools, technical skills and future research/technologies are to be developed.
- Operational challenges: finding the balance between seismic risk mitigation and the impact to production is not always an easy task.

ACKNOWLEDGEMENTS

The authors would like to thank Vale Base Metals for granting the permission to present this information. Technical and operational inputs, along with the collaboration in developing Seismic Risk Mitigation Strategies at Vale's Ontario Operations, are greatly appreciated.

REFERENCES

- Forsythe, A. 2016. Link between Magnitude of Large Seismic Events and the Effectiveness of Sill Pillar Destress Blasting: Two Case Studies at Vale Sudbury mines, 2016. 7th ESG Microseismic Symposium and Workshop, Sudbury, Canada, June 12–15, 2016.
- Yao, M., Forsythe, A., and Chinnasane, D. R. 2019. De-stress Blasting Strategy: Case Studies for Mining in Highly Stressed Sill Pillars at Vale's Ontario Operations. 53rd US Rock Mechanics / Geomechanics Symposium June 23 – 26, 2019 New York, USA.



Geology, safety, value: +/- 40 years

Falmagne, V.

Agnico Eagle Mines, Toronto, Ontario, Canada

EXTENDED ABSTRACT

The RockEng 2022 Symposium provides a remarkable opportunity to sample and showcase the best and brightest of our community, in addition to celebrating achievements in Rock Engineering in Canadian mining. The last objective of this gathering is to define a vision for future collaboration and propose a pathway to achieve it. Before proceeding to the workshop entitled RockEng 2023: Rebirth of the Canadian Rock Mechanics Symposia, this final presentation offers a brief retrospective of the last four to five decades of mining rock engineering. It highlights some of the author's observations of external and internal drivers of the evolution that some of us have witnessed and others have inherited, as well as discussing some of the factors and technologies that are likely to shape the future in mining.

LOOKING BACK 40 YEARS

The early 80s signalled a wake-up call for the Canadian hard rock mining industry, first with the Belmoral crown pillar failure in 1980 and then with the Stevenson Commission following the Falconbridge rockbursts in 1984. The Canadian public, legislators and government, academia and industry reacted to these major events by implementing significant changes to the legislation, defining corporate and individual responsibilities and funding significant research efforts to tackle mine design and ground stability challenges. During this period, major Canadian mining companies such as Inco, Falconbridge, Placer Dome and Noranda (and others) were highly engaged in supporting internal and academic research and developing technologies to improve safety and return on investment. The Cavity Monitoring Survey (CMS), the introduction of new ground support elements/systems (e.g., modified geometry cables, mesh straps, yielding bolts, shotcrete) and equipment (e.g., Maclean bolter) and the development of paste fill are some of the technological game changers that were developed and successfully implemented in the industry. These developments provided the much-needed tools for quantitative unbiased measurements of stope and support performance (i.e., overbreak and underbreak), for enhanced safety and for increases in mining rate and productivity. On the design side, with the introduction of classification schemes in the 70s, the 80s and early 90s came the golden age of empirical design methods. The Stability Graph for open stope design (Mathews et al, 1981, Potvin 1988), pillar design (Hudyma, 1988, Lunder and Pakalnis, 1997), crown pillar design (Golder, 1990), dilution estimation (Clark, 1992), and design span for man-entry stopes (Lang et al, 1991) are a few examples of the design tools that were introduced and are still used extensively today. Fundamental research into ground support and mine design under rockbursting conditions was made accessible to the industry through the Canadian Rockburst Research Project (CRRP), the publication of several handbooks and books (Hutchinson and Diederichs, 1996, Hoek, Kaiser, Bawden, 1995), the suite of Rocscience analysis software and seismic monitoring systems (ESG). This non-exhaustive list is only a portion of the legacy of this highly fruitful period in applied mining research in Canada. In conjunction with heightened industry awareness and regulations, the results of the technical advances were measured in terms of accident reduction and increased mining rates. Figure 1 relates the price of gold to accident frequency and the number of hours worked in the Québec mining sector (data source: APSM annual reports, mining sector statistics).

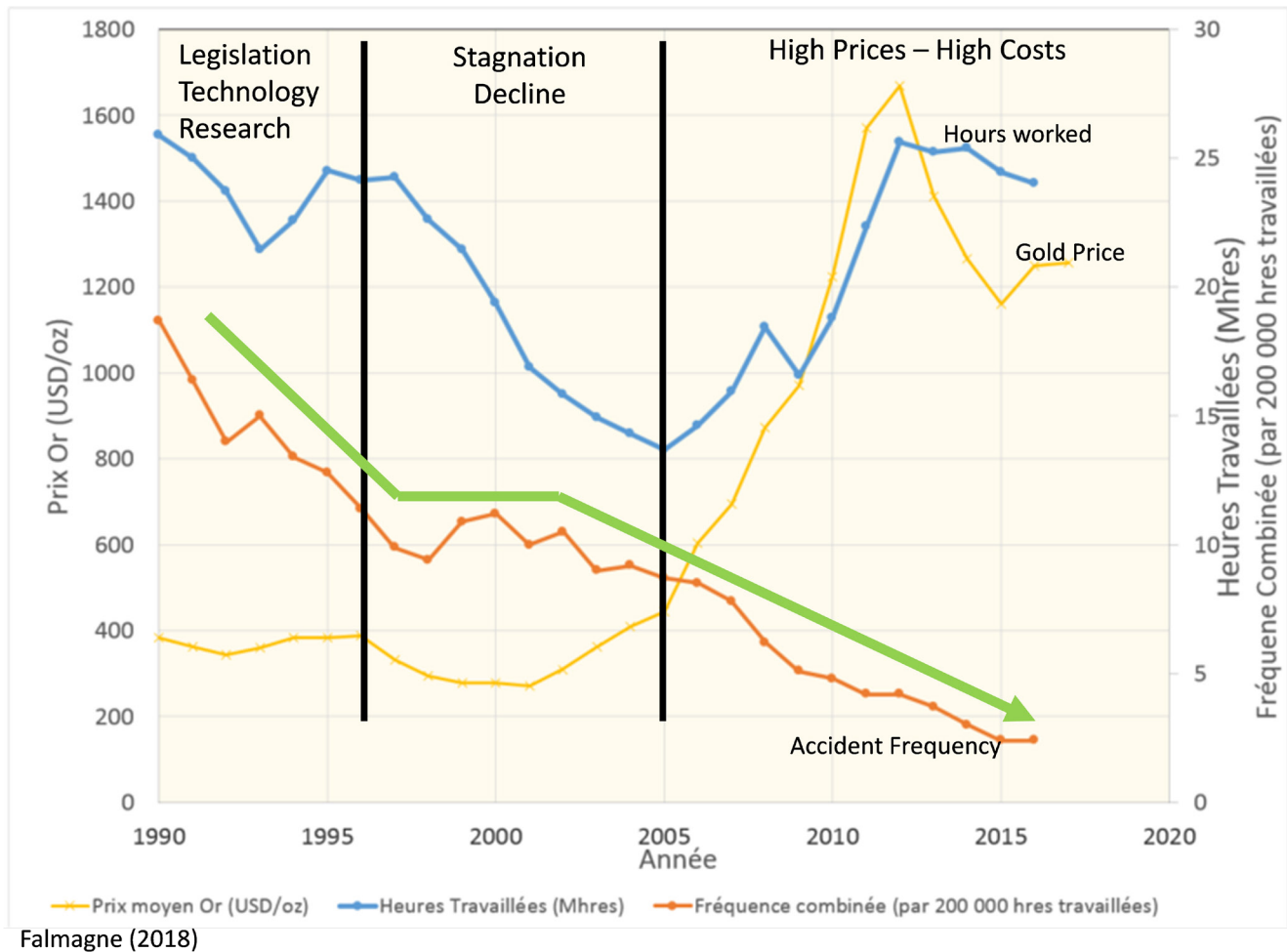


Figure 1: Evolution of the price of gold, the combined accident frequency per 200 000 hours and the number of hours worked in Québec mines from 1990 to 2016. The green arrow highlights the trend in accident frequency.

Three black vertical lines in the graphs on Figure 1 tentatively divide the period into three broad segments. From the early 80s to mid to late 90s, we see the combined benefits of legislation, research and technology developments as well as a general increase in awareness about the importance of ground control in the mining industry reflected in a decline in accident frequency in Québec mines. The decrease in the gold price and relative stagnation in base metal prices from 1996 to early 2000s exerted huge pressure on the industry resulting in inevitable consequences in terms of the loss of qualified people and some economically-driven mine design decisions with inherently higher risk. From 2005 onwards, metal prices increased sharply; however, so did the cost of materials, labour, and energy meaning that although the economic prospects for project development have improved, capital requirements have reached new heights and operating costs exert pressure to increase mining rates or improve ore quality (grade). Rock engineering research in Canada has been more diversified over the last 15–20 years incorporating knowledge and understanding from the nuclear waste disposal and caving geomechanics worlds.

The lean years (1996–2005) were not without some positive impacts that merit highlighting. Under pressure to increase mining rates, the industry became highly effective at safely moving tonnes from non-caving operations (i.e., open stoping with backfill) and making profits from very low grade yet relatively compact and small orebodies. The deepest hard rock mines in Canada have also pushed the envelope in terms of material handling and ventilation. They have led the way in seismic risk management through the development of effective ground support for rockbursting conditions (Cai and Kaiser 2018, Potvin and Hadjigeorgiou 2020), stope sequencing and optimisation of mining layouts (Counter 2014, Sasseville et al 2022). Major advances have also been made in the

management of squeezing and very weak ground. Finally, hard lessons were learned from economically-driven mine design decisions that led to the premature, permanent or temporary closure of operations. These learnings include a renewed understanding of the criticality of geological understanding and modelling based on sufficient data and rock mass characterization, and the commitment to risk evaluation, assessment, and management.

THE NEXT 40 YEARS

It is generally predicted that the world demand for metals (traditional and “new age”) will increase to the point that it is fair to wonder if the global mining industry will be able to meet this demand. As a minimum, it is safe to expect that we will see more large-scale bulk mining of low to moderate grade deposits by very large open pits, caving mines and highly efficient underground open stoping with backfill, progressing to greater depths with higher mining rates. Continued technological advances in mining equipment, instrumentation / monitoring and data management will be needed to meet this demand. To this end, perceived needs in rock mass characterization and excavation / support design are specific to rock engineering and are briefly discussed below.

A geotechnical model relies on the best geological and structural understanding available at each step of project development. With the field analysis and geological modelling tools currently available, geological and structural models can and should be developed from the earliest stages of a project and continuously updated as data is added, including during operation. Time and money are saved when the geology and geotechnical teams (internal and consultants) use a common platform to exchange the most up to date data to plan investigations and instrumentation. Geotechnical site investigations are costly and time consuming, but they are essential and need to be conducted under the direction of experienced rock engineering personnel in the closest cooperation with the exploration / geology team. Several technologies are available or emerging, and we should leverage them fully and support on-going developments. Some examples include televiewer and borehole geophysics, core scanning, and real-time drilling feedback data acquisition. So far, these tools have not evolved to the point of replacing in-person geotechnical logging at the drill to reduce the cost and time of data collection. However, they can be used to massively increase the quantity, spatial distribution and consistency of geotechnically useful data from thousands of meters of exploration holes. As the rock is exposed, mapping is essential to collect data at a larger scale and validate parameters deduced or estimated from core logging such as discontinuity persistence, length and large-scale roughness. Progress is expected with tunnel, stope and pit wall mapping with UAVs in the near future with research and emerging technology firms focusing their efforts on this subject. Geo-data management expertise is becoming essential for large databases and the integration of structural data over several scales in order to generate representative rock mass models. An in situ stress model remains an important component of site characterization that is currently difficult and costly to realize. Technological improvements in this field are needed.

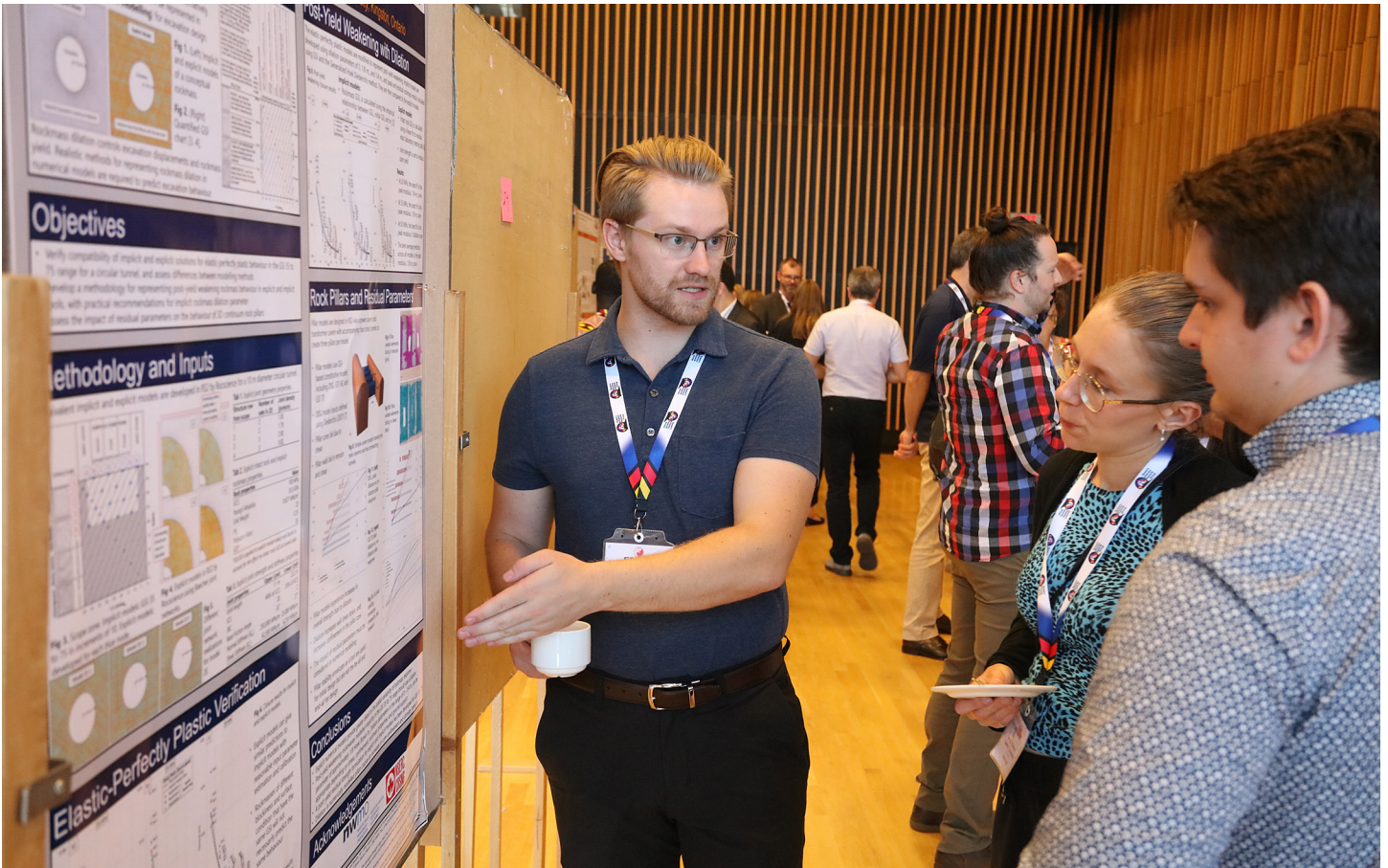
The classification/empirical design combination has served the Canadian mining industry well over the last forty years and will likely continue to be used in the future. However, it is the author’s view that a change is needed for future excavation design. The empirical databases are useful as a sanity check or at the scoping stage of a project; however, they should be refreshed using current conditions and uniformly defined parameters. For example, the Stability Graph and the dilution estimation based on ELOS (Clark 1992) are very popular because a) they have been widely used, studied and “improved” by many researchers b) they can be presented with deterministic and quasi-probabilistic results and c) they provide convenient input for the Minalbe Shape Optimizer (MSO) software for reserve evaluation. The variability in parameter definition (e.g., the A factor) over the years can lead to confusion. Depending on the version of the parameters used by designers, significant differences in the results and subsequent design recommendations have been observed with major impacts on stope dimensions and dilution that directly affect project viability. Other pitfalls of these approaches are well described in Potvin et al (2012). One of the most useful outcomes of site characterization and preliminary analyses is the identification of the potential failure mechanisms, critical parameters and data gaps. All of which should be considered when

selecting the most appropriate analytical/numerical method for assessing stability beyond a scoping level. Numerical modelling using discontinuum mechanics (e.g., Garza-Cruz et al, 2019) and particle-based models can provide useful insights into support performance, failure mechanisms and key factors controlling stability.

The objectives of Ground Control management are to ensure the safety of personnel and the recovery of the mineral reserves and generate value through optimisation of the extraction process. Achieving these goals requires time, effort and resources for geotechnical site investigations to produce a realistic and robust mine design, assessing risks and opportunities and identifying the data gaps that must be tackled to de-risk the projects. Rock engineering has progressed in leaps and bounds over the last 50 to 60 years; however, so have the demands placed on Ground Control engineers and the Rock Engineering and Geotechnical disciplines. Rock engineering specialists are being asked to respond to this ever-increasing demand with an increasing level of “certainty” under rock mass and stress conditions that continually push the limits of our knowledge. In order to accomplish this, they must continue to leverage their unique and essential role as translator and facilitator between geology and engineering, test and implement new technologies for the rapid collection and validation of quality geotechnical data and learn to use, control and fully exploit available sophisticated modelling, data analysis and integration tools.

REFERENCES

- Cai, M. and Kaiser, P.K., 2018. Rockburst support reference book, Volume 1, Rockburst Phenomenon and Support Characteristics, Mirarco – Laurentian University.
- Clark, L.M., 1992. Minimizing dilution in open stope mining with a focus on stope design and narrow vein longhole blasting. M.A.Sc. Thesis, Department of Mining and Mineral Process Engineering, University of Saskatchewan.
- Counter, D.B., 2014. Kidd Mine – dealing with the issues of deep and high stress mining – past, present and future. Deep Mining 2014: Proceedings of the Seventh International Conference on Deep and High Stress Mining, ACG, Sudbury, ON.
- Garza-Cruz, T., Bouzeran, L., Pierce, M., Jalbout, A. and Ruest, M., 2019. Evaluation of ground support design at Eleonore Mine via Bonded Block Modelling. Ground Support 2019: Proceedings of the 9th International Symposium on Ground Support in Mining and Underground Construction, ACG, Sudbury, ON.
- Golder Associates 1990. Report 881-1739 to Canmet on "Crown Pillar Stability Back-Analysis". Report #23440-8-9074/01-SQ, Canada Centre for Mineral and Energy Technology, pp. 90.
- Hoek, E., Kaiser, P.K. and Bawden, W.F., 1995. Support of underground excavations in hard rock, A.A. Balkema/Rotterdam/Brookfield.
- Hudyma, M.R., 1988. Rib pillar design in open stope mining. M.A.Sc. Thesis, Department of Mining and Minerals Processing, University of British Columbia.
- Hutchinson, D.J. and Diederichs, M.S., 1996. Cablebolting in Underground Mines, BiTech Publishers Ltd, B.C.
- Lang, B., Pakalnis, R.C. and Vongpaisal, S, 1991. Span design in wide cut and fill stopes at Detour Lake Mine. 93rd Annual General Meeting CIM 1991, Vancouver, B.C.
- Lunder, P.J. and Pakalnis, R.C., 1997. Determination of the strength of hard-rock mine pillars. CIM Bulletin Vol 90, No 1013, pp51–55.
- Mathews, K.E., Hoek, E., Wyllie, D.C., and Stewart, S.B.V. 1981. Prediction of stable excavations for mining at depth below 1000 metres in hard rock. CANMET Report. Department of Energy, Mines and Resources, Ottawa.
- Potvin, Y. 1988, Empirical stope design in Canada. PhD Thesis, Department of Mining and Minerals Processing, University of British Columbia.
- Potvin, Y., Dight, P.M. and Wesseloo, J. 2012. Some pitfalls and misuses of rock mass classification systems for mine design, The Journal of the South African Institute of Mining and Metallurgy, Vol 112, pp. 697–702.
- Potvin, Y. and Hadjigeorgiou, J. 2020. , Ground Support for underground mines, ACG, University of Western Australia, ISBN 978-0-9876389-5-3.
- Sasseville, G., Turcotte, P. and Falmagne, V., 2022. Control measures to manage seismic risk at the LaRonde Mine, a deep and seismically active operation. American Rock Mechanics Association, 56th Rock Mechanics / Geomechanics Symposium, Santa Fe, New Mexico.



Poster Presentation Abstracts

Multi-modal limit equilibrium analysis of open pit mines using LIPS-R

Li, S.¹, Cami, B.², Javankhoshdel, S.², Corkum, B.², and Yacoub, T.²

¹*University of Waterloo, Waterloo, Ontario, Canada*

²*Rocscience Ltd., Toronto, Ontario, Canada*

ABSTRACT

The slope stability analysis of open pit mines is a multi-modal problem, i.e. there can be multiple regions with critical factors of safety (local minima) with factor of safety values similar to that of the most critical factor of safety (global minimum) but in locations far away from the most critical failure region. In practical multi-modal problems, the information of multiple optima is always desired for practitioners to make better decisions. To achieve such goal, a niching method called locally informed particle swarm algorithm (LIPS) has been proposed by researchers. However, very few have reported the application of LIPS in solving multi-modal geotechnical problems. This paper proposes an algorithm called LIPS radius (LIPS-R), which adds a radius filter to LIPS. This study shows the effectiveness of the proposed algorithm for two open pit mine cases with anisotropic materials. Results showed that LIPS-R is efficient in finding the global minimum, as well as any other minima simultaneously.

Numerical and machine learning based approaches to study the influence of environmental conditions on crack growth in the Theban Necropolis, Egypt

Vasileiou, A.¹, Alcaino-Olivares, R.¹, Loprieno-Gnirs, A.², Bickel, S.², Ziegler, M.³, Khan, U.T.¹, and Perras, M.A.¹

¹Department of Civil Engineering, York University, Toronto, Ontario, Canada

²Department of Ancient Civilizations – University of Basel, Basel, Switzerland

³Department of Earth Sciences, Swiss Federal Inst. of Technology – ETH, Zurich, Switzerland

ABSTRACT

The Thebes Necropolis in Luxor, Egypt, was listed by UNESCO as a World Heritage site since 1979. During the Egyptian New Kingdom (1500 – 1000 BC) many rock-cut tombs were constructed to host funerary chambers for the high cast society, of which 450 of them have been uncovered to-date. The area extends over 6 km² and includes marl and limestone from the Thebes Limestone Formation (Lower Eocene), with structural features such as listric faults, networks of gullies and steep cliffs all across the Thebes Mountains. Efforts have been made to better understand the geo-hazards which could jeopardize the Theban Necropolis' pristine landscape.

Our team has deployed instrumentation in two areas in the Theban Necropolis (Valley of the Kings and Sheikh Abd el-Qurna), in order to examine how the current climatic conditions have impacted the stability of cliffs and tombs in these areas. The monitoring networks record displacements and local climatic conditions, observing the thermally induced stress effect on the rock mass. In the Valley of the Kings our monitoring station is measuring the movement of a lateral fracture that forms part of a rock pillar that is potentially unstable (See Figure 1). This rock pillar has multiple sub-vertical slabs that could potentially collapse onto the entrance of tomb KV42. Lateral fracture movements have been strongly correlated to temperature and solar radiation fluctuations that have recently been replicated in FLAC models. The second location in Sheikh Abd el-Qurna, a pillar inside a rock cut tomb (TT95) has a through going fracture which was a release plane for a large wedge that collapsed during the construction of the tomb in ancient time. Evidence, such as construction tools left behind, suggest that the wedge collapse occurred suddenly, although there appears to have been some effort to support the wedge prior to collapse (see Figure 2). The tomb sites several meters below the ground surface and on the most recent field visit, sand had accumulated on the floor of the tomb after it had been closed to access for nearly 3 years. The sand suggests that there could be some movement on the fracture which daylight at the ground surface. 3D numerical models are currently being constructed to assess the stability of the pillars within tomb TT95 in order to develop a more robust monitoring system and preservation plan.

The climatic and rock movement data has been collected at both sites for several years at KV42, and for several months at TT95. Measurements are taken every 15 minutes and this volume of data collection requires time series and machine learning analysis to understand the relationships between the climatic factors and the rock movement. In addition, a compilation of Egyptological reports, paleo-climatic studies and archaeological findings extend the dataset beyond the digital records and afford the opportunity to include the past historical

and even ancient conditions from the sites. The utmost goal is to reconstruct and represent digitally the geo-environmental history of the sites in order to understand the how the present conditions may have come to be. The sparsity of data points in the ancient records will require the use of fuzzy logic machine learning models to handle this issue. The present article introduces the site investigation and assessment of current progressive crack growth as well as the historical and ancient records that could be related to environmental influences on past crack growth in the Thebes Necropolis near Luxor, Egypt. Preliminary numerical and machine learning models will be presented to demonstrate the importance of capturing the climatic influence to better understand the crack growth driving mechanisms that threaten to slowly deteriorate these ancient monuments and could potentially lead to more dynamic failures in the future.

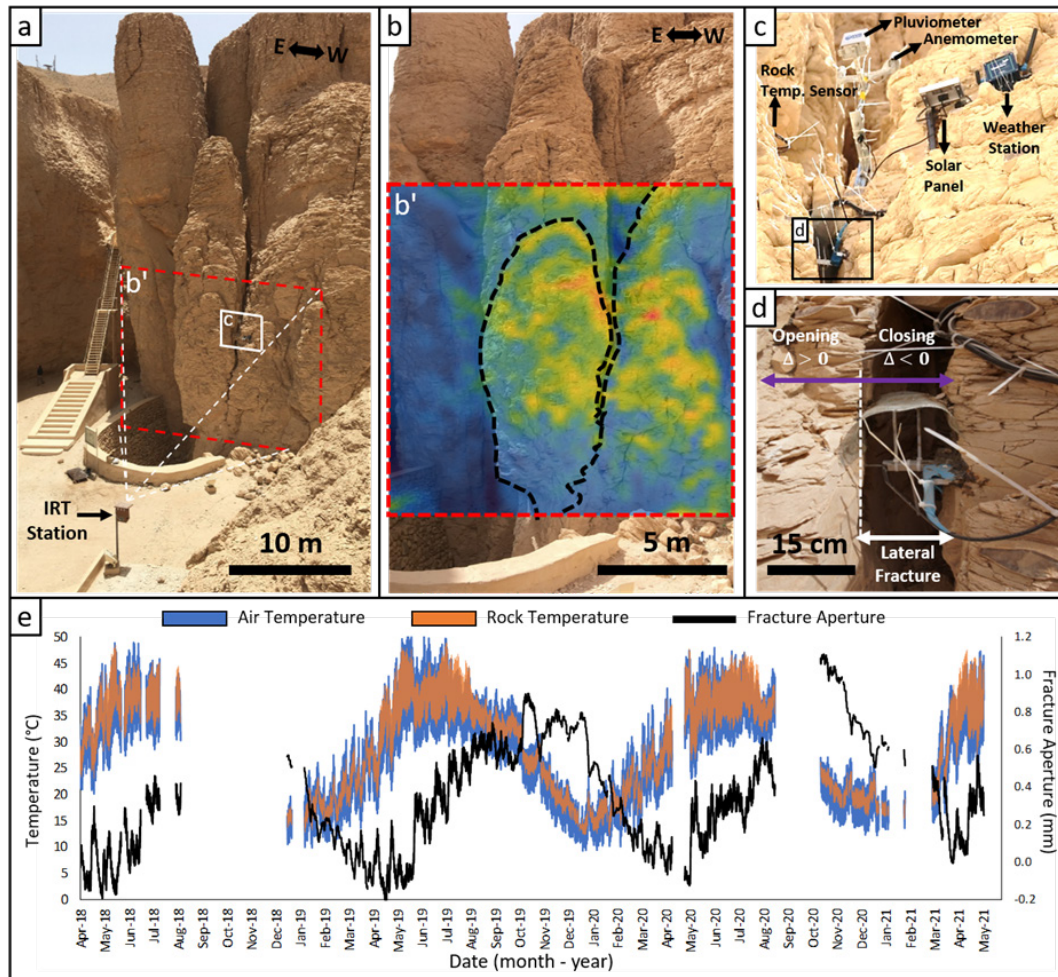


Figure 1: Instrumentation on the rock pillar above tomb KV42, showing a) a panoramic view of the infrared thermographic (IRT) station facing the rock pillar, b) the infrared image over laid on the rock mass, c) the Libelium weather station deployed within the lateral fracture, and d) the crack meter.



Figure 2: Wedge in the roof of tomb TT95 (left) with remains of the final tomb painting indicating the final designed roof location (middle left side) and (right) the displacement sensor placed between the pillar with the through going fracture and an intact pillar, as well as wires for 10 temperature sensors.

A geomechanics research program in support of deep geological disposal in Canada

Kasani, H.

Nuclear Waste Management Organization, Toronto, Ontario, Canada

ABSTRACT

The Nuclear Waste Management Organization (NWMO) is implementing Adaptive Phased Management (APM), Canada's plan for the long-term management of used nuclear fuel in a deep geological repository (DGR). The NWMO is currently investigating two potential rock settings for a DGR in Canada: crystalline rocks of the Canadian shield and the Paleozoic sedimentary rock of southern Ontario. Together with other components such as bentonite buffer, the surrounding geosphere constitutes part of a multi-barrier system preventing radionuclide migration during construction, operation, and post-closure. During the post-closure period, natural processes expected to occur within the next one million years such as earthquake, glacial loading and unloading must be considered. To ensure the best scientific approaches are available to inform engineering design, assist in site selection, and demonstrate long-term safety of a DGR, the NWMO supports fundamental and applied geomechanics research programs at several universities, international research institutes, and underground research laboratories. The ongoing research programs aim to advance the state of knowledge in multiple fronts, including: 1) laboratory characterization of low-porosity and low-permeability crystalline and sedimentary rocks including mechanical, hydraulic, thermal, coupled thermal-hydraulic-mechanical (THM) properties, poroelastic parameters, and long-term strength; 2) fracture characterization and shear behavior at different scales; 3) a joint international program to manufacture and test large shear testing equipment for studying scale effect on rock fracture shear behavior; 4) large-scale triaxial equipment for characterizing a heterogeneous limestone; 5) numerical research programs dedicated to delineation of excavation damaged zone (EDZ); 6) statistical analyses of in situ stress measurement data; 7) development of numerical approaches for upscaling mechanical properties of rockmass containing discrete fracture network (DFN); 8) in situ experiments in international underground research laboratories, associated long-term monitoring programs, and interpretation of the field data; and 9) numerical studies to demonstrate safety of underground openings during construction, operation and post-closure including during heat emission by the used fuel, earthquake loading, fault re-activation, and glacial loading and retreat. This poster provides an overview of NWMO's geomechanical research program in support of characterizing safety attributes of the geosphere in relation to a safe and long-term disposal of used nuclear fuel in hard sedimentary and crystalline rocks.

2022 database update and UCS-Leeb Hardness correlation

Séguin, K.¹, Kinakin, D.¹, and Corkum, A.G.²

¹BGC Engineering Inc., Kamloops, British Columbia, Canada

²Dalhousie University, Halifax, Nova Scotia, Canada

ABSTRACT

The Leeb Hardness Tester (LHT), or Equotip device, is a pocket-sized portable device for non-destructive estimates of material hardness based on the measured ratio of rebound velocity to impact velocity, originally developed for metals (Figure 1). Several authors have conducted studies to predict the Uniaxial Compressive Strength (UCS) of rock from the LHT (Table 1). Since 2018, the authors have maintained a database of LHT and UCS test results for the same rock samples compiled from literature and testing completed by the authors. This study presents the latest database comprising work by Corkum et al (2021) with additional literature sources (Celik et al, 2020; Desarnaud et al, 2018) and further testing by the authors.

The latest database consists of 355 sample data points with intact strengths data between R3 and R5 (ISRM, 1981). The database updates also include additional sample characterization including sample texture, fabric, type, porosity, density, Young's modulus and Poisson's ratio. A revised correlation between LHT hardness and UCS is presented. Recommendations for best practices for using the device and interpretation of the resulting data are also provided.

REFERENCES

- Celik SB, Cobanoglu I, Koralay T. 2020. Investigation of the use of Leeb hardness in the estimation of some physical and mechanical properties of rock materials. *Pamukkale University Journal of Engineering Sciences*, 26(8), 1385-1392.
- Corkum AG, Asiri Y, El Naggar H, Kinakin D. 2018. The Leeb Hardness Test for rock: An updated methodology and UCS Correlation. *Rock Mechanics and Rock Engineering*, 51(3):665-675
- Corkum, AG; Ghasemi, M; Asiri, Y; Kinakin, D. 2021. Leeb Hardness Test and UCS Correlation Data for Rock. <https://doi.org/10.5683/SP2/O52YXA>, Scholars Portal Dataverse, V1, UNF:6:QTbGE9M/SZPVISY2MDilYw== [fileUNF]
- Desarnaud J, Kiriya K, Simsir BB, Wilhelm K, Viles H. 2019. A laboratory study of Equotip surface hardness measurements on a range of sandstones: What influences the values and what do they mean? *Earth Surface Process and Landforms* (Vol. 44, pp. 1419-1429). Chichester : John Wiley & Sons Ltd.
- International Society for Rock Mechanics (ISRM). 1981. ISRM suggested methods for rock characterisation, testing and monitoring. *International Journal of Rock Mechanics, Mining Sciences & Geomechanics Abstracts*, 18: 119 - 121.



Figure 1: Leeb Hardness Tester device (Corkum et al, 2018).

Table 1: Correlations of UCS to LHT from previous studies

Source	Reported Best-fit Equation
Meulenkamp, 1997	$\sigma_c = 1.75 \times 10^{-9} L_D^{3.8}$
Verwaal and Mulder, 2000	$\sigma_c = 4.906 \times 10^{-7} L_D^{2.974}$
Lee et al., 2014	$\sigma_c = 2.3007 e^{0.0057 L_D}$
Yilmaz, 2013	$\sigma_c = 4.5847 L_D - 142.22$
Aoki and Matsukara, 2008	$\sigma_c = 0.079 e^{-0.039 n L_D^{1.1}}$
Meulenkamp and Alvarez Grima, 1999	$\sigma_c = 0.25 L_c + 28.14(\text{density}) - 0.75(\text{porosity}) - 15.47(\text{grain size}) - 21.55(\text{rock type})$
Corkum et al., 2018	$\sigma_c = \alpha L_D \beta \times 10^{-6}$ (α and β based on rock type)

Numerical study of the effects of yielding rockbolts on controlling self-initiated strainbursts

Wang, J., Apel, D.B., Wei, C., and Xu, H.

School of Mining and Petroleum Engineering, University of Alberta, Edmonton, Alberta, Canada

ABSTRACT

Self-initiated strainburst is an unstable rock failure phenomenon at the excavation boundaries of deep openings. It is the most common type of rockbursts and has posed a serious threat to the safety of the facilities, equipment, and workers in mining and civil engineering projects. A popular tactic to control and mitigate strainburst damage is using yielding rockbolts. This type of rockbolts allows yielding to resist the dynamic loads and accommodate large deformations caused by rock fracturing, dilation, and ejection.

Drop test is a common method to evaluate the effects (e.g., the dynamic capacity of energy-absorption) of yielding rockbolts on controlling strainbursts. This test method is simple, straightforward, and repeatable. However, there are some defects for this method. For instance, the dynamic capacity of a rockbolt is not a constant value, and the loading mode of a rockbolt will affect its dynamic capacity. The impact load in drop tests is difficult to represent the impact of ground pressure load, and the existing test system generally cannot reproduce the complex ground support/rock mass interaction that exists in an underground environment. Additionally, original rock stress is not considered in tests. Hence, the impact loading from conventional drop tests might not be able to represent rockburst loading. The complex interaction between seismic waves, rockbolts, and reinforced rock masses during strainbursts requires extensive numerical studies to assess the effects of yielding rockbolts.

In this study, instead of conventional drop tests, a 2D distinct element method (DEM) model of a deep tunnel is built via UDEC to fully evaluate the effects (e.g., the dynamic capacity of energy absorption and control of rock damage) of yielding rockbolts on controlling self-initiated strainbursts. The rationality and capability of UDEC in modeling self-initiated strainbursts are first validated through comparison with laboratory tests. Then, two types of yielding rockbolts (D-bolt and Roofex) and the traditional rockbolt (resin-grouted rebar, for comparison) are modeled via the “rockbolt” element in UDEC after an exact calibration procedure. The numerical modeling was conducted with two stages: (a) static stage: the in situ stress field was applied to the model, and the geo-static equilibrium was achieved. Then, the tunnel was excavated and a total of 15 rockbolts were installed; (b) dynamic stage: the dynamic mode was activated. The local damping ratio was reduced from 0.8 to 0.05. The viscous boundary was used in the dynamic calculation to avoid propagating waves’ reflection and allow the necessary energy radiation. The dynamic calculation time is set to 120 ms.

The velocity distribution of tunnel surrounding rock masses is shown in Figure 1. Only a few rock blocks are ejected from a local zone when the D-bolt is adopted. For the tunnel supported by Roofex and resin-grouted rebar, much more rock blocks with high speeds are ejected from the roof and sidewalls. Some resin-grouted rebar bolts are broken agreeing with many in situ observations. A function was developed using FISH language programming to record the velocity and volume of all the detached rock blocks in the model. The statistical analysis results are illustrated in Figure 2. Figure 2a shows that the average velocity of detached rock blocks in the tunnel supported by D-bolts is only 0.34 m/s, while the average velocities of detached rock blocks in the tunnel

supported with Roofex and resin-grouted rebar are 3.22 and 3.97 m/s, respectively. Additionally, the velocity distributions of rock blocks in these two scenarios are more extensive than those in the tunnel using D-bolts (Figure 2b). Another FISH function was developed to record the variation of the kinetic energy of ejected rock blocks with time (Figure 2c). When the tunnel is supported with D-bolts, the kinetic energy first increases to the peak value from 0 to 26 ms and then gradually declines to almost zero. For Roofex, the kinetic energy experiences fast growth, especially after 80 ms, and reaches the peak value at 103 ms. Then, the kinetic energy drops with time but is still high. When the tunnel is supported by resin-grouted rebar, the kinetic energy first increases rapidly to the peak value from 0 to 54 ms and then suffers a sudden drop. Then, it surges again at 100 ms. These results suggest that the rock ejection is much more violent when the tunnel is supported by Roofex and resin-grouted rebar, indicating that these two types of rockbolts fail to control the strainburst solely. In contrast, the D-bolt can effectively reduce kinetic energy and mitigate strainburst damage.

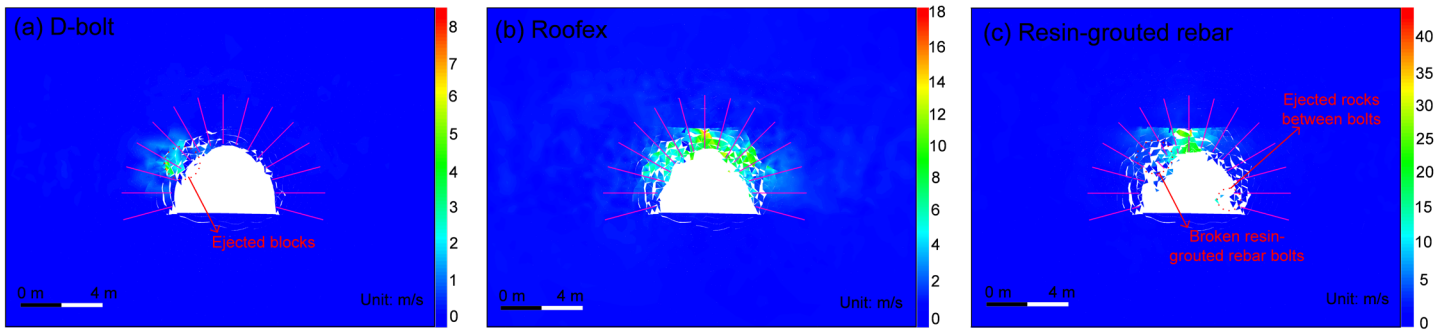


Figure 1: Simulated velocity distribution of the surrounding rock masses along the tunnel supported by different types of rockbolts: (a) D-bolt; (b) Roofex; (c) Resin-grouted rebar.

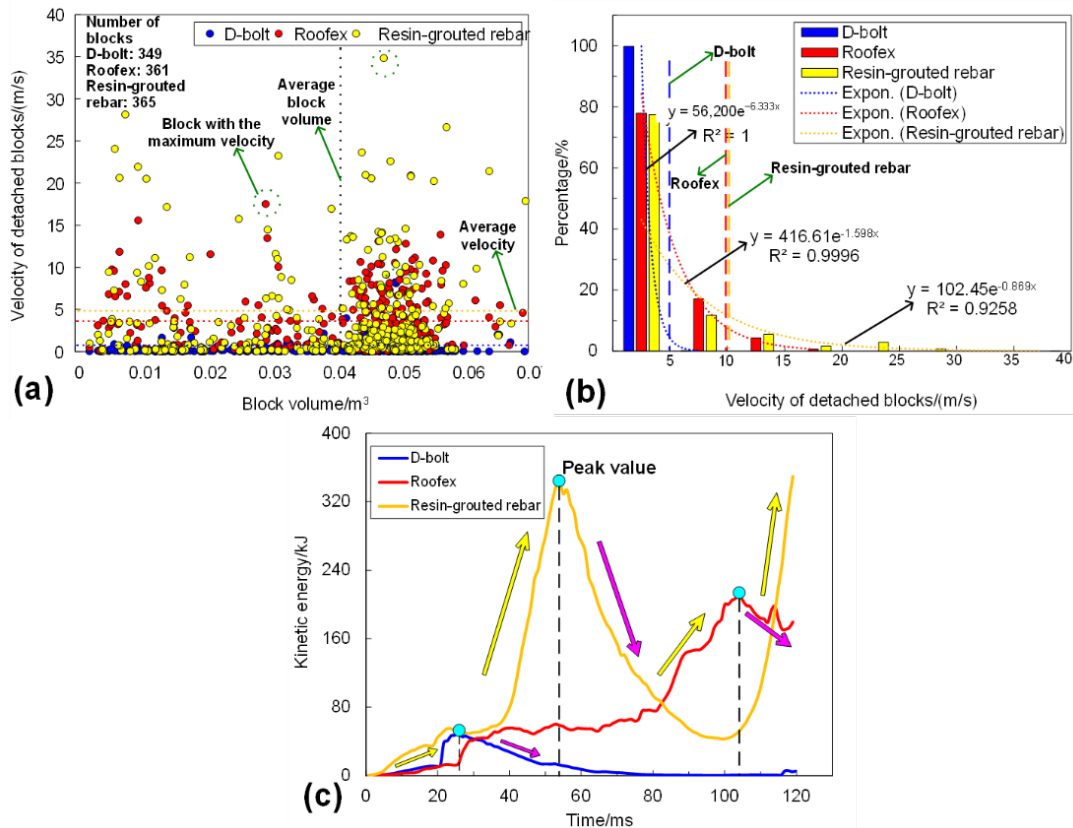


Figure 2: (a) is the velocity of all detached blocks versus block volume. (b) is the velocity distribution of all detached rock blocks. (c) is the evolution of the kinetic energy of ejected rock blocks.

Innovation in underground mapping – digital data collection and streamlined post-processing in industry standard software

Morgenroth, J., Yee, S., and Andrew, J.

RockMass Technologies, Inc., Toronto, Ontario, Canada

ABSTRACT

Underground mapping is typically a tedious paper-based process, which is occasionally done with the support of rugged tablets. In either case, geotechnical data is collected manually and then transcribed to a compatible format based on the software that is being used for post-processing or visualization. These traditional data collection practices offer limited quality control, decreased accuracy, and minimal standardization across geotechnical personnel. RockMass Technologies has developed a commercialized product, the Mapper, that uses the 3-Dimensional Axis Mapping (3DAM) method to digitally collect the orientation of geotechnical features. The RockMass Mapper is a mobile hand-held mapping unit that houses an infrared LiDAR sensor and an inertial measurement unit (IMU) comprised of a gyroscope, magnetometer, and accelerometer. These components allow the LiDAR point cloud to be oriented relative to magnetic north; subsequently software on the RockMass Mapper allows the geological structures measured to be georeferenced relative to the existing survey in the excavation.

The 3DAM method was originally developed by researchers at Queen's University, Canada in 2016 (Gallant, 2016; Gallant & Marshall, 2016a, 2016b). The 3DAM approach uses LiDAR point cloud data to generate axis maps (AM), which represent the orientations of planar surfaces in an environment by parameterizing the normal vectors to each of the surfaces into axes. In the context of rock engineering, the axes represent the normal vectors to the exposed rock surfaces. The axes are grouped into statistically significant clusters, and an orientation is calculated for each cluster. These orientations represent the orientations of the major discontinuities within the point cloud. A summary of the 3DAM method is illustrated in Figure 1.

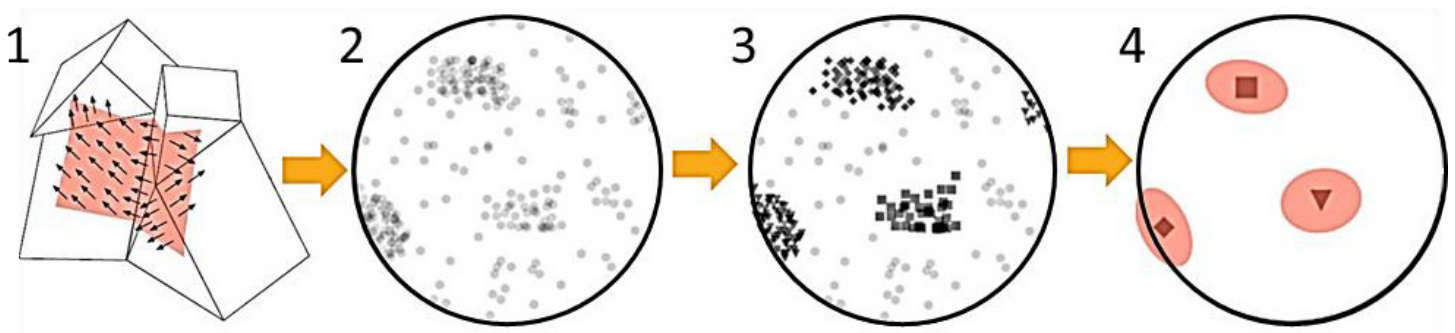


Figure 1: An illustration of the 3DAM method in terms of normal vectors and the resulting stereonets throughout the clustering analysis. (adapted from Gallant & Marshall, 2016a).

The output of the Mapper consists of a LiDAR point cloud, high-definition images of areas scanned, stereonet containing all the clusters from the scanned rock surfaces, tabulated data collected by the user for each discontinuity scanned, and a georeferenced Drawing Exchange Format (.dxf) file of the structures measured. These digital data

formats can be used in a variety of geomechanical post-processing applications, such as Cloud Compare (Figure 2), Rocscience DIPS and Unwedge (Figure 3), Deswik.CAD (Figure 4), and Seequent Leapfrog (Figure 5).

The application of digital mapping technologies is becoming increasingly common as the rock mechanics community seeks to collect more data quickly and accurately. The next hurdle now becomes how to efficiently integrate the digitalized data into existing geomechanical design practices, to lower the barrier to entry for practitioners. The nature of the 3DAM method and the software developed for the RockMass Mapper aim to overcome those post-processing challenges.

REFERENCES

- Gallant, M. J. (2016). Axis Mapping: The Estimation of Surface Orientations and its Applications in Vehicle Localization and Structural Geology (Issue September). <https://qspace.library.queensu.ca/jspui/handle/1974/15025>
- Gallant, M. J., & Marshall, J. A. (2016a). Automated rapid mapping of joint orientations with mobile LiDAR. *Int J of Rock Mech & Min Sci*, 90, 1–14. <https://doi.org/10.1016/j.ijrmms.2016.09.014>
- Gallant, M. J., & Marshall, J. A. (2016b). Automated three-dimensional axis mapping with a mobile platform. *Proceedings - IEEE International Conference on Robotics and Automation*, June 2016, 1049–1054. <https://doi.org/10.1109/ICRA.2016.7487236>

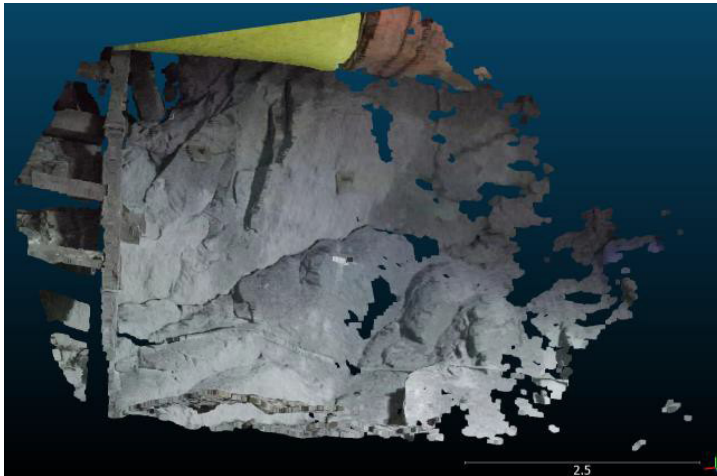


Figure 2: LiDAR point cloud imported into Cloud Compare.

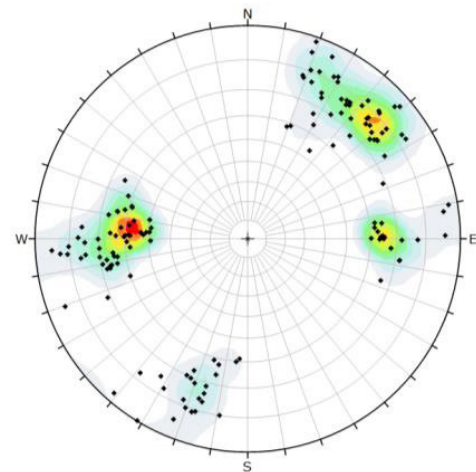


Figure 3: Structural measurements imported into Rocscience DIPS.

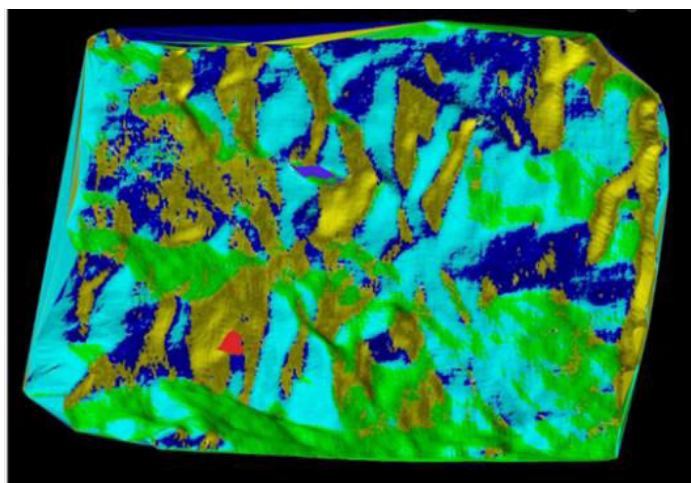


Figure 4: LiDAR point cloud imported into Deswik.CAD.

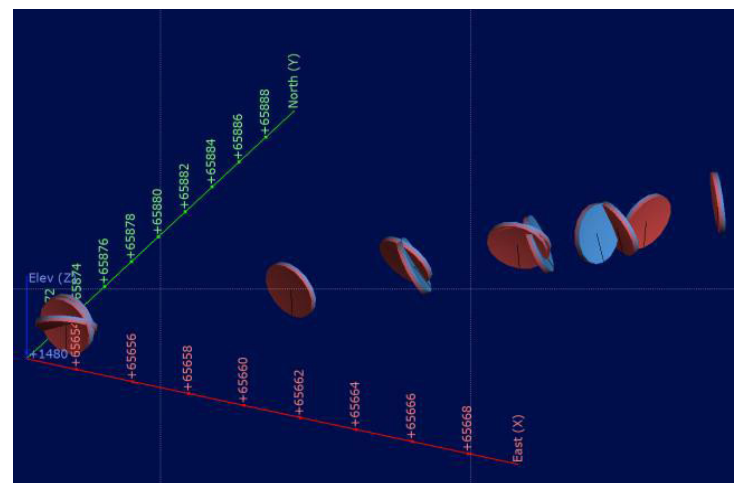


Figure 5: Structural discs generated from orientations measured imported into Seequent Leapfrog.

Forecasting of seismic hazard based on numerical modelling of future mining

Rebuli, D.B.

Institute of Mine Seismology, Canada

ABSTRACT

Static stress models are regularly used to understand the perturbations to the in situ stress field caused by mining. In underground hard rock environments, these stress perturbations may result in seismicity. Extending techniques proposed by Salamon and Linkov, it is possible to generate a synthetic catalogue of seismicity from a static stress model. This catalogue consists of locations and sizes (potency) of seismic events for a given mining geometry. A size distribution of seismic events comes naturally from this catalogue, from which seismic hazard can be estimated. Some uncertainty may exist, for example from incomplete knowledge of future seismically active geological structures, but comparing the synthetic seismic catalogues for different mining sequences yields valuable information. With the use of an appropriate ground motion prediction equation, the probability of exceeding a given ground motion at specified locations can be determined. This ground motion hazard can be translated into the probability of shakedown damage for a given ground support design.

Assessing the extent of blast-induced damage in an open pit bench blast using Discrete Fracture Network (DFN) and combined finite/discrete element methods (FDEM)

Karimi, O.¹, Fillion, M.H.¹, and Dirige, P.²

¹*Bharti School of Engineering, Laurentian University, Sudbury, Ontario, Canada*

²*Ground Control, Workplace Safety North, Ontario, Canada*

ABSTRACT

The most common and cost-effective method used for rock breakage in mining is drilling and blasting. In open pit mining, blast-induced damage can reduce the level of stability of the pit slopes, which is a safety concern. Wall damage is the extra cracking beyond the intended area of fragmentation, and this could lead to slope failures, damage to equipment, loss of production and staff injuries (Silva et al., 2019). A sufficient knowledge of the rock properties and in situ discontinuities is necessary to develop an optimal blast design. Blasting engineers often rely on empirical criteria and rule-of-thumb for the most part of their design (Dyno Nobel, 2020; International Society of Explosives Engineers, 2011), which involves a degree of uncertainty. Often, multiple iterations of blast design are required to reach optimal blast results (e.g., adequate fragmentation and rock movement, minimized wall damage, low vibration levels and minimal fly rocks). This practice is costly and time consuming for the mining operation. Therefore, the use of quantified methods for assessing the extent of the rock damage by blasting enable the engineers to optimize the design for safer excavations.

Rock fragmentation by blasting involves the wave propagation, principles of fracture mechanics, large displacement of materials, and interactions among these processes (Mitelman & Elmo, 2014; Rogers et al., 2015). Rock fracturing is the result of the coalescence of existing and developed fractures in the rock mass, and the presence of in situ joints can have a significant impact on the extent of blast-induced damage. Hence, the numerical analysis of blast-induced damage requires a realistic simulation of the rock fracturing and rock fragmentation processes, governed by the in situ rock and joint properties.

Discrete Fracture Networks (DFN) are representations of joint systems and can estimate the distribution of in situ fractures within a rock mass. A DFN-based analysis relies on quantifiable joints properties and provides realistic fracture networks with the key advantage of preserving the real joint properties during the modelling process. Additionally, the DFN approach can capture discrete fracture characteristics at the local scale more accurately in comparison to large-scale continuum methods (Elmo et al., 2014; Rogers et al., 2009), which is appropriate at the scale of production blasts. Since the blasting process starts from a static phase to a large displacement phase, modeling should include both continuum and discontinuum models for better representation of the blasting process (Han et al., 2020). The combined finite-discrete element modeling (FDEM) provides the necessary analysis tool for simulating the blasting process (An et al., 2017). Finite element method (FEM) is used for calculating stress distributions and displacements in rock before fracturation (static phase) and, once the fracture process begins, discrete element method (DEM) is used for the fractured medium (large displacement phase) (Zhang, 2016).

The principal objective of this research is to use a quantified approach to determine how the in situ joints controls the post-blast fracturing and the associated wall damage. A DFN model is used as an input for a numerical bench blasting simulation performed with the combined FDEM method. Bench blasts are simulated in the 2D environment, including a production blasthole, using the FDEM software Irazu 2D (Geomechanica, 2019). The DFN software FracMan (Golder Associates, 2020) is used to generate the stochastic fractures based on the fracture intensity P32 defined as total fracture area per unit of volume (Elmo et al., 2014).

Two main scenarios were considered for numerical simulations: 1. Bench blast without DFN; and 2. Bench blast with in situ joint systems (DFN). The rock properties and blast design parameters are obtained from an open pit mine operated by Iamgold. The comparison of the two scenarios, in terms of post-blast fracture intensity, quantified the influence of the in situ fracture systems on blast-induced damage assessment. The damage quantification approach used is based on Lupogo et al. (2014) method to characterize the damage area and intensity (D21) related to the yielded elements in the 2D numerical model. This methodology allows for quantifying the effect of in situ joints on rock fracturing and wall damage. The results show that a more realistic blasting simulation and wall damage assessment is obtained when DFNs are included in the modelling process, because of the possibility to consider fracture growth direction and intensity. A better characterization of the blast damage zone can lead to improved slope stability analyses.

REFERENCES

- An, H., Liu, H., Han, H., Zheng, X., & Wang, X. (2017). Hybrid finite-discrete element modelling of dynamic fracture and resultant fragment casting and muck-piling by rock blast. *Computers and Geotechnics*, 81, 322–345. <https://doi.org/10.1016/j.compgeo.2016.09.007>
- Dyno Nobel. (2020). Explosives Engineers' Guide. Dyno Nobel Asia Pacific Pty Limited. <https://www.dynonobel.com/apac/~media/Files/Dyno/ResourceHub/Brochures/APAC/Explosives%20Engineers%20Guide.pdf>
- Elmo, D., Liu, Y., & Rogers, S. (2014). Principles of discrete fracture network modelling for geotechnical applications. In: *Proceedings of the First International DFNE Conference*, 19-23 October. Vancouver, British Columbia, Canada. 8 p.
- Geomechanica, Inc. (2019). Irazu 2D Geomechanical Simulation Software (Computer Software). Theory Manual. Geomechanica Inc., Toronto, ON, Canada. 67 p.
- Golder Associates. (2020). FracMan: DFN software suite [Computer software]. Golder Associates, Toronto, ON, Canada. Retrieved from <http://www.golder.com/fracman/>.
- Han, H., Fukuda, D., Liu, H., Salmi, E., Sellers, E., Liu, T., & Chan, A. (2020). Combined finite-discrete element modelling of rock fracture and fragmentation induced by contour blasting during tunnelling with high horizontal in-situ stress. *Int. Journal of Rock Mechanics and Mining Sciences*, 127, 104214. <https://doi.org/10.1016/j.ijrmms.2020.104214>
- International Society of Explosives Engineers. (2011). *ISEE blasters' handbook*. (18th ed.). Cleveland, Ohio: International Society of Explosives Engineers.
- Lupogo, K., Tuckey, Z., Stead, D., & Elmo, D. (2014). Blast damage in rock slopes: potential applications of discrete fracture network engineering. In *Proc. 1st Int. Discrete Fracture Network Engineering Conf.*, Vancouver, Canada. p (Vol. 14).
- Mitelman, A., & Elmo, D. (2014). Modelling of blast-induced damage in tunnels using a hybrid finite-discrete numerical approach. *J. Rock Mechanics and Geotechnical Engineering*, 6(6), 565–573. <https://doi.org/10.1016/j.jrmge.2014.09.002>
- Rogers, S., Elmo, D., Beddoes, R., & Dershowitz, W. (2009). Mine scale DFN modelling and rapid upscaling in geomechanical simulations of large open pits. In: *Proceedings of the International Symposium on 'Rock Slope Stability in Open Pit Mining and Civil Engineering'*, November 2009, Santiago, Chile: 11 p.
- Rogers, S., Elmo, D., Webb, G., & Catalan, A. (2015). Volumetric Fracture Intensity Measurement for Improved Rock Mass Characterisation and Fragmentation Assessment in Block Caving Operations. *Rock Mechanics and Rock Engineering*, 48(2), 633–649. <https://doi.org/10.1007/s00603-014-0592-y>
- Silva, J., Worsey, T., & Lusk, B. (2019). Practical assessment of rock damage due to blasting. *International Journal of Mining Science and Technology*, 29(3), 379–385. <https://doi.org/10.1016/j.ijmst.2018.11.003>
- Zhang, Z.-X. (2016). *Rock fracture and blasting: Theory and applications*. Elsevier Inc., Cambridge, MA, USA.

Investigating the effect of bedding plane orientation on the mechanical and elastic behaviour of shale rock

Rizehbandi, A., Popoola, A., Seyed Ghafouri, S.M.S., and Grasselli, G.

Department of Civil and Mineral Engineering, University of Toronto, Toronto, Ontario, Canada

ABSTRACT

Anisotropy resulting from the presence of bedding planes, schistosity, foliation, and cleavage, has a significant influence on the deformation and strength properties (Ramamurthy et al., 1993), elastic properties (Awang et al. 2017; Forbes et al. 2018), and failure patterns (Nasseri et al. 1997; Chen et al. 2021) of rocks. Shale is a typical example of an anisotropic rock that constitutes both the source and reservoir rock in unconventional plays (Wang et al., 2018). The laminated and bedded structure in shale results from sedimentation and further hardening of detritus material during its formation (Wenk, 2008). The bedding plane orientation in shale affects the failure behaviour of the rock; specifically, it influences how cracks initiate and propagate (Li et al., 2020). In laboratory testing, bedding plane orientation is generally defined as the angle between the direction of depositional layering and the loading direction during axial compression tests. Chen et al. (2021) stated that as bedding plane orientation increases from 00 to 900, the proportion of shear mode cracks decreases while tensile mode cracks increase. Contrarily, crack density and slip potential did not follow a monotonous trend with bedding plane orientation.

Apart from the transition in failure mechanism, shale's mechanical and elastic behaviour varies depending on the bedding plane orientation along which it is tested. Results from uniaxial compressive strength (UCS) tests from previous studies conducted on shale samples showed a consistent decreasing and then increasing UCS values as bedding plane orientation increases from 00 to 900. These trends were classified into the V shape curve (Zhai et al. 2022), W shape (Zhang, 2021), and the U shape curve (Ramamurthy et al., 1993). However, different results for the effect of bedding plane orientation on the elastic modulus and Poisson's ratio of different types of shale are suggested in literature. For instance, Chandler et al. (2016), Forbes et al. (2018), and Zhong et al. (2015) found that the elastic modulus and P-wave velocity exhibited a continuous decreasing trend when bedding plane orientation changed from 00 to 900, but no apparent relation between Poisson's ratio and bedding orientation. However, Zhang (2021) stated that the elastic modulus and Poisson's ratio showed a V shape curve as bedding plane orientation increases from 00 to 900. Therefore, there is a need to investigate these relationships further.

In this study, we evaluate the effect of bedding plane orientation on the mechanical and elastic properties of shale samples obtained from an outcrop equivalent of the Montney Formation; a famous shale gas plays in Western Canada, under unconfined compressive loading. Four bedding plane orientations, namely, 0°, 30°, 60°, and 90°, are selected for testing. Ultrasonic P-wave and S-wave velocity measurements will be conducted on the samples, followed by UCS testing. The results from this testing campaign will enable us to further understand the dependence of these velocities and UCS on bedding plane orientation. Additionally, there are some empirical relationships developed for different types of shale which investigate the correlation between these velocities and UCS results. Our intention is to assess the validity of these empirical relationships for Montney shale which allows rapid estimation of the strength properties of shale and its directional dependence on bedding orientation.

REFERENCES

- Awang, H., Rashidi, N. A., Yusof, M., & Mohammad, K. (2017). Correlation between P-wave velocity and strength index for shale to predict uniaxial compressive strength value. In *MATEC Web of Conferences* (Vol. 103, p. 07017). EDP Sciences.
- Chandler, M. R., Meredith, P. G., Brantut, N., & Crawford, B. R. (2016). Fracture toughness anisotropy in shale. *Journal of Geophysical Research: Solid Earth*, 121(3), 1706-1729.
- Chen, H., Di, Q., Zhang, W., Li, Y., & Niu, J. (2021). Effects of bedding orientation on the failure pattern and acoustic emission activity of shale under uniaxial compression. *Geomechanics and Geophysics for Geo-Energy and Geo-Resources*, 7(1), 1-17.
- Forbes Inskip, N. D., Meredith, P. G., Chandler, M. R., & Gudmundsson, A. (2018). Fracture properties of Nash Point shale as a function of orientation to bedding. *Journal of Geophysical Research: Solid Earth*, 123(10), 8428-8444.
- Li, Z. Q., Li, X. L., Yu, J. B., Cao, W. D., Liu, Z. F., Wang, M., ... & Wang, X. H. (2020). Influence of existing natural fractures and beddings on the formation of fracture network during hydraulic fracturing based on the extended finite element method. *Geomechanics and Geophysics for Geo-Energy and Geo-Resources*, 6(4), 1-13.
- Nasseri, M. H. B., Rao, K. S., & Ramamurthy, T. (2003). Anisotropic strength and deformational behavior of Himalayan schists. *International Journal of Rock Mechanics and Mining Sciences*, 40(1), 3-23.
- Nasseri, M. H., Rao, K. S., & Ramamurthy, T. (1997). Failure mechanism in schistose rocks. *International Journal of Rock Mechanics and Mining Sciences*, 34(3-4), 219-e1.
- Ramamurthy, T., Rao, G. V., & Singh, J. (1993). Engineering behaviour of phyllites. *Engineering Geology*, 33(3), 209-225.
- Wang, Y., Li, C. H., & Hu, Y. Z. (2018). Experimental investigation on the fracture behaviour of black shale by acoustic emission monitoring and CT image analysis during uniaxial compression. *Geophysical Journal International*, 213(1), 660-675.
- Wenk, H. R., Voltolini, M., Mazurek, M., Van Loon, L. R., & Vinsot, A. (2008). Preferred orientations and anisotropy in shales: Callovo-Oxfordian shale (France) and Opalinus Clay (Switzerland). *Clays and clay minerals*, 56(3), 285-306.
- Zhai, M., Xue, L., Bu, F., Yang, B., Huang, X., Liang, N., & Ding, H. (2022). Effects of bedding planes on progressive failure of shales under uniaxial compression: Insights from acoustic emission characteristics. *Theoretical and Applied Fracture Mechanics*, 119, 103343.
- Zhang, S. (2021). Study on the bedding angle on the mechanical properties of shale. *AIP Advances*, 11(11), 115305.
- Zhong, J., Shengxin, L. I. U., Yinsheng, M. A., Chengming, Y., Chenglin, L., Zongxing, L. I., ... & Yong, L. I. (2015). Macro-fracture mode and micro-fracture mechanism of shale. *Petroleum Exploration and Development*, 42(2), 269-276.

Implementation of Epiroc Cabletec in permafrost condition

Hammoum, S.

Raglan Mine, Rouyn-Noranda, Québec, Canada

ABSTRACT

The Raglan mine is situated in the northern tip of Québec province over the 61st parallel north. The mining complex is composed of 4 actives underground mines that produce Nickel ore. The mining method is a mix of cut and fill and longhole stoping. The Raglan particularity regarding ground support quality control is the permafrost condition of the rock mass. In addition, the mine isn't heated, and the underground drift temperature can go as low -30°C in wintertime. This condition has a direct impact on the grout component of the cablebolting. This poster will cover the implementation of the Epiroc Cabletec. The Cabletec is a fully mechanized drill rig that combines the drilling, installation, and cementation of the cable for UP & DOWN hole. The designed grout mixture necessitates to hold on a vertical hole and strengthen over time in permafrost ground condition.

MATERIALS & METHODS

In situ rock mass temperature is measured by a combination of surface and underground thermistors installed in diamond drill holes. The drift temperature was measured by regular Hobos.

Pull out tests were done on single 7 strands cables with different W:C ratio and added SikaSet RHE accelerator with different proportion as shown on the left picture of Figure 1.

In addition to the pull-out tests, correspondent end-beam compressive tests were done on grout cured at the ambient drift temperature as shown on the right picture of Figure 1.

RESULTS

Figure 2 display the in situ rock mass temperature that is heavily influenced by surface lake in the first 100 m of the permafrost. The trend near surface temperature is -6°C and gain 1°C for each 100 m of depth of Qakimajurq/MP8H (yellow and green dots) mines where a significant part of the mining is done.

The initial grouting test was done with Sika's product for cold weather called Nordic Cabletm. This solution was unsuccessful regarding the cycle time of the Cabletec. The Nordic Cabletm initial set time was too quick in the mixing tube and the grout couldn't be pumped after less than 20 minutes. This issue is largely due that Nordic Cabletm is designed to work between -5 to 5°C and the mixing tube temperature average 15°C while the Cabletec is in operation. Retarding admixture was also added to the mix without success.

The subsequent and successful solution was the use of a general use Portland cement and added accelerant admixture. The SikaSet RHE accelerant performs well in laboratory testing by Sika and field tests were implemented to determine the acceptable range of admixture and Water: Cement proportion. The test's outcome converges toward a W:C ratio of $0.345 \pm$ and 15% (weighted proportion to water) accelerant dosage. This proportion confers the cable grout at least 45 minutes pumpability time window to successfully go through the Cabletec cycle time.

Short embedment (18 to 36") tests were done on single 7 strands steel cables with no bulge grouted with GU Portland cement with SikaSet RHE proportion ranging from 13 to 18%. The mine drift curing temperature was 5°C for the initial test. The equivalent average linear outcome was 128 kN/m after 24 h and 238 kN/m for 72 h (steel cable failure and not the grout). A second set of tests combines with end-beam test on rectangular prism samples was done in winter with a -5°C average drift temperature. As anticipated, the drift temperature had an impact on the grout early-age strength. The 48 and 120 h results were averaging 45.1 kN/m and 150 kN/m respectively. Therefore, the end-beam compressive strength averages a strength 10.0 MPa and 31.5 MPa for a curing time of 24 and 120 h, respectively. Those results build confidence in the use of the end-beam tester for subsequent quality control on cable grout with SikaSet RHE admixture.



Figure 1: Setup for pull out tests on single 7 strands steel cables (5/8") and end-beam tester on 3"x3" grout samples.

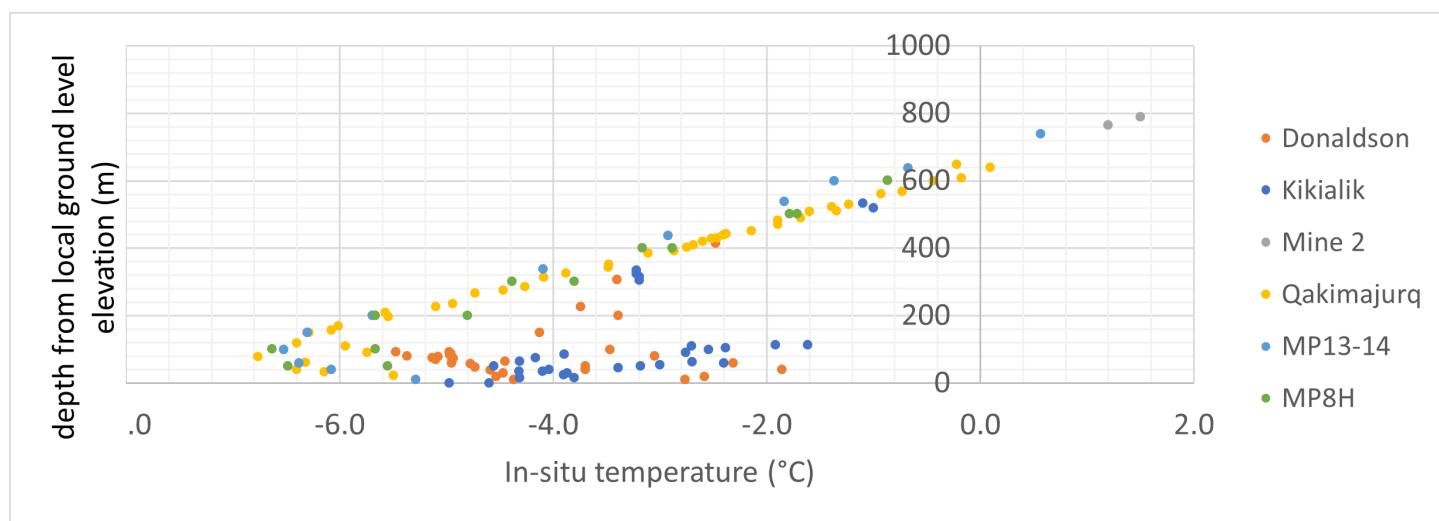


Figure 2: In situ rock mass temperature in regard to depth.

Empirical stability analysis of stopes using MineRoc software® considering the three-dimensional stress condition, Alamos Gold Mine

Vallejos, J.¹, Espinoza, G.¹, Cepeda, E.¹, Espinoza, J.¹, Barberán, A.¹, Xu, Y.H.², Boame, M.², and Blake, T.²

¹*Advanced Mining Technology Center (AMTC), Universidad of Chile, Chile*

²*Alamos GOLD Inc., Young Davidson mine, Ontario, Canada*

ABSTRACT

Sublevel Stopping is an underground exploitation method widely used by the mining industry in Canada, Chile, and around the world. An important aspect of the method is to define the size of the exploitation units in order to maintain control of the recovery and operational dilution, maintaining the stability of the stopes. For this, various methodologies are available in the literature that allow to estimate the stability of the stope walls. Among them, the Mathews empirical method is widely used in the mining industry. In this context, the software MineRoc® has been developed to standardize the generation of databases from the back-analysis of over-break.

This study uses MineRoc® for the development of site-specific over-break curves based on the back-analysis of primary stopes from Alamos Gold Mine, Ontario, Canada. A standardized database of 71 stopes that includes design and CMS geometry, geological and geotechnical information, and stress condition from numerical modeling, is developed. The effect of the three-dimensional stress condition on the empirical stability method is investigated.

The pulverization mechanism of host rocks induced in faulting: Insights from grain-scale fracturing by OpenFDEM

Li, X.¹, Zhao, Q.², and Grasselli, G.¹

¹*Department of Civil and Mineral Engineering, University of Toronto, Toronto, Ontario, Canada*

²*Department of Civil and Env. Eng., The Hong Kong Polytechnic Univ., Hong Kong, China*

ABSTRACT

Rocks in nature contain a large number of defects and exhibit strong heterogeneity at different scales. This study presents a novel multiscale continuum-discontinuum method, implemented in the OpenFDEM software, to investigate the dynamic behaviors and microfracturing in rocks. The open-source package, OpenFDEM, offers a novel and reliable multiscale continuum-discontinuum modelling approach with rigorous microstructural characterizations, and provide insights to understand the role of grain-scale fracturing and micro heterogeneity on the rate-dependency and pulverization.

In this work, using the Grain Base Model (GBM) module in OpenFDEM, the heterogeneity in mineral components is realistically reproduced using the thin section images of rock samples as an input. The rupture strength, temporal deformation fields and failure patterns are compared to experimental results to verify the reasonability and accuracy of the proposed method. The energy items conversion considering residual kinetic energy, the underlying mechanism of grain-scale fracturing leading to fractal fracture surfaces, pervasively grain pulverization and deflection/penetration cracking model are quantitatively discussed. These approaches are further extended to field-scale slips considering the existence of multiscale heterogeneities to capture the faulting mechanism of supershear earthquakes.

REFERENCES

- Rempe M, Mitchell T, Renner J, et al. 2013. Damage and seismic velocity structure of pulverized rocks near the San Andreas Fault. *J Geophys Res Solid Earth* 118:2813–2831.
- Okubo K, Bhat HS, Rougier E, et al. 2019. Dynamics, radiation and overall energy budget of earthquake rupture with coseismic off-fault damage. *J Geophys Res Solid Earth* 1–30.
- Li X F, Li H B, Zhao J. 2021. Transgranular fracturing of crystalline rocks and its influence on rock strengths: Insights from a grain-scale continuum–discontinuum approach[J]. *Computer Methods in Applied Mechanics and Engineering*, 373: 113462.
- Mahabadi O K, Randall N X, Zong Z, et al. 2012. A novel approach for micro-scale characterization and modeling of geomaterials incorporating actual material heterogeneity[J]. *Geophysical Research Letters*, 39(1).

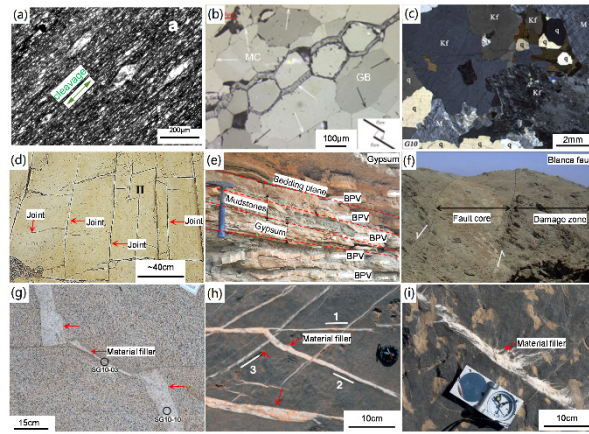


Figure 1: Discontinuities with different scales in rock materials.

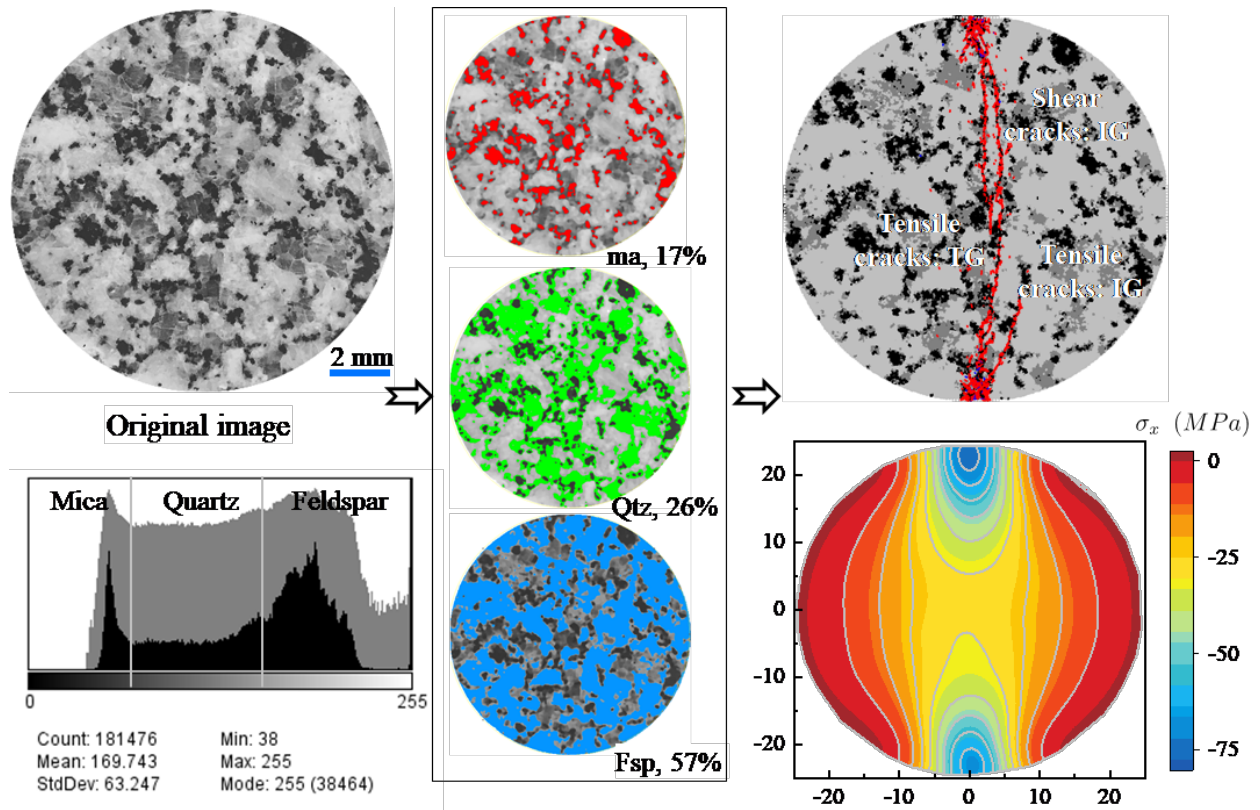


Figure 2: Multiscale framework for realistic 2D fracturing considering the action of micro heterogeneity from theory to numerical models in OpenFDEM.

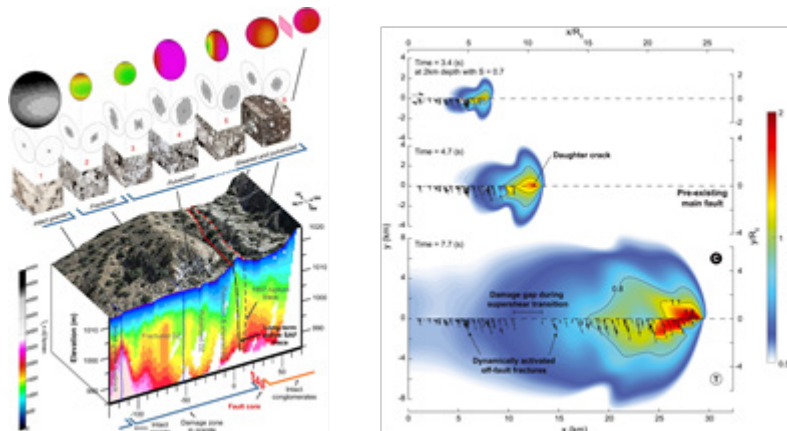


Figure 3: Evidence showing the role of heterogeneity on the grain pulverization in supershear earthquakes (Rempe et al. 2013; Okubo et al. 2019).

Improving confidence in caving-induced subsidence forecasting through surface monitoring validation

Lalang, M.¹, Eberhardt, E.¹, Campbell, R.², and Taylor, K.³

¹*Geological Engineering/EOAS, The University of British Columbia, Vancouver, British Columbia, Canada*

²*Freeport-McMoRan Inc., USA*

³*PT Freeport Indonesia, Indonesia*

ABSTRACT

Subsidence represents a major hazard to block and panel caving operations that persist until the end of the mine's life. This ever-present hazard has attracted much research to investigate its development and the ground response relative to cave propagation and the surrounding geology. Early studies largely focused on surface observations (e.g., ground cracking, breakthrough, collapse) to understand subsidence phenomena. This has since shifted towards the increasing use of advanced numerical modelling to develop a more robust approach with the ability to investigate complex interactions at depth between the cave, geology, and surface topography.

Numerical modelling also provides a means to forecast the future expression of caving-induced subsidence as a function of the mine plan and mine life, which may include multiple expansions (e.g., multiple lifts, panels, etc.). The challenge is that many of the factors that can influence subsidence events vary spatially, change over time, or are unknown as to whether they are present or not. The result is that the extent, asymmetry, and severity of the subsidence hazard as it develops may differ significantly from the modelling forecasts. Therefore, wherever possible, confidence must be improved by validating and updating subsidence forecasts, while accessing and developing available heuristics from monitoring data.

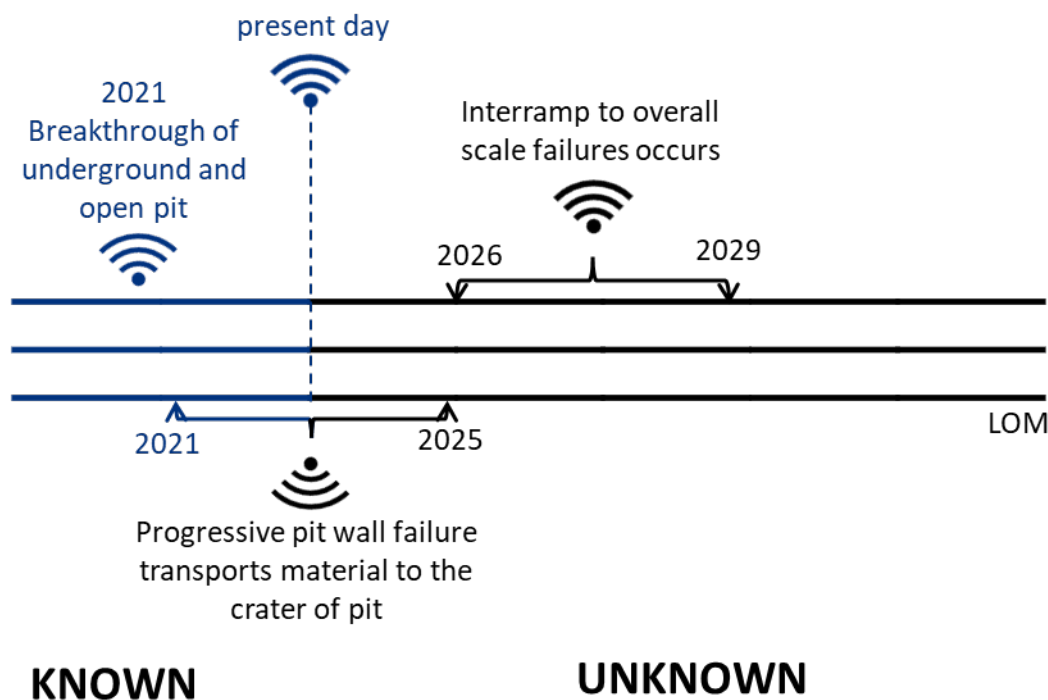
The Grasberg Block Cave (GBC) mine represents a transition to underground to target deeper resources after the overlying open pit reached the end of its mine life. Production in the GBC began in early 2019 and is expected to have a 22-year mine life. Over this time, production is expected to reach 130,000 tpd (in 2023) and mine a total of five production blocks covering a footprint area of 335,000 m². The resulting surface subsidence and cave-pit interactions will eventually impact critical infrastructure on surface with questions of “when” and “how” relying on numerical model forecasts (e.g., see inset figure). For this, the mine has deployed a vast array of monitoring instruments to measure subsidence and confirm/check against numerical model forecasts.

This poster reviews the monitoring technologies being employed at the GBC, which include several newer innovations in surface and subsurface monitoring. The related research highlights the utilization of satellite InSAR to monitor surface subsidence over large areas within and outside the pit area, whereas the use of smart markers provide a unique subsurface dataset showing the progression of caving. These offer a new paradigm of mechanistic understanding of the ground response and interactions to caving as the cave progresses, including early detection and movement pattern confirmation related to the timing and spatial extent of the subsidence. Comparisons between the collected monitoring data and numerical model forecasts are made for cross-validation to establish a variance between the two products to improve the forecasting review and interpretation cycle. Overall, the validated knowledge will be beneficial in scrutinizing dedicated areas of interest (e.g., critical surface facilities for the mine).

By corroborating, and in future improving, numerical modelling forecasts, the collective and added mechanistic knowledge gained through this research will help to bridge the gap between the value, confidence and reliability in the subsidence data products produced. This will in turn aid decision makers in their management of caving-induced subsidence hazards.

REFERENCES

- Donati, D., Rabus, B., Engelbrecht, J., Stead, D., Clague, J. & Francioni, M. (2021). A robust SAR speckle tracking workflow for measuring and interpreting the 3D surface displacement of landslides. *Remote Sensing*, 13(15): 1–20. <https://doi.org/10.3390/rs13153048>
- Eberhardt, E. EOSC 536: Advanced Rock Engineering – Observational Method. 14 Oct. 2021, University of British Columbia, Vancouver. Class lecture.
- Rabus, B., Eberhardt, E., Stead, D., Ghuman, P., Nadeau, C., Woo, K., Severin, J., Styles, T. & Gao, F. (2009). Application of InSAR to constrain 3-D numerical modelling of complex discontinuous pit slope deformations. In *Slope Stability 2009: Proceedings of the International Symposium on Rock Slope Stability in Open Pit Mining and Civil Engineering*, Santiago.
- Woo, K.S., Eberhardt, E., Elmo, D. & Stead, D., (2013). Empirical investigation and characterization of surface subsidence related to block cave mining. *International Journal of Rock Mechanics and Mining Sciences*, 61: 31–42. <http://dx.doi.org/10.1016/j.ijrmms.2013.01.015>.
- Woo, K-S., Eberhardt, E., Rabus, B., Stead, D. & Vyazmensky, A. (2012). Integration of field characterization, mine production and InSAR monitoring data to constrain and calibrate 3-D numerical modelling of block caving-induced subsidence. *International Journal of Rock Mechanics and Mining Sciences*: 53: 166–178. <https://doi.org/10.1016/j.ijrmms.2012.05.008>



Study of bulking displacement and depth of stress fracturing for deformation-based ground support design calibration

Primadiansyah, A.A.¹, Eberhardt, E.¹, Silaen, H.², and Campbell, R.³

¹*Geological Engineering/EOAS, The University of British Columbia, Vancouver, British Columbia, Canada*

²*Freeport-McMoRan Inc., USA*

³*PT Freeport Indonesia, Indonesia*

ABSTRACT

Experiences from historical and existing deep caving operations suggest that brittle failure around underground excavations (e.g., spalling or strainbursting, leading to excessive bulking; Figure 1) has been a key challenge, posing a safety hazard for workers and causing costly interruptions to production. Consequently, effective and efficient ground control strategies need to be adopted to manage these challenging conditions (Kaiser & Moss, 2022).

A transition from conventional energy-based support design approaches (Hedley, 1992; Ortlepp, 1992; Kaiser et al., 1996) to deformation-based support design (DBSD) for brittle ground (Kaiser, 2014; Kaiser & Moss, 2022) has been implemented as a strategic element of ground control for the Deep Mill Level Zone (DMLZ) mine to improve excavation performance. The DBSD approach accounts for support capacity at the critical stage of its utility (remnant support capacity) rather than at the time of support installation and therefore allows for the service of life of the support system to be estimated as displacements induced by stress fracturing after support installation consume the support's capacity. This type of design aspect is not considered in energy-based support design.

To increase the effectiveness and reliability of the DBSD approach, an improved understanding of how the depth of stress fracturing and rock mass bulking progress as the cave abutments and stress path evolve is critical. This poster presents a methodology to calibrate and validate the DBSD parameters through dedicated monitoring stations employed across a production level footprint (Figure 2). Each monitoring station integrates borehole camera (BHC) surveys and multipoint borehole extensometers (MPBX) to determine the depth of stress-induced brittle fracture damage, and convergence measurements and light detection and ranging (LiDAR) surveys to characterize the corresponding rock mass bulking.

REFERENCES

- Hedley, D. G. F. (1992). Rockburst Handbook for Ontario Hardrock Mines. CANMET Special Report SP92-1E.
- Kaiser, P. K. (2014). Deformation-based support selection for tunnels in strainburst-prone ground. Proceedings of the Seventh International Conference on Deep and High Stress Mining, January 2014, 227–240. https://doi.org/10.36487/acg_rep/1410_13_kaiser
- Kaiser, P. K., McCreath, D. R., & Tannant, D. D. (1996). Canadian Rockburst Support Handbook: Prep. for Sponsors of the Canadian Rockburst Research Program 1990-1995. Sudbury, Ontario: Geomechanics Research Centre.
- Kaiser, P. K., & Moss, A. (2022). Deformation-based support design for highly stressed ground with a focus on rockburst

Ortlepp, W.D. (1992). The design of support for the containment of rockburst damage in tunnels – An engineering approach. Support in Mining and Underground Construction, Kaiser & McCreath (eds). Balkema Rotterdam

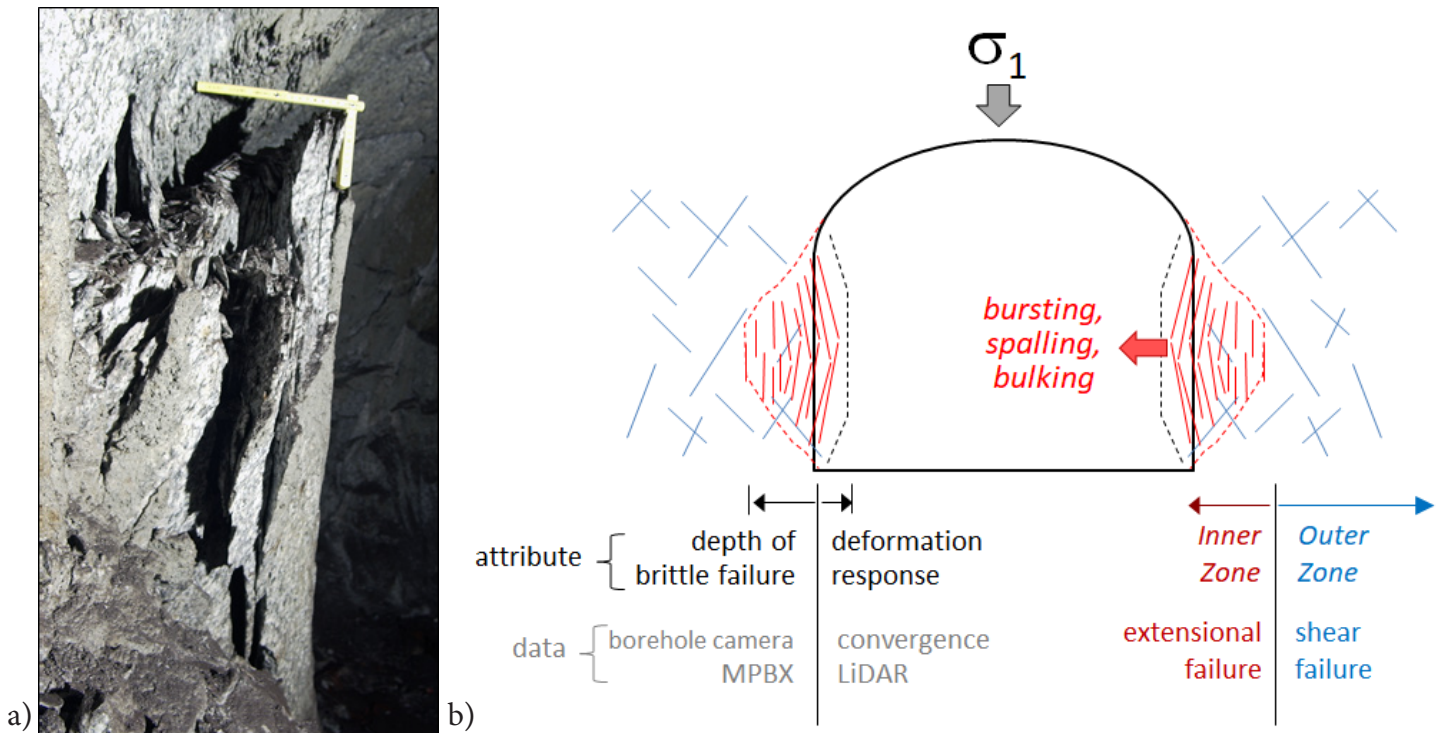


Figure 1: a) Example of rock mass bulking due to stress fracturing. b) Integrated monitoring methodology to measure both depth of stress fracturing and the corresponding rock mass bulking.

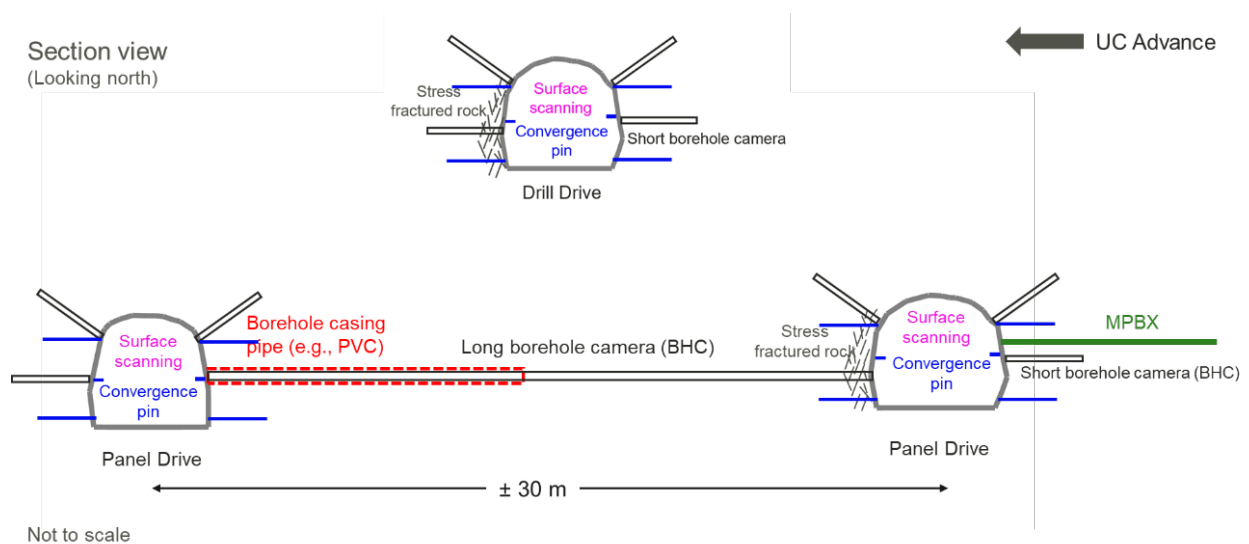


Figure 2: Dedicated integrated monitoring stations for calibration and validation of the DBSD approach.

High resolution imaging and characterization of laboratory fractures in layered anisotropic rocks – geometry, morphology and permeability

Li, M., Magsipoc, E., Sun, L., Peterson, K., and Grasselli, G.

Department of Civil and Mineral Engineering, University of Toronto, Toronto, Ontario, Canada

ABSTRACT

This work will introduce a recently developed laboratory approach for high-resolution 3D imaging of lab scale rock fractures. By quantifying the geometry, morphology and permeability of the fractures, we can add to our knowledge of how rock fabric and anisotropy affect failure mechanisms and how fractures of different origins contribute to fluid producibility.

The laboratory imaging approach based on serial images reconstruction allows high-resolution, high-contrast 3D imaging of fractures in rock samples ranging from centimeters to tens of centimeters in size. High-resolution serial images were successively collected using an integrated experimental set-up that consists of a surface grinder and a digital camera; the high contrast was achieved by fluorescence imaging. The collected serial high-resolution high-contrast fracture images were processed to reconstruct 3D representations of the rock sample and segmented to extract the fracture network inside. The fractures were classified into three categories: parted bedding planes, opened natural fractures, and newly created hydraulic fractures, and were further segmented into individual fracture domains using a machine learning approach. The geometries of the segmented fracture domains were assessed by quantifying fracture volume, aperture, and orientation; the morphology of individual fracture surfaces was evaluated using directional roughness (DR), which permits further characterization of fractures' slip potential. In addition, the fluid producibility of the fracture network was numerically simulated using a finite volume method.

High-resolution ($39 \times 39 \times 50 \mu\text{m}^3$) representations of an 8 cm fractured shale cube were acquired using the proposed imaging approach. The fracture map suggests that lateral growth of the fracture network is favored under the prescribed stress-state, as reflected through activated bedding planes accounting for over 60% of the fracture volume. Hydraulic fractures generated in the matrix dip at 35° – 60° to the minimum principal stress and are noticeably less in volume, which contradicts conventional wisdom of fracture mechanics; however, these fractures encouraged vertical growth of the fracture network by connecting low-angle bedding planes. The bedding planes are shown to have much smaller roughness and are less likely to slip. The fractures' slip potential under different lubrication conditions suggests that fracture orientation likely plays a greater role in the stability of fractures and the potential to generate larger activation energies.

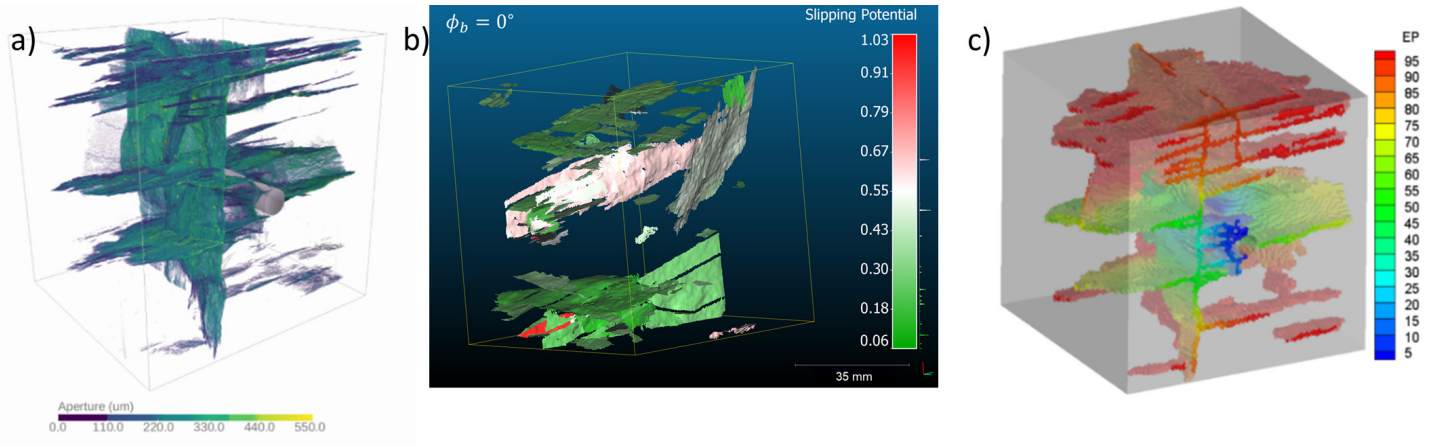


Figure 1: Feature maps of the high-resolution digital fracture network. a) mechanical aperture map, b) slip potential map (fractures not calculated are hidden), and c) fluid pressure map during production.

REFERENCES

- Tatone B. S. A., Grasselli G. 2009. A method to evaluate the three-dimensional roughness of fracture surfaces in brittle geomaterials. *Rev Sci Instrum*, 80(12), 125110.
- Cottrell B, Tatone, B. S. A., & Grasselli G. 2010. Joint replica shear testing and roughness degradation measurement. ISRM-EUROCK-2010-043.
- Li M, Magsipoc E, Abdelaziz A, Ha J, Peterson K, Grasselli G. 2021. Mapping fracture complexity of fractured shale in laboratory: three-dimensional reconstruction from serial section images. *Rock Mechanics and Rock Engineering*. 1-12.
- Li M, Magsipoc E, Abdelaziz A, Ha J, Peterson K, Grasselli G. 2022. Fracture network in laboratory hydraulic fracturing tested shale cube. *Album of Porous Media - Structure and Dynamics*.
- Magsipoc E, Li M, Abdelaziz A, Ha J, Peterson K, Grasselli G. 2020. Analysis of the fracture morphologies from a laboratory hydraulic fracture experiment on Montney shale. *ARMA/DGS/SEG International Geomechanics Symposium*.

Controlled lab-scale evaluation of the secondary permeability represented in a 3D printed discrete fracture network (DFN) model

Baidoo, M.¹, Fillion, M.-H.¹, Hutchison, A.², and González, C.³

¹*School of Engineering, Laurentian University, Sudbury, Ontario, Canada*

²*Mirarco Mining Innovation, Laurentian University, Sudbury, Ontario, Canada*

³*BBA Inc., Ontario, Canada*

ABSTRACT

The evaluation of fluid flow through fractured media is essential for many applications, e.g. oil extraction, geothermal energy extraction, nuclear waste management, mining, etc. (Öhman, 2005; Sight et al., 2014). In hard rocks, fluid flow depends on fracture aperture and connectivity, as fractures are the preferential flow paths within the rock mass (Blyth and De Freitas, 2017). The presence of fractures can increase the permeability by several orders of magnitude (Singhal and Gupta, 2010). Discrete fracture networks (DFN) are 3D representations of fracture systems based upon field observations of fractures properties and can be used to statistically represent a rock mass fracture system (Rogers et al., 2009). Many researchers have investigated fluid flow, using DFN and numerical modelling methods, with fewer lab-scale experiments. With the increasing use and advancements in 3D printing technology, it is possible to build valuable lab-scale physical models representing a fractured medium. A numerical DFN model is built using the DFN software MoFrac and the 3D printed DFN model (volume of 1881 cm³) representing a rock mass with in situ fractures (2 fracture sets) is generated with a Stratasys dimension SST 1200es 3D printer using ABS material (Figure 1). Different volumes are simulated with MoFrac to determine the Representative Elementary Volume (REV) for the 3D printed physical model. The 3D printed DFN model is installed in an experimental set-up to evaluate, with a quantitative assessment, the capability of the secondary permeability (i.e. fracture permeability) in admitting fluid flow.

The experimental set-up (Figure 2) consists of a centrifugal fan, a transition duct, an orifice plate and the 3D printed DFN model. The set-up functions as a differential pressure meter by restricting airflow through the transition duct (Morris and Langari, 2012). The main objective of the lab-scale experiment is to establish the behavior of the changing pressure to fluid flow through fractures.

The results of this study demonstrate that pressure vs. flow measurements can be obtained experimentally with a lab-scale 3D printed DFN model. Direct fluid flow measurements in fractured networks at the lab-scale are highly valuable because the results can be useful to obtain a physically quantified assessment (as opposed to numerical assessment) of the influence of the fracture properties (intensity, connectivity, aperture, persistence, roughness, etc.) on fluid flow.

This laboratory experiment is part of the scope of work of an ongoing collaborative research project (Mirarco, Laurentian University, mining industry) investigating the constructability of a Natural Heat Exchange Engineering Technology (NHEET) system. The NHEET system uses natural means to provide economically significant seasonal/diurnal thermal regeneration capacity through a volume of fragmented rocks for ventilating mine workings (Acuna and O'Connor, 2010; Saeidi et al., 2017). The input pressure and the flow rate obtained from this lab experiment are key data collected to calibrate a subsequent numerical simulation to represent the

experimental results. This is required for upscaling to the actual size of the NHEET system in order to evaluate whether the secondary permeability of a rock mass can admit sufficient flow for thermal regeneration capacity.

REFERENCES

- Acuna, E. and O'Connor, D., 2010. New approach to maximize the natural conditioning system at Creighton Mine. In CIM MEMO Conference, Sudbury, Canada.
- Blyth, F.G.H. and De Freitas, M.H., 2017. A geology for engineers. Seventh Edition, Elsevier.
- Morris, A. S. and Langari, R., 2012. 'Flow Measurment', in Measurement and instrumentation: theory and application. Amsterdam: Academic Press, pp. 426–434.
- Öhman, J., 2005. Upscaling of Flow, Transport, and Stress-effects in Fractured Rock (Doctoral dissertation, Acta Universitatis Upsaliensis).
- Rogers, S., Elmo, D., Beddoes, R. and Dershowitz, W., 2009, November. Mine scale DFN modelling and rapid upscaling in geomechanical simulations of large open pits. In International Symposium on Rock Slope Stability in Open Pit Mining and Civil Engineering, Santiago, Chile.
- Saeidi, N., Romero, A., Fava, L. Allen, C., 2017. Simulation of large scale thermal storage in fragmented rock modelled as a discretized porous medium – Application to the natural heat exchange area at Creighton Mine. In UMT 2017: Proceedings of the first international conference on underground mining technology, Australian Centre for Geomechanics: pp. 153-165.
- Singh, K.K., Singh, D.N. and Ranjith, P.G., 2014. Simulating flow through fractures in a rock mass using analog material. International Journal of Geomechanics, 14(1), pp.8-19.
- Singhal, B. B. S. and Gupta, R. P., 2010. 'Hydraulic Properties of Rocks', in Applied Hydrogeology of Fractured Rocks. Second Edi. New York: Springer, pp. 139–140.



Figure 1: 3D printed DFN model with ABS material.

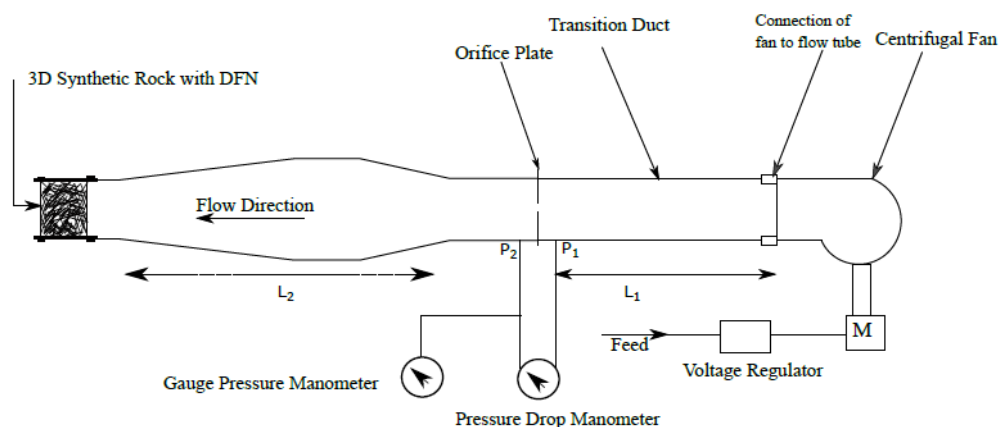


Figure 2: Schematic diagram of anemometer calibration rig.

Studying the effect of roughness-based filtering on structural geology analysis and JRC measurements from LiDAR mapping

Niloufarsadat, S., Akram, D., and Aubertin, J.D.

École de Technologie Supérieure, Montréal, Québec, Canada

ABSTRACT

Remote sensing technologies have become prevalent in the fields of geosciences and geo-engineering applications. Continuous improvements in data processing and automation have greatly broadened capabilities around feature recognition and overall geomechanical characterization. Terrestrial and airborne laser scanners (i.e. LiDAR) and photogrammetry tools allow users to measure a wide range of features and components along exposed rock outcrops. Advanced edge detection algorithms and curvature measurements are used to describe fragmentation distribution, extract structural geology information, and detect instability indicators, and slope failure precursors (Abellan et al., 2014; Battulwar, 2021).

The diversity and engineering depth of applications for remote sensing in geosciences has led to the emergence of processing tools and software to assist with data processing and analysis. Software reliance can lead to dissociative notions between processing and interpretation (i.e. black box effect). In conjunction, a growing number of open-source codes and applications have been developed by the booming geoscience and computer science communities (e.g. Rusu & Cousins, 2011; Girardeau-Montaut, 2016). These tools can be used to develop structured and transparent processing workflows to facilitate the analysis.

Point cloud data sets collected from rock faces require engineered processing techniques to filter noise and extract relevant information. In structural and geomechanical characterization, it is often necessary to filter unwanted occlusions such as vegetation or rock and soil debris. Structural mapping of rock joints must rely on well defined planes which can be misinterpreted with closely spaced asperities or other inconsistencies which would normally be filtered out by conscientious engineers. This study investigates the simple notion of surface roughness as a filtering mechanism in remote sensing assisted rock engineering applications. Roughness is identified here as an intuitive and reliable measurement that can be easily implemented in open-source coding systems.

The present work describes a systematic processing workflow to filter data sets using roughness measurements computed from topographical data. A recursive scale-dependent analysis is implemented to derive characteristic roughness parameters for measured surfaces (Aubertin & Hutchinson, 2022). The scale-dependent trends are applied as a filtering threshold for noise and inadequate surface spans. Special considerations are given to measurement parameters part of the processing workflow. Recommendations are made for systematic parameter testing to ensure optimal results.

The proposed methodology is demonstrated through practical applications with structural mapping and joint roughness measurements. A large rock outcrop surveyed from a limestone quarry South of Montréal was analysed for the purpose of this study. Normal-based structural mapping was carried on the raw data sets as the unfiltered baseline. The structural analysis obtained from the filtered surface is then obtained and compared with the baseline. Geomechanical characterization is performed by measuring the joint roughness coefficient

(JRC) (Barton & Choubey, 1977). In this work, JRC is measured from recursive scale-dependent roughness measurements following the fractal-based geomechanics theory (Tatone & Grasselli, 2013; Magsipoc et al. 2020). JRC measurements are obtained from the raw and filtered data sets to contrast the results.

Observed differences between filtered and raw data processing are discussed in terms of practical implications towards engineering practices. A discussion is given around the viability and limitations of roughness-based filtering. Special considerations are mentioned in regards to the selection of a viable roughness threshold based on the application and scale considered.

REFERENCES

- Abellán, A., Oppikofer, T., Jaboyedoff, M., Rosser, N. J., Lim, M., & Lato, M. J. (2014). Terrestrial laser scanning of rock slope instabilities. *Earth surface processes and landforms*, 39(1), 80-97.
- Aubertin, J. D., & Hutchinson, D. J. (2022). Scale-dependent rock surface characterization using LiDAR surveys. *Engineering Geology*, 301, 106614.
- Barton, N., & Choubey, V. (1977). The shear strength of rock joints in theory and practice. *Rock Mechanics*, 10(1), 1-54.
- Battulwar, R., Zare-Naghadehi, M., Emami, E., & Sattarvand, J. (2021). A state-of-the-art review of automated extraction of rock mass discontinuity characteristics using three-dimensional surface models. *Journal of Rock Mechanics and Geotechnical Engineering*, 13(4), 920-936.
- Girardeau-Montaut, D. (2016). *CloudCompare*. France: EDF R&D Telecom ParisTech, 11.
- Magsipoc, E., Zhao, Q., & Grasselli, G. (2020). 2D and 3D roughness characterization. *Rock Mechanique and Rock Engineering*, 53, 1495-1519.
- Rusu, R. B., & Cousins, S. (2011). 3d is here: Point cloud library (pcl). In 2011 IEEE international conference on robotics and automation (pp. 1-4). IEEE.
- Tatone, B. S., & Grasselli, G. (2013). An investigation of discontinuity roughness scale dependency using high-resolution surface measurements. *Rock Mechanics and Rock Engineering*, 46(4), 657-681.

Delineating numerical excavation damage zone depth limits using machine learning

Golabchi, Y., Morgenroth, J., and Perras, M.A.

York University, Toronto, Ontario, Canada

ABSTRACT

In rock mechanics, empirical methods are used in a variety of ways, such as, to estimate rock mass strength, to establish rock mass classes based on RMR, GSI, or others, or to determine excavation design parameters, such as depth of damage. These methods and approaches were established based on observations and experience from various rock masses and subsequently, the obtained data were analyzed manually or statistically. The advantage of a machine learning (ML) algorithm is that it can learn the underlying patterns given the appropriate input data. ML establishes and learns patterns in the data it is trained with, after which statistical methods can be applied to interpret the patterns and the predicted outputs.

During the construction of underground excavations, the change in the stress regime in the surrounding rock mass leads to damage initiation and crack propagation if the stresses exceed the rock mass strength. The excavation damage zones (EDZs) that develop are a critical aspect for the design of permeability-sensitive excavations, such as deep geological repositories for nuclear waste. The variability of depths predicted using the damage initiation and spalling limit (DISL) method as well as the variability of the inputs evaluated based on former research found that the tensile strength produces the greatest variation in the depth of the EDZs. In this study, logistic regression and support vector machine, two supervised machine learning approaches for classification are used and compared to re-analyze the numerical data that was used to develop EDZ prediction curves to aid in handling the variability from the numerical data. ML can be useful when there is a large volume of observational or numerical points. Logistic regression could classify different excavation damage zone depths with good accuracy, as is shown in the receiver operating characteristic (ROC) curve (Figure 1), however, it considers a straight line as the decision boundary, as it is shown in Figure 2. A more non-linear decision boundary is preferred, so an SVM classification with non-linear kernels was also carried out. Future research will also consider the numerical input parameters to examine influence on the EDZ depth predictions.

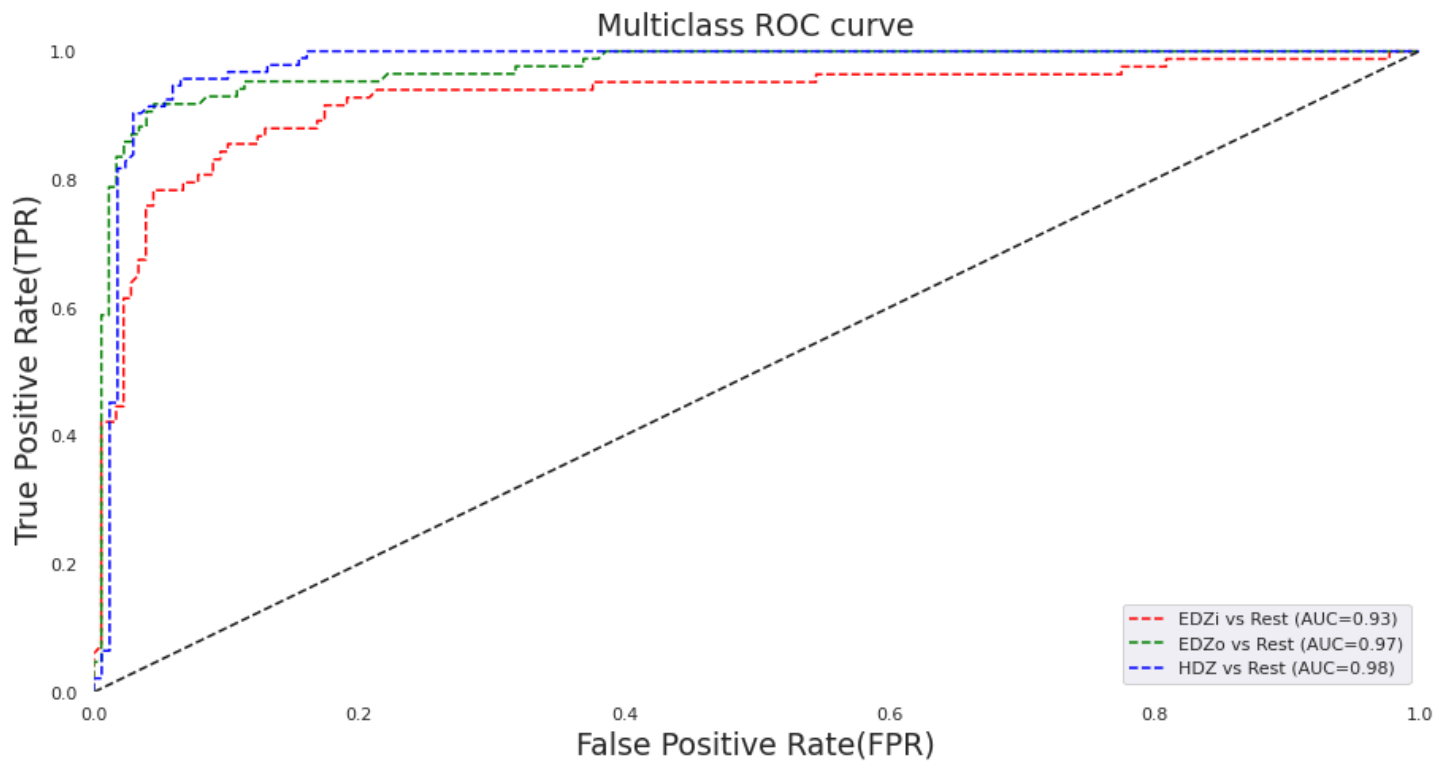


Figure 1: Logistic Regression ROC curve.

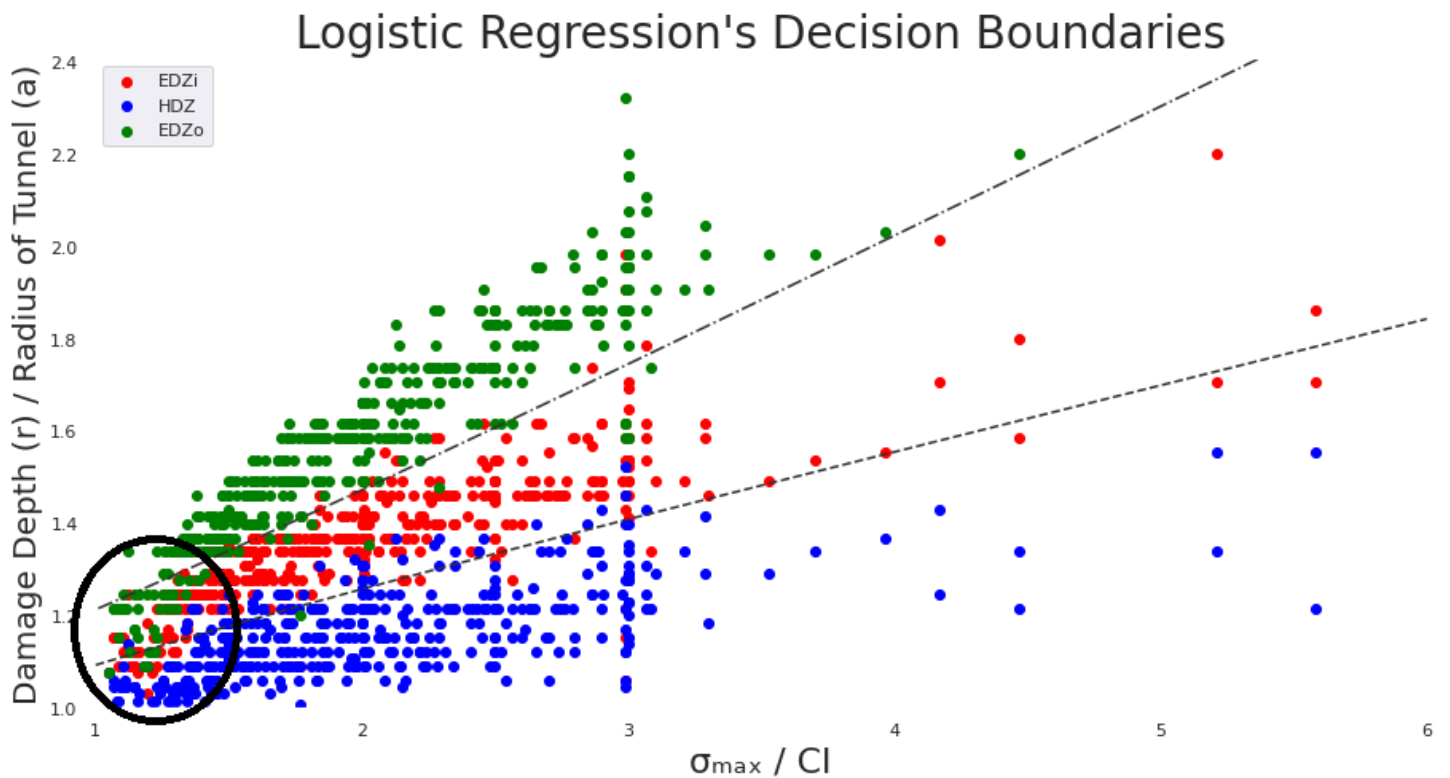


Figure 2: Logistic Regression decision boundaries for HDZ, EDZi, and EDZo.

Verification of numerical models using seismic source mechanisms

Meyer, S.G.¹ and Rigby, A.²

¹*Institute of Mine Seismology, Sudbury, Ontario, Canada*

²*Institute of Mine Seismology, Kingston, Tasmania, Australia*

ABSTRACT

Microseismic monitoring and numerical stress modelling are two of the fundamental and most widely used tools available to geotechnical engineers that aide them to understand and manage the rockmass response to mining. Although there exists a natural, inherent and obvious relationship between stress and seismicity, the fields of stress modeling and seismic monitoring still exist independently from one another. Numerical modelling teases the promise of accurate forecasting of future seismicity, while recorded seismicity should be able to deliver perfect model calibration.

Over the years, there have been a number of methods and aproaches that aim to use seismic data in model calibration. These have had varying degrees success and provided definite improvements in estimating the appropriate model parameters, but remain lacking in some ways. They typically rely more on correlation of parameters, than true, numerically based calibration, for example, comparing the number of events above some magnitude with the modelled rate of energy release, or that events locate in areas with high modelled shear stress.

We present methods that utilize more direct comparisons between model and observed data. These include the generation of catalogues of synthetic seismic source mechanisms for comparison with observed events, differences between the directions of modelled stresses and observed strains, and the difference between observed and modelled slip directions.

Representative Elementary Volume (REV) of a jointed rock mass for determination of the block size

Mahdavi-rad, M., Shahbazi, A., and Saeidi, A.

Université du Québec à Chicoutimi, Québec, Canada

ABSTRACT

In this manuscript, the representative elementary volume of a fractured rock mass that includes three non-persistent joint sets has been investigated using numerical modelling by 3DEC version 7 software and considering the block volume as the interested parameter. The shape and size of the blocks in a fractured rock mass plays significant roles in mechanical properties of the rock; in this regard, joint persistence, orientation and spacing are among the most determining parameters. Determination of the representative size of a numerical model for studying the block size dependent parameter, is the subject of this manuscript.

The methodology that is followed in this research is summarized in the Figure 1. Fourteen datasets of the rock mass from the real data of dams in Australia, USA and Africa (Pells, 2016) comprising three non-persistent joint sets with various orientation and spacing are considered. 3DEC version 7 is used for determination of the volume of the volume blocks. For this purpose, after creation of the model, the blocks that cut by the boundary of the model (boundary blocks) were deleted in order to eliminate the error produced by these blocks (Figure 2).

However, the model that is illustrated in Figure 3 might not be representative to unlimited sizes of the formations (REV). In order to find the REV of the numerical model, it was expanded through all dimensions and simultaneously, the average volume of the blocks in the model (except the boundary blocks), was recorded.

Figure 3 illustrates the variation of the average volume of the blocks in a numerical model by the size of the model. In lieu of the size of the model, its relationship with the average spacing of the joint sets has been considered in calculations. According to Figure 3, the average volume of the blocks varies by variation of the size of the model and in a specific model size, its variation is negligible. For example, diagram (A) and (B) reach to its representative size at 50× and 300× of the average spacing respectively, when the block volume is the parameter of interest.

The reason for considering 50 and 300 as the representative size of the model is that the average volume of the blocks in the numerical model doesn't change anymore in the sizes larger than 50× and 300× of the average spacings of the joint sets and beyond these sizes, the behaviour of the model that is linked to the block volume will be constant.

The REV of the rock mass is a very important parameter that has to be determined prior to running the numerical simulations. According to what was illustrated in this manuscript, the methodology for determining the REV of the model, when the block volume is the parameter of the interest, has been explained. However, this REV is not applicable if the parameter of interest being changed and for each parameter or type of the study (Geomechanical, Hydrogeological), a specific value of the REV has to be determined prior to performing the numerical simulations. On this basis, the conclusions of this manuscript are as below:

- REV is a parameter dependent concept and should be determined separately for each case study
- The REV of the model for the case of volume of the blocks of the rock mass is at least 50× of the average spacings of the joint sets
- In order to accurately define the REV of the model, the error generating parameters have to being deleted from calculations, and for the case of block geometry, the boundary blocks are among error generating parameters

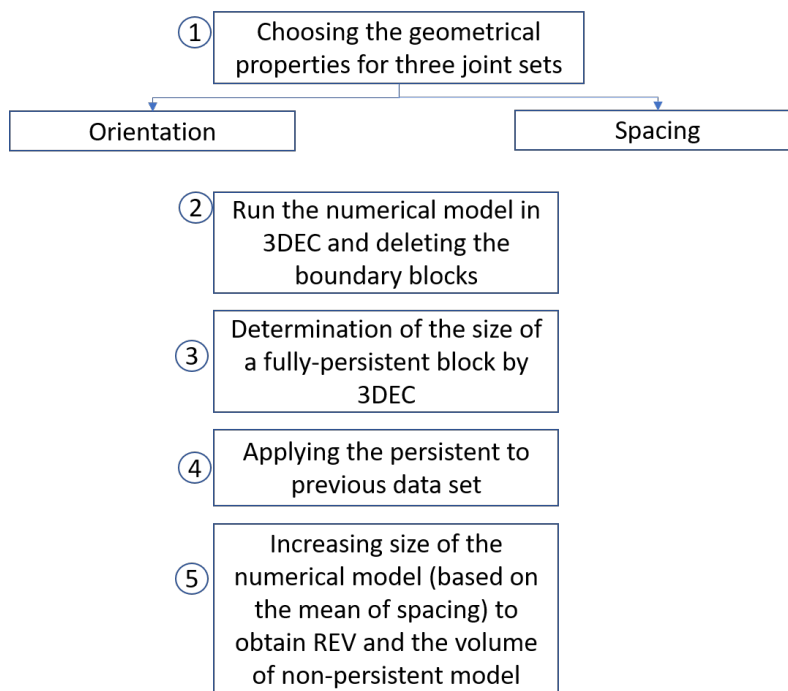


Figure 1: Summary of Methodology.

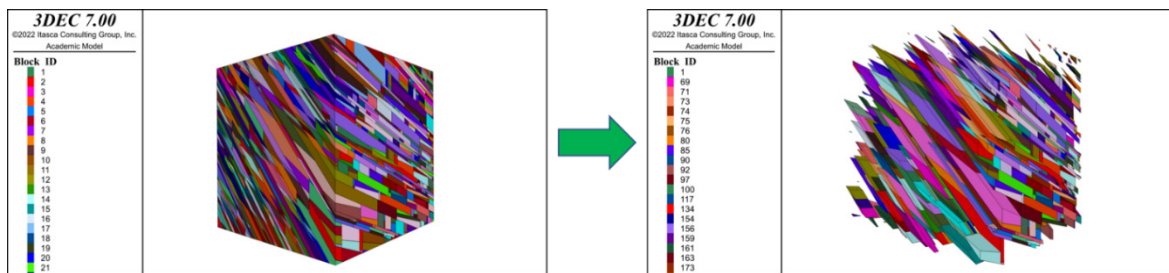


Figure 2: Deleting the boundary blocks to improve the accuracy of the model.

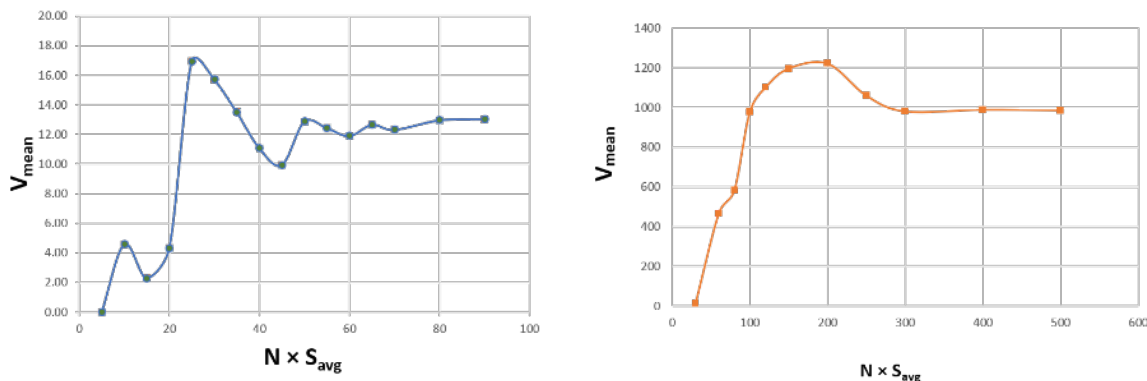


Figure 3: Different REVs for two data sets relating to non-persistent jointed rock mass (The volume of the same dataset for fully-persistent joint sets are in the same ISRM volume categories).

Indication of in situ stress orientation by pressuremeter hold test – experiment and field tests

Liu, L. and Chalaturnyk, R.

University of Alberta, Edmonton, Alberta, Canada

ABSTRACT

In situ stress is considered a key parameter in many rock engineering designs. The in situ stress is the result of the earth's gravitation, geological processes, and tectonic events in history. The in situ stress can have strong local variations due to the heterogeneity in rock mass structure (e.g., discontinuities, layering, and inclusions) and the irregularity of surface topography. Testing methods, such as hydraulic fracturing, have been developed to determine in situ stress in deep formations. However, the determination can be challenging for testing in the weak rocks with relatively low shear strength, where shear yielding before tensile cracking can introduce additional complexity to the interpretation models.

As a conventional in situ testing method in geotechnical site characterization, pressuremeter testing has shown its potential in deriving the in situ stress and its anisotropy in the testing plane based on the measurements from caliper arms at multiple axes (Liu et al., 2021). In a recent experimental study by Liu et al. (2018), the anisotropic expansion of the borehole under pressuremeter loading in soft cement blocks confined by poly-axial boundary stresses was investigated (Figure 1). In this work, the test data is revisited, and the time-dependent expansion of the borehole (or creep) during hold tests after yielding is shown to be closely linked to the anisotropic boundary stresses (σ_H and σ_h) applied in the testing plane (Figure 2). The maximum creep is aligned approximately in the axis of σ_H in three tests under different boundary stress anisotropies σ_H/σ_h .

The experimental findings are explained in a simple theoretical framework, which is then used to interpret the pressuremeter hold tests obtained in Opalinus Clay from a recent field campaign at Mont Terri (Liu et al., 2022). The in situ stress orientation interpreted from four field tests agrees well with the reported in situ stress tensor. The magnitude of in situ stress can not be directly determined but remains possible once the creep rates of the Opalinus Clay under varying deviator stresses are calibrated from the laboratory tests.

REFERENCES

- Liu, L., Chalaturnyk, R., Deisman, N., & Zambrano-Narvaez, G. (2021). Anisotropic borehole response from pressuremeter testing in deep clay shale formations. *Canadian Geotechnical Journal*, 58(8), 1159–1179.
- Liu, L., Fu, H., Chalaturnyk, R., Weng, D., Zambrano, G., & Steve, Z. (2018). An experimental study of pressuremeter testing under polyaxial boundary stress condition. *Proceedings of GeoShanghai 2018 International Conference*, 1, 449–457.
- Liu, L., Giger, S. B., Martin, D., Chalaturnyk, R., Schuster, K., Deisman, N., & Keller, L. (2022). In-situ Shear Modulus Determination by Pressuremeter Tests in Opalinus Clay and Reconciliation with Laboratory Tests. *Rock Mechanics and Rock Engineering*.

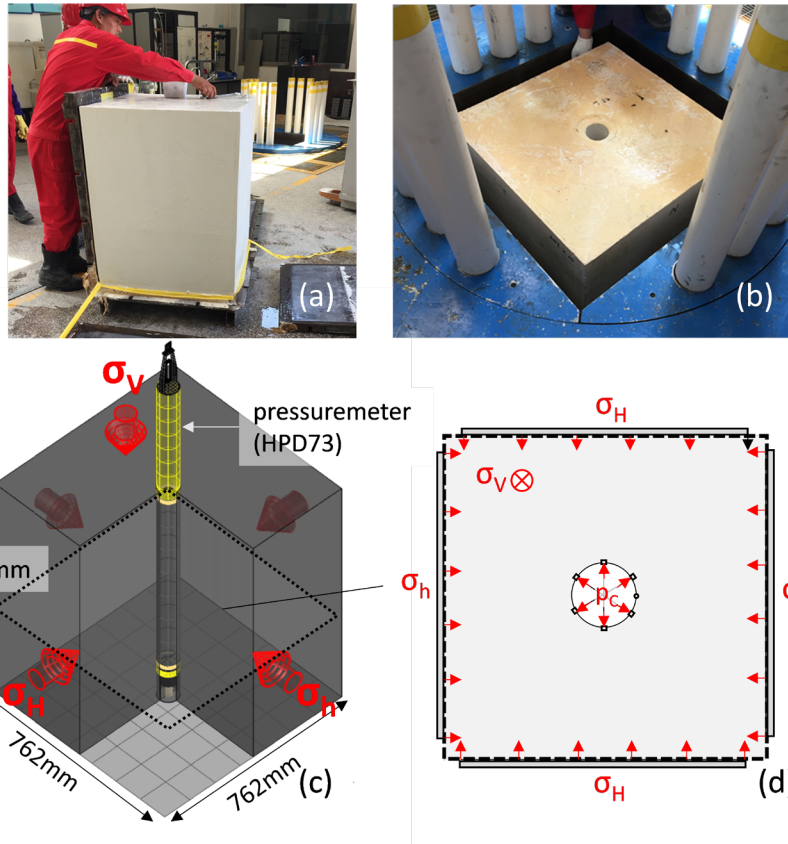


Figure 1: (a) Cubic soft cement specimen after curing. (b) Specimen with a central drilled hole installed in a large-scale poly-axial loading frame. (c) Diagram with pressuremeter set in the central hole of the specimen under poly-axial boundary loading. (d) Horizontal cross-section of the cement specimen under loading.

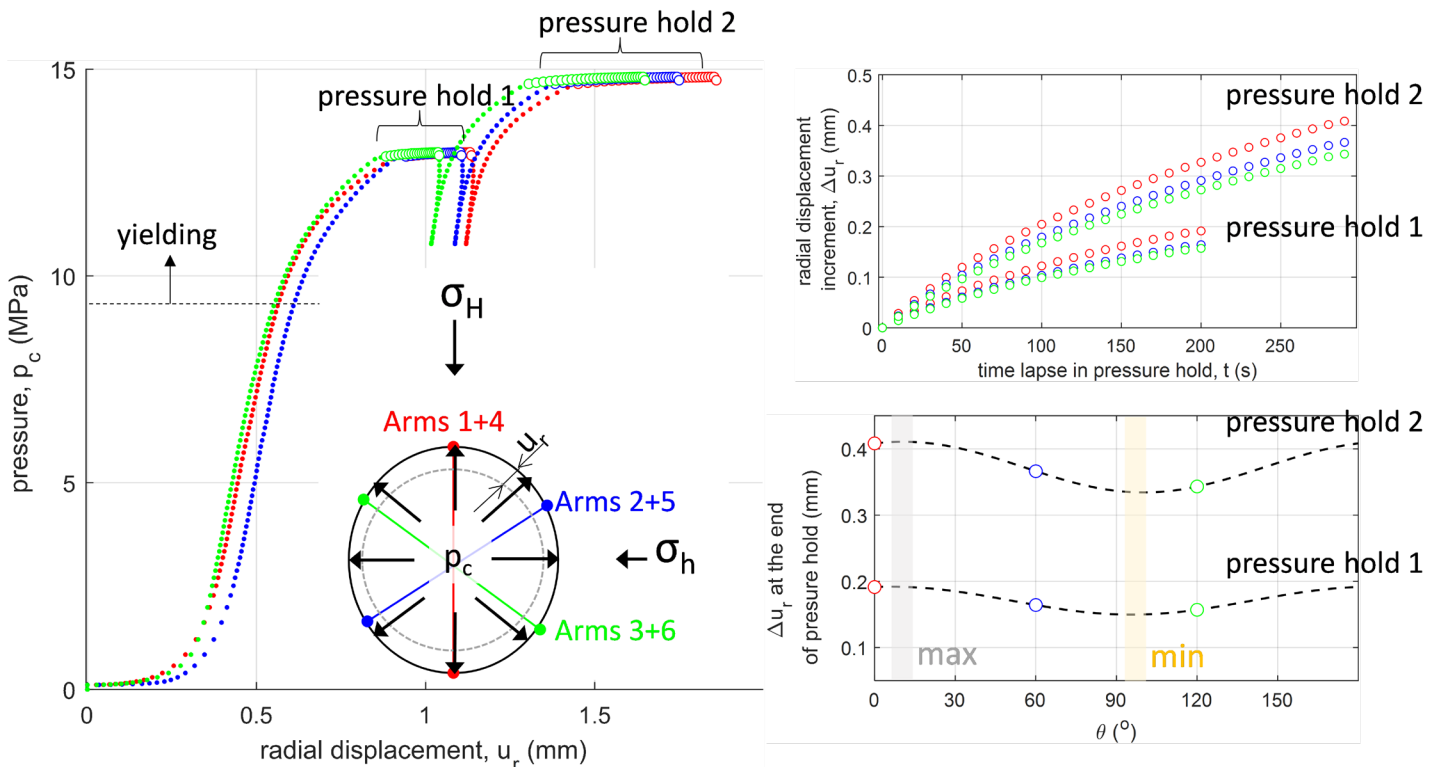


Figure 2: (a) Test curves of pressure versus radial displacements obtained at three independent caliper axes. (b) Radial displacement increments during pressure hold at the three axes. (c) Azimuthal variation of the radial displacement increments at the end of pressure hold.

Impact of layering and fractures in Buckinghamshire shale on strain measurement using digital image correlation (DIC)

Magsipoc, E., Haile, B.F., and Grasselli, G.

Department of Civil and Mineral Engineering, University of Toronto, Toronto, Ontario, Canada

ABSTRACT

The varying stiffness of pre-existing fractures and material layering can have significant effects on strain measurement of laboratory samples due to mineralogy and sample structure (Bandis et al., 1983; Homand et al., 1993). Thus, strain measurement during laboratory testing requires careful placement and critical interpretation to ensure that the material deformation response is accurately characterized. Strain is often measured using linear variable differential transformers (LVDTs) or strain gauges. However, LVDTs only capture the deformation response from end-to-end and may be subject to additional deformation from self-deformation of the LVDT mounting apparatus (ASTM D7012, 2017). Strain gauges also only capture strain in its immediate location and requires careful placement with pre-existing knowledge of the sample structure to capture appropriate strain data. Despite careful planning and interpretation, the produced strain data may still be unexplainable without further information about the sample deformation as these strain measurement methods lacks a “big picture” view of the sample’s mechanical response. To track variation in deformation, digital image correlation (DIC) was used to measure the strain field of various laboratory tests on Buckinghamshire shale. This method of strain measurement allows for continuous deformation tracking over an imaged sample area, providing the ability to see local strain developments that may appear and disappear with time.

The unconfined compressive strength (UCS) and Brazilian disc (BD) tests were performed on Buckinghamshire shale samples that were prepared by computer numerical control (CNC) milling with a vortex tube cold air gun. The samples were subsequently wrapped in a shrink tube to avoid sample disintegration during handling. Because the UCS samples were covered in a shrink tube, a square window sized at approximately 15 mm was cut to expose the surface. The samples were painted with a white matte spray paint and subsequently speckled with a black matte spray paint to provide a pattern to be used for DIC. For both the UCS and BD tests, the samples were prepared and with loading oriented at 0 degrees, 45 degrees, and 90 degrees with respect to the rock fabric (bedding planes).

The DIC was carried out using a stereo-camera system with 5-megapixel cameras. The stereo-camera allows for sensing of sample distance with respect to the viewing axis of the cameras. The system was calibrated after every setup using a calibration panel provided by the manufacturer that determines the camera’s optical and positional parameters that are used for accurate measurement of displacement. The system is sensitive to 0.1% strain when the sample occupies the entire image frame with a minimum image height of 44 mm.

From the DIC analysis areas of localized strain caused by bedding plane orientation or by existing fractures were present in all the samples with well defined bedding planes. The major principal strain fields immediately before failure is presented in Figure 1b, d with tensile strain as the positive colour axis, highlighting the areas of cracking on the exposed surface. The samples after failure are presented in Figure 1a,c. It is immediately apparent that deformation measurements with the UCS sample would cause significant error in strain measurement due

to existing fractures within the sample (Figure 1b). However, DIC provides the capability to measure an intact section of the rock mass that is less disturbed by fracturing. The BD sample also shows an area where fracturing was occurring before the full tensile fracture occurred. This provides test-history insight on when the fractures formed and whether they were involved during failure or occurred as secondary fracturing.

REFERENCES

- ASTM D7012. (2017). Test Methods for Compressive Strength and Elastic Moduli of Intact Rock Core Specimens under Varying States of Stress and Temperatures (No. D7012-14e1).
- Bandis, S. C., Lumsden, A. C., & Barton, N. R. (1983). Fundamentals of Rock Joint Deformation. *International Journal of Rock Mechanics and Mining Sciences & Geomechanics Abstracts*, 20(60), 249–268.
- Homand, F., Morel, E., Henry, J.-P., Cuxac, P., & Hammade, E. (1993). Characterization of the moduli of elasticity of an anisotropic rock using dynamic and static methods. *International Journal of Rock Mechanics and Mining Sciences & Geomechanics Abstracts*, 30(5), 527–535.

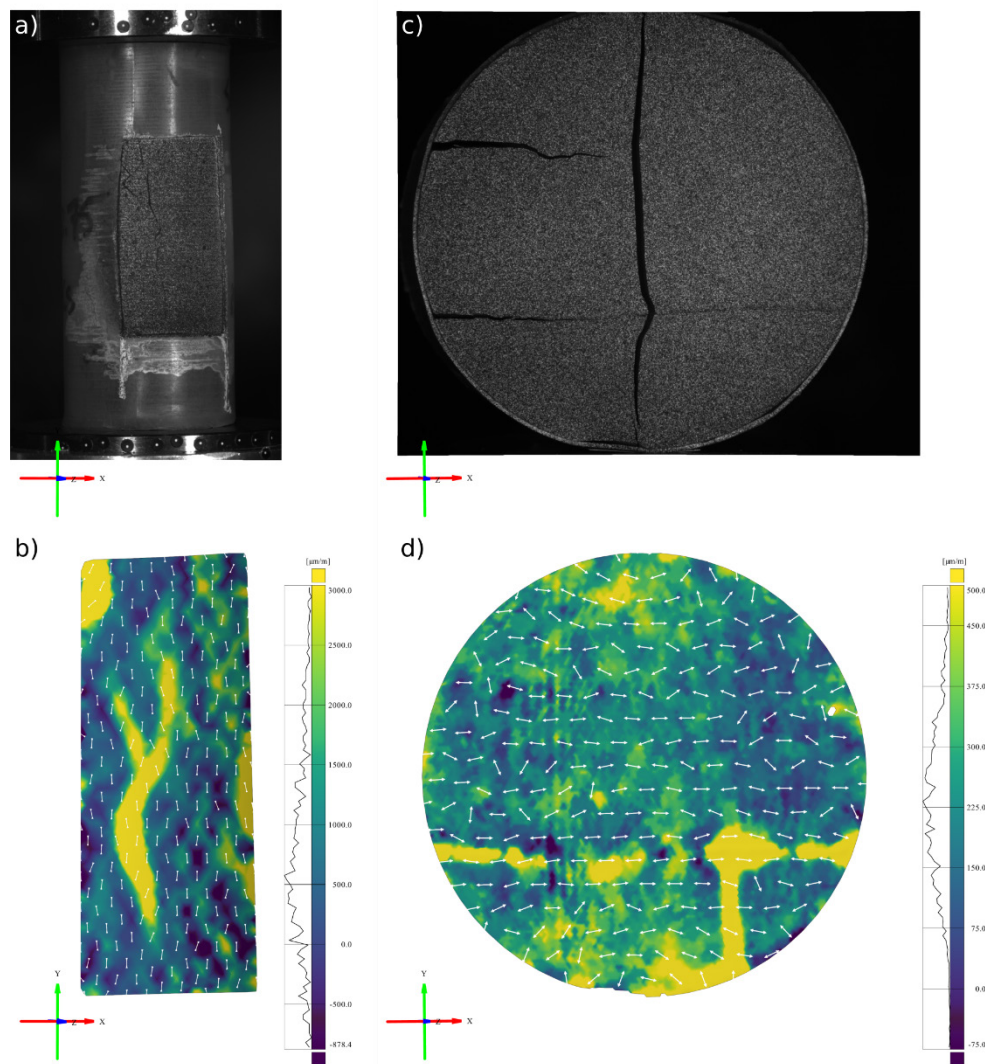


Figure 1: DIC post-failure images and pre-failure major principal strain fields with (a,b) for UCS and (c,d) for BD.

Investigating the thermal cracking process of granitic rocks using digital image correlation (DIC)

Haile, B.F., Aboayanah, K.R., and Grasselli, G.

Department of Civil and Mineral Engineering, University of Toronto, Toronto, Ontario, Canada

ABSTRACT

Most geothermal reservoirs are found in low permeability crystalline rocks, e.g., granite, that are composed of crystalline minerals such as quartz, feldspar, and biotite. Even though these rocks have low permeability and high strength, temperature changes due to production of hot fluids or injection of cold fluids for geothermal applications will induce thermoelastic stresses that can initiate and cause cracks. Experimental investigations of the thermal cracking of granitic rocks have indicated that the mechanical properties of heat-treated rocks are highly dependent on the temperature the rocks have been exposed to (Bauer, 1983). In addition, to study the thermal properties of granite, Nasser et al., (2009) experimentally investigated the rate of formation of thermal cracks, which increased after the sample temperature reached 573 °C. Hence, for various industrial applications, it is essential to investigate the thermal properties of these rocks with novel and state-of-the-art experimental techniques that can help understand the processes involved in the evolution of cracks during thermal heating and cooling.

In this experimental study, to investigate the initiation and propagation of thermal cracks in Stanstead granite, stereo (3D) digital image correlation (DIC), which is a non-contact measurement technique that uses two cameras to measure the displacement and strain fields of deformable materials over time, is used while heating cylindrical samples of the rocks. DIC systems achieve this through a mechanism called facet matching or tracking, which relies on the optimization of optical flow models (Reu, 2012). Using a sequence of digital images from a sample surface painted with a speckle pattern, the DIC algorithm tracks the coordinate changes in the pattern to estimate the deformation and strain of the surface. Stereo-DIC which uses two cameras, allows for the measurement of 3D coordinates of the samples by combining image correlation photogrammetry techniques and allows for accurate measurement of out-of-plane deformation.

The experiment presented in this work lasted for one hour and consisted of both heating and cooling phases (30 minutes each). To heat the Stanstead granite samples of size 50 mm in diameter and 25 mm in thickness, the middles of the samples were drilled, and a heating cartridge was inserted in the middle. Thermocouples were applied close to the hole and the outside of the cylindrical samples to monitor the temperature increase over time. Figure 1 shows the sample setup for the experimental work, and the temperature variations from the heating and cooling cycle.

From the DIC analysis of the strain and displacement fields of the sample surface during the heating and cooling cycle, it was observed that macroscopic crack initiated from the outer boundary of the sample (i.e., cold end) due to tensile stresses exerted by the expansion of the sample interior (i.e., hot end). In addition, as shown in Figure 2 (b) the DIC results showed that the larger resultant displacement was observed in the area where the sample had experienced macroscopic cracking. Hence, using this experimental method we can gain deeper insight into the thermal cracking mechanism of granitic rocks.

REFERENCES

- Nasseri, M.H.B., Tatone, B.S.A., Grasselli, G. and Young R.P., 2009. Fracture Toughness and Fracture Roughness Interrelationship in Thermally treated Westerly Granite. *Pure appl. geophys.* 166, 801–822.
- Bauer, S.J. and Handin, J., (1983). Thermal expansion and cracking of three confined water-saturated igneous rocks to 800 C. *Rock Mechanics and Rock Engineering*, 16(3): 181-198.
- Reu, P.L. (2012) Introduction to Digital Image Correlation: Best Practices and Applications. In \The Art and Application of DIC” article series. *Exp Techniques*, 36(1):3

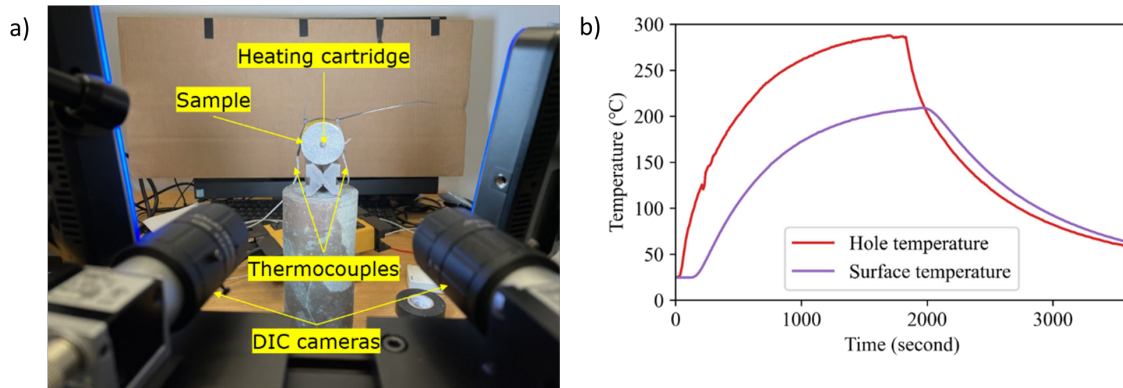


Figure 1: Experiment setup for thermal testing of the Stanstead granite (a) Temperature variation with time for the heating and cooling cycle (b).

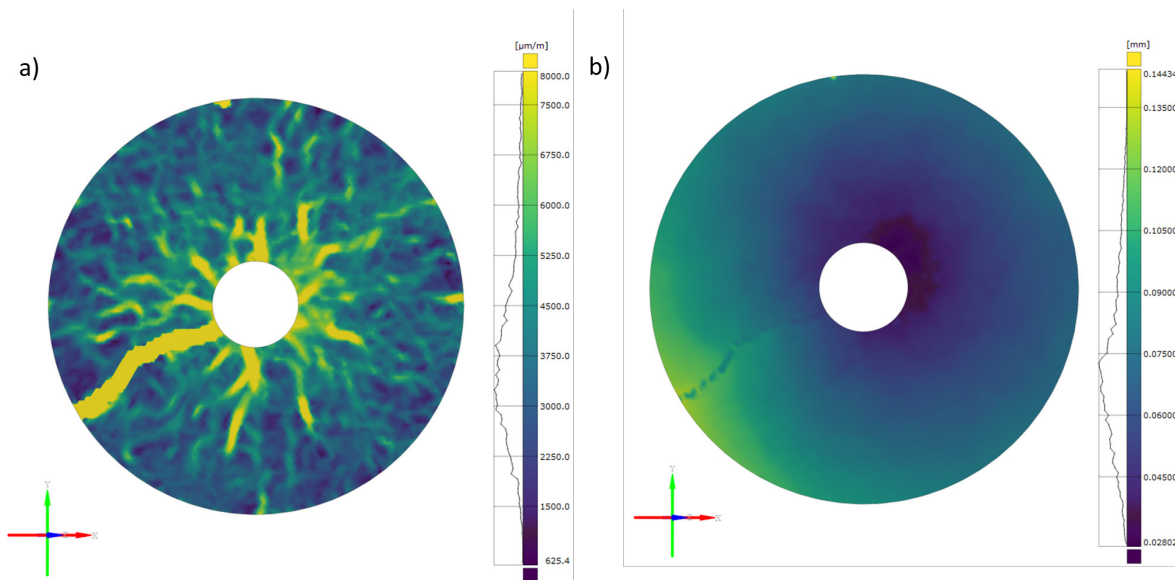


Figure 2: Major strain distribution (a) and resultant displacement in the sample (b) after the 30 minutes heating half-cycle.

Entropy-based probabilistic characterization of rock shear strengths from triaxial tests and its application in rock slope risk

Deng, J.¹, Li, S.J.², Jiang, Q.², and Chen, B.R.²

¹Lakehead University, Thunder Bay, Ontario, Canada

²Institute of Rock and Soil Mechanics, Chinese Academy of Sciences, Wuhan, China

ABSTRACT

The probabilistic approach has been established as a rational method to explicitly deal with ubiquitous uncertainties (e.g., mineral composition, flaws, pores, and micro-cracks) in rock mechanics and engineering as the random nature of rocks can be quantified [1–4]. Modelling and quantifying uncertainties in rock property parameters are the initial and critical steps in probabilistic analysis and design in rock engineering. The cohesive strength of marble has been modelled as a log-normal probabilistic distribution, but the internal friction angle was accepted as a normal distribution [1]. In addition to the most commonly used normal and lognormal distributions, other probabilistic distributions are also popular in modelling various properties of rocks. The range of $(-\infty, +\infty)$ in normal distributions can cause some problems for a rock variable with only positive definition. In order to overcome this problem, the truncated normal distribution is occasionally used so that a minimum and maximum values can be specified and values beyond the specified range are considered invalid [2]. A Weibull distribution was used to describe statistically the rock strength distribution due to its heterogeneity in the meso-scale [3]. Negative exponential, von Mises–Fisher, hyperbolic, and Gamma distributions can also characterize some properties of rocks [4]. Therefore, serious disputes always exist among researchers about which distribution is the best to model a rock parameter.

This paper proposes a new universal probabilistic characterization of rock parameters based on the principle of maximum entropy and finds its application in risk analysis of a rock slope. Firstly, we conducted a series of triaxial compression tests on marble rock from Jinping II hydropower station project, southwest China, to obtain a sample of shear strength, i.e., cohesion and frictional angle (Figure 1). Secondly, a new probabilistic characterization based on maximum entropy and Akaike information criterion is proposed to describe these rock parameters unbiasedly and efficiently (Figure 2). Thirdly, the developed probabilistic model is applied in reliability and risk analysis of a rock slope (Figure 3): Reliability index $\beta = 1.6393$ and the probability of failure $p_f = 0.051$. The probabilistic models of rock shear strengths are objective and distribution-free because no classical distributions were presumed in advance, and the inference result provides a universal form of probability curves which can cover normal distribution and lognormal distribution as special cases. Another advantage of entropy distributions is that one can adjust the distribution's sophistication by adopting different order of sample moments. Thus, accurate probabilistic modelling of rock parameters and risk of rock engineering are obtained.

REFERENCES

- [1] Low BK. (2021). Reliability-Based Design in Soil and Rock Engineering. CRC Press.
- [2] Hoek E, Kaiser PK, Bawden WF (1995). Support of Underground Excavations in Hard Rock. Balkema.
- [3] Tang CA, Kaiser PK (1998) Numerical simulation of cumulative damage and seismic energy release in unstable failure of brittle rock. Int J Rock Mech Min Sci Geomech Abstr 35(2):113–121.
- [4] Cai M. (2011). Rock mass characterization and rock property variability considerations for tunnel and cavern design. Rock Mech Rock Eng, 44(4): 379-399.

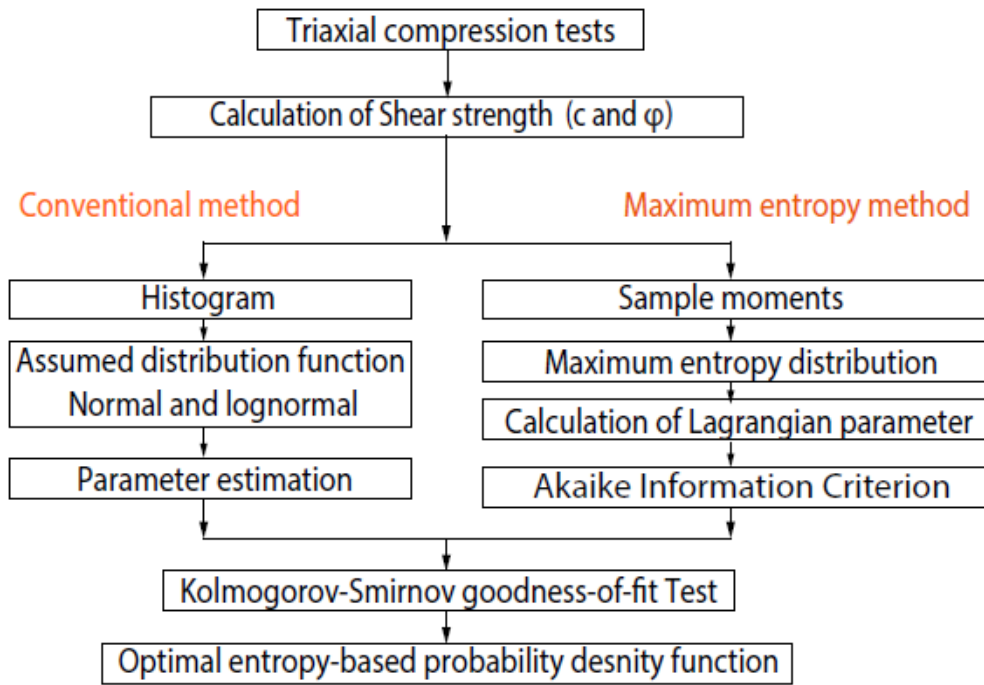


Figure 1: Flowchart of probabilistic characterization of shear strengths using maximum entropy method.

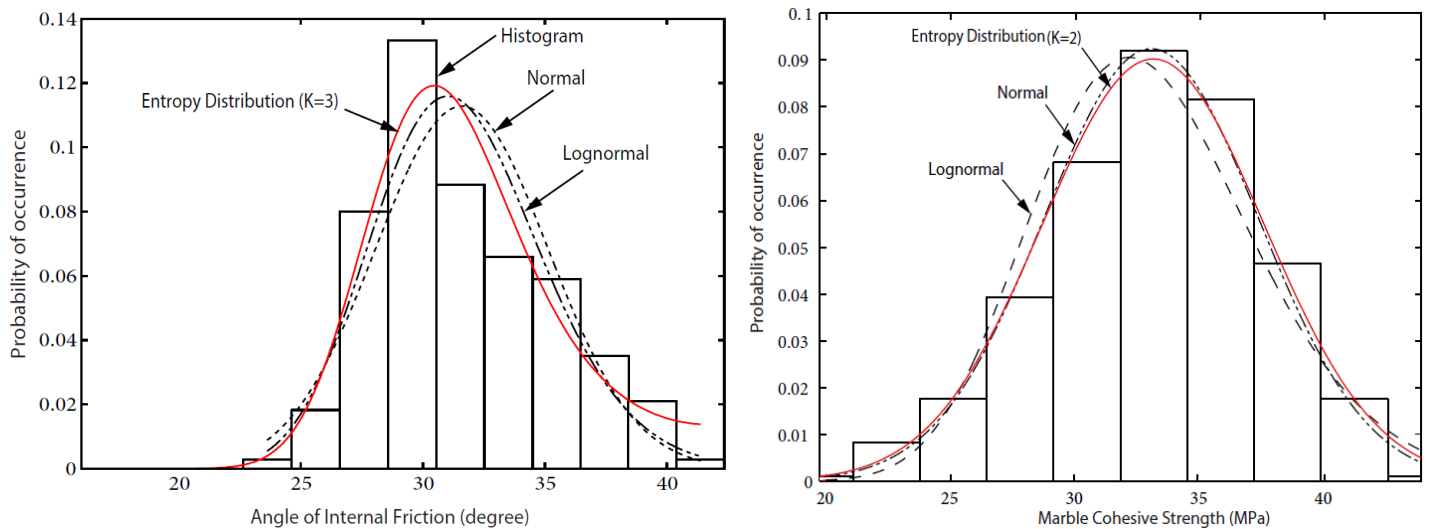


Figure 2: Comparison of entropy distributions for rock shear strength with histogram, normal, and lognormal distribution.

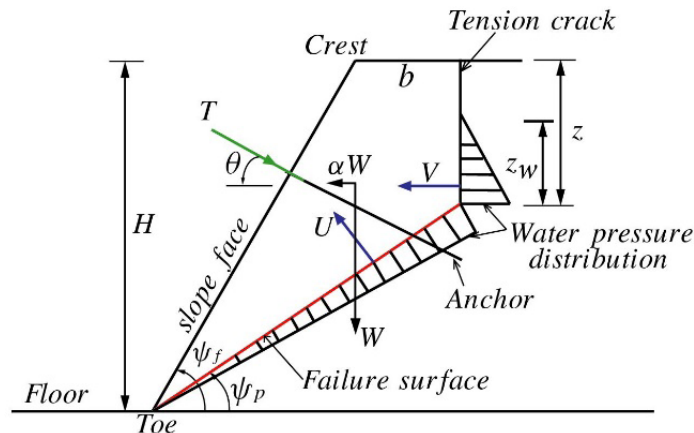


Figure 3: A rock slope in Jinping II project.

Reconstructing roughness of rock discontinuities by geostatistical procedure

Belhaj, M.¹, Rivard, P.¹, and Moradian, O.²

¹*Department of Civil Engineering, Université de Sherbrooke, Québec, Canada*

²*Department of Earth Sciences, ETH Zurich, Zurich, Switzerland*

ABSTRACT

INTRODUCTION

Roughness characterization requires field measurements, with or without contact, which are often time-consuming and expensive to carry out, especially for measuring the roughness of a very large area. Numerous in situ technologies provide precise measurement at a variety of spatial scales. However, roughness measurement in inaccessible/partially exposed areas, has not been studied yet. A major issue arises as how to accurately characterize the roughness of a subsurface discontinuity. A method aiming at reconstructing underneath discontinuity roughness from limited samples obtained from boreholes or exposed surface is then needed.

We have initiated a project to find alternatives to large-scale direct shear tests conducted in the field. The objective was to transfer in situ shear tests to the laboratory. A 50 cm × 50 cm schist outcrop was scanned using a laser scanner profilometer. The generated data was a data file containing the coordinates of each single scanned point, as well as their relative height (in mm) from a horizontal plane. These data will serve as a reference for this paper. We will attempt to reconstruct the original from sparse topographic data using geostatistical techniques. The proposed method aims at characterizing the surface roughness while simultaneously resolving the issue of scale dependency.

METHODOLOGY

The initial stage in geostatistical analysis is to determine the spatial structure of each variable (in this case, the height of the surface points). The variogram was used to describe the continuity and variability of fracture surfaces between every data point. To verify the effectiveness of the prediction analysis approach, a cross validation technique was applied. In each iteration, one of the measured points was removed from the real data set. Kriging analysis was done on the newly obtained data set and contour maps. The estimated values were compared to the true sample values that had been excluded from the sample data set at the start. To compare the actual and estimated values, a graphical plot was created, and error was determined as the root mean square of the differences between the estimated and true elevation values. The model is adjusted by the user based on these results and then a second cross-validation is done, and so on. Following this procedure for each predicted surface, surfaces were reconstructed by systematically dispersing (10 cm × 10 cm) samples. The roughness of the 3D reconstructed surface is evaluated by making a visual comparison to the original surface and analyzing the asperity's height distribution maps and frequency distribution histograms, as well as statistical results.

RESULTS AND DISCUSSION

As expected, as the number of samples increases, the reconstructed surface tends to resemble the original surface. The least accurate reconstructed surface is based on four samples that present 24% coverage, although the most

accurate reconstructed surface is based on thirteen samples that present 77% coverage which is unsurprising given the high coverage.

We may assert that we obtained a surface quite comparable to the original fracture by using 9-sample distribution covering 54% of the whole surface. It is then confirmed by the height of statistical data. This study suggests that it is possible to capture the roughness of a subsurface surface by reconstructing its topographic surface using limited and dispersed samples, but this method potential is limited by the percent of coverage, which is dependent on the number of samples and geometries. We should also point out that, since the weights of the kriging interpolator are dependent on the variogram model, kriging is very sensitive to variations in the variogram model's specification. Furthermore, if the number of sampled observations is small, and the data is restricted in geographical scope, or the data are not sufficiently spatially correlated, it is hard to construct a sample variogram, and therefore kriging may not be the ideal method for making predictions. Finally, we suggest that we compare the roughness parameters of each reconstructed surface, since each parameter present a specific information about the surface topography, then test this approach in an area with complex topography where the spatial autocorrelation of the variable of interest is only visible at a small scale.

CONCLUSION

When in situ rock joints are not accessible or fully exposed, it is often difficult to accurately estimate roughness characteristics of full-scale rock joints. The geostatistical method can solve this problem by using the kriging interpolation technique to predict values at unsampled locations, to obtain a reconstructed rock joint surface. Kriging analysis was performed, using spatial variability models, which provided reconstructed surfaces. The predictions were validated using the cross-validation technique. It was demonstrated that geostatistics can work effectively with 9 samples that present 54% of the coverage of the whole surface. However, a sensitivity analysis to sample locations and sizes is currently performed in order to validate this technique and better understand its limits.

Studying the strength and fracturing properties of rock-concrete interfaces under tensile loading at the microscale

Shams, G.¹, Rivard, P.¹, and Moradian, O.^{2,3}

¹*Department of Civil Engineering, Université de Sherbrooke, Québec, Canada*

²*Department of Earth Sciences, ETH Zurich, Zurich, Switzerland*

³*Civil Engineering Department, Colorado School of Mines, Golden, Colorado, USA*

ABSTRACT

Tensile failure and detachment of rock-concrete interfaces in civil engineering structures such as gravity dams is considered as one of the critical factors in controlling the stability of these structures. Despite a large number of studies, the fracturing process along the rock-concrete interfaces under tensile loading is not yet well understood. In this study, digital image correlation and acoustic emission techniques were employed to investigate the effect of the interface on the strength and the fracture properties of granite-mortar specimens under tensile loading. Our results indicated that the tensile strength of the granite-mortar interfaces was smaller than that of either the granite or the mortar. It was found that the tensile strength of the interface was controlled by both interface (adhesive strength) and the mortar (cohesive strength). The DIC results showed that FPZ is mainly limited to a narrow band along the interface, while the AE analysis revealed that the FPZ covers the interface area and a considerable portion of the mortar. AE better illustrated that the fracture may initiate at the interface and then kink into the mortar. In addition, it was seen that the surface roughness of the generated fractures is material dependent, i.e., fractures generated in granite were roughest, while fractures formed along the interface had the lowest roughness values. The finding of this study can improve our understanding of the tensile strength and behavior of rock-concrete interfaces, leading to the safer design of engineering structures.

25 years of monitoring ground movements around underground excavations: 5 takeaways

Hyett, A.

YieldPoint Inc., Kingston, Ontario, Canada

ABSTRACT

During the last 25 years the investment by mining companies in underground IT has greatly enhanced the opportunity for gathering geotechnical data. At larger mines 100's and in some cases 1000's of instruments monitoring ground movement and support loading are generating significant volumes of data. The budget for geotechnical monitoring projects is justified if ground control engineers can use the data to proactively manage the condition of excavation infrastructure as bulk mining progresses. Based on 5 important takeaways, work continues to develop tools that can unlock the inherent "value" from this data in order to inform proactive ground control decision making.

The five takeaways are:

1. Technology is making a difference.

Deploying electronics in harsh underground environment is challenging but embracing the latest technologies ultimately pays off. For example low cost wireless telemetry integrated into digital instruments can solve many problems related to the vulnerability and cost of regular lead-wires. Also, by leveraging massive industrial and consumer IoT technologies, the volume and quality of geotechnical data has increased to the point where it is no longer accurate to classify all aspects of the geotechnical problem as "data-limited".

2. Time and Space

Due to the diminishing cost of computer storage an estimated 85%+ of geotechnical instruments being combined with low cost autonomous data-loggers. The result is very rich time-series datasets that can be efficiently managed by modern time-series databases and big-data algorithms. However, for all but the biggest projects the spatial density of instruments remains limited. Complimentary technologies such as Distributed Optical Sensing and LIDAR will address this problem over the next 25 years.

3. Stress versus Displacement: "The model calibration conundrum"

Stress is difficult to measure but easy to model whereas displacements are easy to measure but difficult to model. This may be why geotechnical engineers rarely use instrumentation data to calibrate numerical models. While the stress distribution is dictated by the far field in situ stresses and traction free condition at the excavation boundary, displacements that exceed elastic values depend on the constitutive properties (strength/flow) of the rock mass which tend to be highly variable.

4. Understanding geology is critical to the interpretation of displacement datasets.

Consequently, displacements measurements around underground excavations are strongly influenced by rock mass material properties which are primarily a function of geology. Some of the most enlightening case studies

involve displacement monitoring across fault and shear zones, for which without the structural geology overlay the dataset appeared incoherent.

5. Time-dependency is hard rock mining's "inconvenient truth".

Rich time-series dataset reveal that time-dependency is ubiquitous around most underground excavations. Time-dependent behavior is highly correlated not with stress per se but with the excavation scale stress:strength ratio which is in fact a much more valuable parameter for excavation management. Time-dependent displacements have the benefit of quietly releasing energy around excavations, but at the cost of incrementally expending the elongation capacity of support systems.

Excavation and pillar analysis with peak and residual properties in implicit and explicit rockmass models

Fischer, C., Dressel, E., and Diederichs, M.S.

Department of Geological Sciences and Geological Engineering, Queen's University, Kingston, Ontario, Canada

ABSTRACT

The Geological Strength Index (GSI) is a rockmass assessment scheme that incorporates two factors: rockmass blockiness and discontinuity condition. GSI is used worldwide in site characterization for tunnelling, mining, and slope stability. When GSI is used with the Generalized Hoek-Brown strength criterion to represent the strength and stiffness of jointed rockmasses in numerical models, rockmass structure is accounted for implicitly. Such models are termed “implicit models” in this work. Alternatively, dense networks of discrete structural features can be represented in rockmass models using modern numerical modelling tools, termed “explicit models”. Explicit models can show an increased level of detail on rockmass failure mechanisms, although requiring more computational power and additional input parameters for the discrete discontinuity features.

This research aims to verify the compatibility of implicit and explicit numerical rockmass models for elastic-perfectly plastic rockmass behaviour in the moderately jointed rockmass range (GSI 35 to 75) using a circular tunnel model in RS2, and to assess the differences between implicit and explicit results. Following the compatibility assessment, a formulation is developed for representing post-yield weakening rockmass behaviour using implicit and explicit tools. As the pseudo-discontinuous explicit models simulate rockmass dilation by deformation of the joint network, rockmass dilation must be accounted for otherwise in the implicit numerical models which do not contain discrete joints. Practical recommendations are therefore delivered for selecting appropriate dilation parameters for use in implicit post-yield weakening models. This research then uses a series of pillar models to ascertain the influence of the Hoek-Brown dilation parameter on brittle rock pillar behaviour.

Results from the elastic-perfectly plastic tunnel simulations showcase the compatibility of the implicit and explicit modelling methods. The explicit models give similar predictions of tunnel closure and depth of yield when compared to equivalent GSI implicit models, when reasonable input parameters are estimated and calibrated for the explicit models. However, rockmasses that differ in blockiness and surface condition that are nonetheless classified as the same GSI will not necessarily predict the same rockmass behaviour in terms of closure and depth of yield. Based on the explicit representation of the joint network in each model, the localizations of elevated joint yield and closure differ. Additionally, the explicit models show more variability in depth of yield and closure compared to the implicit models, which has practical implications for support design and monitoring.

Upon validation of the elastic-perfectly plastic explicit numerical models, model modifications are implemented to represent rockmass post-yield weakening. In the explicit models, the intact rock block GSI is reduced upon yield, as calculated using a linear fit to residual intact laboratory testing data. Joint strength is reduced to a residual function upon joint yield. For the implicit models, residual GSI is calculated using an empirical relationship between residual GSI, initial GSI, and the rockmass material constant m_i . Implicit models are generated using three different dilation parameters (0 dilation, a dilation parameter of $1/8 m_p$, and a dilation parameter of $1/4 m_p$), and two different rockmass moduli (a peak modulus calculated using initial GSI and the Generalized Hoek-Diederichs formulation, and a residual modulus calculated using residual GSI).

A comparison of the implicit and explicit results for three isotropic stress levels (20 MPa, 35 MPa, and 50 MPa) demonstrates that implicit models using a peak modulus and a dilation parameter of $1/8 m_r$ best represented the explicit model data across the three stresses investigated. However, with increasing isotropic stress, the best fitting dilation parameter decreases ($1/4 m_r$ best fits the data at 20 MPa, while $1/8 m_r$ best fits the data at 35 MPa, and 0 dilation best fits the data at 50 MPa).

These findings were extended through 3D pillar models constructed in RS3 to examine the influence of dilation on confined pillar behaviour. Pillars were formed between adjacent caverns and connecting tunnels to assess strength, failure mode, and the effect of residual parameters. Results showed that dilation increases shear strain along pillar walls and enhances confinement in the pillar core, contributing to an increase in overall pillar strength. The inclusion of dilation in the implicit models produced responses more consistent with explicit simulations, reinforcing the need to consider dilation effects when evaluating post-yield behaviour in numerical design.

While empirical stability charts remain a useful preliminary design tool, they do not account for the influence of rockmass dilation or post-yield degradation of strength and stiffness. These charts typically assume constant input parameters and do not reflect the evolving confinement conditions or anisotropic failure mechanisms observed in jointed rockmasses. As shown in this study, the inclusion of dilation and residual parameters can significantly alter predicted pillar response. Therefore, to capture the true behaviour of brittle rock pillars, especially in moderately jointed ground, numerical modelling with appropriate constitutive inputs is necessary to support safe and realistic design outcomes.

In summary, explicit numerical models were shown to provide greater detail on the spatial variability of moderately jointed (GSI 35 to 75) rockmass response. A post-yield weakening strength formulation was developed for explicit and implicit models, including practical recommendations for the selection of the rockmass dilation parameter.

Innovations in direct shear testing under various boundary conditions

Packulak, T.R.M, MacDonald, N.R., Diederichs, M.S., and Day, J.J.

Department of Geological Sciences and Geological Engineering, Queen's University, Kingston, Ontario, Canada

ABSTRACT

The importance of being able to understand the geomechanical behaviour of rock fractures and intact rock has driven new research. This research includes the use of new laboratory testing equipment and testing protocols, along with the development of numerous constitutive models each addressing a series of different assumptions and variables to better understand the behaviour of intact rock and its fractures. In the case of rock joints (discontinuities), it is one member of two highly influential components of a rockmass, the other member being anisotropy, which have been highlighted as critical areas of study since the International Society of Rock Mechanics was founded in 1962 and further re-iterated by the president of the society (Professor Leopold Muller) at the First Congress. In Professor Muller's opening address to the congress he made the statement "Many experts agree with me that discontinuities and anisotropy are the most characteristic properties of the material rock and that the properties of jointed media depend much more on upon the joints of the unit rock block system than upon the rock material."

In many cases, discontinuities govern rockmass behaviour of rock engineering projects such as natural slopes, surface excavations, and underground openings. For engineering design, laboratory direct shear testing is a critical test used to characterize and measure the stiffness, strength, and dilative behaviour of rock joints and other fractures. These deformation, strength, and dilative properties are needed as input parameters to define the mechanical behaviour of rock joints in explicit and discrete numerical models. Different geological settings for infrastructure projects has meant that fractures are being tested under different boundary conditions to best match expected in situ conditions. The most common and easiest boundary condition to complete in the lab is the Constant Normal Load (CNL) boundary condition where a static normal load is applied to a specimen while measuring the shear resistance of the rock and is used to represent the conditions rock joints experience above ground (e.g. sliding of hydro dams and rock slopes). More complex boundary conditions including the Constant Normal Stress (CNL*) boundary condition, an alternative to the CNL boundary condition, is used to represent for surface cases and the Constant Normal Stiffness (CNS) boundary condition is used to represent fractures in underground settings where dilation is suppressed. The CNL* and CNS boundary conditions are considered to be more complex as they require specialized direct shear machines with servo controlled capabilities.

This poster summarizes recent programs completed on discontinuities in the Queen's University Advanced Geomechanics Laboratory.

A program using crystalline granites and gniesses of NQ and NQ3 size diamond drill core of the Canadian Winnipeg River Complex within the Pointe Du Bois batholith was completed to study the behaviour of clean, rough, discontinuities under CNL* and CNS boundary conditions and saw cuts under the CNL* boundary condition. Rough discontinuities were tested under applied normal stresses of 1, 2, 4, 8, or 16 MPa and normal stiffnesses of 0 (CNL*), 6 or 12 kN/mm. Saw cut specimens were tested under CNL* conditions with applied normal stresses of 1, 2, 4, 8, 10, 16, or 20 MPa. In this study the influence of boundary conditions on strength, dilation, and stiffness was compared. For joint shear strength it was concluded that the boundary condition has

no influence on strength in terms of Mohr-Coloumb or Barton-Bandis parameters. However, it was noted that the CNS boundary condition results in measurements with a high degree of variability. With regards to dilation, it is observed that as normal stress increases the amount of dilation the joint undergoes decreases. Additionally, a new secant dilation that is used to describe the entire dilation curve in terms of total dilation potential, secant dilation angle, and critical shear displacement. All three of these terms can be used as inputs in numerical models with explicit joint structures.

In most cases, joint shear stiffness and joint normal stiffness should not be influenced by the boundary condition, as normal stiffness is measured during the normal loading stage before the boundary condition comes into effect and joint shear stiffness is measured pre-yield prior to joint dilation. However, these parameters will be influenced by the machine components depending where deformation measurements are being taken. In the case of available commercial machines the shear gap is not large enough to install instruments directly on the sample and therefore most instruments are installed outside of the encapsulating material. While this location is in most cases the only feasible location, deformations associated with other components including but not limited to the encapsulating grout or resin, rock specimen, and steel housing will also be measured. In order to overcome this limitation a new procedure based upon work by Goodman (Methods of geological engineering in discontinuous rocks. West Publishing Company, St. Paul, 1976) was created to correct measured deformations and remove all non-fracture deformation. The correction is made by testing an intact specimen of the same geologic material of which the fractures are found in, in direct shear under the same boundary conditions and measuring this baseline deformation. These deformations are then subtracted from all direct shear tests on fractures. In the same study, the normal stiffness was measured using four different methods, a power law (Swan in Rock Mech Rock Eng 16:19–38, 1983), a hyperbolic law (Bandis et al. in Int J Rock Mech Min Sci Geomech Abstr 20:249–268, 1983), and two semi-logarithmic laws (Bandis et al. 1983; Evans et al. in Geotherm Resour Counc Davis Calif USA 16:449–456, 1992). Through the evaluation of the four different laws, it was found that measured instantaneous normal stiffness increased with stress and as most joints had a non-linear normal stress – normal deformation curves. For measured shear stiffness, joint shear stiffness was positively correlated with applied normal stress.

As rock fractures are mostly unique, evaluating measured joint properties is affected by the differences in joint topology and mineral make up of the fracture surface. In an effort to remove the influence of varying surface topology and lithological make up, a replication process using structure from motion (SfM) photogrammetry, 3-D printing technologies, and commercially available non-bleed, non-shrink grout was created to mass produce synthetic joint replicas. The use of synthetic joint replicas allows for laboratory direct shear testing to be completed on controlled samples to evaluate the difference in geomechanical properties of rock joints when following multiple direct shear testing procedures. In this study, a series of synthetic joint replicas utilizing two parent rocks and two different water to cement ratios were produced for the testing program. Measured geomechanical properties when following a multi-stage direct shear testing procedure with repositioning and limited displacement direct shear test procedure were compared to the results of single stage direct shear testing to evaluate the impact each testing procedure has on the results.

Laboratory testing for the characterization of heterogeneous rockmasses

Gagnon, É., Woodland, S.K., Packulak, T.R.M., Hegger, S., Clark, M., and Day, J.J.

Department of Geological Sciences and Geological Engineering, Queen's University, Kingston, Ontario, Canada

ABSTRACT

Rock is seldom a homogeneous material; at the meso-scale, defects such as veins, phenocrysts, and foliation often form representative parts of the intact rock and must be included in laboratory testing specimens in order to properly capture the expected rock behaviour. The ISRM recommends use of three direct contact extensometers to measure axial and circumferential strains during Uniaxial Compressive Strength (UCS) testing. Strain gauges can also be used for UCS testing but should cover at least ten grain diameters of the rock microstructure. Due to the spatial importance of intrablock features at the specimen scale, a proper understanding of the stress-strain field of the rock during testing is critical to identify shape-, scale-, and end-effects, and derive appropriate intact rock strength characteristics. The conventional strain measurement methods listed above are blind to localized deformation outside of the central zone of a specimen, which greatly hinders our ability to properly interpret test results.

To address this limitation, members of the Queen's Geomechanics and Geohazards Group (QGGG) carried out testing programs on heterogeneous rockmasses to characterize spatial variability in mechanical behaviour, and developed full-field strain measurement techniques—specifically Fiber Optic Sensing and 2D Digital Image Correlation (DIC)—to more accurately capture the complete deformation field during UCS and BTS testing.

An intensive UCS testing program was conducted on the Legacy Skarn Deposit in New Brunswick to evaluate the geomechanical influence of hydrothermal veins and phenocrysts, and to assess the suitability of standard geotechnical logging and sampling protocols for heterogeneous rockmasses. A total of 50 UCS tests were completed across five lithologies, including both matrix-type and veined specimens. Results show that mineralogy significantly affects strength: calcite veins weakened granodiorite but strengthened calcareous mudstone. Phenocrysts increased stiffness and peak strength by arresting cracks. Conventional methods for identifying elastic properties and damage thresholds were evaluated, with Lateral Strain Nonlinearity (LSN) found most effective for Crack Initiation (CI), and Instantaneous Young's Modulus and Axial Strain Nonlinearity (ASN) best suited to Crack Damage (CD), depending on lithology. Four sampling approaches were compared, highlighting the importance of including both matrix and veined specimens in a testing program. A fixed-interval sampling approach is recommended for heterogeneous rockmasses, considering availability, budget, and lithological complexity.

The observations in this testing program motivated the development of improved, full-field strain measurement techniques. A novel distributed optical strain sensing (DOS) technology using Rayleigh optical frequency domain reflectometry (ROFDR) was integrated with UCS testing to measure full-field strain with 0.65 mm spatial resolution. The method was applied to five Cobourg limestone specimens instrumented with helically wrapped optical fibers, axial extensometers, and foil strain gauges. Results showed DOS effectively captured heterogeneous strain responses, with circumferential strain differing by only 15.6% from foil gauges. Strain mapping correlated localized strain concentrations to veins and clay-rich seams, revealing failure modes controlled by stiffness contrasts within the rock.

Work was also done to adapt 2D DIC for rock testing. The QGGG Lab compared speckle pattern application methods—including spray paint, ink, stencils, and a novel laser engraving technique—with laser engraving producing the highest quality, most repeatable patterns. This was validated by comparing DIC strain measurements on BTS specimens with strain gauges. DIC effectively captured strain in foliated meta-basalt, revealing strain and microcrack development outside the strain gauge area, which is critical since fractures in heterogeneous rocks don't always occur centrally. Thus, DIC provides valuable full-field strain data beyond conventional contact methods.

In conclusion, conventional laboratory methods for rockmass characterization were developed for homogeneous rocks and often fall short when applied to heterogeneous specimens containing veins, phenocrysts, or foliation. The results highlight the importance of including specimens which capture the complexity of geological fabric in testing programs to avoid bias and achieve a comprehensive geomechanical understanding. Full-field strain measurement techniques such as distributed optical sensing and 2D Digital Image Correlation provide critical insights by capturing localized strain concentrations and deformation patterns that conventional point measurements miss. These advanced methods improve interpretation of stress-strain behaviour and failure mechanisms in complex rockmasses, enabling more accurate characterization essential for engineering and geotechnical applications.

Modelling sea stack and shoreline cliff failure modes in RS3

Hyslop, A., Hoyle, W. and Day, J.J.

Department of Geological Sciences and Geological Engineering, Queen's University, Kingston, Ontario, Canada

ABSTRACT

Sea stacks are natural pillars of rock that have been detached by wave action and other erosional processes from cliff-lined shores. They are popular geotourism destinations due to their unique and beautiful geometry. Hopewell Rocks Provincial Park in New Brunswick, Canada, which is situated on the coast of the Bay of Fundy, hosts numerous sea stacks and shoreline cliffs that are composed of coarse-grained, poorly sorted, polymictic conglomerates and arkosic sandstone. These layers are interbedded with silt and fine-grained sandstone. Clasts within the conglomerate range in size from small pebbles to cobbles, generally being less than 20 cm in diameter. The Bay of Fundy experiences the world's highest tides, which exposes approximately up to 5 m of the bottom of sea stacks and cliff face to significant tidal and wave erosion that drives undercutting.

Rockfalls from the shoreline cliff in the Park occur annually but no system is in place to predict future occurrences. This study focuses on analyzing different sea stack and cliff failure modes using 3D Structure-from-Motion digital photogrammetry models and 3D finite element method (FEM) geomechanics numerical models (RS3 software by Rocscience Inc.). This work aims to understand the driving forces behind sea stack and cliff rockfalls, as well as the estimated timeline and geometry conditions that are likely to induce failure. The findings of this study provide valuable information that can be used to evaluate the rockfall geohazard risk to public safety and potential impacts to geotourism at the Park.

Challenges in calibration and verification of hydromechanical models for excavations in rock

Markus, S.¹, Kennedy, M.¹, Vazaios, I.², and Diederichs, M.S.¹

¹*Department of Geological Sciences and Geological Engineering, Queen's University, Kingston, Ontario, Canada*

²*ARUP, London, United Kingdom*

ABSTRACT

Management of groundwater is critical in the execution of underground construction projects, but there is inherent uncertainty in the methods used for estimating groundwater inflow into rock tunnels. For excavations in rock, the coupled relationship between the mechanical properties of the rockmass and the groundwater pressures and associated flow has implications on the design of underground spaces. Our understanding of this process and its application in engineering models impacts our estimates of tunnel inflow and stability.

Without well established guidelines, calibration and verification of hydromechanically coupled (HMC) numerical models can be challenging and highly project dependent. Determination of HMC model input parameters requires complex laboratory testing and there are limited studies available in literature for rocks with low permeability. There is a high computational cost and time associated with the numerical models due to the processing of coupled calculations. Models also require limits and boundary conditions for both mechanical and fluid calculations which may be different. In HMC models, the boundary conditions can have a large impact on the resultant values, particularly on pore fluid pressures and fluid flow.

This research explores some of the challenges associated with implementing HMC into numerical models of homogeneous rock, highlighting the limitation of permeability due to the impact of stress, how poor fluid affects the elastic response of the rock, the use of analytical solutions in verification of HMC models, and challenges in HMC model calibration and sensitivities.



Technical Programme

Awards

CARMA's Inaugural 2022 Prof. Doug Stead PhD Award Winner

Jonathan D. Aubertin



RockEng22 Symposium Best Poster Award Winner

Vasileiou, A., Alcaïno-Olivares, R., Loprieno-Gnirs, A., Bickel, S., Ziegler, M., Khan, U.T., and Perras, M.A.



Social Programme

Kingston and 1000 Islands Dinner Boat Cruise



Social Programme

Brockville Tunnel Tour and Banquet Dinner



Symposium Sponsors

Gold Sponsors



Silver Sponsors



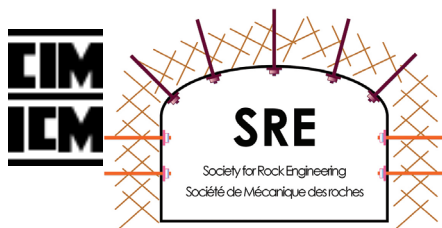
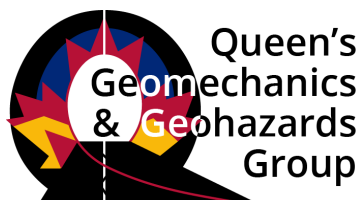
Bronze Sponsors



Friend Sponsor



Event Sponsors



Support a Student Sponsor



Lanyard Sponsor







CARMA

CANADIAN ROCK MECHANICS ASSOCIATION

